



www.csiro.au

COLLINGWOOD PARK MINE REMEDIATION – Subsidence control using fly ash backfilling

Baotang Shen, Habib Alehossein, Brett Poulsen, Cameron Huddleston-Holmes, Binzhong Zhou, Xun Luo, Hongwei Wang, Johnny Qin, Joey Duan, Zak Jecny, Matt Van de Werken, David Williams¹

CSIRO Earth Science and Resource Engineering Report EP105068

¹ University of Queensland

Enquiries should be addressed to:

Dr Baotang Shen
CSIRO Earth Science and Resource Engineering
Queensland Centre for Advanced Technologies (QCAT)
PO Box 883, Kenmore Qld 4069 Australia
Tel. +61 7 3327 4560
Fax +61 7 3327 4455
Email Baotang.Shen@csiro.au

Copyright and Disclaimer

© 2010 CSIRO To the extent permitted by law, all rights are reserved and no part of this publication covered by copyright may be reproduced or copied in any form or by any means except with the written permission of CSIRO.

Important Disclaimer

CSIRO advises that the information contained in this publication comprises general statements based on scientific research. The reader is advised and needs to be aware that such information may be incomplete or unable to be used in any specific situation. No reliance or actions must therefore be made on that information without seeking prior expert professional, scientific and technical advice. To the extent permitted by law, CSIRO (including its employees and consultants) excludes all liability to any person for any consequences, including but not limited to all losses, damages, costs, expenses and any other compensation, arising directly or indirectly from using this publication (in part or in whole) and any information or material contained in it.

EXECUTIVE SUMMARY

Introduction

This executive summary provides background to the mining induced subsidence events in Collingwood Park and outlines CSIRO's technical report into these events.

CSIRO explains why the events occurred and provides options that if actioned, could help prevent future mining-related subsidence.

This summary does not outline the costs associated with CSIRO's suggested options. The CSIRO report is a technical one and costs were not part of the terms of reference.

Background

Part of the Ipswich suburb of Collingwood Park is underlain by two decommissioned underground coal mines – Westfalen Number 3 and New Redbank Collieries. These mines used the “bord and pillar” method of mining at depths from approximately 60m to 140m.

Bord and pillar mining at the collieries created numerous underground pillars ranging up to 11m in height in some areas of Westfalen Number 3, and with various dimensions and shapes left behind to support the load from the rock above the mine after coal was extracted.

In mining terminology, the *Factor of Safety* (FoS) is a measure of stability, defined as the ratio of the maximum strength of a pillar to the load applied to the pillar. A low FoS implies a high risk of mechanical failure. If the calculated FoS is lower than the requisite value, a pillar may fail, triggering overload of neighbouring pillars, leading to roof failure and caving of rock above pillars into the previously excavated roadways or mine voids, and ultimately ground subsidence which may penetrate to the surface.

In December 1988, a subsidence event occurred near Lawrie Drive, Milgate Street and Rush Court in Collingwood Park. In April 2008, a second subsidence event occurred, resulting in surface movement and damage to houses within an area near the intersections of Duncan, McInerney, McLaughlin and Moloney Streets. Both subsidence events occurred as a result of pillar failure within the Westfalen No. 3 Colliery.

Westfalen No. 3 Colliery

The Westfalen No. 3 Colliery extracted coal from the Ipswich Coal Measures from 1965 to 1987. At this mine, multiple coal seams coalesce into a single seam more than 11m thick. The full thickness of the seam was mined in some areas, while in other areas only part of the seam was mined.

Bord-and-pillar mining at Westfalen No. 3 initially used *ad hoc* pillar designs, but after 1976 a modern pillar design was employed. This latter method, characterised by regular square shaped pillars designed to a specific FoS, is evident in the panels to the east of Kruger Parade. To our knowledge, these pillars are still stable (the term “panels” denotes a collection of coal pillars that are spatially and geometrically grouped).

Earlier *ad hoc* mining resulted in irregularly shaped pillars of varying height. Inundation of Westfalen No. 3 in the major flood of 1974 caused pillar damage and roof and floor scouring. Some of these *ad hoc* pillars in the panels that were mined early in the life of Westfalen No. 3 have collapsed, resulting in the 1988 and 2008 surface subsidence events.

CSIRO Engagement

At the request of the Department of Employment, Economic Development and Innovation (DEEDI) and the Department of Infrastructure and Planning (DIP) of the Queensland Government, CSIRO studied mining-induced subsidence at Collingwood Park associated with the Westfalen No.3 Colliery with the goal of providing options for prevention of future mining-related subsidence.

This Executive Summary describes CSIRO's Final Technical Report that documents a 12-month work program.

Numerical modelling by CSIRO estimated the present stability of the workings in order to understand the effectiveness of remediation methods. These models are limited by complex and uncertain subsurface mine geometry and unknown parameters in mine working details. It is unlikely that further field investigation will reduce this uncertainty significantly.

Stability Analysis

Observed ground subsidence directly indicates pillar and/or panel failure. CSIRO assessed the stability of underground panels using the modern pillar design approach to estimating pillar strength from pillar width and height. CSIRO found that pillar strength in the two already failed panels was well below that required for long-term stability where pillars are located beneath a residential area, validating the overall modelling method.

CSIRO estimated that the Central Panel is approximately 20% stronger than the adjacent panel to the south-west that failed in 2008. Further, CSIRO estimated that, of the areas studied, the Central Panel is the next most likely to subside in the future, and that remediation is needed to ensure long-term stability of the Central Panel.

A three-dimensional seismic investigation suggested that pillar collapse in 2008 may have damaged pillars in the Central Panel, reducing its Factor of Safety and compromising its integrity.

CSIRO considers that, if another panel failure occurs, the event will be characterised by failure of one or more pillars and subsequent load transfer to adjacent pillars, resulting in over-stressing and further cycles of pillar failure and load transfer until barrier pillars or unmined coal halt the process. Given the irregular nature of the pillars and the widely varying geometrical attributes of width and height, CSIRO considers that the resulting failure will develop gradually over hours or days rather than an uncontrolled violent manner known as cascading pillar failure. CSIRO also considers that the surface expression of any potential failure will be subsidence developing to a magnitude comparable with the 2008 event (approximately 1.5m).

Monitoring

CSIRO recommended a monitoring system combining a micro-seismic network to monitor seismic events as a result of fracturing in coal pillars and rock strata above the coal seam with an extensometer installed deep in a borehole to monitor deformation of the rock strata focused on the Central Panel. This recommendation has been accepted by the Queensland Government. The hybrid monitoring system is in place and is working as designed. Early results from the monitoring system have identified minor seismic events and some potential stratal deformation. Some of seismic events may be associated with the 2008 failure and the monitored strata movement may partially be instrument related.

From the monitoring results to date, CSIRO considers that parts of the Central Panel are moving slowly. Accordingly, CSIRO recommends that additional extensometers and an additional seismic station be installed above the Central Panel to increase the accuracy and reliability of the monitoring network. Should there be significant increases in the seismic events and/or the rate of deformation, these indications would suggest increasing potential for a surface subsidence event.

Gas

CSIRO considers that rapid escape of mine gas to the surface is possible but unlikely in the case of non-violent panel failure.

Tests conducted by Simtars determined that the mine gas is typical of an unventilated closed coal mine and is a mixture of methane, carbon dioxide, nitrogen and oxygen. Combustion of this gas mixture at the measured levels is not possible. However, if mine gas escapes to the atmosphere, the resulting mixture could potentially be combustible until dispersed. Further monitoring is needed.

Water

Apart from inundation in the 1974 flood event, Westfalen No. 3 Colliery was considered by mine managers to be a dry mine with little water ingress. Existing studies and piezometer monitoring indicate that the workings are currently partially flooded, with rising water levels. Because the CSIRO study coincided with above average rainfall in southeast Queensland, long-term trend of water levels cannot be determined from a single snapshot of current monitoring data.

Rising water levels will reduce coal pillar strength to an uncertain degree. CSIRO determined that the pillars that failed in 2008 were not affected by water. However, it is not known if rising water level was associated with the 1988 subsidence. CSIRO recommended investigating the influence of water interacting with the coal of the specific mineralogy of the Westfalen No. 3 mining seam, because these results could influence the stability assessment and remediation options for the Westfalen No. 3 Colliery. Future work will require studies to assess potential for leaching, erosion, pollution and migration of chemical elements in the fly ash into the underground water.

Backfill Remediation

CSIRO investigated a range of remediation options to reduce the likelihood and consequence of future mine-induced surface subsidence. Backfilling mine voids was identified as the most likely method to achieve success.

CSIRO and University of Queensland researchers tested mixtures of fly ash, crusher dust, sand, cement and water for flowability, stability, strength and overall suitability as potential backfill material. These mixtures included a non-cohesive mix of fly ash and water to a 50-60% solids-water concentration, and a cohesive mix that adds cement to the non-cohesive mix to give a conservative 0.5MPa strength backfill.

The major advantage of the non-cohesive mix over the cohesive mix is that its properties do not change rapidly with time and can penetrate more reliably into smaller voids. This reduces the number of holes needed to be drilled for filling when compared to a cohesive mix. Flowability tests indicate that 90% fill of the mine voids should be achievable, particularly and preferably with a non-cohesive mix.

CSIRO estimated that after backfilling, a typical Westfalen No. 3 coal pillar would be approximately 30% stronger using the non-cohesive mix and 57% stronger using the cohesive mix if the surrounding mine voids are filled to 90%. Panel strength increases resulting from backfill are predicted to be of a similar magnitude.

Unstable pillars, and pillars that have already failed, should become stable after confined bulk filling. Modelling indicates that backfilling to 90% with a non-cohesive mix will increase pillar FoS to a minimum of 1.6, the value often used in rock engineering design for long-term stability.

CSIRO recommended bulk filling of the mine voids with a fly ash mixture from the nearby Swanbank Power Station. A similar approach has been adopted to ensure mine pillar stability as part of the nearby Ipswich Motorway Upgrade.

CSIRO considered two backfilling options in detail. **Option 1** is isolation and subsequent backfilling of the Central Panel, and **Option 2** is the backfilling of all Westfalen No. 3 mine voids that undermine the Collingwood Park residential area northwest of Lawrie Drive and east of Collingwood Drive. CSIRO considered the strength improvement and associated risk reduction together with the potential consequences for both options.

CSIRO assessed undermined areas to the west of Collingwood Drive within the project boundaries, based on the Factor of Safety calculations, as stable for the long-term due to the shallower mining depths and bigger pillars used and were therefore not considered in either option.

Option 1 strengthens the Central Panel, identified as the area of Westfalen No. 3 where future pillar failure is most likely. However, it does not reduce the subsidence risk in areas other than the Central Panel. It also requires building underground barrier walls around the Central Panel which are often expensive, making it less cost-effective than Option 2.

Option 2 strengthens all Westfalen No. 3 mine voids that undermine the Collingwood Park residential area north-west of Lawrie Drive and east of Collingwood Drive, increases the calculated FoS to 1.6, believed to be sufficient for the long-term stability of coal pillars, and minimising potential for mine-induced surface subsidence. Even in the unlikely event of pillar failure after backfilling, CSIRO estimated surface tilt will be less than 5mm/metre, which would result in insignificant to minor damage to the existing Collingwood Park housing stock of slab on ground dwellings.

*CSIRO recommended that the Queensland State Government use remediation **Option 2** with non-cohesive backfill, i.e. backfilling all open mine voids of the Westfalen No. 3 Colliery north of Lawrie Drive and east of Collingwood Drive using a backfill grout consisting of fly ash and water with 50-60% solids-to-water concentration to a minimum of 90% void volume.*

CSIRO recommended that this remediation be undertaken as soon as outstanding environmental and technical issues are resolved.

Further Studies Ensuring the Successful Remediation of Westfalen No.3 Colliery

A backfilling project of this scale has to CSIRO's knowledge not been previously attempted. The table below summarises CSIRO's recommendations to resolve the technical and environmental issues necessary to proceed with remediation of Westfalen No. 3 Colliery.

Table: Summary of further studies to ensure the successful remediation of Westfalen No.3 Colliery

Recommendation	Scope	Reason	Duration
Expansion of the existing monitoring network	Install two additional extensometers and one micro-seismic station in the Central Panel. The existing monitoring network consists of one extensometer and three seismic stations	<ol style="list-style-type: none"> 1. Verify if sections of the Central Panel are stable or deforming. 2. Improve the accuracy and reliability of the monitoring system for any future mine related surface subsidence event, if any. 	2 months
Large scale laboratory modelling of backfill	Build a scaled-down bord-and-pillar mine model in laboratory; conduct injection tests by injecting different grout materials into the mine voids; observe the process of backfilling.	<ol style="list-style-type: none"> 1. Simulate to verify various injection scenarios for the ability to achieve the critical minimum 90% fill. 2. Understand both visually and analytically the process of backfill and its effect. 	8 months
Field full scale test of roadway backfill	Excavate a mine roadway-sized trench at the surface; carry out a full-scale grout injection operation; measure grout flow details including profile and distance in the backfilling process.	Determine potential backfilling issues that can arise in the actual underground backfill operation. Ascertain the most effective and optimum backfilling procedure and process for the real underground mine backfill operations.	8 months
Water: effect of rising levels	Conduct a focused study to quantify the effect of rising water in Westfalen No.3 on the ground stability, including laboratory tests of dry and wet coal samples and analytical/numerical modelling.	<ol style="list-style-type: none"> 1. Understand the effect of rising water level on ground stability; 2. Determine if pumping out mine water before or during backfill operation is needed. 	10 months
Water: groundwater quality after backfill	Investigate and monitor groundwater flow and chemical transport during and after fly ash backfilling; predict the effect of fly ash back fill on groundwater quality.	Determine whether or not backfilling and backfill mix will cause any unacceptable concentrations of any potentially harmful elements in the underground water system.	8 months
Continuous ground monitoring and data analysis, including gas	Maintain the monitoring system in working condition; analyse and interpret the data on a weekly basis before and during backfilling, and monthly after backfilling; recommend actions if subsidence risk is found to increase; continue monitoring during and after backfilling for the long term.	<ol style="list-style-type: none"> 1. Develop a historical record of the current geotechnical environment. 2. Identify any trends suggesting an increased potential for future subsidence events 3. Assess effect of backfilling on ground stability in both short and long-term periods. 	Ongoing (until risk is considered to be fully controlled)

New Redbank Colliery

New Redbank Colliery mined coal during the 1920s in an area that now underlies the north-east corner of Collingwood Park. Coal was extracted from the Bluff, Middle and Bottom seams in a pattern that resulted in overlapping mine panels at different elevations. This approach is called *multi-seam mining*.

Stability assessment of New Redbank Colliery is difficult because few reliable data exist that describe mining operations. A mine plan exists, but its accuracy has not been confirmed and little additional information is available on mining heights and working conditions.

CSIRO believes that further investigation of New Redbank Colliery is needed to establish what remediation may be necessary.

Summary of Recommendations

1. Backfill all open mine voids of the Westfalen No. 3 Colliery north of Lawrie Drive and east of Collingwood Drive using a backfill grout consisting of fly ash and water with 50-60% solids-to-water concentration to a minimum of 90% void volume.
2. Expand the existing monitoring network in Collingwood Park by installing two additional extensometers and one micro-seismic station above the Central Panel of the former Westfalen No. 3 Colliery.
3. Conduct a large-scale laboratory modelling of backfill.
4. Conduct a full-scale field test of roadway backfill.
5. Conduct a focused study to quantify the effect of rising water in Westfalen No.3 on the ground stability.
6. Investigate and monitor groundwater flow and chemical transport during and after fly ash backfilling
7. Continue ground monitoring and data analysis, including gas, in Collingwood Park.

Contents

Executive Summary	I
Technical Summary	1
3D seismic survey	1
Geotechnical investigation and monitoring	2
Microseismic monitoring	4
Numerical modelling and pillar/panel stability assessment	4
Hazard mapping and risk assessment	6
Laboratory tests and injection material recommendation	7
Recommendation of remediation scenario and further work	7
1. Introduction	10
1.1 New Redbank Colliery	10
1.2 Westfalen No. 3 Colliery	10
1.3 Mine subsidence events	11
1.4 Scope of this study	11
2. 3D seismic survey	14
2.1 Summary	14
2.1.1 Project objectives	14
2.1.2 Outcomes	14
2.1.3 Recommendations	15
2.2 3D seismic trial survey	16
2.2.1 Survey site and survey design	16
2.2.2 Data acquisition	19
2.3 Data processing	23
2.4 Data analysis and interpretation	26
2.4.1 The “known” geology	26
2.4.2 Seam reflection identification	27
2.4.3 Pillar failure mapping	28
2.4.4 Fault identification	37
2.4.5 Mapping underground roadways	40
2.5 Conclusions and recommendations	42
3. Geotechnical investigation and monitoring	44
3.1 Summary	44
3.2 Introduction	45
3.3 Drilling	46
3.4 Geological model	50
3.4.1 Regional geology	50
3.4.2 Site geology	50
3.5 Piezometer monitoring	58

3.6	Water effect on pillar stability	60
3.7	Extensometer monitoring	63
3.8	Water sampling and analysis	66
3.9	Gas sampling and analysis	71
4.	Microseismic monitoring.....	74
4.1	Summary	74
4.2	Objectives of the microseismic monitoring	74
4.3	Microseismic monitoring plan	75
4.3.1	Geophone locations	75
4.3.2	Microseismic data acquisition system	76
4.3.3	Geophones.....	77
4.3.4	Calibration of the microseismic system	77
4.4	Data processing and interpretation	82
4.4.1	Discrimination between traffic and seismic events	82
4.4.2	Seismic waveforms of traffic related events and seismic events	83
4.4.3	Seismicity analysis	86
4.4.4	Event location estimation	86
4.5	Conclusions	91
5.	Numerical modelling and pillar/panel stability assessment	93
5.1	Summary	93
5.2	Introduction	95
5.2.1	Pillar strength formula	95
5.2.2	Pillar effective width.....	96
5.2.3	Pillar load formula	96
5.2.4	Numerical model calibration	97
5.3	Summary of results on coal pillar strength	100
5.3.1	Post peak strength	100
5.3.2	Pillar shape influence on strength	101
5.3.3	Additional findings	102
5.4	Roadway backfill and pillar strength improvement	103
5.4.1	Numerical results and analysis.....	103
5.4.2	Post peak pillar strength increase	104
5.4.3	Backfill for diamond shaped pillars	104
5.4.4	Backfill placed after significant pillar yield	104
5.5	3D models of 2008 failure panel and adjacent regions.	109
5.5.1	Results from 2008 event region model.....	110
5.5.2	Results from numerical model of the central panel.....	112
6.	Hazard mapping and risk assessment.....	113
6.1	Summary	113
6.2	Introduction	114
6.2.1	Hazard maps.....	114
6.2.2	Mining zones	116

6.3	Hazard maps with and without backfill	117
6.3.1	Hazard map of Westfalen No. 3 Colliery without backfill	119
6.3.2	Hazard map with targeted 0.5MPa cohesive backfill.....	122
6.3.3	Hazard map with total non-cohesive backfill	123
6.3.4	Hazard map with total cohesive backfill	124
6.4	Consequence maps – Surface subsidence.....	125
6.4.1	Potential subsidence map assuming total failure without backfill	128
6.4.2	Potential subsidence map assuming failure of central region only without backfill	129
6.4.3	Potential subsidence map assuming total failure after targeted backfilling	130
6.4.4	Potential subsidence map assuming total failure after total backfilling.....	131
6.5	Consequence maps – Surface tilt.....	132
6.5.1	Potential tilt map assuming total failure without backfill.....	134
6.5.2	Potential tilt map assuming failure of central region without backfill.....	135
6.5.3	Potential tilt map assuming total failure after targeted backfilling	136
6.5.4	Potential tilt map assuming total failure after total backfilling	137
7.	Laboratory tests and injection material recommendation.....	138
7.1	Scope.....	138
7.2	Recommendation.....	138
7.3	Result summary.....	140
7.4	Conclusions on laboratory tests	148
8.	Remediation scenarios and further investigations	149
8.1	Summary	149
8.2	Introduction	150
8.3	Remediation scenarios at Westfalen No. 3 Colliery	150
8.4	Recommended further studies for remediation scenarios at Westfalen No. 3 Colliery.....	152
8.4.1	Scenarios 1 and 2 – No remediation.....	152
8.4.2	Scenario 3 – Targeted remediation.....	154
8.4.3	Scenario 4 – Non-cohesive total backfill	154
8.4.4	Scenario 5 – Cohesive total backfill	156
8.5	Recommended further work for developing remediation scenarios for New Redbank Colliery	156
9.	Conclusions	158
10.	Acknowledgements	161
11.	References	163
APPENDIX A	167
APPENDIX B	168
APPENDIX C	169

TECHNICAL SUMMARY

During various stages in the 19th and 20th Century, the “bord and pillar” method of underground mining was implemented in a number of mines throughout the Ipswich area, including two mines operated in the vicinity of Collingwood Park, the “New Redbank Colliery” (worked during the 1920s – Bluff: Top, Middle and Bottom Seams) and the more recent “Westfalen No. 3 Colliery” (worked until 1987 – Main Seam).

Two major subsidence events have occurred within the area of Westfalen No. 3, the first on 7 December 1988 and the second on 25 April 2008. The Department of Employment, Economic Development and Innovation (DEEDI) and the Department of Infrastructure and Planning (DIP) of the Queensland Government are investigating the possibility for remedial treatments to control (e.g. prevent or minimise) further surface subsidence within the Collingwood Park suburb where it sits above the workings of the New Redbank and Westfalen Collieries. DIP/DEEDI commissioned CSIRO Earth Science and Resource Engineering (CESRE) to provide technical assistance for these investigations and to utilise CSIRO’s expertise and technologies in ground subsidence control. This report outlines the study that CSIRO has conducted to assist DIP/DEEDI in developing optimal scenarios for controlling and minimising future subsidence.

Working closely with the DEEDI and DIP key personnel and their associated consultants and contractors, the following studies, as planned in the original project proposal, have been completed:

- Small scale 3D seismic survey and analysis – to map underground failure boundaries and geological structures
- Design, technical supervision and data analysis of site investigation – to assess the current conditions of the mines
- Microseismic system installation, monitoring and data analysis – to monitor future rock mass movements and failures
- 3D geotechnical modelling and pillar stability assessment – to understand the stability of the pillars and panels (a “panel” is a group of bords and pillars).
- Risk assessment of future subsidence – to assess the risk of further subsidence
- Investigation of remediation scenarios – to recommend possible remediation plans and actions influenced by budget and cost constraints
- Grout tests and design – to find the best grout material and placement mechanism for backfilling.

The key findings from this study are summarised as follows.

3D seismic survey

A trial 3D seismic survey was carried out at Collingwood Park. The objective of the survey was to demonstrate the feasibility of 3D seismic surveys for identifying and locating areas of pillar collapse, subsurface structures and features such as faults and old mining workings.

The field work component of the trial 3D seismic survey was conducted during the period of 19-23 October 2009 in an area including part of the 2008 subsidence area and adjacent unaffected area. The seismic data were collected and processed by Curtin University using CSIRO's specifications. From CSIRO's analysis of the seismic data, the following observations and remarks are made:

- The location of the "Waterline fault" is confirmed by the 3D seismic data. According to the seismic data, this is a normal fault dipping to the south-west with a vertical displacement varying from 3 m to 13 m. This observation is consistent with the mine managers' recent description of their experiences at the mine during 1970s.
- Caving related to the subsidence event can be identified from seismic data based on the quality and characteristics of seismic reflections from the subsidence and non-subsidence zones. The mapped failure area at the seam level is larger than the subsidence boundary on the surface. The estimated angle between the failure boundary and the vertical depth axis is about 21°.
- The failure area at seam level interpreted from the 3D seismic data provides important information on the extent of the failed pillars. Based on this interpretation, it is likely that the zone of pillar failure at seam level has extended across the Waterline fault to the north-east. Boreholes drilled after the 3D seismic survey also support the suggestion that pillar failure may have been extended to the eastern side of the Waterline fault.
- The underground workings/roadways could not be imaged with these seismic data. The possible reasons for this were: 1) Poor original data due to surface and traffic noises; 2) Insufficient energy generated by the weight-drop source; 3) Dominant (i.e. average) data frequency of 30 Hz was not high enough; 4) Width of roadways within the workings (about 5m) was too small when compared to the generated seismic wave length of about 86 m (i.e. 2600/30).

Geotechnical investigation and monitoring

The main objective of the geotechnical investigation and monitoring programme was to provide additional data on geological, geotechnical and mining conditions to help understand the causes of the 2008 subsidence event and then develop an optimal remediation scenario.

Drilling

A total of 15 open and cored holes were drilled in Westfalen No. 3 and New Redbank Collieries. Most of the holes drilled in Westfalen No. 3 Colliery ended in the intended target (roadways or pillars). This indicates that the mine plan available is reasonably accurate. The mining heights obtained from this drilling programme are generally consistent with those previously reported from various sources.

Two boreholes were drilled into the New Redbank Colliery and they encountered large irregular voids. It is likely that the investigated section of the mine has collapsed in the past.

Piezometers and extensometers

Three piezometers were installed across the two mines. The monitoring results until September 2010 indicate that the water level in New Redbank Colliery is stable at 83m below sea level. The water level in Westfalen No. 3 is at 108m below sea level in September 2010 and is increasing at a rate of about 11m/year.

One 20-anchor surface extensometer was installed in Hole CP_O07 at the central panel or region with relatively small pillars. The limited monitoring results until 24 September 2010 indicate that there was a 8mm movement in the overburden strata during a period of 47 days. It may indicate that the ground in the borehole vicinity is likely to be moving or “creeping” which could lead to a future subsidence event. We recommend the following actions be taken: 1) Install two additional extensometers close to either ends of the Central Panel to determine the size of the area with movement; 2) Install one additional geophone station close to CP_O07 to help detect and locate small seismic events in the Central Panel; 3) Continue the weekly data analysis and, if significant increase in the rate of displacement and seismicity is observed, increase the data analysis frequency (both extensometer and microseismic data) to a minimum of twice a week; and 4) DEEDI considers developing a response plan for any potential subsidence events.

Water

Four sets of water samples have been collected in the past five months from the two mines. The results of chemical analysis show that the water in both mines is typical “old” aquifer water that may not directly linked with the surface fresh water. It is believed that the aquifer water is continuing to flow into the mines, causing the water level increase in Westfalen No. 3 Colliery and a noticeable water chemical change with time.

An analysis was carried out to understand the effect of mine water on the 2008 mining induced subsidence event. It was found based on the drill hole data that, at the time of the event, the mine water level in Westfalen No. 3 Colliery was unlikely to have reached the key area of subsidence. However, the effects of water on pillar strength and panel stability should not be underestimated as past experience in geotechnical engineering shows that ground water can play a key role in rock mass instability. Further investigations on water effects are required.

Gas

Two sets of gas samples were collected and tested from Westfalen No. 3 Colliery. The mine gas contains 17-18% methane (CH₄), 10% carbon dioxide (CO₂) and 71% nitrogen (N₂). The oxygen (O₂) content was 0.5-0.6% in April 2010, but it was increased to 1.1% in July 2010. The risk of underground gas explosion is low at present due to the very low oxygen content. However, because the methane content is close to the explosive range of 5-15%, this risk should not be ignored as the oxygen content is currently increasing and any further subsidence events could accelerate the oxygen increase rate. Further gas monitoring and studies are hence required.

Microseismic monitoring

A CSIRO microseismic monitoring network with three seismic stations was installed at Collingwood Park and all seismic sensors and data recording instruments have been in good working condition.

The objective of the microseismic monitoring network is to detect and locate any ground fracturing at the Collingwood Park above the abandoned Westfalen No. 3 Colliery, and hence provide indication for future failure events, if any. It is also aimed at providing evidence of ground stability or instability in both subsided and non-subsided areas at Collingwood Park.

The monitoring system was calibrated through firing small explosive shots on 3 June 2010. All of the shots were clearly recorded by the system. The shot data were used to determine geophone orientations and provide data to calibrate a ground velocity model for seismic event location.

Data recorded from 1 July to 5 September were manually processed. During this period, the three stations recorded more than 2,000 trigger events. Most of the triggers are associated with moving vehicles. Only 50 events were recognised to be induced by ground movement.

The 50 seismic events were all observed at station S1 (near Collingwood Drive). No seismic event has been identified on the records of stations S2 (near the church) and S3 (at Cnr Duncan St. and Herman Av.). None of the events that triggered S1 were also recorded by S2 and S3.

Few events were recorded from May to June 2010. It appears that there is a tendency of increasing seismicity from July. Most of the seismic events are weak.

Seismic particle motion analysis indicated that ground instability may exist either northeast or southwest to borehole S1, at a distance less than 200m. The extensometer borehole CP_O07 is located east of S1 at a distance of about 300m. Unfortunately, the locations of these events cannot be determined due to insufficient number of geophone stations.

The microseismic results appear to support the extensometer monitoring results, and both indicate a ground movement in the Central Panel (located adjacent to and north-east of the 2008 event).

Numerical modelling and pillar/panel stability assessment

CSIRO carried out a systematic numerical study to determine strength and stability of pillars with common shapes and dimensions found in Westfalen No. 3 Colliery. The effect of backfill on pillar strength and stability using both cohesive fill material (fly ash and cement) and non-cohesive material (fly ash) was investigated. Following this fundamental study, large scale 3D numerical models were built to simulate the 2008 subsidence event and investigate the panel stability in an area of Westfalen No. 3 Colliery considered to have higher risk of failure than other areas.

The key findings from the pillar stability investigation are summarised below.

- Coal pillar peak strength and post-peak residual strength were estimated for pillar shapes common in Westfalen No. 3 Colliery. Of specific interest was diamond shaped pillars. It was found that the effective width of diamond shaped pillars can be estimated by the hydraulic radius analogy (i.e. effective width = minimum width).
- It is predicted that pillars exhibit strain-softening behaviour at a width-to-height ratio below approximately 5 and strain-hardening above this value. This is in agreement with field observations by Das (1986) in Indian mines. The residual strength of a pillar has been estimated from these models and the results have been used in estimating panel stability where stress transfer from yielded pillars to their neighbours is critical.
- Backfill is predicted to increase pillar strength. The percentage of strength increase is found to depend on the roadway fill percentage. For example, as displayed in the following table, the percentage of strength increase from 0.5MPa cohesive fill for a 20m x 20m square pillar with a height of 7m is 39% at a 60% backfill, and 57% at 90% backfill.

% roadway fill	Non-cohesive backfill	0.5 MPa cohesive backfill
	% strength increase	% strength increase
60	13.5	38.8
70	18.3	43.2
80	20.8	47.4
90	29.1	57.2

The key observations from the 3D numerical models of mining panels include:

- The mine panel in the 2008 event model is predicted to fail where the pillar height is 9m.
- The panel in the central region adjacent to the 2008 event is predicted to be 20% stronger than the panel that failed in the 2008 event.
- Effect of backfill on panel strength is predicted to be similar to that on a single pillar.
- With an 83% backfill in the 2008 event model, the predicted maximum surface subsidence from a forced failure is approximately 220mm.
- Stresses in the pillars surrounding the 2008 subsidence area are predicted to be elevated above the *insitu* level. The zone of influence is predicted to extend a horizontal distance of approximately 80m from the edge of the failed panel. The central panel (identified as the high risk panel located adjacent to and north-east of the 2008 event) is likely to be affected by the 2008 subsidence due to elevated stresses from the failed panel.

Hazard mapping and risk assessment

Some of the undermined residential areas at Collingwood Park may have a high risk of future subsidence. To assist the risk management process, an attempt was made to map and identify areas with a high likelihood of future subsidence. This exercise was limited to the Westfalen No. 3 Colliery within the given study area in Collingwood Park, where detailed information about the mining geometry and condition is available. No such attempt was made for the New Redbank Colliery due to the limitation in information available about this mine.

In mining terminology, the *Factor of Safety* (FoS) is a measure of stability, defined as the ratio of the maximum strength of a pillar to the load applied to the pillar. A low FoS implies a high risk of mechanical failure. If the calculated FoS is lower than the requisite value, a pillar may fail, triggering overload of neighbouring pillars, leading to roof failure and caving of rock above pillars into the previously excavated roadways or mine voids, and ultimately ground subsidence.

The key results from this investigation are listed below.

- Hazard maps were created by estimating Factors of Safety (FoS) for every pillar based on the pillars depth-of-cover, mining height and unique size attributes. Pillars interact with each other by shedding load from failed pillars to adjacent pillars, reducing the FoS of these pillars. The amount of load shed by a 'failed' pillar is dependent on its width-to-height ratio.
- Hazard maps produced in this study predict a pillar FoS less than 1.0 in the two regions that subsided in 1988 and 2008 for an "after-mining" case. This agrees with the actual observation.
- Four remediation strategies were analysed; the first is a "Status Quo" approach, the second involves targeted cohesive backfill of 0.5MPa strength in the central panel and the third and fourth approaches involves total backfilling with cohesive and non-cohesive fill respectively.
- From CSIRO modelling calculations, the Factors of Safety (FoS) of the pillars in the central panel, located from Strachan Ct and Heysen Ct in the north extending southeast to Duncan St and beyond, are predicted to be mostly less than 1.4, which is considered to be too low to warrant long term stability.
- Non-cohesive backfill to 90% roadway height is predicted to raise FoS in the central panel to above 1.6, which is the number often used in rock engineering design for long term stability. A cohesive backfill with uniaxial compressive strength of 0.5MPa is predicted to raise FoS to greater than 2.0 in the central region.

Consequence maps have been created to estimate the amount of surface subsidence and surface tilt based on empirical formula modified by observations from the site and numerical models. It is predicted that if pillars were to fail after backfilling roadways to 90% (regardless of the fill material) the surface subsidence would be less than 200mm and the surface tilt less than 5 mm/m. Overall tilts in buildings less than 5 mm/m would generally have negligible impact on building structures (Mine Subsidence Engineering Consultants, 1997)

Laboratory tests and injection material recommendation

A set of laboratory experiments were conducted using fly ash and crusher dust supplied by Swanbank Power Station and Keller's batching plant at the Ipswich Motorway Upgrade construction site respectively. These experiments were conducted to establish the properties of potential slurry fill materials. The properties examined included: viscosity and consistency; stiffness and strength (both under undrained and drained and consolidated conditions); long term stability of deposited material; cohesive and non-cohesive behaviour when used with or without cement, liquefaction, cementation, sedimentation, settlement and deposition rate, erosion, bleeding, segregation and dispersion due to water and dynamic loads. In addition to these tests of material properties, extensive flume tests were conducted by the University of Queensland (UQ) to investigate the fly ash slurry flow, deposition and beach profile behaviour. Strength tests have also been conducted on hardened, dried, cohesive mixes as well as standard soil mechanics tests.

From these laboratory studies, CSIRO's recommendation for backfilling a confined mine void structure is a *non-cohesive slurry mixture* of fly ash and water mix using 50 to 60 % solids by weight concentration. The injected non-cohesive fly ash will consolidate with time and becomes stiffer, harder and denser by the gradual drainage and dissipation of excess water accumulated in its pores. During the consolidation process, the friction angle of the confined consolidated fly ash can increase to close to 40 degrees and its hydraulic conductivity can reduce to less than one micrometre per second. Under high loads fly ash can be compacted and consolidated so that it only has 10% maximum moisture content.

A closed, confined, consolidated fly ash would not only provide sufficient confinement to the previously failed pillars and prevent them from further failure and collapse, but also would minimise any further ground subsidence by filling 90% or more of the voids left in the underground workings of the West Falen No. 3 Colliery. However, in the lack of a closed or confined void structure, sealed barrier walls would need to be built using cohesive slurry, in which cement and crusher dust has to be added to the mix as well. These are similar to the cohesive mixes used in the Ipswich Motorway Upgrade underground backfilling project.

Recommendation of remediation scenario and further work

Based on the investigation results and technical feasibility studies from the current DIP/CSIRO project, we recommend the *Non-cohesive total backfill* approach for Collingwood Park mine remediation

This scenario is also called "Complete non-cohesive backfill". All the mined areas between Collingwood Drive and Lawrie Drive/Namatjira Drive should be backfilled using non-cohesive fill material (pond ash from Swanbank Power Station and water). Barrier walls should be built along Lawrie Drive/Namatjira Drive using cohesive grout, the same as that used for the Ipswich Motorway Upgrade project, to stop grout escaping to other regions of the mine. The void filling ratio is expected to achieve a

minimum 90%. With this backfill, the mine panels are estimated to retain long term stability. In the unlikely event that panel instability still occurs, the ground subsidence is expected to be reduced to less than 0.2m and the surface tilt less than 5 mm/m. Overall tilts in buildings less than 5 mm/m would generally have negligible impact on building structures (Mine Subsidence Engineering Consultants, 1997).

The major advantage of the non-cohesive mix over the cohesive mix is that its properties do not change rapidly with time and can penetrate more reliably into smaller voids. This reduces the number of holes needed to be drilled for filling when compared to a cohesive mix. Flowability tests indicate that 90% fill of the mine voids should be achievable, particularly and preferably with a non-cohesive mix.

It is recommended that further work as listed below should be conducted to ensure a successful remediation operation. Details of the recommendations are given in Chapter 8.

For remediation of Westfalen No. 3 Colliery

Six key tasks are identified and should be carried out to ensure a successful remediation operation using the non-cohesive backfill:

- (1) Expand the existing monitoring network in Collingwood Park by installing two additional extensometers and one micro-seismic station above the Central Panel of the former Westfalen Number 3 Colliery.
- (2) Conduct a large-scale laboratory modelling of backfill.
- (3) Conduct a full-scale field test of roadway backfill.
- (4) Conduct a focused study to quantify the effect of rising water in Westfalen No.3 on the ground stability.
- (5) Investigate and monitor groundwater flow and chemical transport during and after fly ash backfilling
- (6) Continue ground monitoring and data analysis, including gas, in Collingwood Park.

For remediation of New Redbank Colliery

The information available to date for New Redbank Colliery is very limited and does not provide CSIRO with sufficient confidence to develop and recommend a feasible remediation solution.

It is therefore recommended that a three dimensional seismic survey be carried out in this region to determine the extend of the mine collapse. Depending on the findings from the seismic survey, further site investigations for remediation recommendations may or may not be required.

Important note

This study is based on the most up-to-date information and the best knowledge available to project team. A number of assumptions and novel geotechnical assessment methods have been employed, which may not have been sufficiently validated due to the limited data and time available. It is strongly advised that users of the results contained in the report should be aware of the limitations. If any doubt, clarification should be sought from CSIRO.

1. INTRODUCTION

During various stages in the 19th and 20th Century, the “bord and pillar” method of underground mining was implemented in a number of mines throughout the Ipswich area, including two mines operated in the vicinity of Collingwood Park, the “New Redbank Colliery” and the more recent “Westfalen No. 3 Colliery”. Two subsidence events occurred in Collingwood Park in 1988 and 2008 respectively, both in the mined region of Westfalen No. 3 Colliery. A brief description of mine history and the subsidence events are given as follows.

1.1 New Redbank Colliery

In the Redbank area, coal was first encountered in a prospecting shaft in 1913 which led to the establishment of the New Redbank Colliery on the site that now contains the Redbank Plaza shopping centre. New Redbank Colliery operated until 1932 and is located below Mine Street, Redbank Plaza and Namatjira Drive. The coal was extracted from a 15m thick coal seam (called the ‘Main Seam’) with about 6.5m of workable coal. The northern section of the mine was worked in three sections of approximately 1.8m high each, called the top, middle and bottom workings.

Available mine layout plans from 1920s indicate that several sections overlapped leading to the presence of up to three levels of workings at the same location. In the southern section of the mine, however, coal was generally extracted from only one level. The workings in New Redbank Colliery are expected to have a depth of cover of between about 70m in the north and 120m in the south.

1.2 Westfalen No. 3 Colliery

In 1965, the Westfalen Company took up the Authority to Prospect over the area of the New Redbank Colliery and the area to the south. The Department of Mines began drilling in October 1965 and continued exploration until August 1969.

Westfalen No. 3 Colliery was operated between late 1960s until 1987 and it extends over a much larger area compared to the New Redbank Colliery. It extends over the eastern, western and southern side of New Redbank Colliery with the Redbank Fault and a large safety barrier separating the two mines.

The North Eastern part of the Westfalen No. 3 Colliery, called the septum area (close to Ipswich Motorway, and away from Collingwood Park), was worked at two levels, separated by a septum (rock layer) of 2 to 5m thick and is present at depths of 60 to 90m below ground surface, with the total working height ranging between 5 to 15m. Original pillars in the septum area were typically 25 to 30m squares and these are believed to have been split while retreating from the mines in order to extract more coal, thus leaving rectangular pillars of 10 to 11m width and 25 to 30m length.

The main section of the mine (including beneath Collingwood Park) was believed to have been worked at only one level with the working heights ranging between 3m and

11m. Most of the pillars were in a diamond or square shape with sides ranging between 20m and 30m and the roadways between 5m to 7m wide.

The mine was flooded in 1974 and the upper parts of the mine workings were damaged. After the 1974 floods, the mine was pumped out and mining recommenced. Mining continued on the eastern side of Goodna Creek until 1987 when the mine was closed.

1.3 Mine subsidence events

Two mine subsidence events have previously occurred in Collingwood Park, the first on 7 December 1988 and the second on 25 April 2008. Both occurred in the areas underlain by Westfalen No. 3 Colliery and have been attributed to the failure of the coal pillars. The surficial extent of the two subsidence at Collingwood Park is shown in Figure 1–1.

1988 subsidence incidents

On 7 December 1988, the Department of Mines was notified of alleged ground subsidence in the general area bounded by Lawrie Drive, Milgate Street, Reerden Street and McBay Street. A reported up to 570 mm of subsidence was recorded by November 1989 from the survey conducted after the initial subsidence. The total subsidence was estimated to be around 1.7m. A number of slab-on-ground houses were damaged, with a number of houses damaged beyond repair and consequently demolished.

2008 subsidence

On 25 April 2008, a ground subsidence event occurred in an area near the intersection of Duncan Street, Moloney Street and McLaughlin Street. The maximum total subsidence was estimated to be around 1.4m. It is reported approximately 30 to 40 houses within the immediate subsidence area were damaged to varying degrees and many houses were damaged beyond economic repair and were demolished.

1.4 Scope of this study

The Department of Employment, Economic Development and Innovation (DEEDI) and the Department of Infrastructure and Planning (DIP) of Queensland Government are investigating the possibility for remedial treatments to control (e.g. prevent or minimise) further mine related surface subsidence within the Collingwood Park suburb where it sits above the workings of the New Redbank and Westfalen No. 3 Collieries. DIP commissioned CSIRO Earth Science and Resource Engineering (CESRE) to provide technical assistance for these investigations and to utilise CSIRO's expertise and technologies in ground subsidence control. This report outlines the work that CSIRO has conducted to assist DIP/DEEDI in developing the optimal scenarios for controlling and minimising future subsidence.

Working closely with the DEEDI and DIP officers and their associated consultants and contractors, the following studies, as planned in the original project proposal, have been completed:

- Small scale 3D seismic survey and analysis – to map pillar failures and geological structures
- Design, technical supervision and data analysis of site investigation – to assess the current conditions of the mines
- Microseismic system installation, monitoring and data analysis – to monitor future rock mass movements and failures
- 3D geotechnical modelling and pillar stability assessment – to understand the stability status of the pillars and panels
- Risk assessment of future subsidence – to assess the risk of further subsidence
- Investigation of remediation scenarios – to recommend possible remediation plans and actions influenced by budget and cost constraints
- Grout tests and design – to find the best grout material and placement mechanism for backfilling.

This report describes the details of the above studies and their results. The present report is focused only on the Westfalen No. 3 Colliery, where detailed information and data are available from the past and current investigations. The data sets available for the New Redbank Colliery are very limited and insufficient for developing a detailed remediation plan. Further investigations for New Redbank Colliery are required.

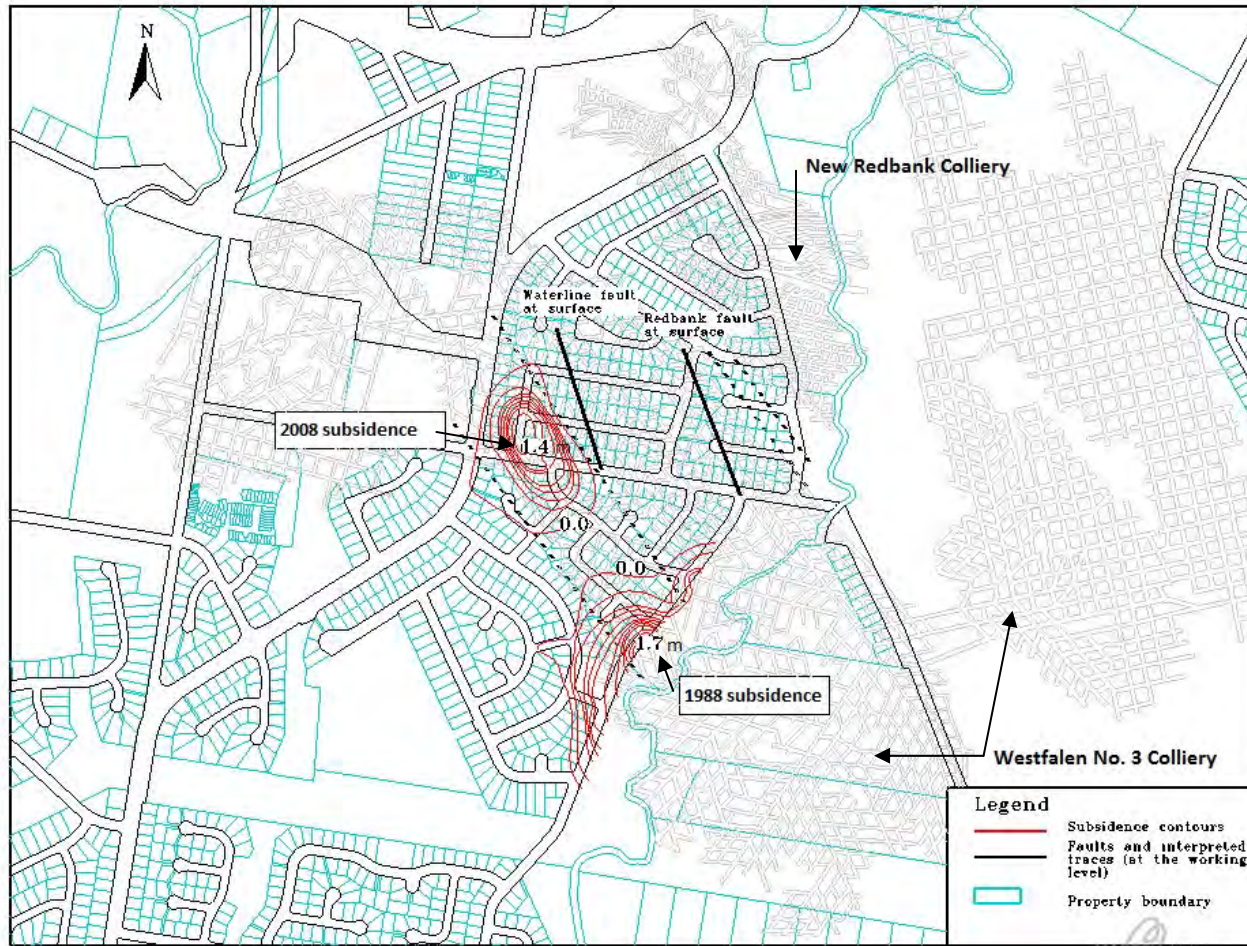


Figure 1-1 Location of two subsidence events in Collingwood Park.

2. 3D SEISMIC SURVEY

2.1 Summary

2.1.1 Project objectives

A trial 3D seismic survey was carried out at Collingwood Park as part of this study. The objective of the survey was to investigate the feasibility of 3D seismic surveying for identifying and locating pillar collapse, subsurface structures and features such as faults and old mining workings. This chapter reports the outcomes of this trial 3D seismic survey.

2.1.2 Outcomes

The field work component of the trial 3D seismic survey at Collingwood Park was conducted during the period 19-23 October 2009 in an area that included part of the 2008 mine subsidence area as well as adjacent unsubsidised ground. The seismic data were collected and processed by Curtin University according to CSIRO's specifications. From our analysis of the seismic data, the following observations and remarks are made:

- The signal-to-noise ratio of the acquired seismic data was generally low, due to traffic noise and the low energy of the weight-drop method, which had to be used as the seismic source in the residential area. The processed seismic data were of reasonably good quality in the unsubsidised areas, but relatively poor in the subsidised region. This observation is consistent with Velseis' (1989) results from their 2D seismic survey in the area that subsidised in 1988.
- The location of the "Waterline fault" was confirmed by the 3D seismic data. According to the seismic data, this is a normal fault dipping to the south-west with a vertical displacement varying from 3 m to 13 m. This observation is consistent with the mine managers' recollections of their experiences at the mine during 1970s.
- A normal fault disturbance (dipping to the north-east) is observed in the north-east corner of the survey area from the seismic data. This fault may be associated with the nearby Redbank fault and may explain why this zone has not been mined. The fault properties cannot be reliably determined from the seismic data due to the poor quality of the data on the edge of the survey area.
- Caving related to the subsidence event can be identified from seismic data based on the quality and characteristics of seismic reflections from the subsidised and unsubsidised zones. The seismic data can be used to map out the subsidence boundary at the ground surface and this mapping matches well with the boundary measured in the field. In addition, the seismic data can also be used to map the failure boundary at the seam level. The mapped failure area at the seam level is larger than the subsidence boundary on the surface. The estimated angle between the subsidence failure surface and the vertical axis is about 21°. This angle may

vary from location to location. This subsidence surface area due to bord and pillar mining method is different from subsidence pattern observed in long wall mining, where the area of ground surface subsidence is normally greater than the associated void area at the coal seam level.

- The projected failure area at seam level provides important information on the extent of the failed pillars. Based on the seismic interpretation, it is likely that the zone of pillar failure at seam level has extended across the Waterline fault to the north-east. Drill holes drilled after the 3D seismic survey also support the suggestion that pillar failure may have been extended beyond to the east side of the Waterline fault.
- The underground working/roadways could not be imaged with these seismic data. The possible reasons for this were: 1) Poor original data due to surface and traffic noises; 2) Insufficient energy generated by the weight-drop source; 3) The dominant frequency of 30 Hz was not high enough; 4) The width of the mine workings (about 5m) was too small when compared to the generated seismic wave length of about 86 m (i.e. $2600/30$).

2.1.3 Recommendations

From the analysis of the seismic data, it is evident that seismic surveying can be used to map the zone where pillars have collapsed and to delineate geological structures in the Collingwood Park area. This study has shown that three dimensional seismic monitoring may be a useful technique to identify mine subsided ground at the New Redbank colliery and other regions of Westfalen No. 3 colliery outside of the current investigation area. It is recommended that:

- A further 3D seismic survey should be carried out in New Redbank Colliery area to identify areas where subsidence may have occurred in the past but not been recorded.
- A further 3D seismic survey should be conducted in the South-East part of Westfalen No. 3 (where the retirement village and two sport grounds are located) to determine if any underground panel failures have occurred.
- Better seismic sources need to be tested to increase the energy and frequency content range with the aim of getting better seismic resolution and seismic data quality.

2.2 3D seismic trial survey

The objective of the geophysical survey is to demonstrate the feasibility of 3D seismic surveying for identifying and locating pillar collapse, subsurface structures and features such as faults and old mining workings. This chapter discusses the results of this 3D seismic trial survey.

2.2.1 Survey site and survey design

A 2D seismic survey was conducted at Collingwood Park in 1989 after the 1988 subsidence event (Velseis, 1989). Two 2D seismic lines were acquired crossing the subsidence area by Velseis using MiniSosie as the seismic source. Good reflections from the Main Seam were obtained in the unsubsided areas, while poor reflections were observed in the subsided zone. This suggests that seismic methods can be used to understand subsurface features associated with subsidence events.

The small trial 3D seismic survey covers part of the 2008 subsidence area around Duncan Street as shown in Figure 2-1 and Figure 2-2, which is in the area of the abandoned Westfalen No. 3 Colliery. This 3D seismic survey area is approximately $390\text{m} \times 210\text{m} = 0.0819 \text{ km}^2$, which is considered to be close to the minimum area required for quality results. The surface is relatively flat with a gentle gradient towards the southeast, sub-parallel to the coal seam dipping towards the same direction. The survey covers the central part of the 2008 subsidence as outlined by the red contour in Figure 2-1 and includes part of a major fault (i.e. Waterline Fault), which might have had impacts on the distribution of the subsidence and ground stability. The trial 3D seismic survey was conducted in a relatively open area, as is evident by the aerial view of the survey site in Figure 2-2. There are only about 27 houses in this area, as shown in Figure 2-2, where three houses are currently owned by the Queensland government and one of them had to be demolished due to damage severity. In addition to the houses, there are also two major roads and 4 small streets in the survey area. This made it relatively easy to carry out the seismic field work in this low residential density area.

The 3D seismic survey was designed with the following desirable parameters:

- Shot Line Spacing = 30 m
- Shot spacing = 4 m
- Number of Shot Lines = 13
- Receiver Line Spacing = 30 m
- Number of Receiver Lines = 8
- Receiver spacing = 4 m
- Desired Survey Fold (repeated measurements) = 30
- Processed Bin Size (seismic grid size) = 2 m x 2m



Figure 2-2. Aerial view of the 3D seismic trial survey location from Google map



Figure 2-3. Basic 3D seismic survey layout of receiver and shot lines. The red/blue dots are the designed shot locations while the light-blue triangles are the receiver/geophone locations. The blue shot points are designed for repeating shots.

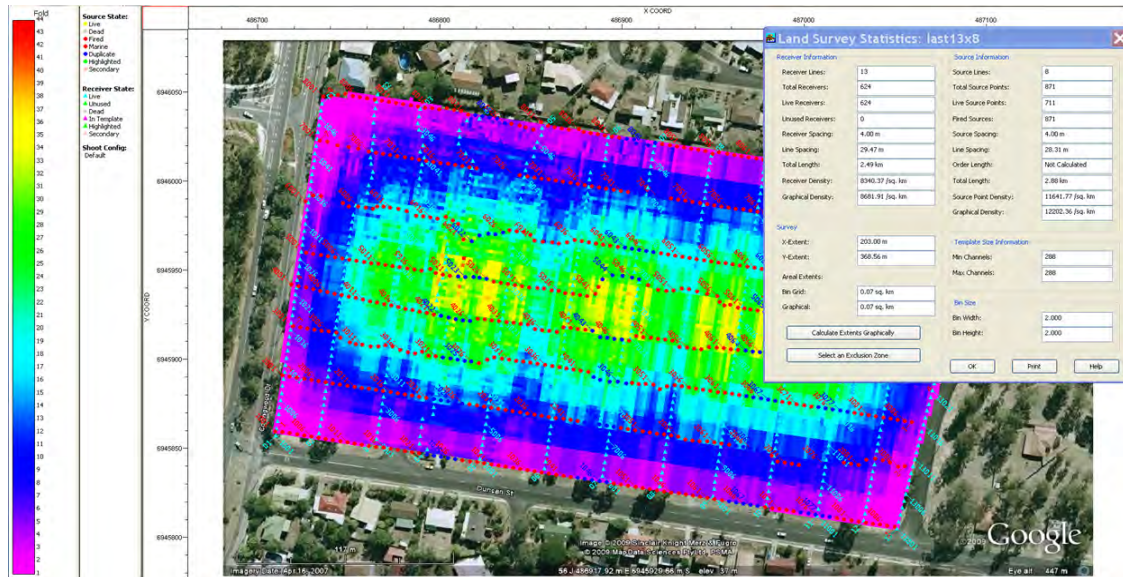


Figure 2-4. Final designed fold map with 6 active receiver lines and 4 moves of the receiver line.

2.2.2 Data acquisition

To run the seismic survey smoothly, we developed a process of support from engaged residents together with the government's coordination and assistance in key areas defined before the survey began. They are listed below.

- **The right to access back yards of the residential houses:** Backyard access was required for the most of the houses in the survey area as shown in Figure 2-2 and Figure 2-3. This was essential. The ideal survey design is on the straight lines. We had to have the access right to the residents' backyards for
 - Adjusting the designed survey lines and shot/receiver locations to the suitable positions around the houses
 - Pegging and surveying the actual geophone and shot positions
 - Planting necessary geophones around the houses
 - Making ground impacts (weight drop) to generate seismic waves.
- **Traffic control:** During the seismic survey, seismic crews were setting up recording cables across the streets and recording seismic ground vibrations generated by the manmade seismic sources. The local traffic is normally the main source of noise for seismic recording. There are also safety implications for the seismic crew during their working. To minimise the noise level and protect the seismic crew, traffic control were put in place by DIP/DEEPI during the survey period. The traffic control included
 - Slow-down the traffic for Collingwood Road and Duncan Street (see Figure 2-1 and Figure 2-2)
 - Close-down and slow-down other small streets for a given period during the day.

- **Overnight equipment protection:** Overnight protection for the equipment was essential. The survey required five days to complete, and the crew had to leave their installed equipment (geophones) on the site, without having to redo all the equipment installation preparations every morning.
- **Seismic source approval:** The seismic source was the accelerated weight drop. Although this seismic source generates minimum vibrations, their usage around the residential houses might raise some concerns from the local community and therefore we needed to seek approvals from the local authorities and residents. The liaison processes with local residents were carried out by DEEDI officers.
- **Pegging and surveying:** All shots and receiver positions were pegged and surveyed by Conics Surveying before actual seismic data acquisition.

The seismic data acquisition was conducted by Curtin University from 19-23 October 2009. A Seistronix' EX-6 distributed seismic system was used. The EX-6 is a high performance, distributed refraction/reflection seismograph designed for 2D and 3D seismic surveys. The system combines 24-bit A/D performance in a rugged six-channel box that supports 600 channels of real-time seismic data acquisition in single line operation, and up to 2400 channels on 32 lines in Multiline (3D) operation. The main elements of the EX-6 system are the Windows laptop running the EX-6 System Software, the EX-6 Acquisition Units (AU), Line Tap Units (LTU), AUX unit, and Line Interface Unit (LIU). AUs are connected together with eight-pair spread cables with six geophone takeouts between boxes and may be distributed arbitrarily around the LTU. New boxes are automatically recognised and addressed by the EX-6 System Software, making the system easy to expand. A radio triggering system was used between the seismic source and seismic recording system.

There were eight receiver lines laid out with 48 channels per line for this survey. Six active receiver lines with 48 channels per line were used in this 3D seismic trial survey as illustrated by Figure 2-5. The two spare receiver lines were used to speed up the field operation during rolling up the receiver lines. Figure 2-6 shows a few snapshots of the seismic survey. The actual seismic survey layout is presented in Figure 2-7 and the actual seismic recording parameters are listed in Table 2-1. The final fold map achieved by the survey is shown in Figure 2-8, which is consistent with the designed fold expectation – a nominal of 30 folds on average. The data acquisition was completed within the planned time.

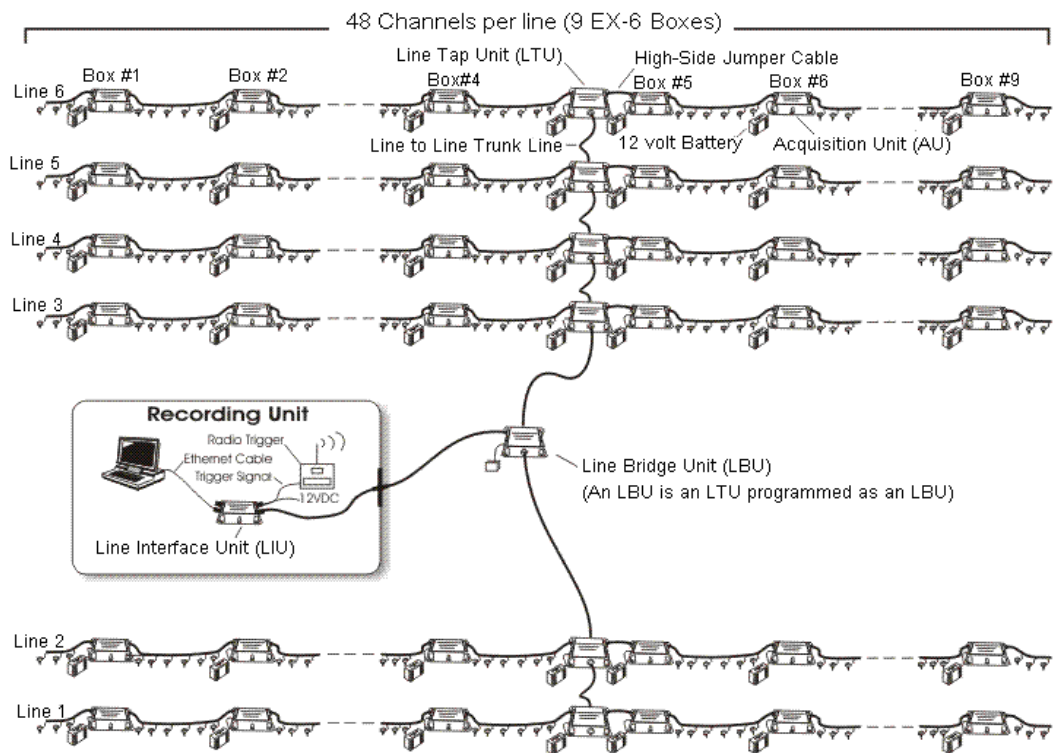


Figure 2-5. Illustration of the field layout for the Seistronix' EX-6 distributed seismic recording system for this 3D seismic trial survey at Collingwood Park.



Figure 2-6. Seismic surveying in action at Collingwood Park. Top left: the seismic team; Top middle: Shooting in the backyard with accelerated weight drop device Digipulse 120 AE; Top right: Seismic recording computer; Bottom Left: Line cables, Line Tap Unit, Acquisition Unit and Batteries; Bottom right: Seismic receiver line running across the road and geophones (next to the traffic cones) planted on the road.



Figure 2-7. The actual 3D seismic survey layouts of receiver and shot lines. The magenta dots are shot locations while the black dots crosses are the receiver/geophone locations.

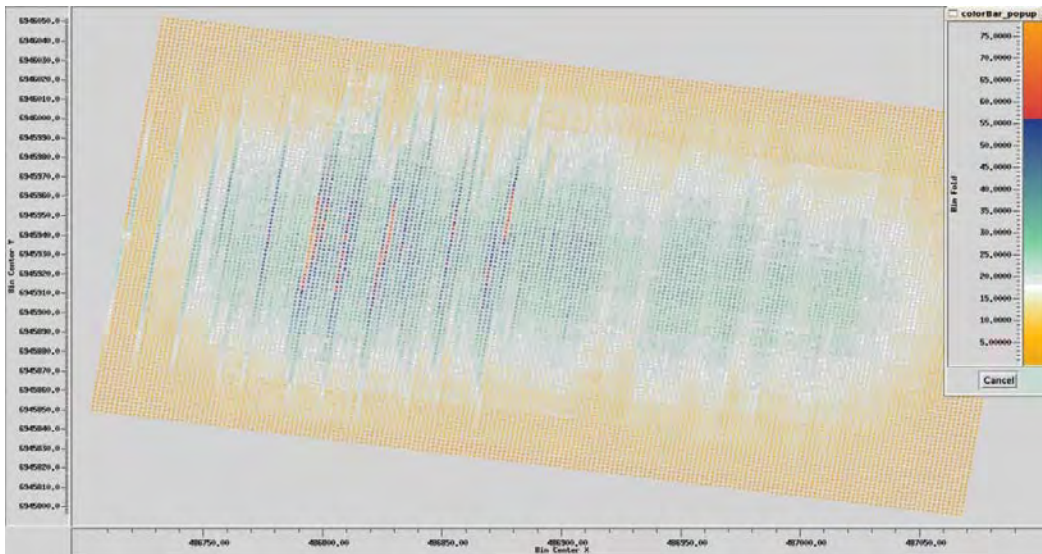


Figure 2-8. The actual fold map of the 3D seismic survey at Collingwood Park. A nominal of 30 folds in the middle part of the area is achieved as designed.

Table 2-1 Seismic recording parameters

Survey Grid Design	Orthogonal receiver and shot lines
Bin Dimensions	2 m x 2 m
C.D.P. coverage (fold)	30 fold (nominal)
Maximum In-Line Offset	120 m
Maximum X-Line Offset	210 m
Maximum Offset	241 m
Recording Patch	6 Receiver Lines x 48 Traces/Line (288 traces)
Shot Line Separation	~30 m
Shot Point Interval	4 m
Total number of Shot Points	798
Receiver Line Separation	~28 m
Receiver Point Interval	4 m
Total number of Receiver points	624
Shot point interval	4 m
Seismic Source	Weight drop
Number of live geophone channel	240 (5 receiver lines)
Geophone stringing array	Single geophone
Geophone element type	10 Hz geophone
Recording system	Seistronix EX-6
Number of Total Shots	1045

2.3 Data processing

The seismic data were processed by Curtin University with parameters specified by CSIRO. Figure 2-9 (a) shows a typical seismic shot record from Collingwood trial 3D seismic survey and its corresponding frequency amplitude spectrum is presented in Figure 2-9 (b). The data quality is relatively poor. The dominant frequency of the record is around 30 Hz, relatively low compared to a typical coal seismic frequency of about 70 Hz. The reason for this is the difference in the physical characteristics of the source, namely weight-drop vs explosive. From Figure 2-9, one can identify the direct wave, air wave, surface waves/ground-rolls and other noise, but one can hardly recognise the useful reflections from the target seam from these reading records. This makes it very hard, if not impossible, to interpret a useful seismic outcome from such records.

In general, these seismic shot records from the survey need to be converted into a much easier and more interpretable seismic data format, called stacked sections, such as the one shown in Figure 2-10, through seismic data processing using advanced mathematical algorithms and procedures in signal processing and noise filtering.

However, practical seismic data processing is both science and art. Too much filtering can cause damage to and loss of the actual signal. Hence, there are no well-established universal methods for processing such seismic data. Different data need different treatments, procedures, algorithms and parameters to process. The options depend on the quality of the data, nature of the objectives to be imaged, the algorithms in use and their corresponding parameters. In general, seismic data processing focuses on filtering, or de-convolution, to suppress random and coherent noise such as air waves and ground-rolls. In other words, this is a de-convolution process to increase seismic resolution by compressing the seismic wavelets, statics corrections to compensate for the effects of topographic variation and low velocity layers at near surface, and velocity analysis for normal moveout correction and migration for collapsing diffraction energies and moving the dipping reflectors to their correct spatial positions. These are the key processing procedures normally used for processing seismic data. In all these procedures, the static correction and velocity analysis are the critical stages of seismic data processing in a coal mining environment. The details of the basic seismic data processing techniques and procedures can be found in most text books on seismic data processing (e.g. Yilmaz, 2001).

After processing, the seismic frequency content was improved as shown by Figure 2-11. Using Fourier transforms, the dominant frequency is increased from the original ~30 Hz to ~50 Hz. The increase in seismic bandwidth and dominant frequency is mainly attributed to the surface-consistent de-convolution and the zero-phase spectrum whitening process used in the processing. This is a common practice in seismic data processing to improve resolution.

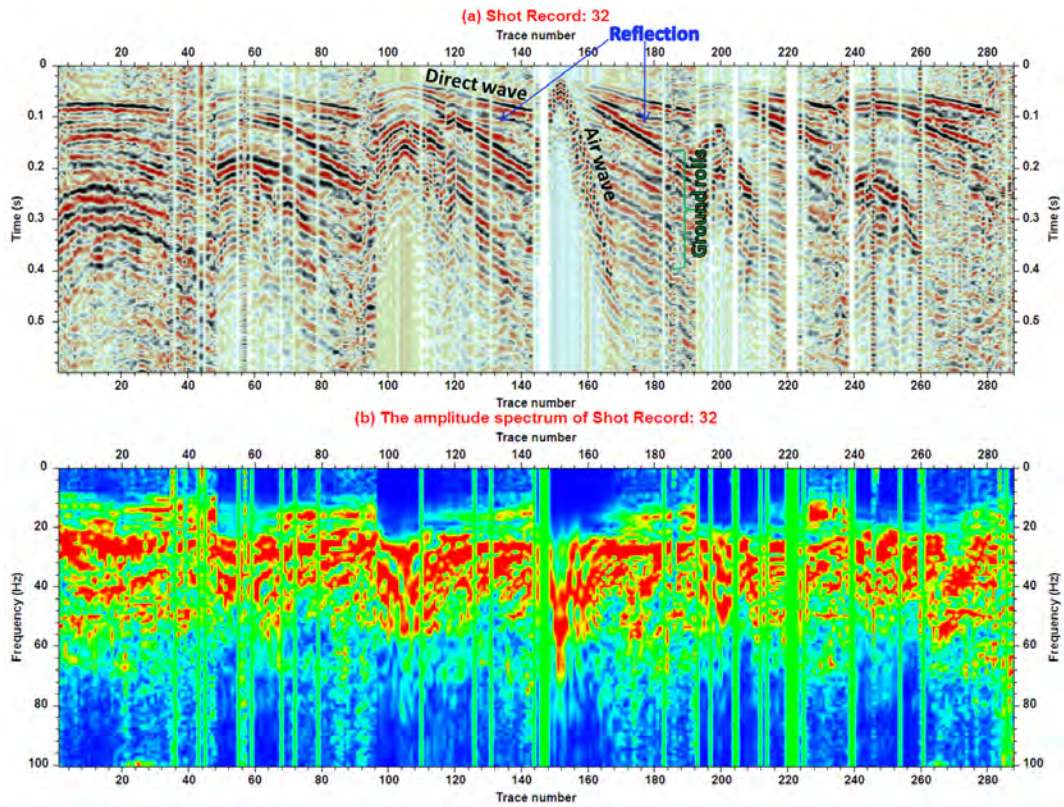


Figure 2-9. (a) A typical seismic shot gather from the Collingwood Park seismic survey; (b) The frequency amplitude spectrum of the shot gather in (a). The dominant energy of the data is in the frequency range of 20-50 Hz with a dominant frequency at 30 Hz.

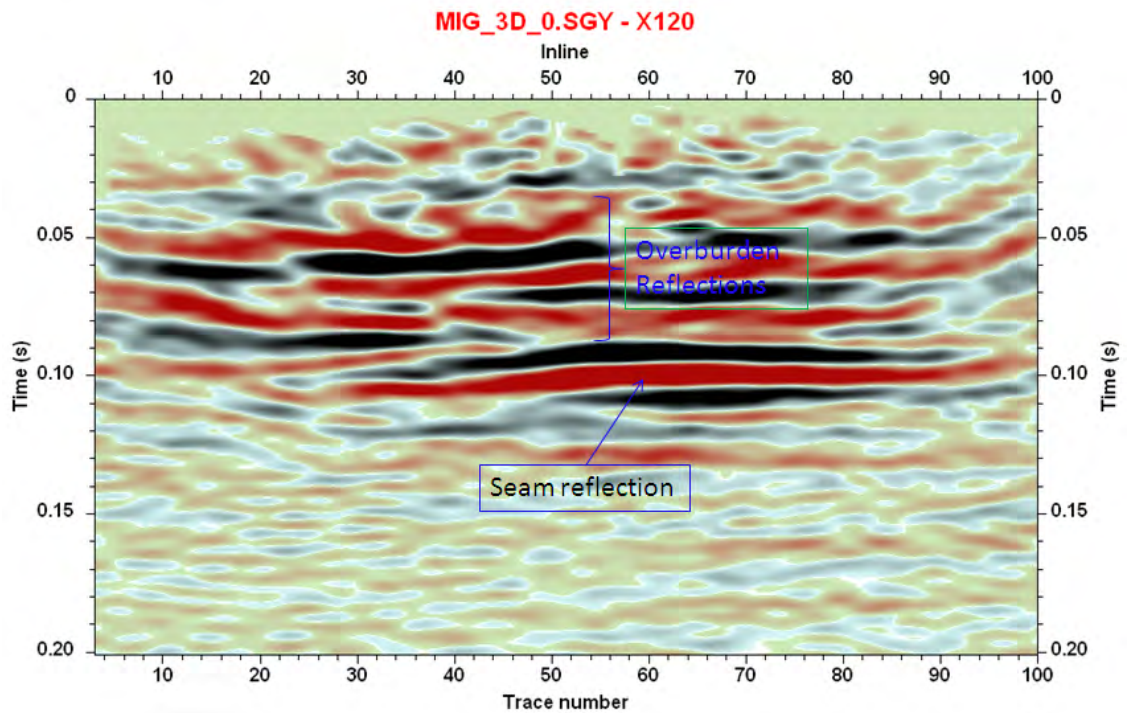


Figure 2-10. Processed migrated stack cross-section X120 from Collingwood Park 3D seismic trial survey, showing coherent reflections which are much easier to interpret than the shot record in Figure 2-9.

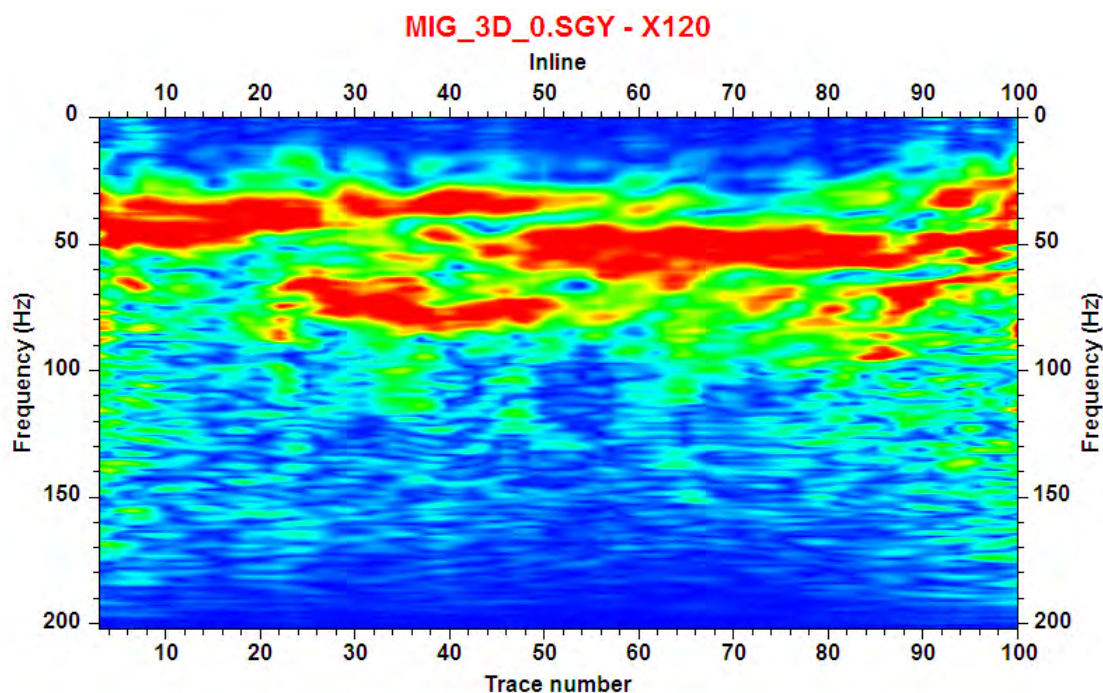


Figure 2-11. Frequency amplitude spectrum of the processed section in Figure 2-10. The frequency range of the processed data is 20-80Hz with a dominant frequency at 50 Hz.

2.4 Data analysis and interpretation

2.4.1 The “known” geology

Figure 2-12 shows the “known” geology in the 3D seismic trial survey area. The mined seam at the Duncan Street is part of the Triassic Blackstone Formation. It is called the Main Seam, which has an average thickness of 10m, as shown in the figure (140-130=10m). The seam depth relative to the surface elevation of 40m (the datum) is from 125m to 145m gently dipping towards the South-East or South. The Waterline fault, mentioned earlier, is reported to have a 0.5m displacement and runs from the NW to the SE. According to the mapped fault on the surface and at the seam level, this fault dips to the SW. Based on recent quotations from previous mine managers, the “Waterline fault” is a misleading name for this fault, as they had never noticed any water leaking out from this fault (at the time of mining). Furthermore, the fault was noticed to be a normal fault with much larger displacement than the nominated 0.5 m at the working location of the fault (note that they mined 6-8 m coal there). The mine managers also indicated that the fault is a scissoring fault, i.e. some locations have large displacements and some locations have small displacements. The subsidence on the surface is located on the west side of the Waterline fault. In addition to the Waterline fault, there is potentially another fault at the NE corner of the survey area as the underground workings are also not mined through and there is a fault line mapped in that general direction of the larger unmined barrier pillars.

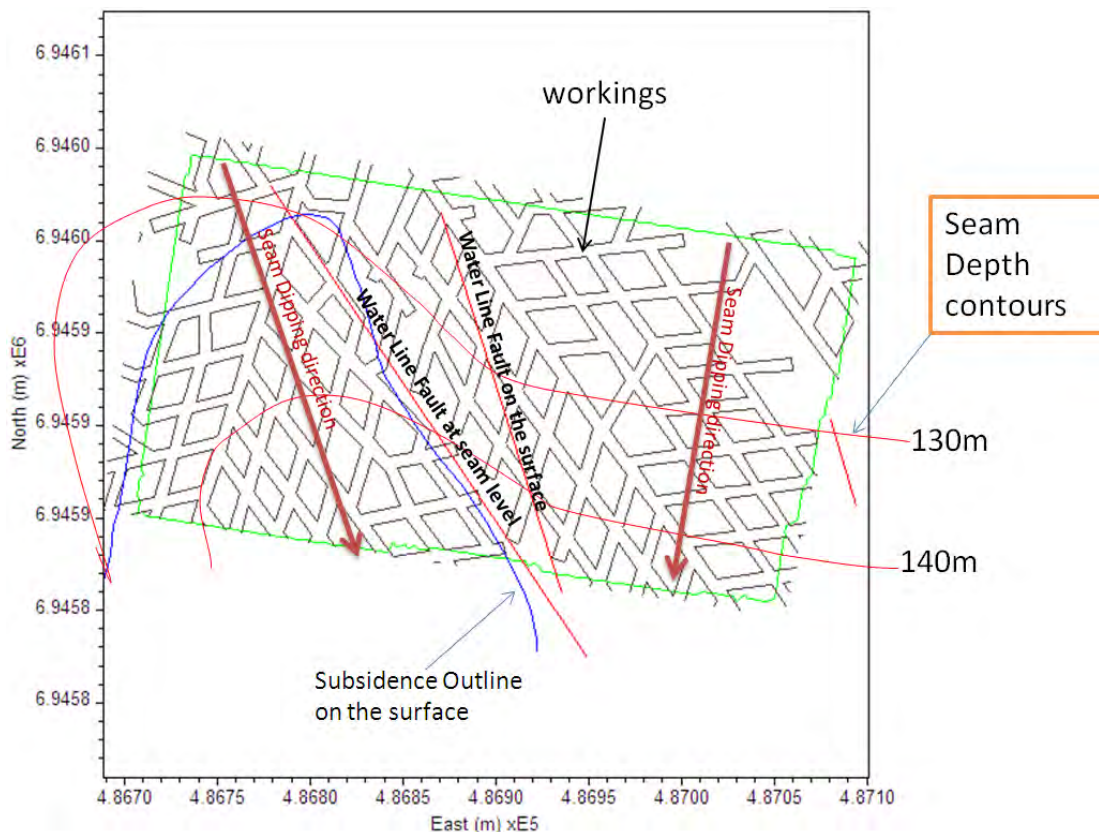


Figure 2-12. The “known” geological knowledge at the 3D seismic trial area.

2.4.2 Seam reflection identification

The first step in the interpretation is to link the target coal seam with reflections on the seismic section. This is normally done by stretching and correlating the geophysical logs from drilling or the synthetic seismograms with the seismic reflections on the section. The seam reflection could not be identified with such an approach as there were no geophysical logs available to help at the time of data processing. Fortunately, as pointed out before, the knowledge that the coal seam depth is about 130 m in the area. Due to the poor quality of the seismic data, only a single root-mean-square (RMS) stacking velocity profile as listed in Table 2-2 was used to process the seismic data onto a datum of elevation 40 m. According to this velocity profile, a 130 m deep coal seam will appear at ~100 ms (0.1 s) on a processed stack section with a stacking velocity of 2600 m/s. With this guidance, we can easily identify the seam reflections on the inline and the cross-line sections in Figure 2-13.

There are drill holes drilled after the seismic data were collected and processed. Drill hole CP_O11 at the intersection point of the two sections in Figure 2-13 was drilled through the coal seam – see the geophysical logs in Figure 2-14. The seam floor depth, relative to the datum (at elevation 40m) and based on the borehole collar elevation at 29.40 m, is 143.20 m. Assuming a wave velocity of 2600 m/s for the depth-to-time conversion, this leads to a seam floor two-way reflection time of 0.11 s (Two-way-time = $2 \times \text{Depth}/\text{Velocity}$, i.e. $2 \times 143.2/2600 \approx 0.11$ s) at this location, as marked by

the two light blue arrows on the seismic sections in Figure 2-13, which is matched with the actual seam reflection.

2.4.3 Pillar failure mapping

The data quality of the processed inline section IN051 (left top) in Figure 2-13 varies significantly from the poorly imaged seam at the left side (west side in the subsidence area) to the well imaged reflection at the right side (east side where no subsidence occurred). This observation is consistent with the 2D seismic survey data from Velseis (Dixon, 1989) in the subsided and unsubsidied areas associated with the 1988 subsidence event. This quality variation is attributed to the failure of pillars, which causes further fracturing or caving of the overburden strata, and hence increases the absorption and attenuation of the seismic waves. In addition, the collapsed underground pillars and workings make the coal seam less continuous laterally and so that it does not form a smooth strong reflector. Therefore, continuous, clear reflections of the coal seam boundary could not be obtained in this disturbed and collapsed zone. The purposely increased “fold” in the collapsed zone also did not help to resolve such wave reflection issues in poor reflective zones.

Figure 2-15 shows two examples mapping the collapsed zone in both subsided and non-subsided sections. It shows the contrast of the failure boundaries between the subsided and non-subsided areas from the inline and cross-line sections. The blue lines drawn on the section figures are the failure boundaries obtained from the seismic reflection contrasts. As indicated by the figures, the seismic reflections on the left side of the blue line are of poor quality, while those on the right are good and well imaged. Based on these contrasts, one can easily project the boundaries at the seam level (the yellow dots) and on the surface (the green and light blue dots) on to the seismic survey base map. As shown in the figures, the projected collapse boundaries on the surface, measured by the 3D seismic data, not only match the independently measured subsidence boundaries in the field, but also produced extra important information underground. It is worth noticing that the area of the surface subsidence boundary is not the same as that of the failure boundary at the seam level. The failure area at the seam level is larger than what was observed on the ground surface. Based on the mapped failure boundaries from the inline section IN064 and the cross-line section X080, it is estimated that there is an angle of about 21° between the failure boundary and the vertical depth axis. This angle may vary from location to location.

As stated before, the quality and strength of the seismic wave reflection from coal seam void is used as an indicator for pillar failure and caving. To map the failure boundary at the seam level, the coal seam reflection data have been identified and their amplitudes have been extracted and plotted in Figure 2-16. A failure boundary at the seam level is drawn by a thick blue curve, based on the seam reflection amplitude distribution. It clearly shows that the pillar failure effects on the surface and at the seam level are different. To verify the pillar failure boundaries with the observations from the seismic sections, two boundary locations, the two yellow dots of Figure 2-15, are re-mapped and plotted in Figure 2-16, showing subsidence at two levels of the mine. As

shown in the figure, these two yellow points sit almost exactly on the subsidence contour line at the seam level, i.e. the thick blue curve.

Results of Figure 2-16 suggest that the pillar failure has extended across a relatively larger area than what is evident on the ground surface from surface subsidence observations and measurements. Barrier pillar failure is possibly due to the existing Waterline fault running through these pillars. Also shown in Figure 2-16 are the locations of several drill holes drilled after the 3D seismic survey. Drill hole CP_C02 is located in the subsidence area; drill hole CP_O11 is in the extended failure area; and drill hole CP_O07 is in the area with no surface subsidence. Figure 2-17 shows the optical drill hole scan/Televue images from the drill holes CP_C02, CP_O11 and CP_O07. From Figure 2-17, it is evident that one can observe fractures from top to the bottom (above the coal seam) of drill holes CP_C02 and CP_O11 while one can hardly see any fractures in the borehole CP_O07. The similarity of the fracturing pattern in both drill holes CP_C02 and CP_O11 suggests that the pillars around drill hole CP_O11 may have already failed, which supports the hypothesis that the pillar failure has extended beyond the larger barrier pillars separating the two mined zones.

Table 2-2. Stacking velocity used during the data processing.

Two-way reflection time (ms)	RMS Velocity (m/s)
0.0	2150.0
50.0	2350.0
100.0	2600.0
130.0	2700.0
200.0	2900.0
400.0	3200.0

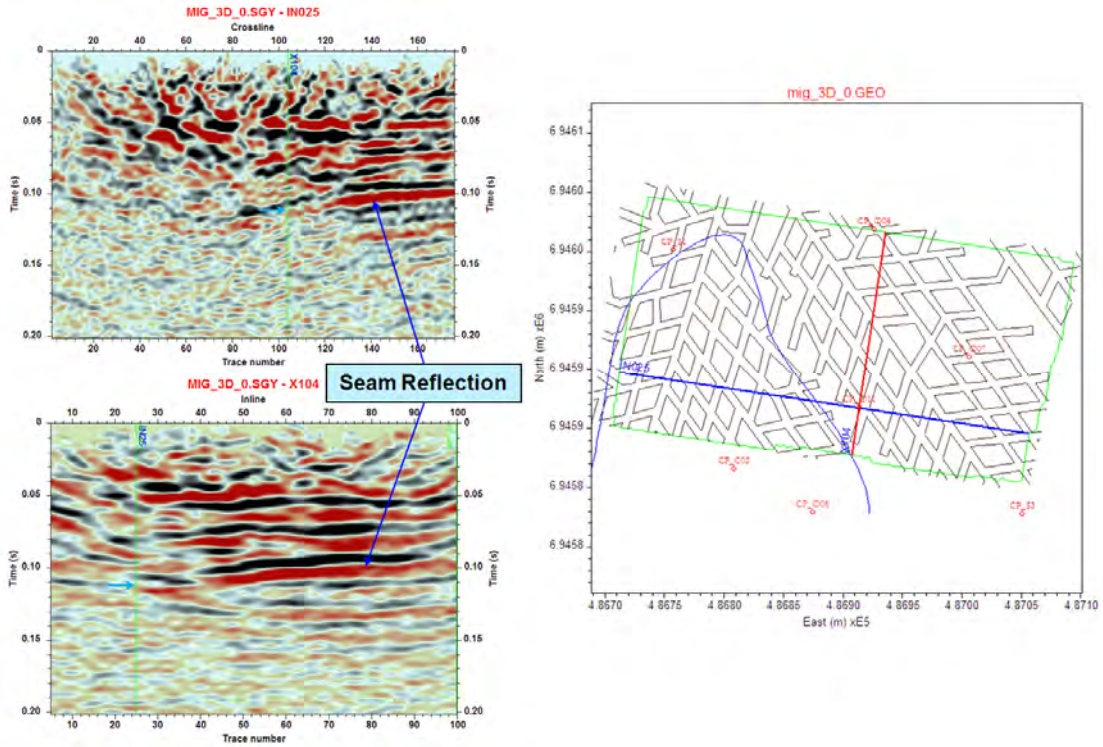


Figure 2-13. Identified seam reflection from the seismic data in two cross sections based on the reflection time and the average stacking velocity assumed during the data processing. The inline section (left top) runs from the west to the east and the cross-line section (left bottom) runs from the south to the north. The red dots indicate the boreholes drilled afterwards for further site investigation.

Geophysical Logs for CP_O11 at Collingwood Park

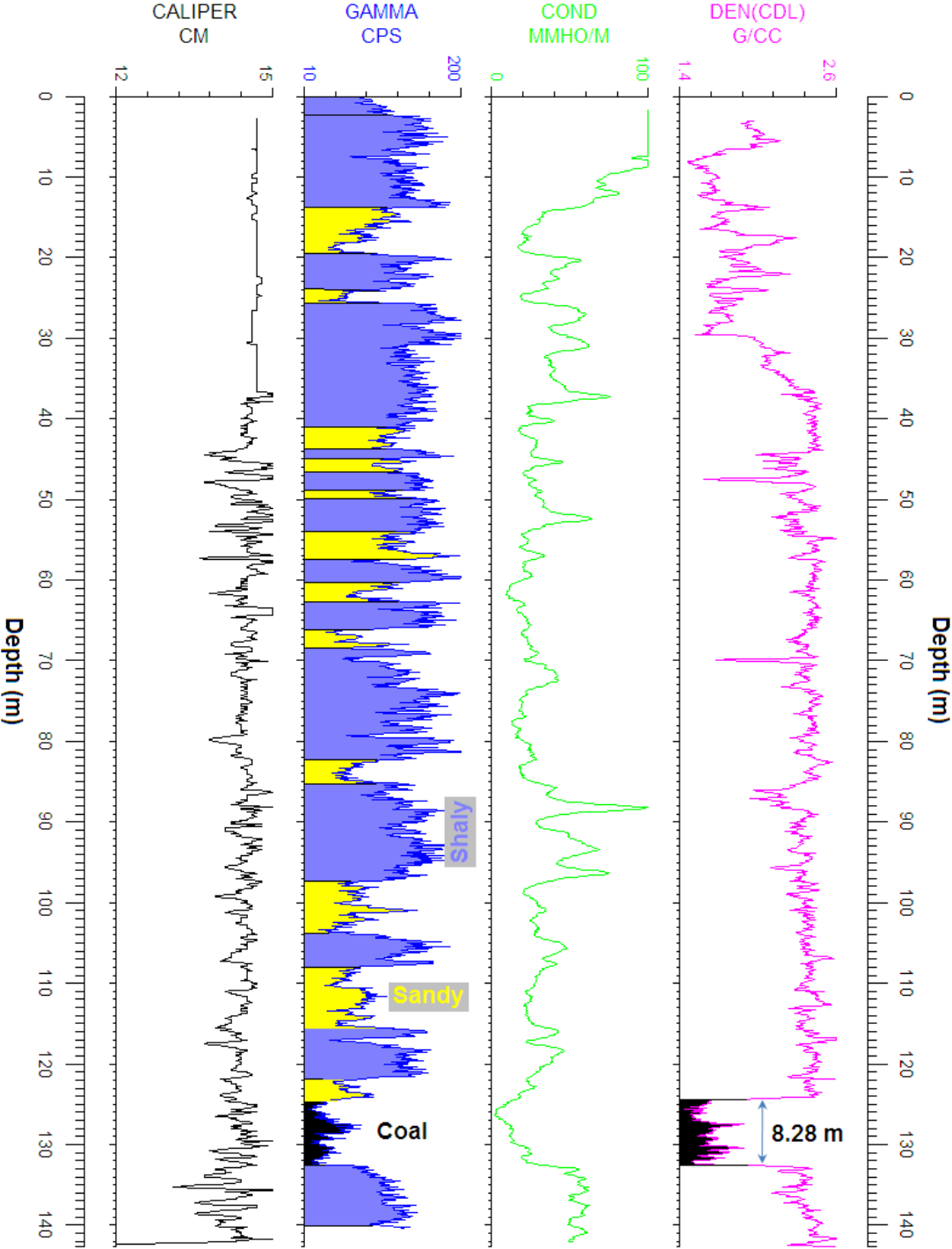


Figure 2-14. Geophysical logs from borehole CP_O11 at the intersection of the inline IN025 and cross-line X104 in Figure 2-13. Seam floor is at 132.6m from the collar.

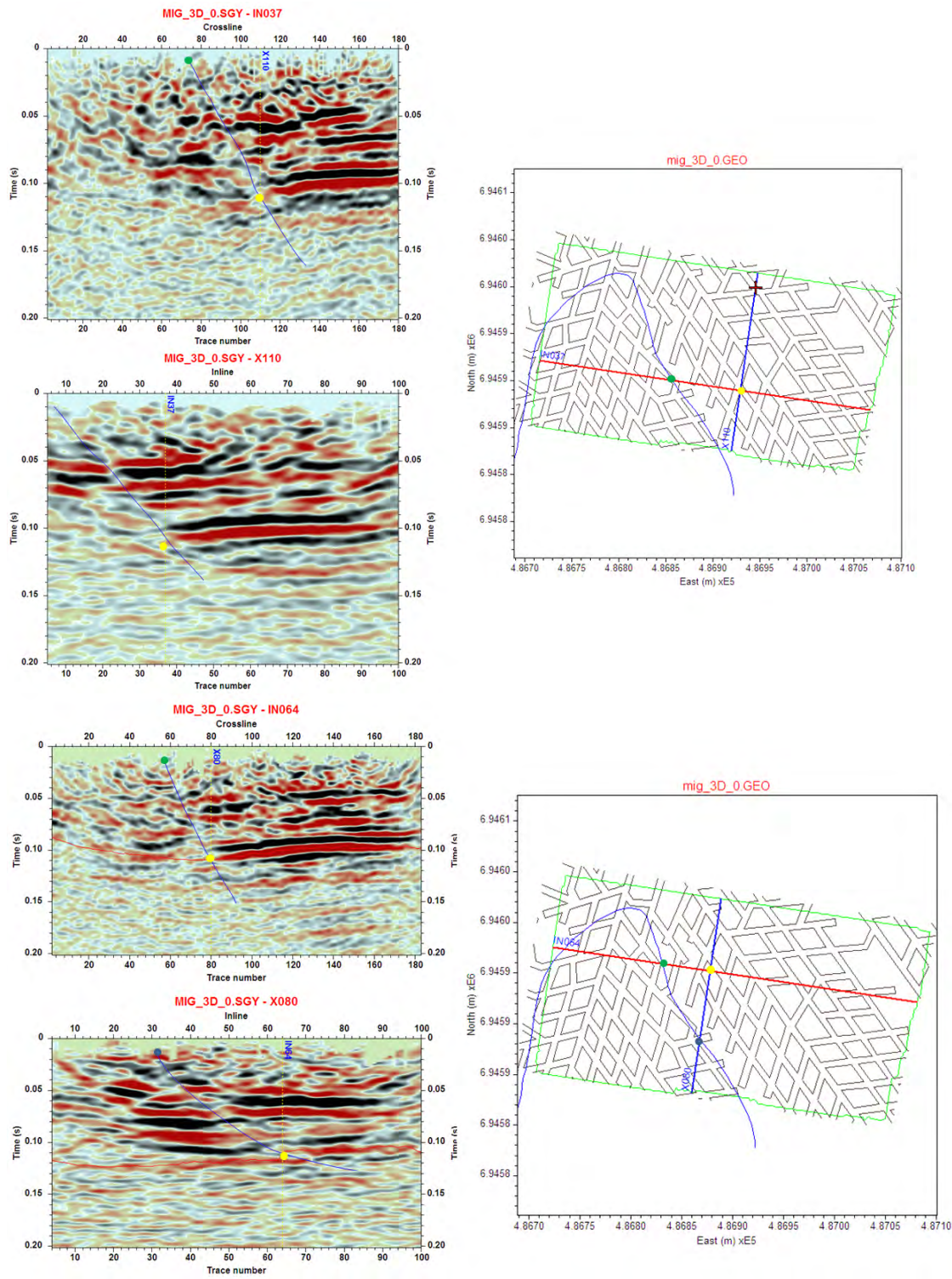


Figure 2-15. Mapping the caving boundaries (blue curves) based on the reflection features. The yellow dots are the mapped failure boundaries at the seam level and the green and light blue dots are the subsidence boundaries on the surface.

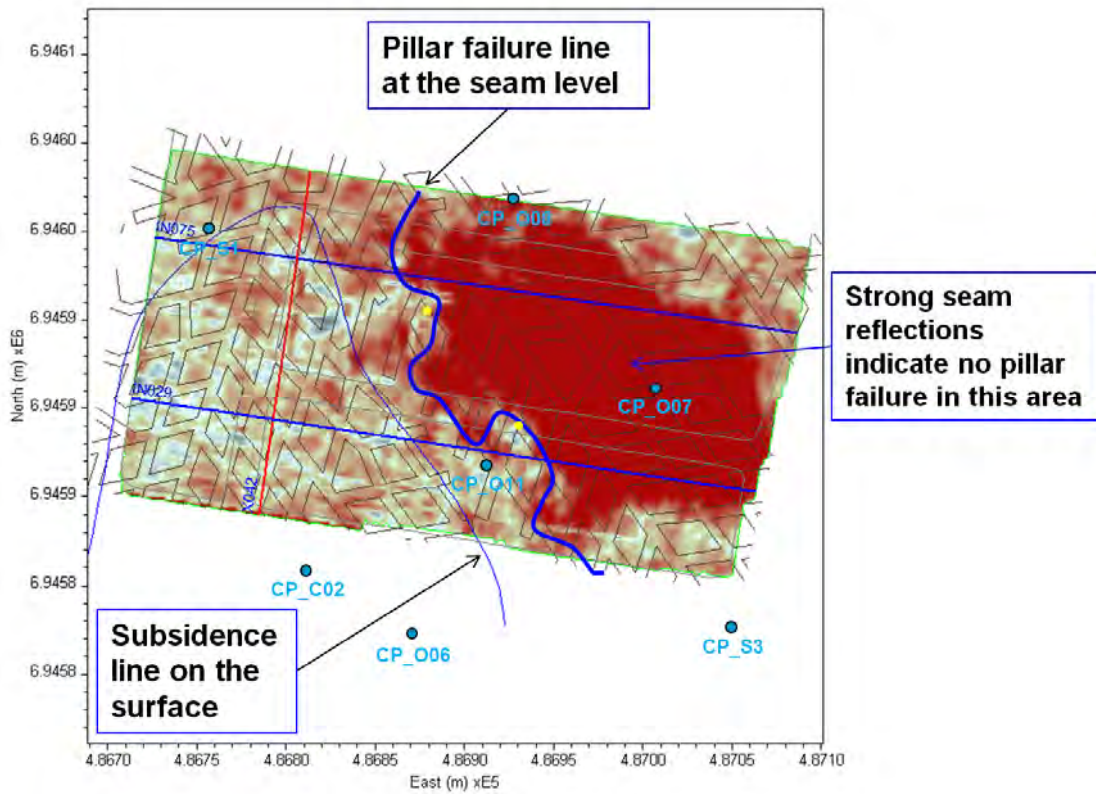
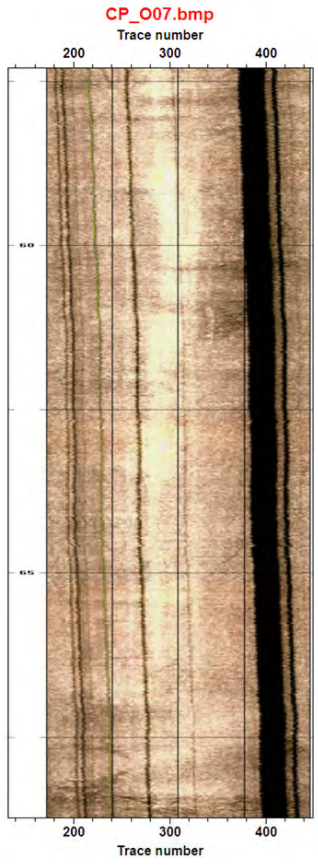
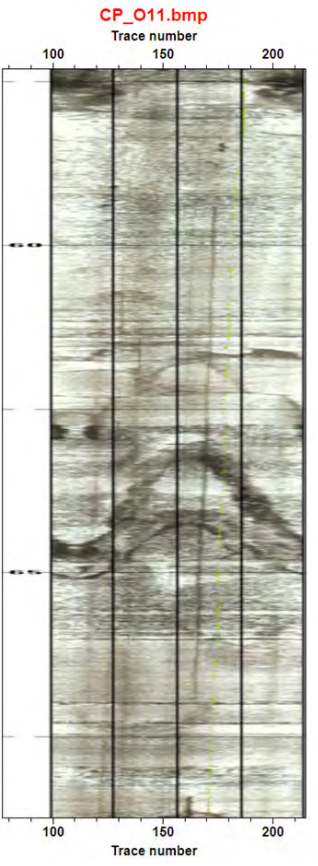
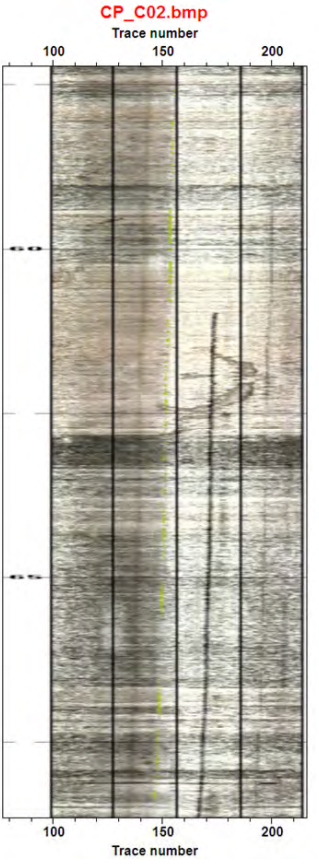
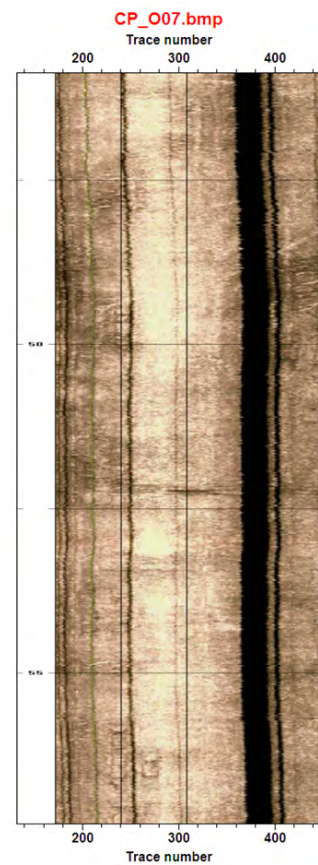
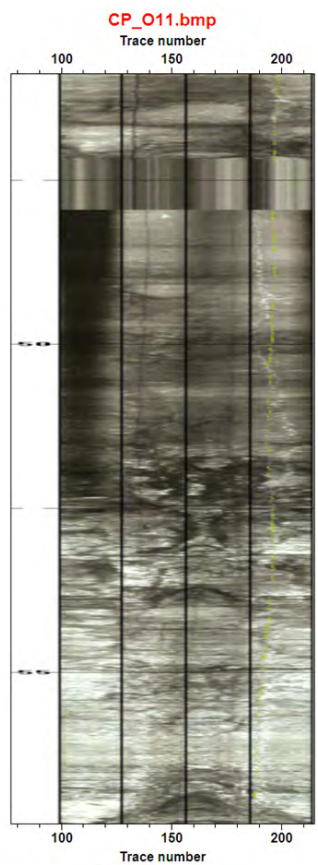
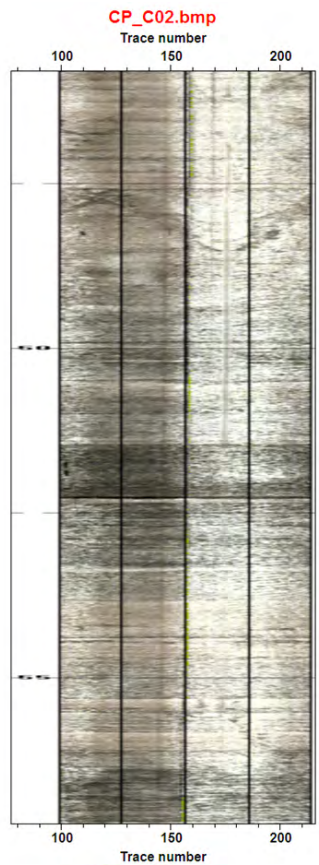
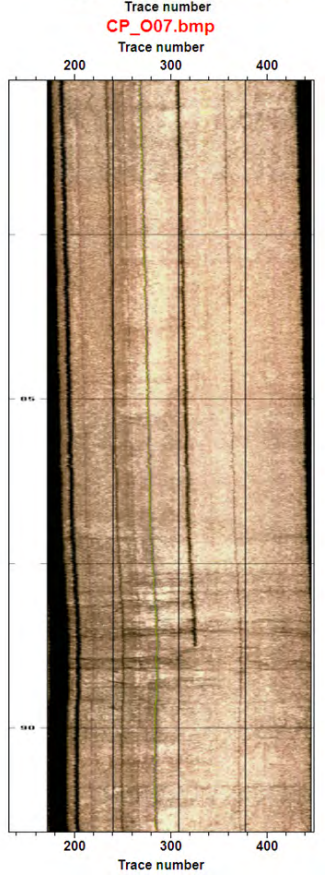
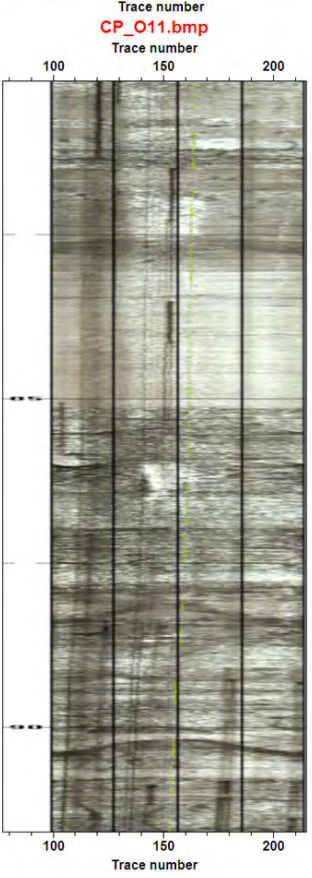
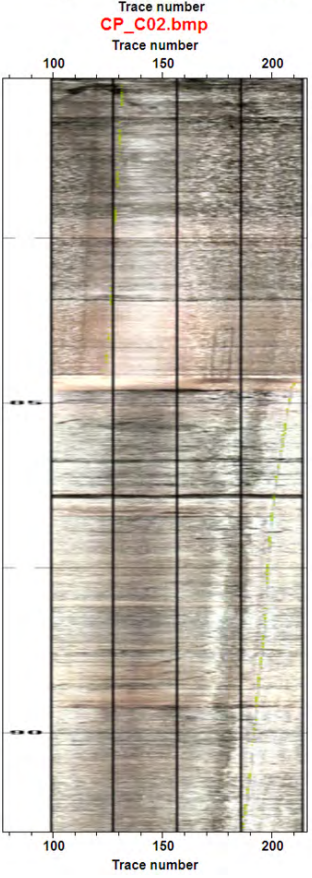
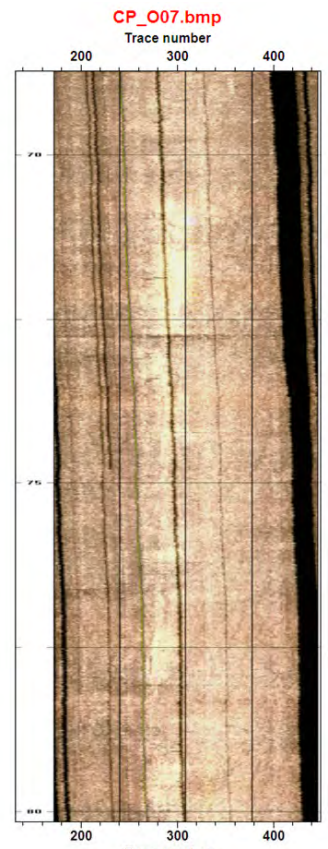
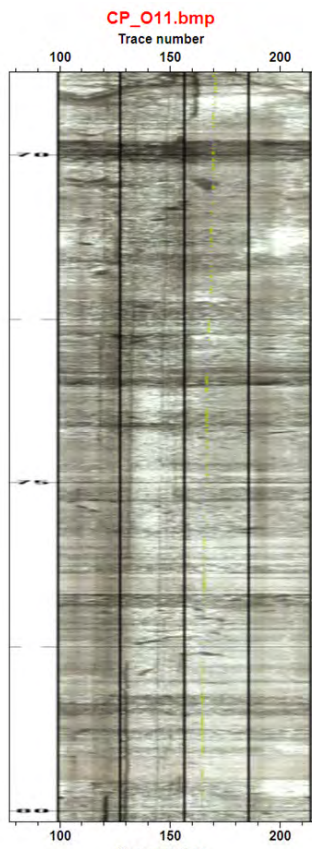
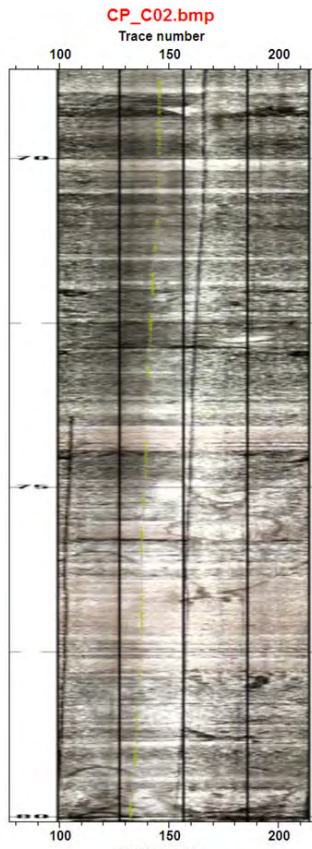
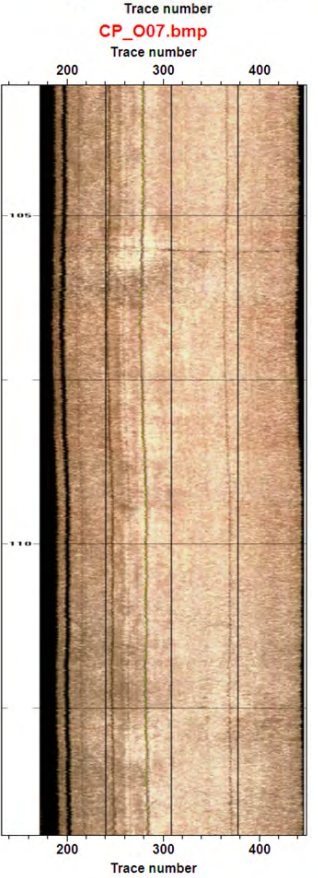
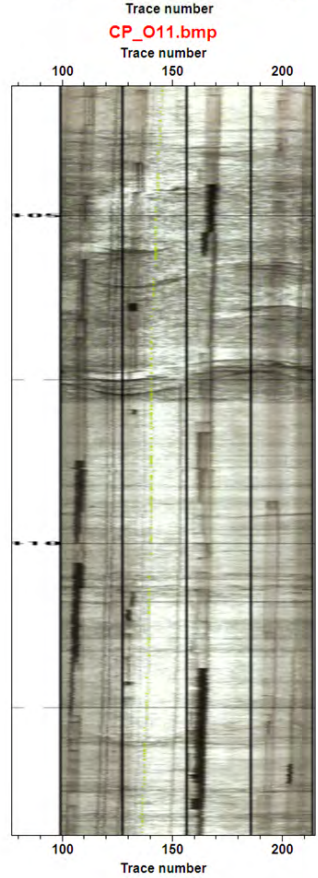
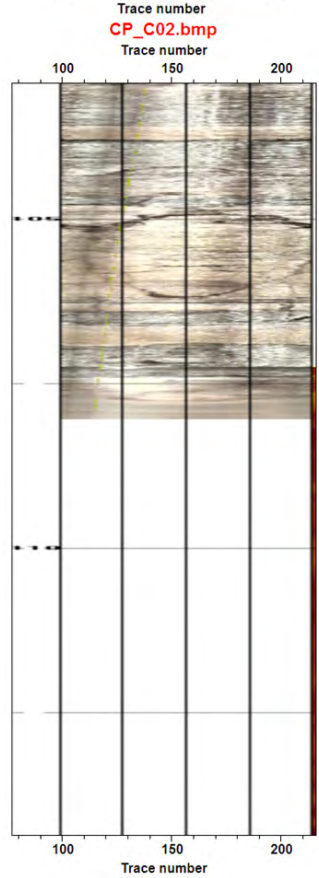
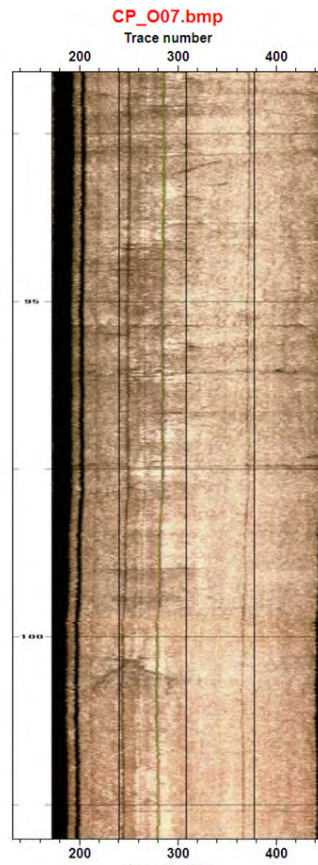
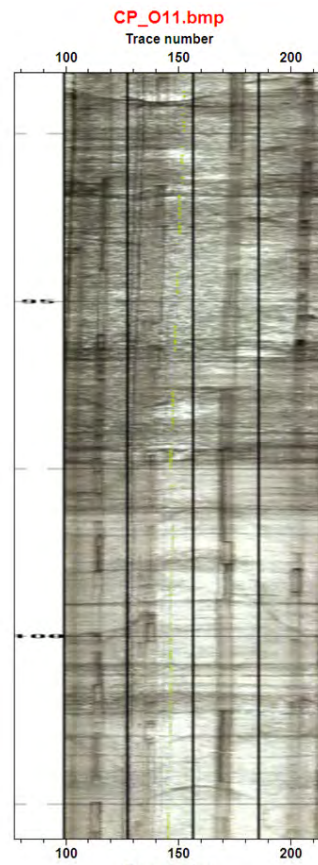
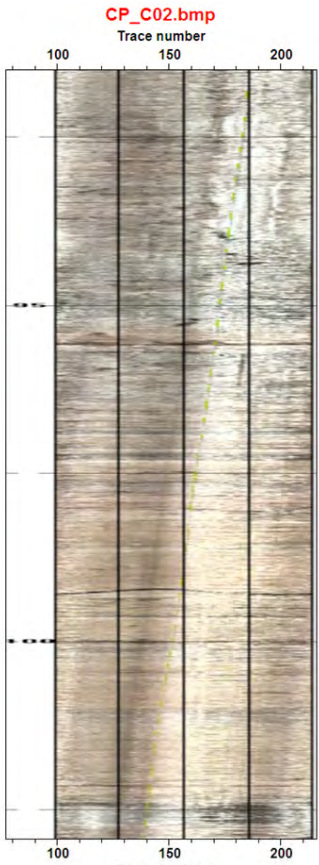


Figure 2-16. Amplitude distribution of seam reflections for mapping the failure at the seam level, clearly showing that the subsidence area on the surface and failure area at the seam level are different. The yellow dots are the failure boundary locations at the seam level mapped from seismic sections in Figure 2-15. The thick blue curve describes the failure boundary at the seam level based on the reflection amplitude strength. Amplitudes are clipped to make the selection of the subsidence boundary at the seam level easier. The light blue dots are the boreholes drilled after the 3D seismic field work.







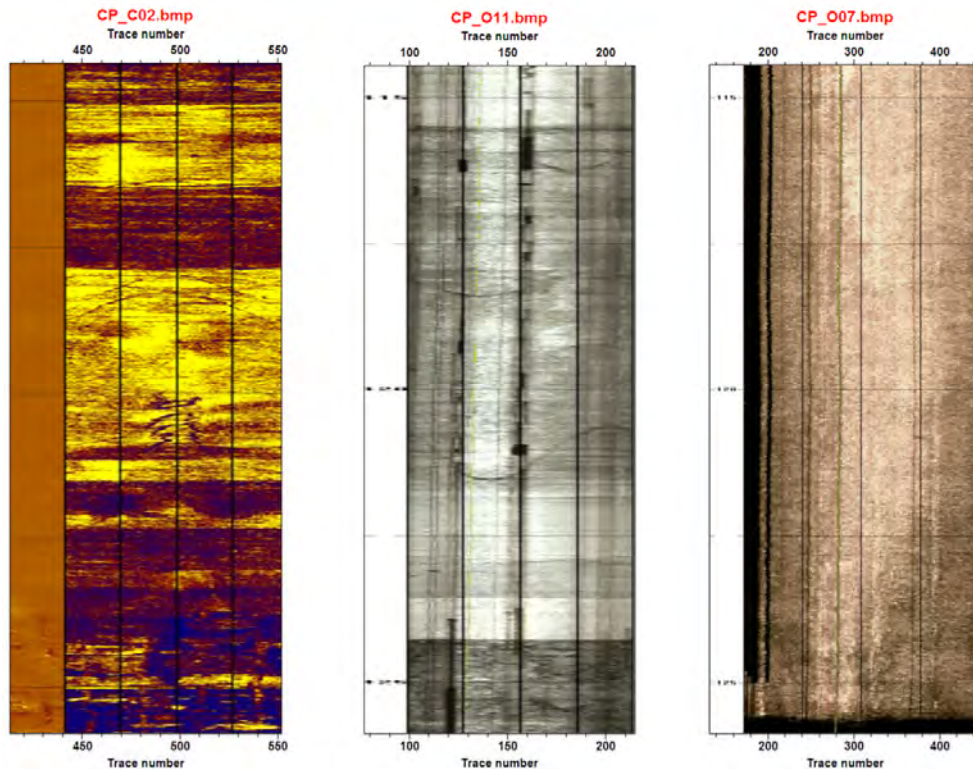


Figure 2-17. Optical scan images from boreholes CP_C02, CP_O11 and CPO07.

2.4.4 Fault identification

There are various ways to identify faults from seismic data. Faulting structures normally appear as abrupt shifts on the seismic reflections. Therefore, one simple and quick way to identify faults is to pick the reflection times of the coal seams and locate them on the cross section to see if there is any discontinuity in the data. In fact, the failure line identified in the previous section in the barrier pillars is directly related to such fault. This is evident from wave reflections in the seismic sections of Figure 2-15.

As stated before, the south-west dipping Waterline fault is in the seismic survey area. From Figure 2-18 to Figure 2-21, one can easily confirm the existence of this Waterline fault from the seismic data. This Waterline fault has been identified as a normal fault with a fault displacement range between 3 to 13 m depending on the location. The fault displacement is consistent with the experience of the mine managers.

The up thrown side of the fault is on the right or East side of the fault. However, this fault could be a thrust fault with a fault plane dipping to the northeast as shown on the cross-line section X089 in Figure 2-20. However, because the area has been disturbed by subsidence, and the data quality is relatively poor, it is possible that the thrust fault appearance on section X089 is actually a reflection of the failure (or caving) boundary.

In addition to the Waterline fault, we also observed a disturbance in the seismic data (indicated by the light blue arrows) in the north-east corner of the survey area as shown by Figure 2-18. This disturbance is likely to relate to the faulting structure. It can

be a thrust fault as currently drawn on the section, but the data quality does not warrant its correct identification of the fault type.

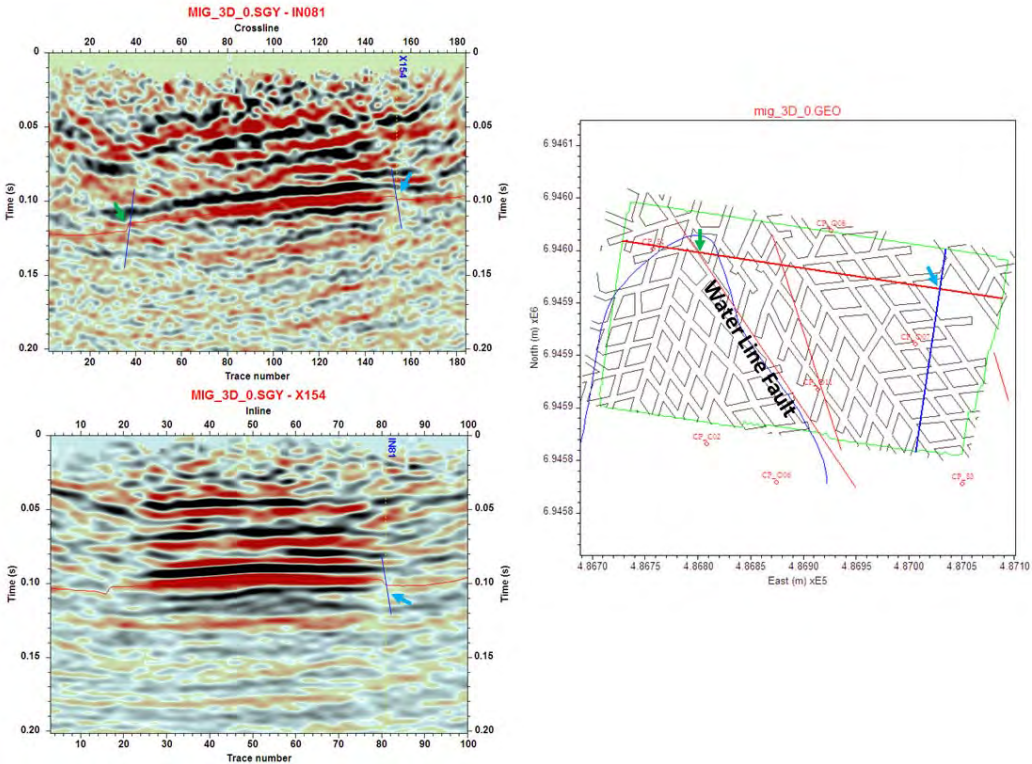


Figure 2-18. Two faults identified from the inline IN079 and cross-line X164 as indicated by arrows. The fault indicated by the green arrow is associated with the Waterline fault while the fault indicated by the light blue arrow is a newly identified one which might be the reason for not mining through the region.

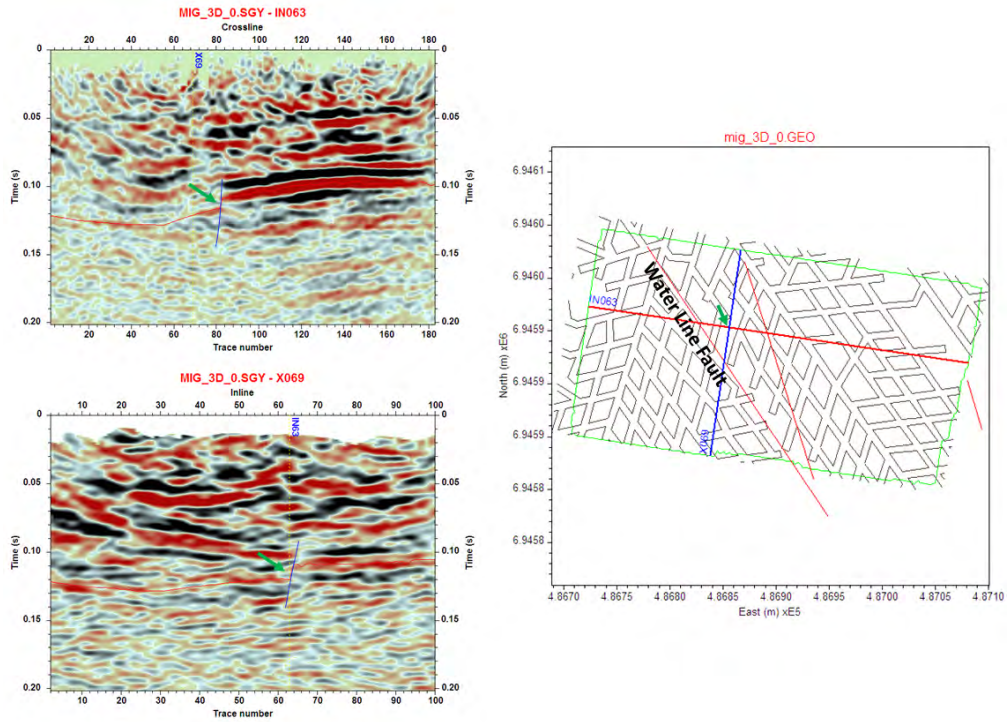


Figure 2-19. One fault identified from the inline IN063 and cross-line X069 as indicated by arrows. This fault is associated with the Waterline fault. The estimated fault displacement at this location is about 8-13 m based on the seismic data.

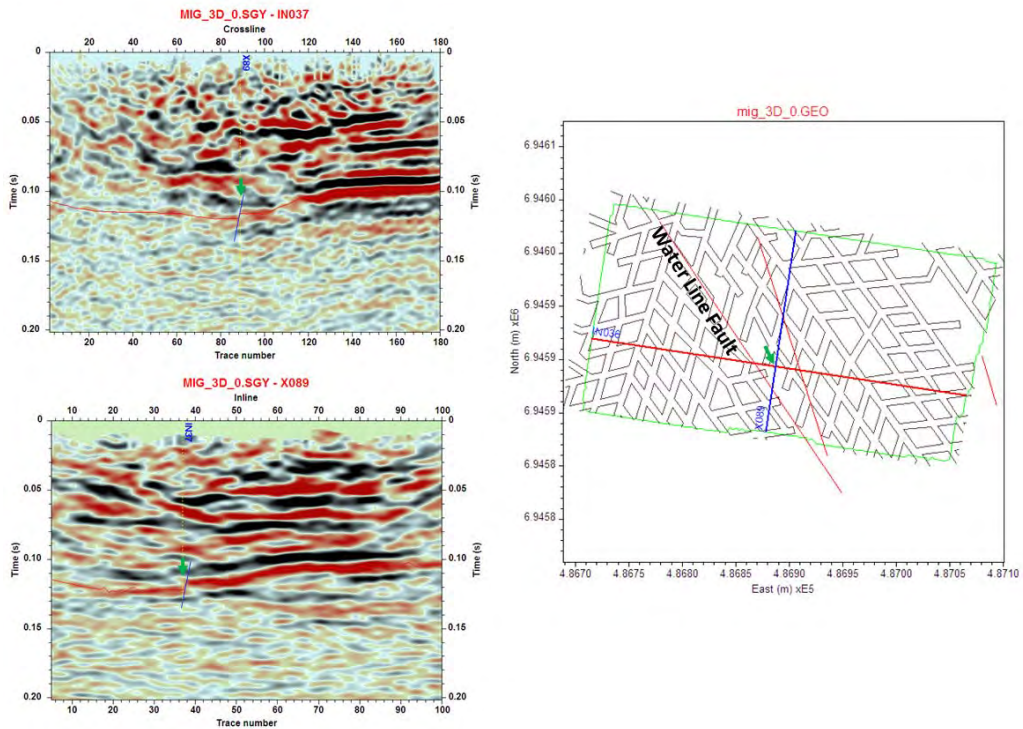


Figure 2-20. One fault identified from the inline IN037 and cross-line X089 as indicated by arrows. This fault is associated with the Waterline fault. The estimated fault displacement is about 3 - 5m.

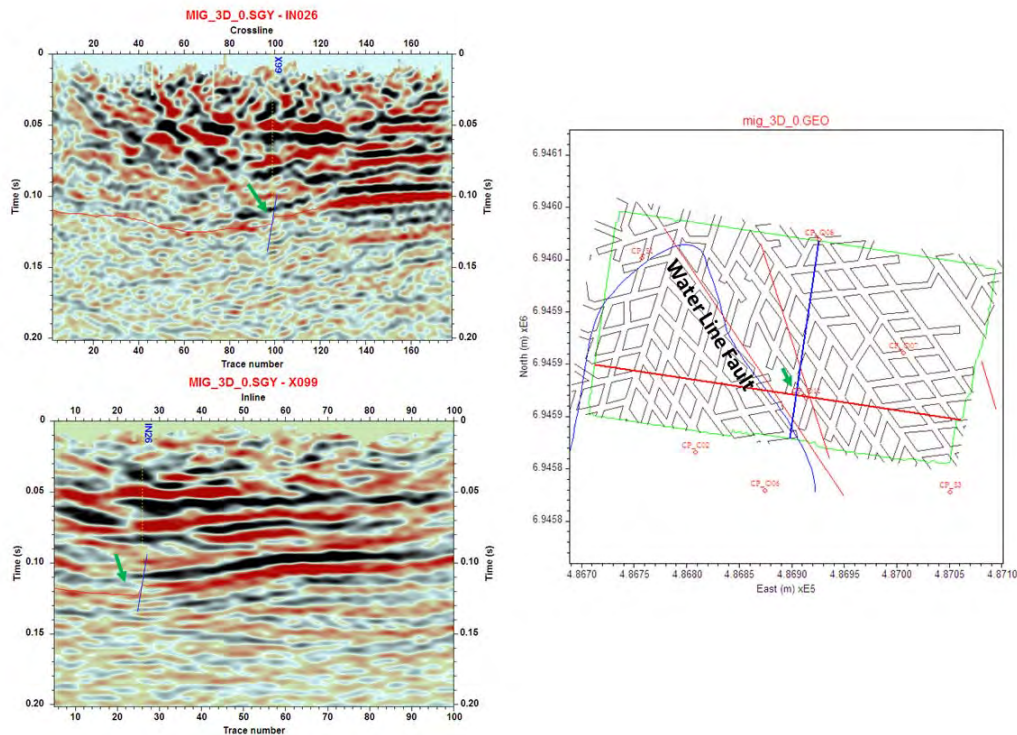


Figure 2-21. One fault identified from the inline IN026 and cross-line X099 as indicated by arrows. This fault is associated with the Waterline fault. The estimated fault displacement is about 3-6 m at this intersection location.

2.4.5 Mapping underground roadways

One of the objectives for this 3D seismic survey is to test if the underground workings/roadways can be mapped in the area. This is similar to the mapping of paleochannels by 3D seismic surveys in the petroleum industry, as shown in Figure 2-22 (Chopra et al, 2009). This is normally achieved by mapping out the amplitude distribution like the one shown in Figure 2-16. Unfortunately, we were not able to correlate any amplitude variations with the underground workings. The reason for this was that the seismic data were mainly processed for structural interpretation, which does not strictly speaking maintain the true relative amplitudes of the seismic wave.

Seismic signals lose their energy due to spherical divergence (geometrical spreading), absorption, source and receiver coupling related conditions and energy partitioning at interfaces and between modes. Some of these factors need to be corrected or compensated for during seismic data processing. Currently, coal seismic data processing is mainly oriented towards structural interpretation. Structural information is best determined on the basis of abrupt shifts in the reflectors. The more reflectors showing a shift, the more obvious is the feature. In other words, it is a standard practice to boost the amplitudes on all seismic reflections. However, in doing this, relative amplitudes (signal strengths from one observation point to another) may also be lost. Also important is to maintain the relative amplitudes from trace to trace and from sample to sample for stratigraphic interpretations, e.g. looking for the

underground workings based on the amplitude differences in reflections from the pillars and the mined-out roadways/workings.

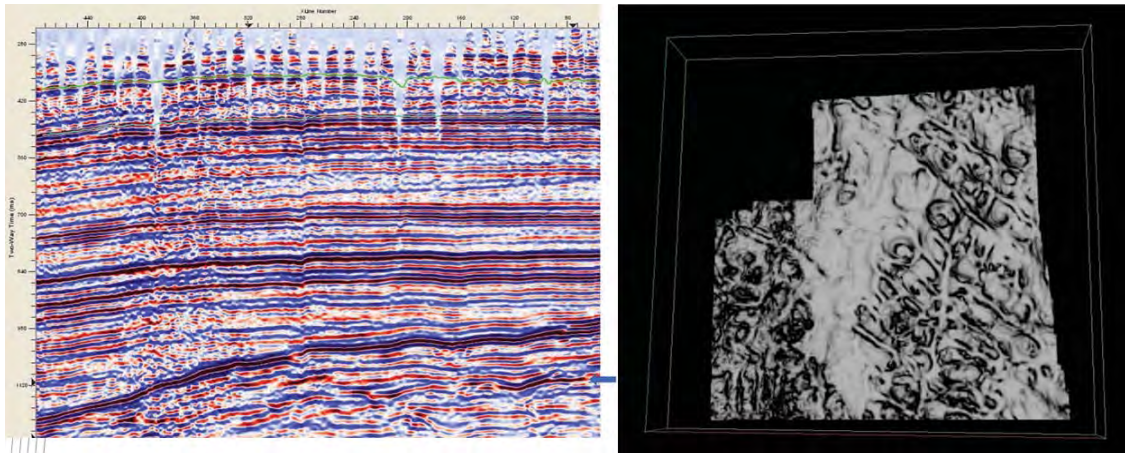


Figure 2-22. Example of mapping paleochannels from petroleum 3D seismic. From Chopra, Negut and Cilensek (2009).

The key process affecting seismic amplitudes is the gain control applied for increasing the weak signal for visual and data display purposes. The gain for geometric spreading is applied to compensate for wavefront divergence early in the process, before deconvolution (a process to recover the high frequency loss of the wave propagation in the earth) and filtering process. Exponential gain is also normally applied to compensate for attenuation losses. It is also possible to compensate for the variations near the source and receiver using a surface-consistent amplitude model where the corrections are statistically determined from the redundancy in the data. Another correction involves applying automatic gain control (AGC)-type gain functions to bring up weak signals. This type of gain must be used with care as it will destroy signal characters important for seismic attribute interpretation.

To improve the characteristics of true relative amplitudes the seismic data were reprocessed with true amplitude processing procedures and algorithms and the resulting amplitude distribution of the seam reflections is displayed in Figure 2-23. Unfortunately after this reprocessing we were still unable to map the underground workings. After excluding improper processing as the failure reason, other possible reasons for the failure can be:

- *Noise*: poor original data due to surface and traffic noise
- *Energy*: insufficient source energy generated by the weight-drop
- *Frequency*: the dominant frequency of the data (30 Hz) was not high enough
- *Width*: the working width (about 5m) was too small compared with the seismic wave length (about $86 \text{ m} = 2600 / 30$).

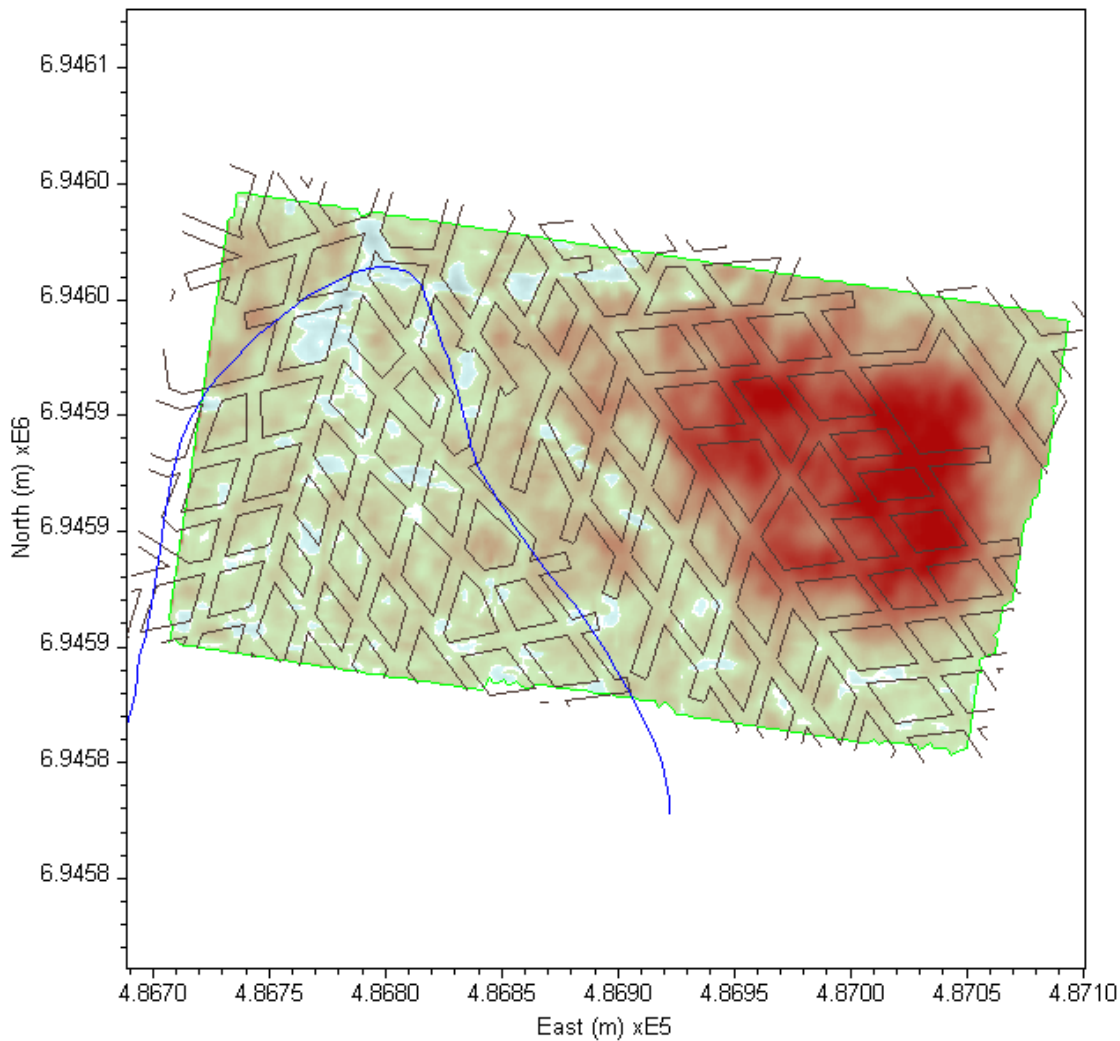


Figure 2-23. Seam reflection amplitude distribution extracted from true-amplitude processed volume is displayed with full-amplitude range. No workings can be identified from this amplitude map.

2.5 Conclusions and recommendations

A trial 3D seismic survey was conducted at Collingwood Park in the 2008 subsidence and adjacent areas from 19-23 October 2009. The seismic data were collected and processed by Curtin University to CSIRO's specifications. From the analysis of the seismic data, the following observations and conclusions are drawn:

- Acquired seismic data have low signal-to-noise ratio in general due to traffic noise and the low-energy weight-drop method used as the seismic source. However, the processed seismic data are of reasonably good quality especially in the zone where no subsidence occurred but relatively poor in the subsided region. This observation is consistent with the 1989 2D seismic survey results by Velseis.
- The location of the Waterline Fault is confirmed by the 3D seismic data. According to the seismic data, this is a normal fault dipping to the southwest with a vertical

displacement varying from 3 m to 13 m. This observation is consistent with the mine managers' experiences at the mine.

- A normal fault disturbance (dipping to the northeast) is observed from the northeast corner of the survey area from the seismic data, which may be the extension of an existing fault near-by and may explain the reason for not mining through this zone. The fault properties cannot be reliably determined from the seismic data due to the poor quality of the data on the edge of the survey area.
- The caving zone related to the subsidence event can be identified from seismic data based on the quality and characteristics of seismic reflections from the subsided and unsubsidized zones. The seismic data can be used to map out the surface subsidence boundary that matches well with the boundary observed in the field. In addition, the seismic data can also be used to map the failure boundary at the seam level in relation to the subsidence event. The mapped failure area at the seam level is larger than the subsidence boundary on the surface. The estimated angle between the failure (caving) boundary and the vertical axis is about 21°. This angle may vary from location to location.
- The projected failure area at seam level yields some important information for definition of the extent of pillar failure. It is possible that pre-existing geological structures (i.e. the Waterline Fault) may result in the extension of the large pillar failure based on observations from the seismic data. The data from drill holes drilled after the 3D seismic survey support the idea that the pillar failure has extended beyond to the east side of the Waterline Fault.
- The underground working/roadways cannot be imaged with these seismic data. Possible reasons include: 1) Poor original data due to surface and traffic noise; 2) insufficient source energy generated by the weight-drop; 3) the dominant frequency of the data (30 Hz) is not high enough; 4) the working width (about 5m) is too small compared with the seismic wave length (about 86 m).

From these observations, we conclude that seismic surveying can delineate the geological structures in the Collingwood Park area and help us to understand underground conditions for future subsidence assessment. It is recommended that:

- A 3D seismic survey should be carried out in New Redbank Colliery to identify areas where subsidence may have occurred in the past but not been recorded.
- Further 3D seismic surveys may be conducted in the southeast part of Westfalen No. 3 (where the retirement village and two sport grounds are located) to determine if any underground panel failure has occurred in the past.
- Better seismic sources need to be tested to increase the energy and frequency range with the aim of getting better seismic resolution and seismic data quality.

3. GEOTECHNICAL INVESTIGATION AND MONITORING

3.1 Summary

The main objective of the geotechnical monitoring programme was to provide additional data on geological, geotechnical and mining conditions to help understand the causes of the 2008 subsidence event and then develop an optimal remediation scenario. CSIRO worked closely with DIP and DEEDI to design a site investigation to provide this data. SMEC was contracted to undertake and to manage the site investigation activities.

A total of 15 open and cored holes were drilled in Westfalen No. 3 and New Redbank Collieries. Most of the holes drilled in Westfalen No. 3 Colliery intercepted the intended target (roadways or pillars). This indicates that the mine plan map available is reasonably accurate. The mining heights obtained from this drilling programme are generally consistent with those previously reported from various sources.

Both of the boreholes drilled into the New Redbank Colliery encountered large irregular voids. It is likely that the investigated section of the mine has collapsed.

Three piezometers were installed in the two mines. The monitoring results to date indicate that the water level in New Redbank Colliery is stable at 83m below sea level. Water level in Westfalen No. 3 is currently (September 2011) at 108m below sea level and is increasing at a rate of about 11m/year however further data is required to confirm if this is a long term trend.

One 20-anchor surface extensometer was installed in Hole CP_O07 in the central region of Westfalen No. 3 Colliery with relatively small pillars. The limited monitoring results from 9 August to 24 September 2010 indicate that there was a 8mm movement in the overburden strata and the movement is increasing at a rate of about 1mm/week. The trend of strata movement is worrisome and it could be a precursor of a subsidence event. If this trend continues in the subsequent monitoring period and the total movement greater than 10mm, we recommend a set of actions be taken, including to install two new extensometers and a microseismic station, and to develop an emergency response plan for potential mine subsidence.

Four sets of water samples were collected over the past five months from the two mines. The chemical analysis results show that the water in both mines is typical "old" aquifer water that may not be directly linked with the surface fresh water. It is believed that the aquifer water is continuing to flow into the mines, causing the water level increase in Westfalen No. 3 Colliery and a noticeable water chemistry change with time.

Two sets of gas samples were collected and tested from Westfalen No. 3 Colliery. The mine gas contains 17-18% methane (CH₄), 10% carbon dioxide (CO₂) and 71% nitrogen (N₂). The oxygen (O₂) content was 0.5-0.6% in April 2010, but it was

increased to 1.1% in July 2010. The risk of gas explosion underground is low at present due to the very low oxygen content. However, because the methane content is close to the explosive range of 5-15%, this risk should not be discounted as the oxygen content is currently increasing and any further subsidence events could accelerate the oxygen increase rate. An oxygen concentration of approximately 12% will move the methane concentration in to the explosive range

An analysis was carried out to understand the effect of mine water on the 2008 subsidence event. Based on the drill hole data from this most recent program, it was found that at the time of the subsidence event the mine water level in Westfalen No. 3 Colliery was unlikely to have flooded the key area of subsidence. However, there is a discrepancy in the seam floor depths from the underground survey data and from drill hole data. The survey data suggest that the water level might have “wetted” up to six pillars at the edge of the subsidence area. The recent drill hole data are considered to be more reliable.

The effect of water on pillar/panel stability is not sufficiently understood at present. It should not be dismissed because evidence in other geotechnical engineering studies have indicated that water could be a major factor in rock mass instability. More studies are required to quantify this effect.

3.2 Introduction

Scattered data and information are available for Westfalen No. 3 Colliery and New Redbank Colliery, and they have largely been summarised by Dept of Mine and Energy (2008) in a scoping study after the 2008 subsidence. For Westfalen No. 3 Colliery, a detailed mine plan, believed to be reasonably accurate and reliable, is available together with general knowledge of mining heights. By comparison, the data available for New Redbank Colliery is very limited except for an old mine plan the accuracy of which is very questionable.

At the start of this study, the scattered and mostly unverified data did not provide sufficient confidence necessary for the design of an optimal remediation scenario. Additional site investigation was required in order to improve the level of confidence.

Working closely with DIP/DEEDI personnel, CSIRO had recommended and designed a geotechnical investigation and monitoring programme at Collingwood Park. The programme consisted of the following key components:

- Drilling a total of 15 holes, 13 of which are in Westfalen No. 3 and 2 in New Redbank Colliery. The main objectives of the drilling include
 - to verify the mine plan
 - to check the mining heights
 - to inspect the current roadway/pillar conditions
 - to obtain additional geological data to build a reliable geological model

- to allow for the installation of various monitoring instrumentation and water/gas samplings.
- Monitoring water levels in the two mines by installing piezometers in three boreholes. It has been suggested that the water level may have played a key role in the previous subsidence events. Hence it is essential to understand the water level and its change over time.
- Installing a microseismic monitoring system in three boreholes. The system will be able to pick up rock fracturing related seismic event and hence provide information for any ongoing or future ground failure events.
- Installing a 20-anchor extensometer in the high risk central region of the Westfalen No. 3 Colliery. It will monitor any movement in the overburden strata associated with slow pillar deformation and failure.
- Sampling and analysing the mine water and gas over a period of six months. This program was designed to analyse the source of the mine water and gas.
- Geophysical logging and rock sampling and testing to provide detailed geological and geotechnical information for geotechnical assessment of panel stability.

DIP/DEEDI contracted SMEC to carry out the site investigation, with the exception of the installation of the microseismic system, which was carried out by CSIRO with assistance from SMEC. The field components of the investigations were conducted between February and April 2010. SMEC provided a draft factual report containing the data collected during the investigation (SMEC, 2010). The outcomes of the geotechnical investigation and monitoring programme are provided in the sections below.

3.3 Drilling

The drilling component of the site investigation consisted of drilling a total of 15 cored and open boreholes as designed by CSIRO. The drilling objectives and targets included: pillars within the Main Seam; roadway intersections within the Main Seam; and holes terminated above the Main Seam for seismic installation. Once completed, a suite of geophysical logs were run and the drill holes were used for remote visualisation and inspection of the workings using a down-hole video camera.

Selected drill holes were installed with monitoring instruments including a microseismic network, three piezometers and an extensometer. In addition, underground water and gas samples were taken from some boreholes for chemical analyses.

Within the geotechnical site investigation programme the following drilling was completed. Figure 3-1 shows the locations of these drill holes:

- Three 125mm diameter drill holes were drilled using percussive techniques to about 20m above the projected Main Seam depth. These holes were used to install a total of 9 geophones for the microseismic monitoring network. These holes are named CP_S1, CP_S2 and CP_S3. The microseismic monitoring network has

been installed to monitor future ground fracturing behaviour of both subsided and non-subsided areas.

- Three HQ cored (100mm diameter) drill holes were drilled targeting the pillar locations. These are holes CP_C01, CP_C03 and CP_C04. CP_C01 and CP_C03 are in the non-subsided area of Westfalen No. 3 Colliery whereas CP_C04 is in New Redbank Colliery where the ground may have already collapsed. A piezometer has been installed in C04. CP_C02 was originally designed as a cored hole targeting the 2008 subsidence area. Due to the drilling difficulties experienced in broken ground elsewhere this hole was later changed to be an open hole.
- Nine 150mm diameter drill holes were drilled with percussive techniques to penetrate the mine workings at the intersections of the mine roadways, both in subsided and non-subsided areas. These holes are named CP_O05 to CP_O12, plus CP_C02. An extensometer is installed in CP_O07 and piezometers in CP_O05 and CP_O09.

In general, the drilling went smoothly and according to the design and majority of the targets were hit as planned. However target drilling, or verticality control, is still more of an art than science with the equipment used and needs further technology improvement. The costs of directional drilling methods were considered to be too expensive for a site investigation. There were situations where there were less controls on the propagation of deviation employed, resulting in large horizontal deviations from the target. However, drill holes designed to penetrate mine voids were purposely located at the roadway intersections. This measure ensured that some of the drill holes with large deviation still ended up in the roadways.

A summary of the drilling program carried out during the investigation together with some drilling operation results are provided in Table 3-1. More discussions and details of the drilling and borehole survey results are provided in a separate report by the site drilling contractor, SMEC (2010).



Drawn by Mapping and Survey Services | 19-01-2010 | GGS155_A4_propdrill_jan2010.mxd

Figure 3-1. Locations of 15 drill holes designed by CSIRO distributed in both historical subsided and non-subsided areas.

Table 3-1. Drilling summary (after SMEC 2010)

Hole_ID	Type	Planned Depth to roof of coal	Target	Drilling Metres						Actual Depth to Roof of Coal	Actual Depth to Void Ceiling	Actual Depth to Void Floor	Geo Physics			Verticality	Visual Data	Additional Notes
				Date Started	Date Completed	Cored Hole (m)	Length of Core (m)	Microseismic Hole (m)	Open Hole (m)				Date	Depth Logged to (m)	Water Level below surface			
CP_C01	Core	60	Pillar	15/02/2010	1/03/2010	63.8	34.2	-	-	53	N/A	N/A	N/A	N/A	N/A	N/A	-	Core barrel and rods left in hole, backfilled.
CP_C02	Core	122	Pillar	22/03/2010	29/03/2010	-	-	-	142.0	127.0	N/A	N/A	1/04/2010	128.8	108	4.7m, 298 deg. WNW	30/03/2010	PCD Air Drilling from 85 to 142m Coal Seam 127 to 135 Hole blocked at 128.8 during geophysical survey, 1-4-10.
CP_C03	Core	115	Pillar	24/02/2010	18/03/2010	131.2	79.2	-	-	127.5	N/A	N/A	17/03/2010	125.0	97	3.3m, 311.3 deg. NW	-	Core barrel left in hole below 127.5m
CP_C04	Core	90	Pillar	10/03/2010	24/03/2010	133.5	21.4	-	-	N/A	130.0	133.5	30/03/2010	128.3	96	9.7m, 358.7 deg. N	25/03/2010	PCD Air Drilling from 85 to 105m & 126.4 to 133.5, Intact rock at 133.5, No Rubble noted, Vibrating wire piezometer
CP_O05	Open	145	Intersection	10/03/2010	11/03/2010	-	-	-	151.3	-	149.5	150.0	13/03/2010	147.0	136	10.6m, 342.4 deg. NNW	19/03/2010	0.8m loose material below 150.0m, Vibrating wire piezometer
CP_O06	Open	135	Intersection	17/03/2010	18/03/2010	-	-	-	126.1	-	121.6, 123.1	-	31/03/2010	120.3	Dry	4.5m, 333.7 deg. NNW	19/03/2010	Two voids encountered
CP_O07	Open	125	Intersection	15/02/2010	17/02/2010	-	-	-	137.0	-	127.0	134.9	23/02/2010	126.0	Dry	5.5m, 328.5 deg. NNW	22/02/2010	0.4m of loose material on floor, Deep hole extensometer
CP_O08	Open	125	Intersection	26/02/2010	5/03/2010	-	-	-	130.5	122.0	124.5	128.5	12&15/3/2010	122.5	Dry	4.5m, 3.6 deg. N	10/03/2010	No loose material on floor noted
CP_O09	Open	135	Intersection	15/03/2010	16/03/2010	-	-	-	137.0	-	131.0	134.9	16/03/2010	129.0	Dry	1.1m, 354 deg. N	19/03/2010	Varying strength from 134.9 to 137m Visual data includes sonar below water level. Vibrating wire piezometer
CP_O10	Open	60	Intersection	24/02/2010	25/02/2010	-	-	-	66.0	-	59.2	63.1	3/03/2010	58.0	Dry	2.7m, 277.7 deg. W	10/03/2010	1.1m of loose material on floor
CP_O11	Open	125	Intersection	19/03/2010	22/03/2010	-	-	-	143.0	125.0	No Void	No Void	30/03/2010	142.6	129	6.0m, 330.0 deg. NNW	25/03/2010	Floor of coal 133m
CP_O12	Open	90	Intersection	8/03/2010	9/02/2010	-	-	-	126.0	-	-	-	12&16/3/2010	122.0	98	9.2m, 5.3 deg. N	10/03/2010	Possible ceiling collapse below 120m, 80mm PVC standpipe grouted to 58m inside, 40m outside
CP_S1	Microseismic	125	-	17/02/2010	18/02/2010	-	-	105.0	-	N/A	N/A	N/A	24/02/2010	104.9	92 / 82	2.1m, 329.deg. NNW	-	Microseismics installed, grouted 4/3/10
CP_S2	Microseismic	140	-	19/02/2010	22/02/2010	-	-	120.0	-	N/A	N/A	N/A	2/03/2010	120.0	73 / 28	24.6m, 230.39 deg. SW	-	Microseismics installed, grouted 5/3/10
CP_S3	Microseismic	130	-	23/02/2010	23/02/2010	-	-	110.0	-	N/A	N/A	N/A	3/03/2010	109.8	10	4.0m, 298.5 deg. WNW	-	Microseismics installed, grouted 4/3/10
						Totals	328.5	134.8	335.0	1158.9								

3.4 Geological model

Based on the recent and previous site investigation data, CSIRO has developed a geological model for the Collingwood Park region and it is described in this Section.

3.4.1 Regional geology

The New Redbank Colliery and Westfalen No. 3 Colliery extracted coal from the Bluff, Four Foot and Bergin Seams of the Late Triassic Blackstone Formation of the Ipswich Coal Measures. The Bundamba Group unconformably overlies these coal measures, and a summary of the stratigraphy in the study area as described by Carr (1977) is presented in Table 3-2.

Table 3-2.: Summary of Stratigraphy of the Goodna - Redbank district from Carr (1977)

Bundamba Group	Raceview Formation	Fine to Medium grained sandstone interbedded with siltstone and shale. Minor carbonaceous shales and thin coal seams
	Aberdare Conglomerate	Pebble conglomerate, pebbly sandstone and/or pink-grey shale; minor carbonaceous mud bands
~~~~~ unconformity ~~~~~		
Ipswich Coal Measures	Blackstone Formation	(Upper) Coal, interbedded shale, siltstone and fine sandstone, variable depositional thickness
		(Lower) Coal, medium to coarse grained sandstone, minor siltstone
	Tivoli Formation	Interbedded sandstone and mudstone with some siltstone and coal

North-west trending normal faults are the dominant structures in the region. Faults with down thrown north-eastern blocks cutting through all stratigraphy while faults with down thrown south-western blocks do not cut across the unconformity at the base of the Aberdare Conglomerate.

Open folds with sub horizontal north-north-west trending fold axes are present throughout the area. The most significant is the Bundamba Anticline, approximately 4 km west of the study area.

#### 3.4.2 Site geology

This interpretation of the geology of the Collingwood Park area is based on the results of the site investigation completed by SMEC (SMEC 2010) as well as historical data made available by the Department of Employment, Economic Development and Innovation (DEEDI). Drilling data was available from a 1989 program conducted by the

Mines Department (3 holes, DME BH1-BH3), a mining subsidence assessment report completed in 1994 by Moreton Geotechnical Pty. Ltd. (7 holes with no geological data except for depth of roof, Grubb, 2004), and a report on the coal resources of the Redbank – Goodna area (34 holes drilled, Carr, 1977). Other available data included survey data from the mine workings and various reports on subsidence in Collingwood Park.

### *Coal seams*

The mined seams in the Goodna area are from the upper part of the Blackstone Formation. Table 3-3 summarises the correlations between the nomenclature of the coal seams mined and their regional equivalents. The majority of the workings of the Westfalen No. 3 Colliery are in what is locally known as the Main Seam. This seam is interpreted to be the equivalent to the combined Bluff and Four Foot Seams (Carr, 1977). Elsewhere in the region these seams are separated by as much as 30 m (Falkner et al. 1988). The Main seam has an average thickness of approximately 10 m, varying between 6 m and 15 m in the study area. The best quality coal is at the top of the seam with stone bands increase in proportion towards the base of the seam.

A lower level of the mine, extracting coal from the X seam, was worked to a small extent in the western part of the study area. The X Seam is interpreted to be stratigraphically equivalent to the Bergin Seam. The interburden between the X Seam and the Main Seam varies from as little as 10 cm in the north of the study area to 40 m in the south. The nature of the X seam is highly variable with numerous partings and splits. The seam's average thickness is around 3 m, in the area mined at Westfalen No. 3.

Table 3-3. Correlation of seams worked at the Westfalen No. 3 Colliery with regional described

Westfalen No. 3 Colliery	Regional Name	New Redbank Colliery
Main Seam	Bluff Tops	Tops?
	Bluff Middles	Tops?/Middles?
	Bluff Bottoms	Middles?
	Four Feet Tops	Middles/Bottoms?
	Four Feet Bottoms	
X Seam	Bergin Seam	Bottoms?

### *Lithologies*

**Blackstone Formation:** The Blackstone Formation consists of coal, interbedded shale, siltstone and fine sandstone (Figure 3-2), and has been interpreted as being deposited in a fluvial environment with floodplains, meandering channels and peat forming mires (Falkner et al. 1988). This environment results in stratigraphy that has a high degree of lateral variation. For example, the two seams that make up the Main Seam, the Bluff and Four Foot Seams, are separated by tens of metres of interburden elsewhere in the

basin, whereas they are in contact in the study area. There are numerous clay bands (tonsteins) in the formation that have been interpreted as volcanic ash falls. Where drilled, the floor of the Main Seam (CP_C01, CP_C02, CP_O11, DME BH2) consists of siltstone and carbonaceous mudstone (Figure 3-2d). Carr (1977) suggested that the top of the Main Seam has been eroded by the overlying Aberdare Conglomerate in the Westfalen No. 3 area. Recent drilling suggests that this overlying unit is several metres above the roof of the Main seam throughout most of the mine area, and that the seam is largely intact (Figure 3-2a and b). The immediate roof of the coal seams consists of fine grained sandstone thinly interbedded with siltstone and carbonaceous mudstone and appear to conformable with the coal in CP_C01, CP_C03 and DEM BH2. These sediments are interpreted to be part of the Blackstone Formation.

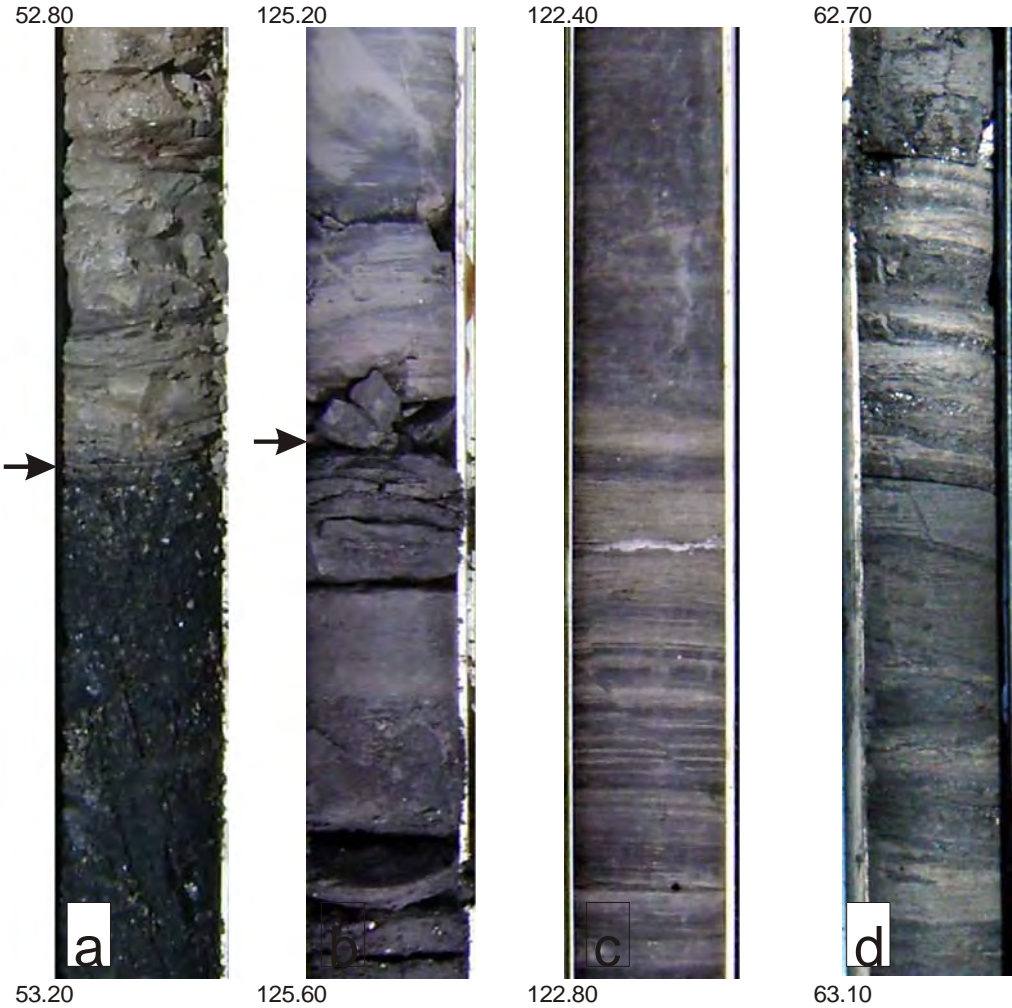


Figure 3-2. Lithologies from the Blackstone Formation. a) top of the Main Seam in CP_C01, b) top of the main seam in CP_C03, c) interbedded fine sandstone, siltstone and carbonaceous mudstone in the roof of the Main Seam (CP_C03), and d) interbedded siltstone, carbonaceous mudstone and coal bands in the floor of the Main Seam (CP_C01).

**Aberdare Conglomerate:** The Blackstone Formation is unconformably overlain by the Aberdare Conglomerate. This unit consists of pebble conglomerate, pebbly sandstone, sandstone, siltstone and carbonaceous shale, representative of a high energy fluvial

environment, most likely as a series of point-bar deposits (Cranfield et al. 1976) with a high degree of lateral variability. This unit is also represented by grey shale with needles of red iron carbonate. As discussed above, the base of this unit appears to be several metres above the roof of the Main Seam in the study area, although this is difficult to determine in the percussion holes. In DEM BH2 the grey shale is prominent. This shale was not observed in the three cored holes drilled in the most recent program with conglomerates and coarse sandstones the dominant lithologies (Figure 3-3). The thickness of bedding in this formation is very thin to medium (2 cm to 60 cm). Beds in this formation are likely to have been deposited in lenses with limited lateral continuity

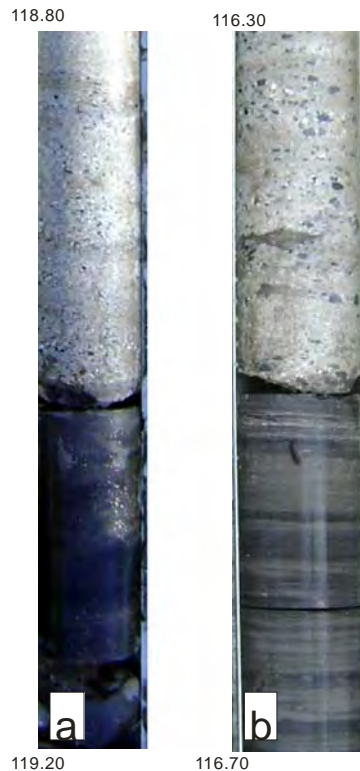


Figure 3-3. The base of the Aberdare Conglomerate and underlying Blackstone Formation in a) CP_C03 and b) CP_C04. In both cases the exact nature of this contact is obscured due to damage to the core as a result of drilling.

**Raceview Formation:** The Aberdare Conglomerate is conformably overlain by the Raceview Formation. This unit consists of fine to medium grained sandstone interbedded with siltstone and shale (Figure 3-4), indicative of a lacustrine to fluvial environment. Minor carbonaceous shales and thin coal seams are also present. The bedding in this formation is generally very thin to medium (2 cm to 60 cm). The Raceview Formation crops out through out the study area, with up to three metres of soil and alluvium cover except in the vicinity of Goodna Creek where up to 7 m of alluvium was observed. The base of weathering is at a depth of between 12 m and 20 m.

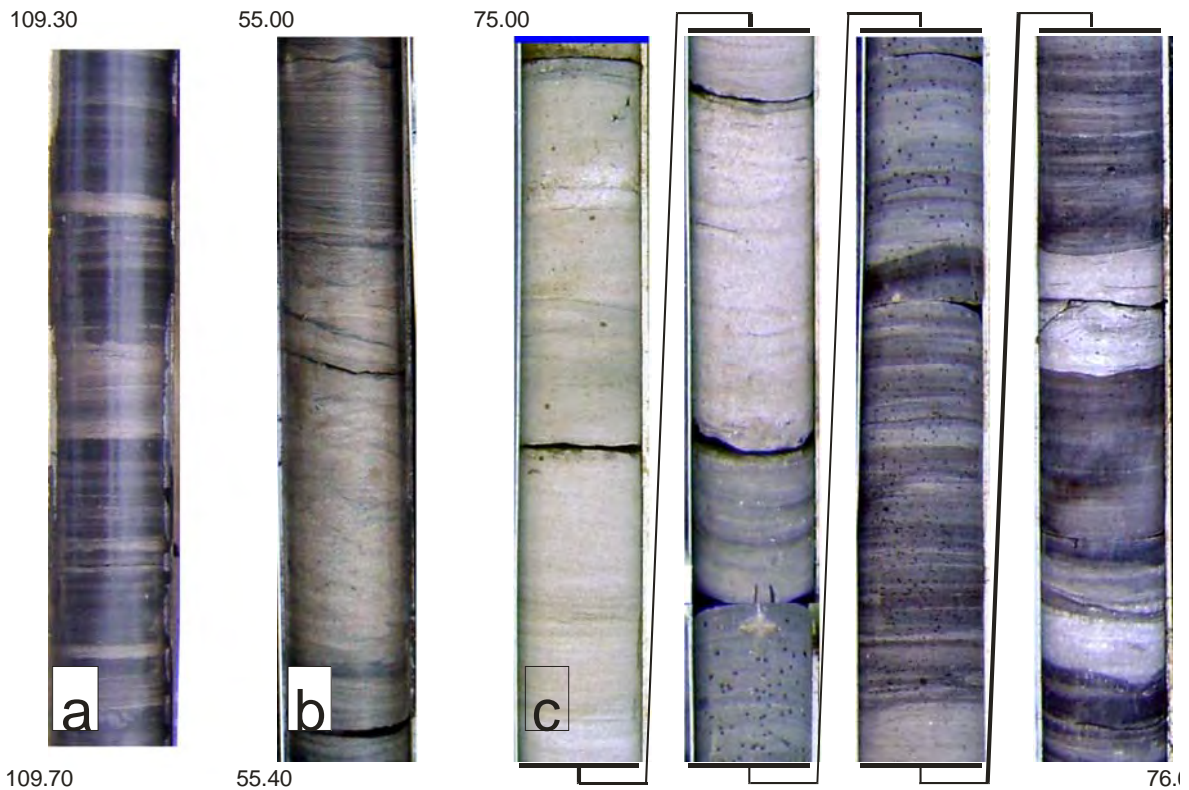


Figure 3-4. Examples of the lithologies of the Raceview formation in a) CP_C04 and b) CP_C03. c) is a 1.60m section of CP_C03 showing the variation from fine sand dominated to silt and mud dominated layers.

### Structure

The strata in the study area generally dip gently in a southerly direction. A large fault zone that defines the eastern margin of Westfalen No. 3 Colliery's workings is the most significant structure in the area. This fault zone has been interpreted as a 20 m wide series of normal faults, dipping approximately of 60° towards the east-northeast. The

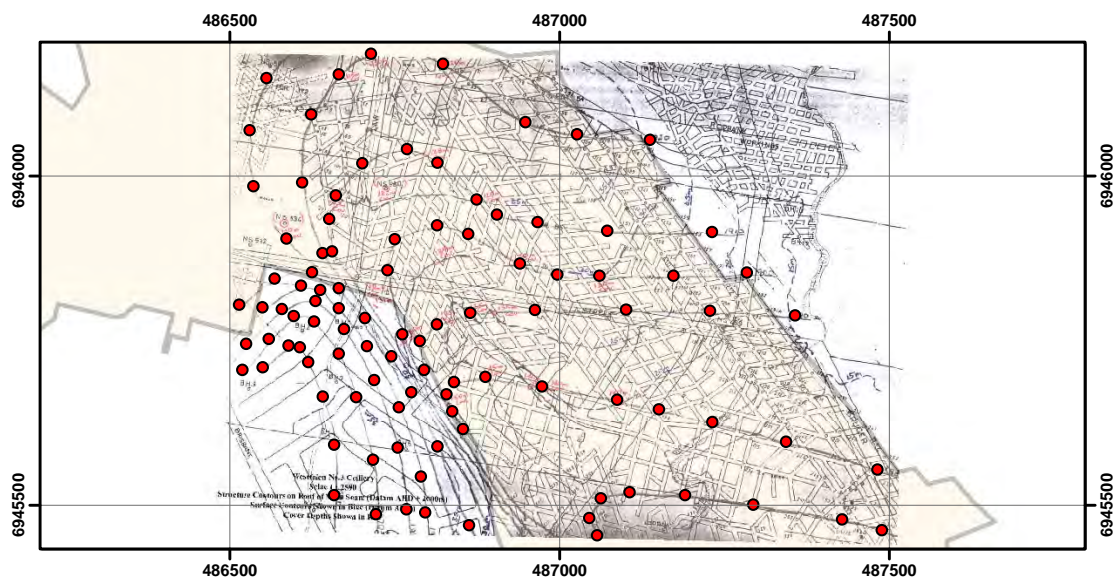


Figure 3-5. Map showing data points digitised from a contour plot of depths to the seam roof at Westfalen No. 3 Colliery

throw across the fault is up to 40 m (Maconochie and Forster, 1982). To the southwest of the Westfalen No. 3 mine workings the strata is locally domed upwards by as much as 100m. A scissor fault on the eastern margin of this dome structure was intersected in the mine workings below the intersection of Collingwood Drive and Duncan Street. This fault and the steep dips associated with the doming form the southern boundary of workings near the pit top area and the western boundary of the mine workings in the southeast of the study area. No information is available on the dip of this fault so it has been assumed to be vertical. The Waterline Fault is a structure that was intersected in the underground workings. This fault is reported to have had a moderate amount of water seepage associated with it as well as 0.5m of throw although the sense of movement has not been recorded (Maconochie and Forster 1982). The dip of the Waterline Fault is assumed to be steep to the south-west based on reported seam level and surface traces and the 3D seismic survey.

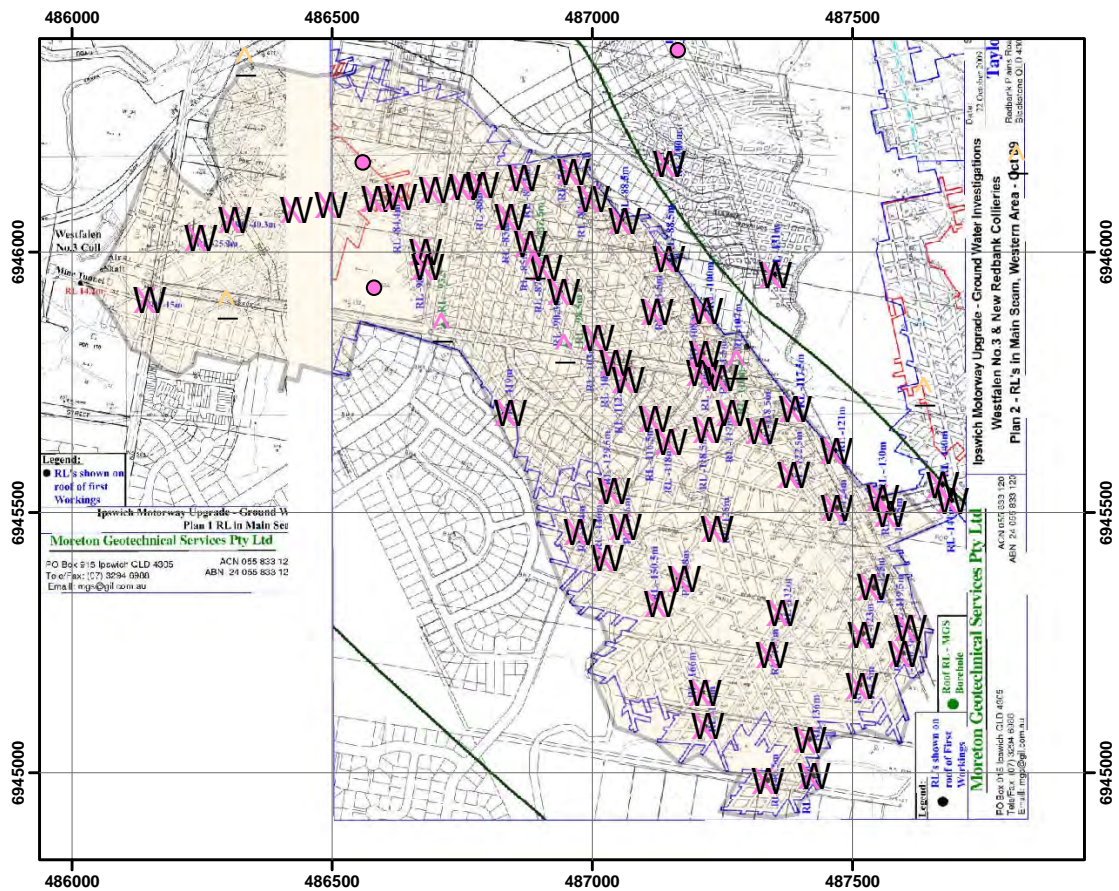


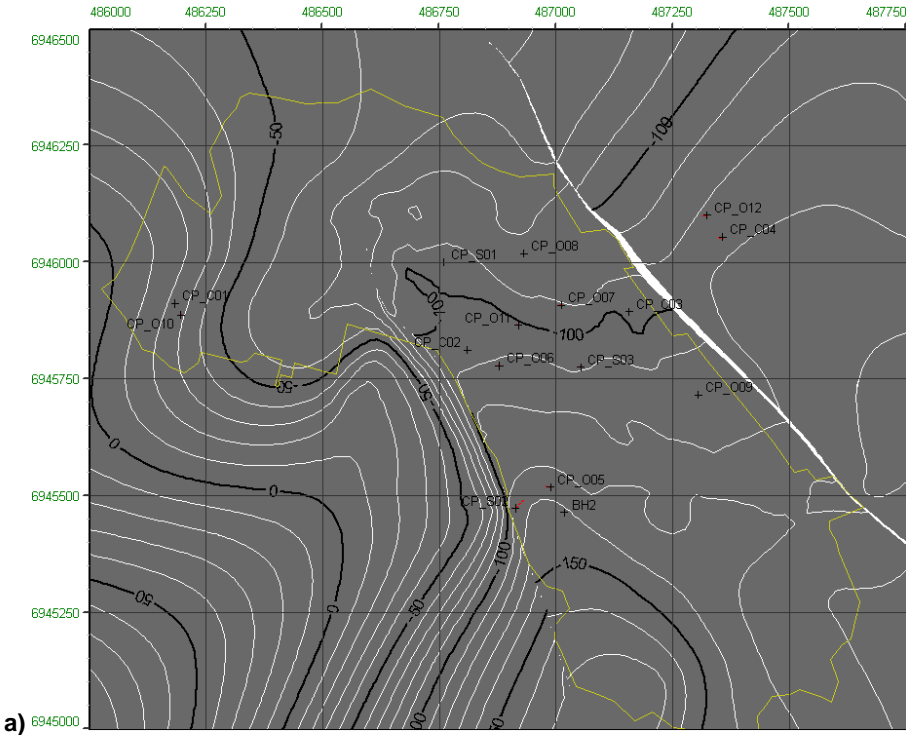
Figure 3-6. Depth to seam roof data prepared by Ken Grubb of Moreton Geotechnical Services Pty. Ltd. in 2009 for the Ipswich Motorway Upgrade. Pink diamonds represent underground survey data, pink stars represent seam roof depths from the 1994 drilling program, pink circles represent stratigraphic holes used by Grubb and orange stars represent data added in this study from regional stratigraphic holes.

Of key importance to this study is the 3D geometry of the Main Seam. This is necessary for understanding the water levels in the mine and where backfill may flow. The geometry of the Main Seam roof was modelled in the GOCAD geological modelling package (<http://www.pdgm.com/products/gocad.aspx>) incorporating all available data sets. The roof was chosen as the reference horizon as mining was from the roof down and the majority of available data is for this horizon. Results from the

drilling campaign completed by SMEC as part of the site investigations for this study are deemed to provide the most reliable data. However, the spatial distribution of this data is poor. A contour plot of unknown origin provides good coverage but its accuracy is not known (Figure 3-5). A compilation of earlier data provided by Moreton Geotechnical Services (Figure 3-6) provides good coverage of the area of interest for this study and includes underground survey data.

Two models of the Main Seam roof were built: one incorporating the historical data and the other including the results from the recent drilling activities (Figure 3-7). The modelled results show that the historical data are accurate for most of the mine with the exception of the area below the intersection of Collingwood Drive and Duncan Street. In this area the recent drilling results show that the Main Seam roof is not as deep as suggested by the roof contours (Figure 3-5) or mine survey data (Figure 3-6) by as much as 15 m. The drilling data from the recent program correlate well with data from holes drilled in the mid-1990's by Moreton Geotechnical Pty. Ltd.

A snapshot of the 3D model built of the project area is shown in Figure 3-8. An interactive version of the model is available in PDF format in the attached file (cp_3D.pdf).



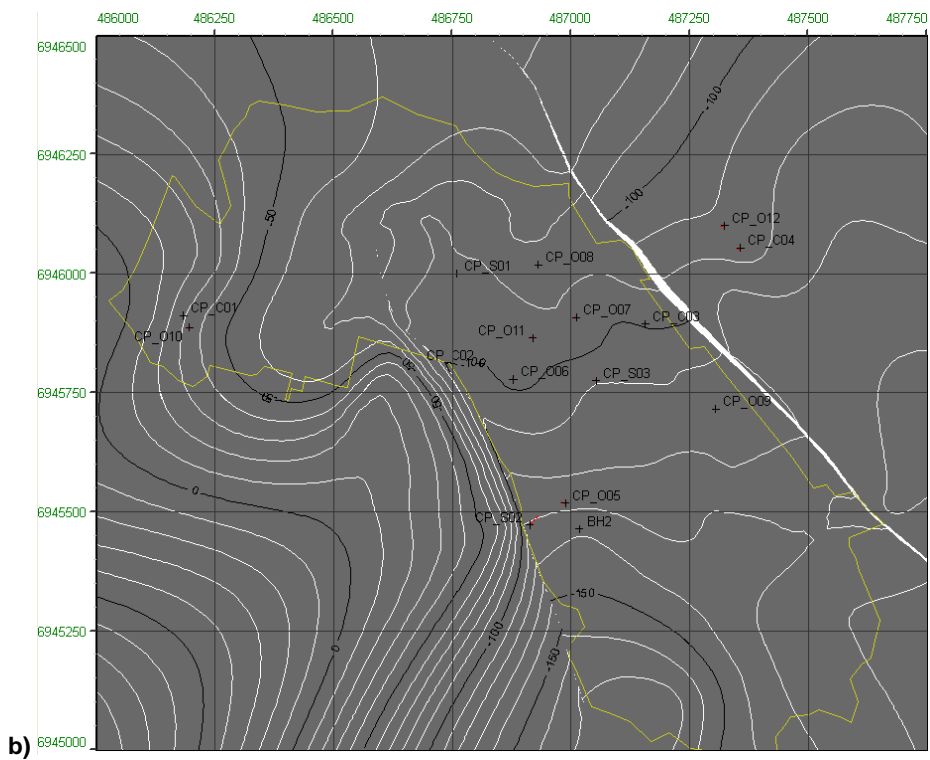


Figure 3-7. Main Seam roof contours for a) historical data and b) incorporating recent drilling results. The area of most significant difference is around CP_006. The outline of the Westfalen No. 3 Colliery's workings are shown in yellow.

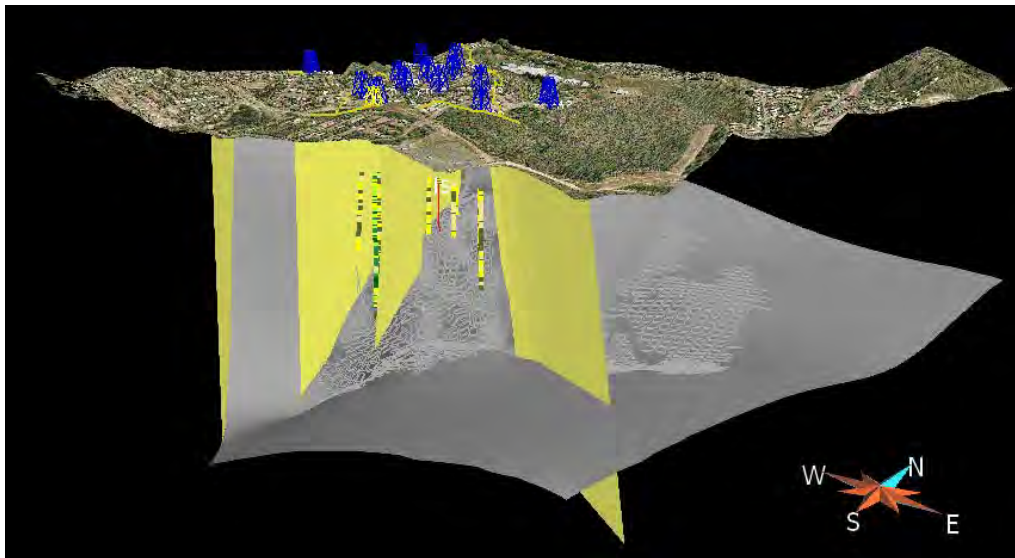


Figure 3-8. Snapshot of the 3D model of the Collingwood Park study area built in GOCAD for this project. 5 x vertical exaggeration. The grey surface is the roof of the Main Seam. Yellow surfaces are faults.

### 3.5 Piezometer monitoring

Single piezometers were installed in three boreholes, CP_C04, CP_O05 and CP_O09. CP_O05 and CP_O09 are in the Westfalen No. 3 Colliery, whereas Piezometer CP_C04 is in the New Redbank Colliery.

The aim of the piezometer monitoring is to observe the water level at the two mines over a long time period. The piezometers were located close to the bottom of the open holes and are freely suspended by their cables. Data loggers at the ground surface record the piezometric data every 30 minutes.

The data recorded up to 17 September 2010 are plotted in Figure 3-9 to Figure 3-11. All the water level data shown refer to the Reduced Level (RL, or metres above sea level).

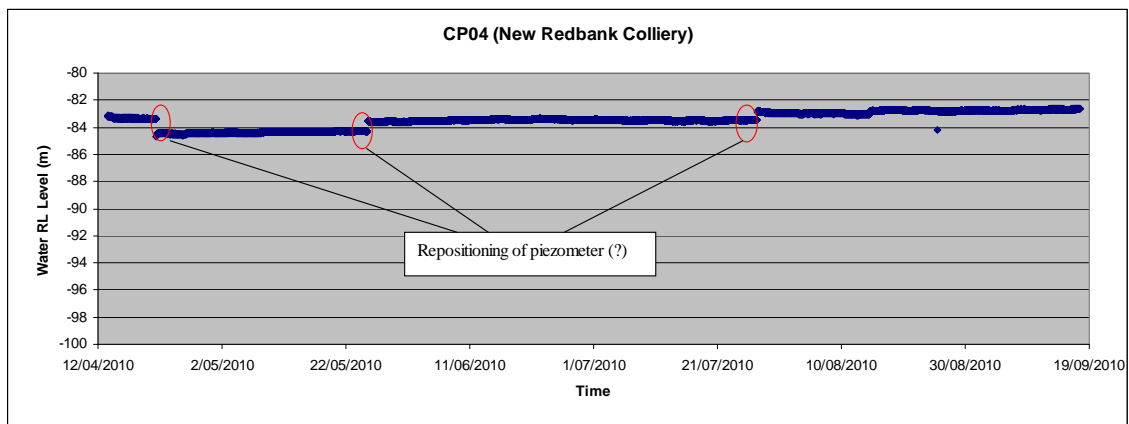


Figure 3-9. Recorded water level in Hole CP_C04, New Redbank Colliery – The water level is more or less stable at about 83m below sea level. The sudden change in the water level data is likely due to the removal and re-installation of the piezometer for water sampling.

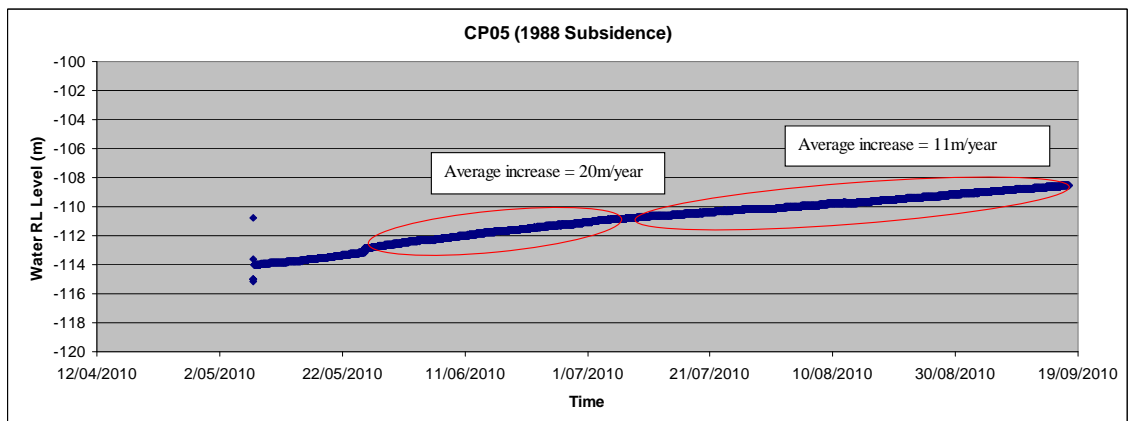


Figure 3-10. Recorded water level in Hole CP_C05, Westfalen No. 3 – The water level is increasing at a rate of about 20m/year during May to June but at a reduced rate of 11m/year during July to September.

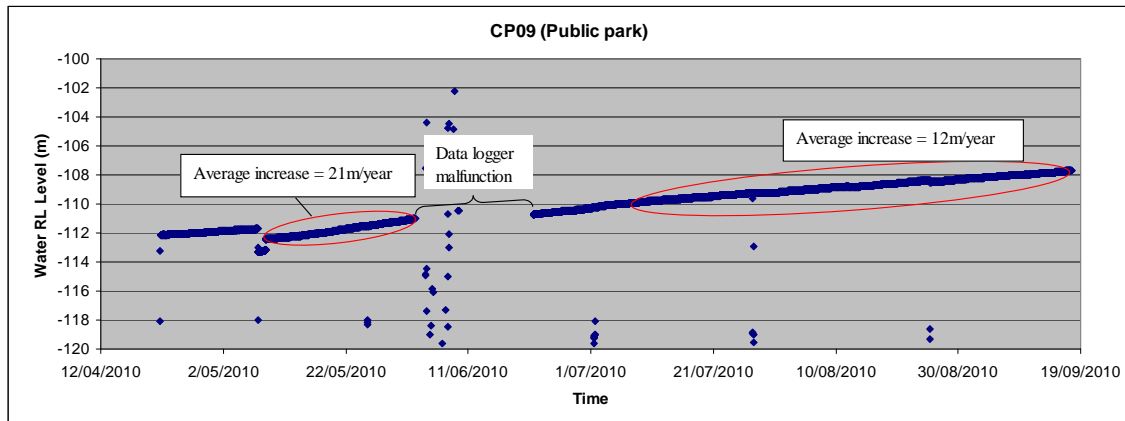


Figure 3-11. Recorded water level in Hole CP_C09, Westfalen No. 3. – about 21m/year during May to June but at a reduced rate of 12m/year during July to September.

The monitoring data up to 17 September 2010 indicate that the water level in Westfalen No. 3 Colliery was increasing at an estimated rate of 20-21m/year in May and June 2010 but that the rate was reduced to 11-12m/year during July to September. The water level on 17 September 2010 was at RL = -108m, which implies that the southern 1/3 of Westfalen No. 3 Colliery within the Collingwood Park investigation region is flooded. More detailed analysis of the water levels is given in later sections.

The water level in Westfalen No. 3 Colliery determined from this study is generally consistent with that from Mills (2010, personal communication) for the Ipswich Motorway Project. In the study by Mills (2010), a piezometer was grouted in a coal pillar in the eastern branch of the Westfalen No. 3 Colliery in September 2009. The monitored water level was -112m in mid May 2010 (Figure 3-12), compared with our result of -112 to -113m at the same time.

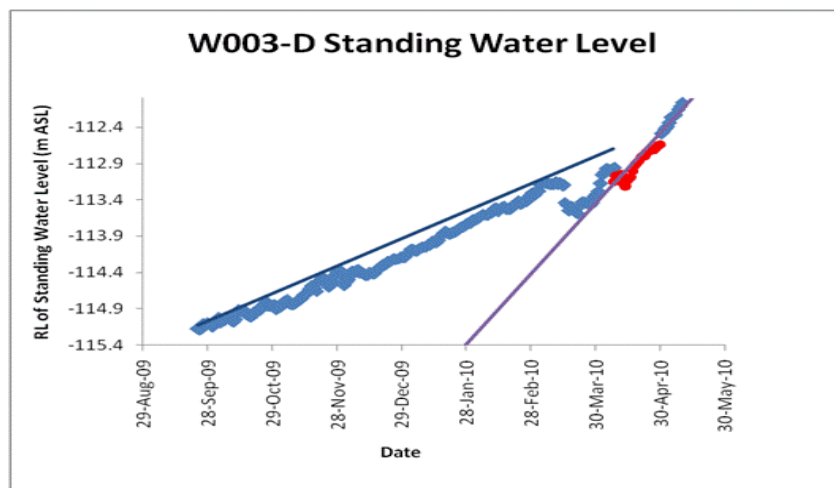


Figure 3-12. Water level in the eastern branch of Westfalen No. 3 Colliery. After Mills (2010, personal communication)

It is noticed from Mills' results that, during September 2009 – February 2010, the water level in Westfalen No. 3 Colliery was increasing steadily at a rate of about 3.5m/year. The rate significantly increased in April 2010 (Figure 3-12). Based on this study, the rate peaked at about 20m/year in May - June 2010 (Figure 3-10 and Figure 3-11), before reducing to 11-12m/year in July - September 2010.

The initial change of water level increase rate coincided with the drilling activities at Collingwood Park. It is possible that the new drill holes led to water leakage from perched aquifers in the overburden to the underground workings which caused a faster increase in the water level. With time however, the water flow into the drill holes may have reduced as the aquifers around them were drained. This would reduce the rate of water level change as observed during July to September 2010.

Another explanation could be rainfall events. There were several significant rainfall events in February and March and these months had more than double their long term average rainfall in 2010. The rain water might have found its way into the mine and caused a faster increase in the mine water level.

In the New Redbank Colliery, the current water level is at RL= -83m, and it has remained stable so far. The sudden changes in the plot of Figure 3-10 were likely to be caused by the relocation of the piezometer which was removed and re-installed during water sampling. The removal of the piezometer is necessary as this hole was drilled at a smaller diameter (100 mm) than the other piezometer holes.

The stable water level at New Redbank Colliery was not expected considering that a large amount of water inflow was observed in the two boreholes (CP_O12 and CP_C02) drilled in this mine. There may be a path for water to flow out of the mine, possibly through the barrier pillars, to the Westfalen No. 3 Colliery. Note that the water level in the New Redbank Colliery is about 30m higher than that at Westfalen No. 3 Colliery, implying that water seepage between the two mines are possible.

The workings of the New Redbank Colliery are flooded at least in the area of boreholes CP_O12 and CP_C02. The mine workings in this area are at an RL of approximately -110m, well below the current water level. Further studies are required to develop a comprehensive hydrological model of the underground water in these two areas.

### **3.6 Water effect on pillar stability**

Water in the mine may have two opposite effects on long and short term pillar stability. On the negative side, it may reduce the cohesion and internal friction angle of the coal mass, and hence reduce the pillar strength. It could also exacerbate the spalling process by washing away material at the edges of pillars, reducing the pillar size. On the positive side, and considering only short term stability, the applied gravity load on a submerged pillar can be reduced by the upward water buoyancy forces acting on the coal seam roof and overburden strata. Hence, its short term Factor of Safety (FoS) can increase, if we assume that there is no reduction in the strength properties due to the presence of water.

Overall, the effect of water on long-term pillar strength and stability is largely unknown and requires further study. However, it may help to understand the significance of this process by examining the water level at the time of the 2008 subsidence event.

Mills (2009) reports that the water level in Westfalen No. 3 was at RL=-115m and was increasing at an average rate of 3.5m/year during the time period between 23 September to 14 October 2009. If this rate was also persistent during the period between April 2008 to October 2009, the water level in Westfalen No. 3 Colliery is expected to have been RL=-120m on April 2008, the time when the latest subsidence event occurred.

Using the seam floor contour map provided by Mills (2009) based on underground survey data, at this mine water level (RL=-120m), most of the pillars in the 2008 subsided area should be above the water table with exceptions of some pillars which might have started to experience just becoming wet at the floor level, as shown in Figure 3-13.

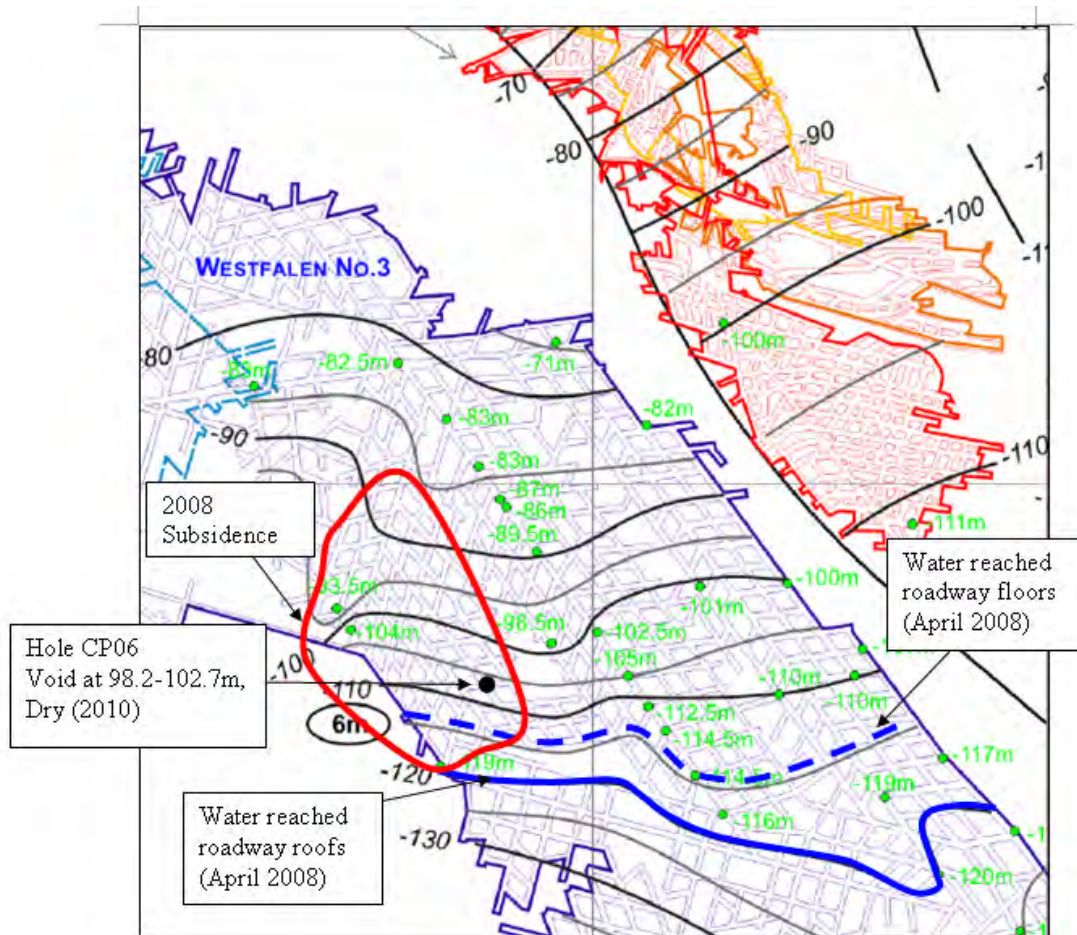


Figure 3-13. Predicted water level in Westfalen No. 3 Colliery at the time of the 2008 subsidence events based on data from Mills (2009).

The data from the recently completed drilling and observation records at borehole CP_O06 in the subsided area confirms that the central part of the 2008 subsidence was dry in April 2010.

The seam floor contours derived from the previous and new drill hole data are different from those based on the underground survey data (Figure 3-14). Overall, the drill hole data suggest that the floor level in the 2008 subsidence area is about 10m-14m higher than the survey data suggest. Some doubts about the survey data accuracy were also expressed by the previous mine managers during an interview.

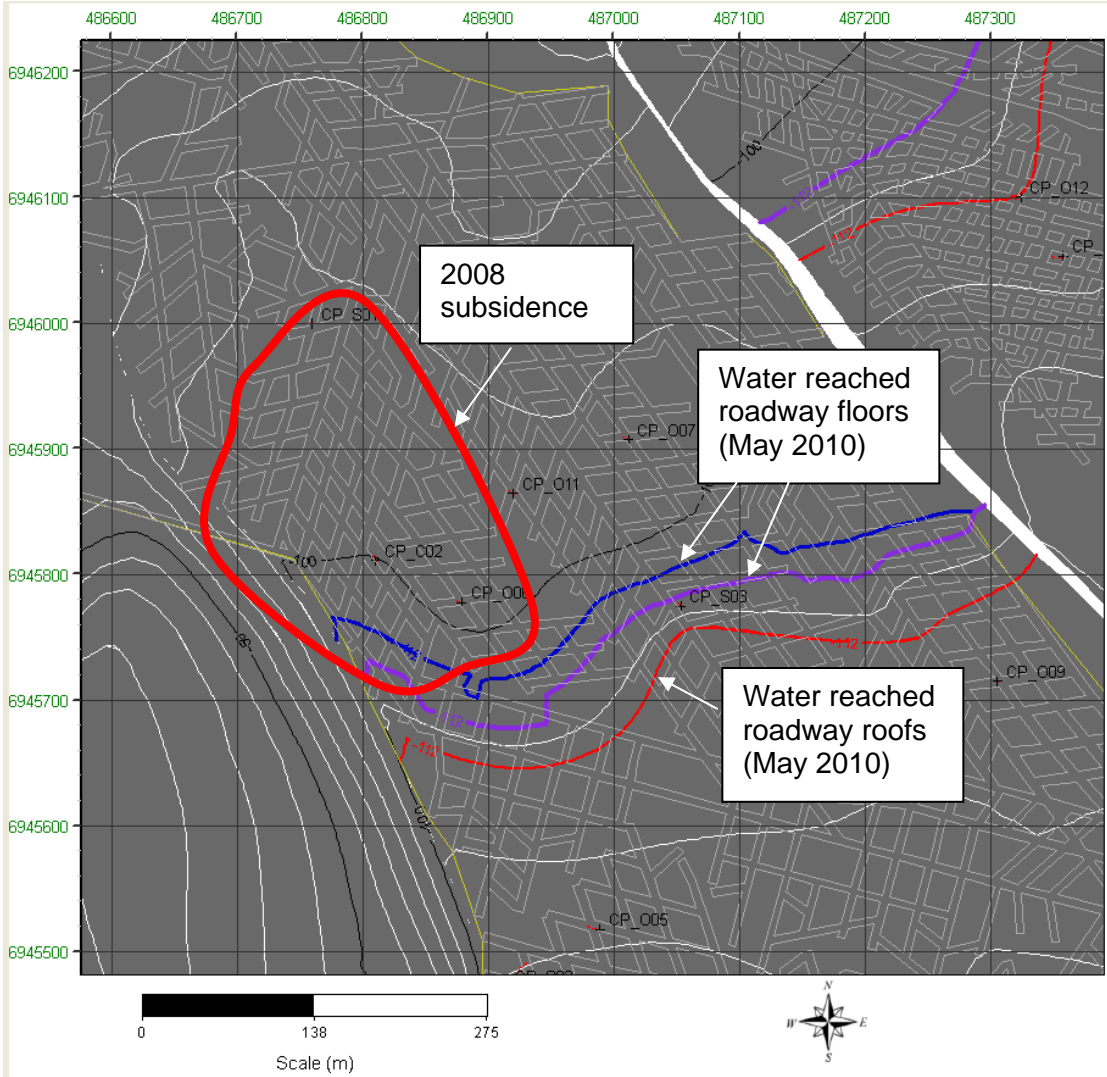


Figure 3-14. Depth contours (RL level) of seam roof and predicted water level in Westfalen No. 3 Colliery as at May 2010, based on recent drill hole data. The blue and purple lines provide the estimated water level at the roadway floor, based on the mining height ranges presented in Figure 6-3.

Based on the drill hole roof contours, the extents of water level in May 2010 is shown in Figure 3-14. This result suggests that all pillars in the 2008 subsidence area were basically above the water table at the time of the subsidence event if the water levels have not decreased, which is considered highly unlikely.

This result may indicate that mine water was unlikely to be the crucial factor contributing to the initiation of the 2008 subsidence event, although the overall effect of water on panel stability is still unknown and should never be ignored.

With the current water rising at a rate of approximately 11-12m/year, it can be expected that the Westfalen No. 3 Colliery will be flooded in 3-4 years however a longer period of water level monitoring is required to confirm the long term trend. It is therefore very important to understand the effect of water by further research.

### **3.7 Extensometer monitoring**

One deep hole surface extensometer was installed in Hole CP_O07 on 9 August 2010 to monitor any movement of the underground strata. The extensometer monitoring is complimentary to the microseismic monitoring that detects sudden rock fracturing events from seismic waves. The extensometer will be able to detect slow strata movements, which cannot be detected by the microseismic network's geophones.

Since borehole CP_O07 is located inside the central high-risk zone at Westfalen No. 3 Colliery (see Chapter 6 for details), it is best suited for the extensometer installation and monitoring.

The extensometer has 20 anchors that are distributed across the entire depth of the borehole. The depths of the anchors are given in Table 3-4.

Each anchor is firmly attached to the borehole wall, and has a thin steel wire linking it to the headframe on top of the borehole. When the strata move, they bring the anchor with them and hence move the wire in the headframe. The potentiometer linked with the wire in the headframe then transfers the wire displacement to an electronic signal that is recorded by a data logger.

Each anchor records the relative displacement between its host rock stratum and the ground surface. After knowing the relative displacements from all 20 anchors to the ground surface, the relative displacements between different anchors (or strata) are known.

Table 3-4. Anchor depth of the extensometer installed in hole CP_O07.

Anchor No.	Depth in hole (m)	Distance above roadway roof (m)
20	20	107
19	30	97
18	40	87
17	50	77
16	60	67
15	65	62
14	70	57
13	75	52
12	80	47
11	85	42
10	90	37
9	95	32
8	100	27
7	105	22
6	110	17
5	114	13
4	118	9
3	121	6
2	124	3
1	126.5	0.5
Roadway roof	127.0	0

The extensometer monitoring results at Collingwood Park are shown in Figure 3-15 and Figure 3-16. During the monitored period of 9 August to 24 September 2010, the extensometer results showed a maximum displacement of 8mm between the seam roof and the ground surface (Figure 3-15). The movement has been increasing at approximately 1mm per week. The displacement occurred mostly in the depth zones of 0-20m and 60-100m.

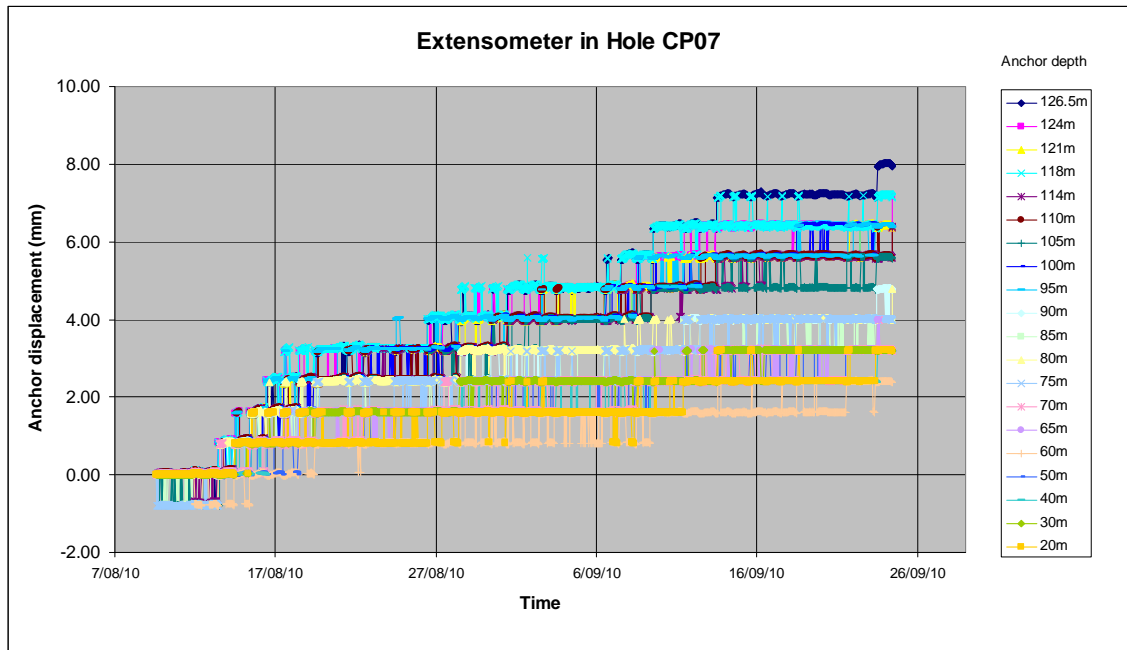


Figure 3-15. Extensometer readings during 8 August – 24 September 2010.

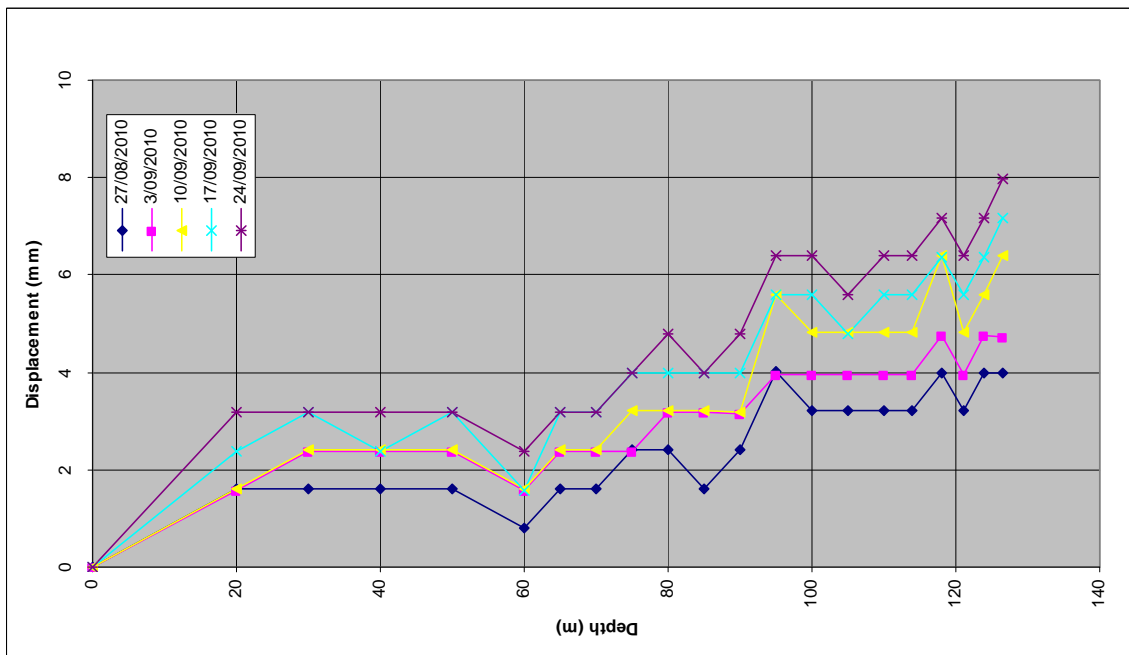


Figure 3-16. Profile of strata movement in overburden strata recoded in CP_O07 during August – September 2010.

Although the monitored strata movement is still small, the trend of the data clearly suggests that the overburden strata are “expanding”, ie the strata close to the seam are moving downward relative to the ground surface which may also be moving. This kind of movement is often observed in the early stage of a panel failure when strata

near the excavation start to deform. The displacement may then propagate to the ground surface at a later stage forming surface subsidence.

The short data duration and small magnitude of displacement do not yet provide high confidence that the pillars/panel in the vicinity of Hole CP_O07 are indeed deforming or creeping. If the trend is verified by future monitoring data, its implication could be very significant. It could indicate that the central region identified as high risk zone in Westfalen No. 3 Colliery may be moving toward an instability.

The extensometer data need to be closely monitored and interpreted. If the strata deformation continues to increase, we recommend the following actions:

- Install two additional extensometers close to either ends of the Central Panel to determine the size of the area with movement
- Install one additional geophone station close to CP_O07 to help detect and locate small seismic events in the Central Panel
- Increase the data analysis frequency (both extensometer and microseismic data) to minimum twice a week if significant increase in the rate of displacement and seismicity is observed
- DEEDI considers developing a response plan for any potential mine subsidence events.

### **3.8 Water sampling and analysis**

Water samples have been scheduled for collection from three boreholes (CP_C04, CP_O05, CP_O09) every 1-2 months for a total period of six months. The samples will be analysed for composition and general parameters so that any changes over time can be determined. The objective of the groundwater investigation is to determine quality of the water in the mine voids, and to possibly trace the source of the mine water. To date, four sets of samples have been collected on 21 April, 25 May, 1 July, and 25 August respectively and analysed by ALS Laboratory Group.

The initial suite of tests are:

- pH
- Electrical conductivity (EC)
- Major cations and anion
- 27 Metals
- Total petroleum hydrocarbons

Further in-situ water quality tests have been added and completed using a TPS 90 FL-T Field Lab. These include:

- pH
- Electrical conductivity
- Oxygen

- Temperature

Table 3-5 - Table 3-8 summarise the analysis results of all the samples.

Table 3-5. Water analysis results for samples collected on 21 April 2010.

Analytical Results			Client sample ID			
Sub-Matrix: WATER			Client sampling date / time			
			CPC04	CPC05	CPC09	QC1
			21-APR-2010 15:00	21-APR-2010 15:00	21-APR-2010 15:00	21-APR-2010 15:00
			EB1007042-001	EB1007042-002	EB1007042-003	EB1007042-004
Compound	CAS Number	LOR Unit				
<b>EA005: pH</b>						
pH Value		0.01 pH Unit	7.40	7.40	7.88	7.75
<b>EA010P: Conductivity by PC Titrator</b>						
Electrical Conductivity @ 25°C		1 µS/cm	6150	9570	8070	9180
<b>ED037P: Alkalinity by PC Titrator</b>						
Hydroxide Alkalinity as CaCO3	DMO-210-001	1 mg/L	<1	<1	<1	<1
Carbonate Alkalinity as CaCO3	3812-32-6	1 mg/L	<1	<1	<1	<1
Bicarbonate Alkalinity as CaCO3	71-52-3	1 mg/L	569	593	523	565
Total Alkalinity as CaCO3		1 mg/L	569	593	522	566
<b>ED040F: Dissolved Major Anions</b>						
Sulfate as SO4 2-	14808-79-8	1 mg/L	54	337	143	112
<b>ED045G: Chloride Discrete analyser</b>						
Chloride	16887-00-6	1 mg/L	1630	3330	2610	2640
<b>ED093F: Dissolved Major Cations</b>						
Calcium	7440-70-2	1 mg/L	86	139	49	52
Magnesium	7438-95-4	1 mg/L	98	222	29	30
Sodium	7440-23-5	1 mg/L	1220	1830	1770	1770
Potassium	7440-09-7	1 mg/L	9	20	10	10
<b>EG094F: Dissolved Metals in Fresh Water by ORC-ICPMS</b>						
Aluminium	7429-90-5	5 µg/L	<5	<5	<5	<5
Iron	7439-89-6	2 µg/L	68	462	111	8
Antimony	7440-36-0	0.2 µg/L	<0.2	<0.2	<0.2	<0.2
Selenium	7782-49-2	0.2 µg/L	<0.2	<0.2	<0.2	<0.2
Arsenic	7440-39-2	0.2 µg/L	0.3	0.9	1.9	1.7
Barium	7440-39-3	0.5 µg/L	2080	131	1180	1370
Beryllium	7440-41-7	0.1 µg/L	<0.1	<0.1	<0.1	<0.1
Boron	7440-42-8	5 µg/L	1410	764	1530	1560
Bismuth	7440-89-9	0.05 µg/L	<0.05	<0.05	<0.05	<0.05
Cadmium	7440-43-9	0.05 µg/L	<0.05	<0.05	<0.05	<0.05
Chromium	7440-47-3	0.2 µg/L	<0.2	<0.2	<0.2	<0.2
Cobalt	7440-48-4	0.1 µg/L	<0.1	0.1	5.0	4.8
Copper	7440-50-8	0.5 µg/L	<0.5	<0.5	1.1	1.1
Lead	7439-92-1	0.1 µg/L	0.1	0.3	0.1	0.1
Lithium	7439-93-2	0.5 µg/L	111	171	121	124
Manganese	7439-96-5	0.5 µg/L	51.9	29.8	28.4	24.3
Molybdenum	7439-98-7	0.1 µg/L	0.2	0.8	6.4	5.4
Nickel	7440-02-0	0.5 µg/L	<0.5	3.1	5.6	5.4
Silver	7440-22-4	0.1 µg/L	<0.1	<0.1	<0.1	<0.1
<b>EG094F: Dissolved Metals in Fresh Water by ORC-ICPMS - Continued</b>						
Strontium	7440-24-6	1 µg/L	2920	4940	3450	3480
Thallium	7440-29-0	0.02 µg/L	<0.02	0.04	<0.02	<0.02
Thorium	7440-29-1	0.1 µg/L	<0.1	<0.1	<0.1	<0.1
Tin	7440-31-5	0.2 µg/L	0.2	0.2	<0.2	<0.2
Titanium	7440-32-6	1 µg/L	<1	<1	<1	<1
Uranium	7440-61-1	0.05 µg/L	<0.05	0.14	0.11	0.11
Vanadium	7440-63-2	0.2 µg/L	0.3	0.3	0.4	0.5
Zinc	7440-66-6	1 µg/L	29	53	209	138
<b>EN055: Ionic Balance</b>						
△ Total Anions		0.01 meq/L	59.4	113	87.0	88.2
△ Total Cations		0.01 meq/L	61.3	106	82.2	82.2
△ Ionic Balance		%	2.44	3.31	2.84	3.63
<b>EP080/074: Total Petroleum Hydrocarbons</b>						
C6 - C9 Fraction		20 µg/L	<20	99	<20	<20
C10 - C14 Fraction		50 µg/L	<50	<50	<50	<50
C15 - C28 Fraction		100 µg/L	<100	<100	<100	<100
C28 - C36 Fraction		50 µg/L	<50	<50	<50	<50
△ C10 - C36 Fraction (sum)		50 µg/L	<50	<50	<50	<50
<b>EP080S: TPH(V)/BTEX Surrogates</b>						
1,2-Dichloroethane-D4	17060-07-0	0.1 %	105	108	113	109
Toluene-D8	2037-26-5	0.1 %	96.7	108	100	94.8
4-Bromofluorobenzene	460-00-4	0.1 %	96.3	101	98.4	96.1

Table 3-6. Water analysis results for samples collected on 25 May 2010.

Analytical Results									
Sub-Matrix: WATER									
Client sample ID									
Client sampling date / time									
CP C004									
CP C005									
CP C009									
QC01									
-----									
Compound	CAS Number	LOR	Unit	EB1009279-001	EB1009279-002	EB1009279-003	EB1009279-004	-----	-----
<b>EA005: pH</b>									
pH Value	---	0.01	pH Unit	7.58	7.57	7.53	7.51	-----	-----
<b>EA010P: Conductivity by PC Titrator</b>									
Electrical Conductivity @ 25°C	---	1	µS/cm	6720	10200	8360	8360	-----	-----
<b>ED037P: Alkalinity by PC Titrator</b>									
Hydroxide Alkalinity as CaCO ₃	DMO-210-001	1	mg/L	<1	<1	<1	<1	-----	-----
Carbonate Alkalinity as CaCO ₃	3812-32-6	1	mg/L	<1	<1	<1	<1	-----	-----
Bicarbonate Alkalinity as CaCO ₃	71-52-3	1	mg/L	578	609	537	552	-----	-----
Total Alkalinity as CaCO ₃	---	1	mg/L	578	609	537	552	-----	-----
<b>ED040F: Dissolved Major Anions</b>									
Sulfate as SO ₄ 2-	14808-79-8	1	mg/L	44	346	146	142	-----	-----
<b>ED045G: Chloride Discrete analyser</b>									
Chloride	16887-00-6	1	mg/L	1890	3270	2670	2640	-----	-----
<b>ED083F: Dissolved Major Cations</b>									
Calcium	7440-70-2	1	mg/L	62	140	48	50	-----	-----
Magnesium	7439-95-4	1	mg/L	48	219	28	29	-----	-----
Sodium	7440-23-5	1	mg/L	1360	1840	1780	1780	-----	-----
Potassium	7440-09-7	1	mg/L	8	19	10	10	-----	-----
<b>EG094F: Dissolved Metals in Fresh Water by ORC-ICPMS</b>									
Aluminium	7429-90-5	5	µg/L	<5	<5	7	7	-----	-----
Iron	7439-89-6	2	µg/L	451	722	9	9	-----	-----
Antimony	7440-36-0	0.2	µg/L	<0.2	<0.2	<0.2	<0.2	-----	-----
Selenium	7782-49-2	0.2	µg/L	<0.2	<0.2	<0.2	<0.2	-----	-----
Arsenic	7440-38-2	0.2	µg/L	0.2	1.2	1.5	1.5	-----	-----
Barium	7440-39-3	0.5	µg/L	1850	62.7	554	644	-----	-----
Beryllium	7440-41-7	0.1	µg/L	<0.1	<0.1	<0.1	<0.1	-----	-----
Boron	7440-42-8	5	µg/L	1580	778	1490	1510	-----	-----
Bismuth	7440-69-9	0.05	µg/L	<0.05	<0.05	<0.05	<0.05	-----	-----
Cadmium	7440-43-9	0.05	µg/L	<0.05	<0.05	0.14	0.09	-----	-----
Chromium	7440-47-3	0.2	µg/L	0.2	0.3	0.6	0.4	-----	-----
Cobalt	7440-48-4	0.1	µg/L	<0.1	0.2	3.2	3.3	-----	-----
Copper	7440-50-8	0.5	µg/L	<0.5	<0.5	3.9	1.4	-----	-----
Lead	7439-92-1	0.1	µg/L	<0.1	0.2	0.3	0.3	-----	-----
Lithium	7439-93-2	0.5	µg/L	109	182	130	128	-----	-----
Manganese	7439-96-5	0.5	µg/L	49.6	30.9	14.6	15.2	-----	-----
Molybdenum	7439-98-7	0.1	µg/L	0.2	0.9	1.4	1.5	-----	-----
Nickel	7440-02-0	0.5	µg/L	1.1	0.8	6.4	4.7	-----	-----
Silver	7440-22-4	0.1	µg/L	<0.1	0.1	<0.1	<0.1	-----	-----
<b>EG094F: Dissolved Metals in Fresh Water by ORC-ICPMS - continued</b>									
Strontium	7440-24-6	1	µg/L	2920	5050	3220	3280	-----	-----
Tellurium	25541-49-7	0.2	µg/L	<0.2	0.3	<0.2	<0.2	-----	-----
Thallium	7440-28-0	0.02	µg/L	0.14	0.05	0.02	0.03	-----	-----
Thorium	7440-29-1	0.1	µg/L	<0.1	<0.1	<0.1	<0.1	-----	-----
Tin	7440-31-5	0.2	µg/L	<0.2	<0.2	<0.2	<0.2	-----	-----
Titanium	7440-32-6	1	µg/L	<1	<1	<1	<1	-----	-----
Uranium	7440-61-1	0.05	µg/L	<0.05	0.15	0.07	0.07	-----	-----
Vanadium	7440-82-2	0.2	µg/L	0.3	0.5	0.6	0.6	-----	-----
Zinc	7440-66-6	1	µg/L	31	2	87	64	-----	-----
<b>EN055: Ionic Balance</b>									
^ Total Anions	---	0.01	meq/L	65.8	112	89.1	88.5	-----	-----
^ Total Cations	---	0.01	meq/L	66.3	105	81.4	82.7	-----	-----
^ Ionic Balance	---	0.01	%	0.40	2.84	4.54	3.39	-----	-----

Table 3-7. Water analysis results for samples collected on 1 July 2010.

Analytical Results				CP 04	CP 05	CP 09	QC 01	---
Sub-Matrix: WATER				01-JUL-2010 15:00	01-JUL-2010 15:00	01-JUL-2010 15:00	01-JUL-2010 15:00	---
Client sample ID				EB1011592-001	EB1011592-002	EB1011592-003	EB1011592-004	---
Client sampling date / time				EB1011592-001	EB1011592-002	EB1011592-003	EB1011592-004	---
Compound	CAS Number	LOR	Unit	EB1011592-001	EB1011592-002	EB1011592-003	EB1011592-004	---
<b>EA005: pH</b>								
pH Value	---	0.01	pH Unit	7.48	7.34	7.51	7.64	---
<b>EA010P: Conductivity by PC Titrator</b>								
Electrical Conductivity @ 25°C	---	1	µS/cm	6320	10200	8450	6530	---
<b>ED037P: Alkalinity by PC Titrator</b>								
Hydroxide Alkalinity as CaCO3	DMO-210-001	1	mg/L	<1	<1	<1	<1	---
Carbonate Alkalinity as CaCO3	3812-32-6	1	mg/L	<1	<1	<1	<1	---
Bicarbonate Alkalinity as CaCO3	71-52-3	1	mg/L	583	624	554	412	---
Total Alkalinity as CaCO3	---	1	mg/L	583	624	554	412	---
<b>ED040F: Dissolved Major Anions</b>								
Sulfate as SO4 2-	14808-79-8	1	mg/L	56	340	133	50	---
<b>ED045G: Chloride Discrete analyser</b>								
Chloride	16887-00-6	1	mg/L	1860	3460	2890	1870	---
<b>ED093F: Dissolved Major Cations</b>								
Calcium	7440-70-2	1	mg/L	85	129	48	62	---
Magnesium	7439-95-4	1	mg/L	57	217	26	53	---
Sodium	7440-23-5	1	mg/L	1330	1960	1960	1380	---
Potassium	7440-09-7	1	mg/L	10	21	12	10	---
<b>EG094F: Dissolved Metals in Fresh Water by ORC-ICPMS</b>								
Aluminium	7429-90-5	5	µg/L	<5	<5	<5	<5	---
Iron	7439-89-6	2	µg/L	332	320	105	335	---
Antimony	7440-36-0	0.2	µg/L	<0.2	<0.2	<0.2	<0.2	---
Selenium	7782-49-2	0.2	µg/L	<0.2	<0.2	<0.2	<0.2	---
Arsenic	7440-38-2	0.2	µg/L	0.4	1.1	1.9	0.4	---
Barium	7440-39-3	0.5	µg/L	2910	46.6	1170	3000	---
Beryllium	7440-41-7	0.1	µg/L	<0.1	<0.1	<0.1	<0.1	---
Boron	7440-42-8	5	µg/L	1350	685	1310	1430	---
Bismuth	7440-69-9	0.05	µg/L	<0.05	<0.05	<0.05	<0.05	---
Cadmium	7440-43-9	0.05	µg/L	0.06	0.08	0.10	0.07	---
Chromium	7440-47-3	0.2	µg/L	<0.2	0.2	0.3	<0.2	---
Cobalt	7440-48-4	0.1	µg/L	<0.1	0.6	11.1	<0.1	---
Copper	7440-50-8	0.5	µg/L	<0.5	<0.5	1.9	<0.5	---
Lead	7439-92-1	0.1	µg/L	0.3	0.6	0.4	0.3	---
Lithium	7439-93-2	0.5	µg/L	86.4	144	111	91.0	---
Manganese	7439-96-5	0.5	µg/L	35.9	29.0	50.9	34.8	---
Molybdenum	7439-98-7	0.1	µg/L	0.2	1.0	3.5	0.2	---
Nickel	7440-02-0	0.5	µg/L	<0.5	1.2	4.3	<0.5	---
Silver	7440-22-4	0.1	µg/L	<0.1	0.1	0.1	<0.1	---
<b>EG094F: Dissolved Metals in Fresh Water by ORC-ICPMS - Continued</b>								
Strontium	7440-24-6	1	µg/L	3430	5260	3720	3440	---
Tellurium	22541-49-7	0.2	µg/L	0.2	0.2	0.2	<0.2	---
Thallium	7440-28-0	0.02	µg/L	<0.02	<0.02	<0.02	<0.02	---
Thorium	7440-29-1	0.1	µg/L	<0.1	<0.1	<0.1	<0.1	---
Tin	7440-31-5	0.2	µg/L	0.2	0.7	0.4	0.2	---
Titanium	7440-32-6	1	µg/L	<1	<1	<1	<1	---
Uranium	7440-61-1	0.05	µg/L	<0.05	0.16	0.08	<0.05	---
Vanadium	7440-62-2	0.2	µg/L	0.4	0.2	0.4	0.4	---
Zinc	7440-66-6	1	µg/L	12	13	179	13	---
<b>EM055: Ionic Balance</b>								
* Total Anions	---	0.01	meq/L	65.3	117	95.4	62.0	---
* Total Cations	---	0.01	meq/L	66.0	110	90.1	67.8	---
* Ionic Balance	---	0.01	%	0.54	3.10	2.85	4.42	---
<b>EP080/071: Total Petroleum Hydrocarbons</b>								
C6 - C9 Fraction	---	20	µg/L	<20	140	20	---	---
C10 - C14 Fraction	---	50	µg/L	<50	<50	<50	---	---
C15 - C28 Fraction	---	100	µg/L	<100	<100	370	---	---
C29 - C36 Fraction	---	50	µg/L	<50	<50	60	---	---
* C10 - C36 Fraction (sum)	---	50	µg/L	<50	<50	430	---	---
<b>EP080S: TPH(V)/BTEX Surrogates</b>								
1,2-Dichloroethane-D4	17060-07-0	0.1	%	125	89.9	91.5	---	---
Toluene-D8	2037-26-5	0.1	%	110	102	107	---	---
4-Bromofluorobenzene	460-00-4	0.1	%	110	97.1	97.3	---	---

Table 3-8. Water analysis results for samples collected on 1 July 2010. Samples were only collected from CP_O04 and CP_O09. Hole CP_O05 was decided not to collect samples in order to protect the borehole stability.

Analytical Results				Client sample ID			QC 01		CP 04		CP 09			
Sub-Matrix: WATER				Client sampling date / time			25-AUG-2010 11:00		25-AUG-2010 11:00		25-AUG-2010 11:00			
Compound	CAS Number	LOR	Unit	EB1015075-001		EB1015075-002		EB1015075-003						
<b>EA005: pH</b>														
pH Value		0.01	pH Unit	7.56	7.67	7.53								
<b>EA010P: Conductivity by PC Titrator</b>														
Electrical Conductivity @ 25°C		1	µS/cm	6450	6420	7590								
<b>ED037P: Alkalinity by PC Titrator</b>														
Hydroxide Alkalinity as CaCO ₃	DMO-210-001	1	mg/L	<1	<1	<1								
Carbonate Alkalinity as CaCO ₃	3812-32-6	1	mg/L	<1	<1	<1								
Bicarbonate Alkalinity as CaCO ₃	71-52-3	1	mg/L	571	567	541								
Total Alkalinity as CaCO ₃		1	mg/L	571	567	541								
<b>EDM40F: Dissolved Major Anions</b>														
Sulfate as SO ₄ 2-	14806-79-8	1	mg/L	45	44	153								
<b>EDM45G: Chloride Discrete analyser</b>														
Chloride	16887-00-6	1	mg/L	2380	2290	2760								
<b>ED083F: Dissolved Major Cations</b>														
Calcium	7440-70-2	1	mg/L	67	67	51								
Magnesium	7439-95-4	1	mg/L	52	52	30								
Sodium	7440-23-5	1	mg/L	1480	1460	1860								
Potassium	7440-09-7	1	mg/L	10	10	11								
<b>EG094F: Dissolved Metals in Fresh Water by ORC-ICPMS</b>														
Aluminium	7429-90-5	5	µg/L	7	14	12								
Iron	7439-89-6	2	µg/L	380	445	14								
Antimony	7440-38-0	0.2	µg/L	<0.2	<0.2	<0.2								
Selenium	7782-49-2	0.2	µg/L	<0.2	<0.2	<0.2								
Arsenic	7440-38-2	0.2	µg/L	0.3	0.3	1.2								
Barium	7440-39-3	0.5	µg/L	2680	2670	488								
Beryllium	7440-41-7	0.1	µg/L	<0.1	<0.1	<0.1								
Boron	7440-42-8	5	µg/L	1460	1380	1270								
Bismuth	7440-69-9	0.05	µg/L	<0.05	<0.05	<0.05								
Cadmium	7440-43-9	0.05	µg/L	0.05	<0.05	0.12								
Chromium	7440-47-3	0.2	µg/L	<0.2	<0.2	0.6								
Cobalt	7440-48-4	0.1	µg/L	0.3	0.3	3.4								
Copper	7440-50-8	0.5	µg/L	<0.5	0.9	3.5								
Lead	7439-92-1	0.1	µg/L	0.2	0.2	0.3								
Lithium	7439-93-2	0.5	µg/L	100	96.8	118								
Manganese	7439-96-5	0.5	µg/L	45.1	46.0	17.3								
Molybdenum	7439-98-7	0.1	µg/L	0.1	0.2	0.9								
Nickel	7440-02-0	0.5	µg/L	<0.5	<0.5	3.3								
Silver	7440-22-4	0.1	µg/L	<0.1	<0.1	<0.1								
<b>EG094F: Dissolved Metals in Fresh Water by ORC-ICPMS - Continued</b>														
Strontium	7440-24-6	1	µg/L	3620	3640	3750								
Thallium	7440-28-0	0.02	µg/L	0.15	0.12	0.06								
Thorium	7440-29-1	0.1	µg/L	<0.1	<0.1	<0.1								
Tin	7440-31-5	0.2	µg/L	0.5	0.4	0.3								
Titanium	7440-32-6	1	µg/L	<1	<1	<1								
Uranium	7440-61-1	0.05	µg/L	<0.05	<0.05	0.08								
Vanadium	7440-62-2	0.2	µg/L	<0.2	<0.2	0.3								
Zinc	7440-66-6	1	µg/L	10	14	206								
<b>EN055: Ionic Balance</b>														
^ Total Anions		0.01	meq/L	79.5	76.8	91.8								
^ Total Cations		0.01	meq/L	72.1	71.3	86.4								
^ Ionic Balance		0.01	%	4.87	3.80	3.09								
<b>EP080/071: Total Petroleum Hydrocarbons</b>														
C6 - C9 Fraction		20	µg/L		<20	<20								
C10 - C14 Fraction		50	µg/L		<50	<50								
C15 - C28 Fraction		100	µg/L		110	110								
C29 - C36 Fraction		50	µg/L		<50	<50								
^ C10 - C36 Fraction (sum)		50	µg/L		110	110								
<b>EP080S: TPH(V)/BTEX Surrogates</b>														
1,2-Dichloroethane-D4	17060-07-0	0.1	%		118	84.6								
Toluene-D8	2037-26-5	0.1	%		125	84.2								
4-Bromofluorobenzene	460-00-4	0.1	%		121	78.5								

Several key observations from the water analysis results to date are given below:

- Water in both Westfalen No. 3 and New Redbank Collieries have a pH close to neutral.
- The levels of Electrical Conductivity (EC) of the water from both Collieries (EC = 6150 – 10200µS/cm) are much higher than fresh rain water (EC < 1000µS/cm). This implies that the mine water is an “old” formation water reservoir.
- The water in New Redbank Colliery is different from that in Westfalen No. 3 Colliery. The EC level at New Redbank Colliery is about 6000-6800 µS/cm, whereas it is 7500-10000µS/cm in Westfalen No. 3. This indicates that the two collieries may not be hydraulically linked.

- The piezometer readings taken over the three month period indicate that there has been an increase in water level at Westfalen Colliery. At the end of four month period, an increase in height of about 5 m was noticed at CP_05 and about 4 m at CP_09. However, there was not much variation in water level after three months at New Redbank Colliery, represented by borehole CP_04.
- Over the four month period, the total Alkalinity of water from both collieries showed an increasing trend during April – June 2010 but a decreasing trend during July – August 2010. It is inconclusive on what caused this change. One possible scenario is that some fresh water may find its way into the mine workings in July and August, and hence reduced the total Alkalinity.

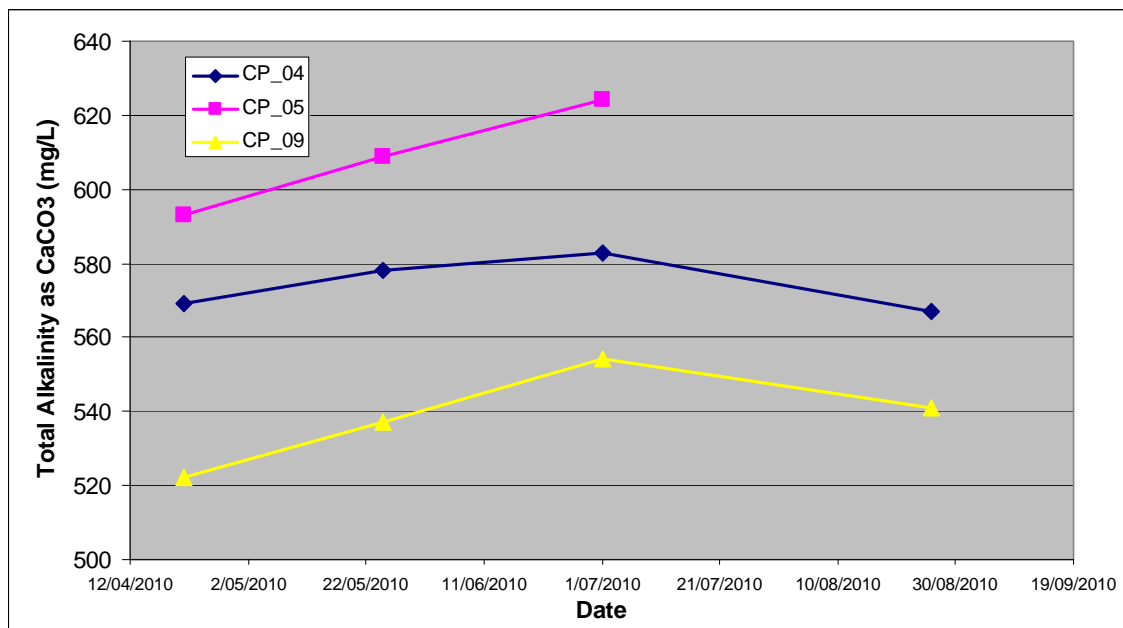


Figure 3-17. Alkalinity change in water samples from New Redbank Colliery (CP_04) and Westfalen No. 3 Colliery (CP_05 and CP_09)

- Overall, the water from neither of the mines is suitable for environmental purposes. At such high levels of EC and chlorine contents, the water can be classified as brackish. For reference, the EC levels for various types of water are:
  - Freshwater: 50-1000  $\mu\text{S}/\text{cm}$ ,
  - Industrial water: around 10,000  $\mu\text{S}/\text{cm}$
  - Seawater: about 50,000  $\mu\text{S}/\text{cm}$ .

### 3.9 Gas sampling and analysis

Gas samples have been scheduled to be collected from two boreholes (CP_008, located near McLaughlin Street, and CP_010, located at the western end of Duncan Street) every six months. Both boreholes are located in the Westfalen No. 3 Colliery. No gas sampling is possible for the New Redbank Colliery because the two drill holes in this colliery are flooded. The objective of the gas investigation was to determine the

gas contents within the mine voids. Two sets of samples were collected to date: one on 21 April and the other on 28 July 2010. They were sampled and analysed by SIMTARS.

SIMTARS collected gas samples from pit bottom of each borehole and analysed them for (as a minimum) oxygen (O₂), methane (CH₄), carbon monoxide (CO), carbon dioxide (CO₂), and hydrogen sulphide (H₂S) components. This suite of gas analyses was extended to include helium (He), hydrogen (H₂), nitrogen (N₂), ethylene (C₂H₄) and ethane (C₂H₆) as they can be covered within the same GC methodology.

Analysis for oxygen, methane, carbon monoxide and carbon dioxide was conducted in-situ using a Maihak S710 infra-red and paramagnetic analyser. Bag samples were collected for subsequent laboratory analysis by Gas Chromatography (GC) using Thermal Conductivity Detection (TCD) and Flame Photometric Detection (FPD).

As the boreholes were un-cased below 20m, sampling was conducted at various depths within the borehole to identify any changes in the gas makeup caused by overlying strata.

Table 3-9 summarises the results from sample analysis.

Table 3-9. Gas analysis results for samples collected on 21 April and 28 July 2010.

Sampling date 21 April 2010

Borehole ID	CP-O08					CP_O10		
Sample depth	110m	100m	80m	60m	40m	65m	40m	20m
Methane (CH ₄ )	18.20%	18.20%	18.10%	18.20%	18.10%	18.40%	18.20%	18.20%
Carbon Dioxide (CO ₂ )	9.22%	9.22%	9.19%	9.16%	9.19%	9.29%	9.29%	9.11%
Nitrogen (N ₂ )	71.20%	71.20%	71.30%	71.20%	71.30%	71.00%	71.20%	71.20%
Oxygen (O ₂ )	0.60%	0.60%	0.60%	0.60%	0.50%	0.50%	0.50%	0.60%
Carbon Monoxide (CO)	<0.0005%	<0.0005%	<0.0005%	<0.0005%	<0.0005%	<0.0005%	<0.0005%	<0.0005%

Sampling date 28 July 2010

Borehole ID	CP-O08	CP_O10
Sample depth	130m	68m
Methane (CH ₄ )	18.20%	18.20%
Carbon Dioxide (CO ₂ )	8.70%	8.50%
Nitrogen (N ₂ )	71.00%	71.00%
Oxygen (O ₂ )	1.10%	1.10%
Carbon Monoxide (CO)	<0.0005%	<0.0005%

The key observations from the gas analyses can be summarised as follows:

- The gas concentrations obtained from this sampling were typical of a sealed section of a coal mine. The gas makeup of all samples was found to be consistent across the various depths sampled in each borehole and between the two boreholes.
- The methane contents in both boreholes were very similar, although borehole CP_O10 is at a much shallower part of the Westfalen No. 3 Colliery. This implies that the methane gas in the mine has been there for a long duration and is well mixed with other gas components. It is unlikely that there is any major gas being released from the coal seam indicating inactive coal seam gas at present.
- The oxygen content in Westfalen No. 3 Colliery was 0.5-0.6% on 21 April 2010. It however increased to 1.1% on 28 July 2010. This is an indication that air has entered the mine during this period. It was not known, however, if this was caused by the recent site drilling activities, nearby Ipswich Motorway Upgrade activities or any other unknown factors.
- The risk of gas explosion underground is low at present due to the low oxygen content. However, because the methane content is close to the explosive range of 5-15%, this risk should not be discounted as the oxygen content is currently increasing and any further subsidence events could accelerate the oxygen increase rate. An oxygen concentration of approximately 12% will move the methane concentration in to the explosive range

In order to minimise the potential risk imposed by underground methane, it is recommended that the current frequency of gas sampling and analysis should be increased to every three months for at least 2 years to confirm any long term trends. In the event of any major ground movement in the future (e.g. subsidence), the gas sampling frequency should be increased to weekly. If the oxygen content is greater than 5% and the trend is continuing, remediation measures (such as injection of nitrogen) should be considered.

## **4. MICROSEISMIC MONITORING**

### **4.1 Summary**

- A three-station CSIRO microseismic monitoring network has been installed at Collingwood Park. All seismic sensors and data recording instruments were in good working condition through out the monitoring period from 4 May to 5 September 2010.
- Data recorded from 1 July to 5 September 2010 were manually processed. During this period, the three stations recorded more than 2,000 triggered events. Most of these events are associated with moving vehicles. Only 50 events were recognised to be induced by ground movement.
- The 50 seismic events were all observed at station S1 (near Collingwood Drive). No seismic events have been identified on the records of stations S2 (near the church) and S3 (at Cnr Duncan St. and Herman Av.). None of the events triggered and recorded at S1 were detected by S2 and S3.
- Few events were recorded from May to June 2010. It appears that there is a tendency of increasing seismicity from the start of July. Most of the seismic events are weak.
- Seismic particle motion analysis indicated that ground instability may exist either northeast or southwest to borehole S1, at a distance of less than 200m. The locations of these events cannot be determined due to the events being detected by an insufficient number of geophone stations.
- It has been demonstrated that the microseismic monitoring network is an effective tool for detecting rock fractures associated with ground instability at Collingwood Park. We recommend two more seismic stations be installed approximately 200m northeast of S1 in order to accurately locate seismic events.
- Routine data processing and interpretation are in progress. Instrument working condition is checked daily through wireless communication and data is downloaded twice a week at the site.

### **4.2 Objectives of the microseismic monitoring**

- Detect and locate any ground fracturing at the Collingwood Park above the abandoned Westfalen No. 3 underground coal mine.
- Provide indication for future failure events, if any.
- Provide evidence of ground stability or instability in both subsided and non-subsided areas of concern at Collingwood Park.

## 4.3 Microseismic monitoring plan

### 4.3.1 Geophone locations

To ensure the largest possible area was monitored, three geophone strings, each with three triaxial geophones, were installed in drill holes drilled approximately 300 m apart in a triangular pattern (Figure 4-1). This arrangement covers about 1 square kilometre and includes areas subsided during the 2008 event as well as unsubsided ground. The triangular geometry is ideal for accurate location of seismic events that occur within or near the monitoring array. Explosive shots were used to provide known seismic events that would trigger the geophones so that their spatial orientations and locations could be determined. Accurate event locations were achieved from the three geophones in each drill hole. Table 4-1 lists the location parameters of the geophone stations.



Figure 4-1. Locations of three geophone boreholes CP-S1, CP-S2 and CP-S3, weight drop points (red square) and suggested shot holes (large red dots).

Table 4-1. Parameters of the geophone locations.

Borehole	Geophone	Easting (m)	Northing (m)	Elevation RL (m)	Depth (m)	Orientation* (degrees)
S1	S14	486758.5	6946000.3	36.4	0	0
	S13	486758.5	6946000.3	-27.6	64	155
	S12	486758.5	6946000.3	-47.6	84	-47
	S11	486758.5	6946000.3	-67.6	104	-136
S2	S23	486929.9	6945491.1	-17.5	43	-160
	S22	486929.9	6945491.1	-42.5	68	-115
	S21	486929.9	6945491.1	-67.5	93	45
S3	S33	487051.6	6945778.0	-38.6	65	50
	S32	487051.6	6945778.0	-58.6	85	79
	S31	487051.6	6945778.0	-78.6	108	-6

*Orientation: Azimuth of the geophone north component clockwise from Geometric North, determined using calibration shots.

### 4.3.2 Microseismic data acquisition system

The microseismic data acquisition system used in this project is the Kelunji EchoPro seismometer made by Environmental Systems & Services Pty Ltd (an Australian company, [www.esands.com](http://www.esands.com)). The instrument's specifications include a sampling rate of up to 1000 samples/second, up to 32 times gain, GPS time synchronisation, 24 bit analogue to digital converter, 12 channel capacity and USB based data storage. The global positioning system (GPS) based time synchronisation allows the internal clock in the EchoPro to be corrected automatically every one second to ensure the time error between clocks in different acquisition units is not greater than ten micro-seconds.



Figure 4-2. Microseismic stations S1, S2 and S3. The data acquisition system and battery are within the enclosure. The battery is charged using a solar panel installed on the top of the post.

Next G based modems provide wireless communications to each of the acquisition units. This communication system is used to monitor the status of the acquisition units. The power supply for each data acquisition system consists of two 12V deep cycle absorbent glass mat lead-acid batteries connected to a solar panel and regulator. The

EchoPros consume little power and an external deep-cycle 72 Ah 12V battery can run the instrument for up to 7 days without charging. All of this equipment is installed in a system enclosure at the top of each drill hole.

### 4.3.3 Geophones

Three geophone strings manufactured in China have been used in this project. Two of the geophone strings have three triaxial geophone sensors spacing at 20 m (S1 and S3) and one has the geophones spaced at 25 m. The geophones have a sensitivity of 21.4 V/m/s and a flat frequency response from 10-300 Hz. The geophone strings are cemented in the drill holes to achieve the best possible coupling with the ground.

### 4.3.4 Calibration of the microseismic system

As rock deforms or fractures, seismic signals and waves are emitted at a constant speed, indicating the occurrence of a microseismic event. To determine the location of a seismic event requires both knowledge of the seismic arrival-time of the wave (distance) and its ray direction (orientation). In order to determine seismic ray direction, the orientation of a geophone in the ground must be known. However, during installation of the geophones in a deep drill hole, their orientation cannot be controlled. After an unsuccessful weight drop trial, calibration shots by explosives at three known locations were applied to determine and calibrate the in-situ geophone orientations.

#### *Weight drop*

A weight drop method for the calibration was tried first. The weight drop machine and field service were provided by Terra Geophysics Pty Ltd. The weight is a 50kg solid steel cylinder, which is dropped from a height of 0.5m on to a steel plate laid on the ground (Figure 4-3). The ground impact force of the cylinder was enhanced by an accelerator. On soft ground or over a landfill site, the weight drop method can transfer and deliver seismic energy of the order of kilo-Jules up to a 300m horizontal distance.



(A)



(B)

Figure 4-3. Weight drop machine provided by Terra Geophysics (A). Weight drop on ground surface (B). A reference geophone is located about 0.5m from the impact point.

Three weight drop points were arranged around each geophone borehole (see Figure 4-1), at a distance of 30-60m from the drill hole. At each point, 10-20 consecutive weight drops were applied for the purpose of signal stacking to increasing the signal to noise ratio.

The weight drop experiment was carried out on 18-19 March 2010. During the experiment, the seismic instruments were set to record seismic data continuously. A reference geophone was planted near each drop point in order to capture the timing of each drop impact (Figure 4-3).

The results showed that the weight drops did not provide the energy required to orient the geophones. Figure 4-4 shows typical seismic waveforms recorded on the three components of one of the triaxial geophone in S2. The signal to noise ratio is too poor to determine the orientation.

After stacking of seismic waveforms associated with the 20 weight drops at each drop point, the seismic signal to noise ratio was improved. Figure 4-5 (A, B, C) shows waveforms associated with the three geophones in S2, after stacking of 20 waveforms.

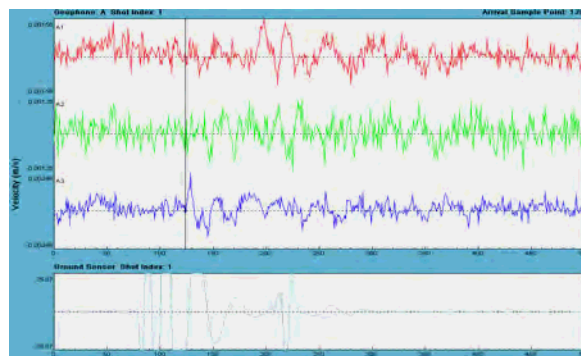
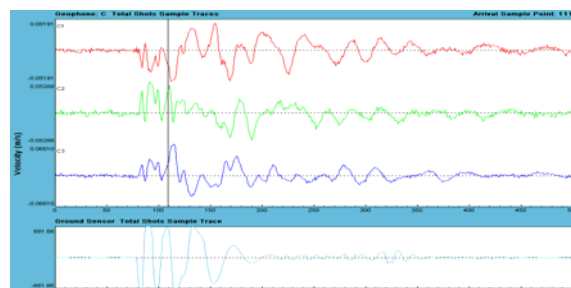
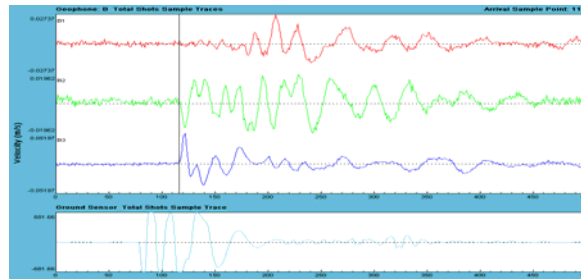


Figure 4-4. Typical seismic waveforms from the weight drop trial at a distance of 35m recorded at the S2 station. The red line is for the east component, green for the north and blue for the vertical. The bottom waveform is captured by the reference geophone near the weight drop testing point.

A. Top geophone, 55m deep: arrival-time=111 ms. The trigger sensor time=81 ms.



B. Middle geophone, 75m deep: arrival-time=118 ms



C. Bottom geophone, 95m deep: arrival-time=126 ms

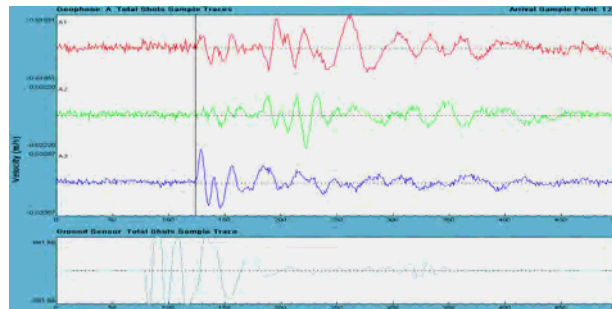


Figure 4-5. Seismic waveforms associated with the three geophones inside CP-S2, after stacking waveforms of 20 weight drops.

Although the signal to noise ratio was improved after stacking, the seismic energy on the horizontal components was still not strong enough to reliably determine geophone orientation.

### *Calibration shots using explosives*

Three 25m deep shot holes were drilled for the explosive calibration shots. Figure 4-6 shows the locations of the shot holes. In each of the holes, 1-2 shots were fired using a charge size of 400gm pre cast primer with two detonators (Table 4-2). All of the shot holes collapsed to some extent below the surface casing limiting the depth at which the shots could be placed. Orica Quarry and Construction was subcontracted by CSIRO to conduct the shot firing.



Figure 4-6. Locations of dynamite calibration shots.

Table 4-2. Parameter of the calibration shots.

Shot	Easting	Northing	Depth (m)	Charge size (gm)	Record quality
1	486998.3	6945947.2	5	400 + 2 detonators	Excellent
2	486812.8	6945798.3	16	400 + 2 detonators	Excellent
2	486812.8	6945798.3	13	400 + 2 detonators	Excellent
3	487200.1	6945698.0	5.8	400 + 2 detonators	Excellent

All of the shots were recorded with a good signal to noise ratio. Figure 4-7 shows the seismic waveforms associated with the four shots. The seismic data obtained from the shots were used for both the geophone orientations and seismic velocity determination.

### *Seismic velocity model*

The seismic arrival times of the calibration shots at each geophone station were accurately determined (Table 4-3). These arrival times were then used to construct a velocity model for event location. In this study, only an average velocity model has

been obtained. Figure 4-8 shows the distance - arrival time curves obtained for the shot signals. An average velocity of 3,430 m/s was determined.

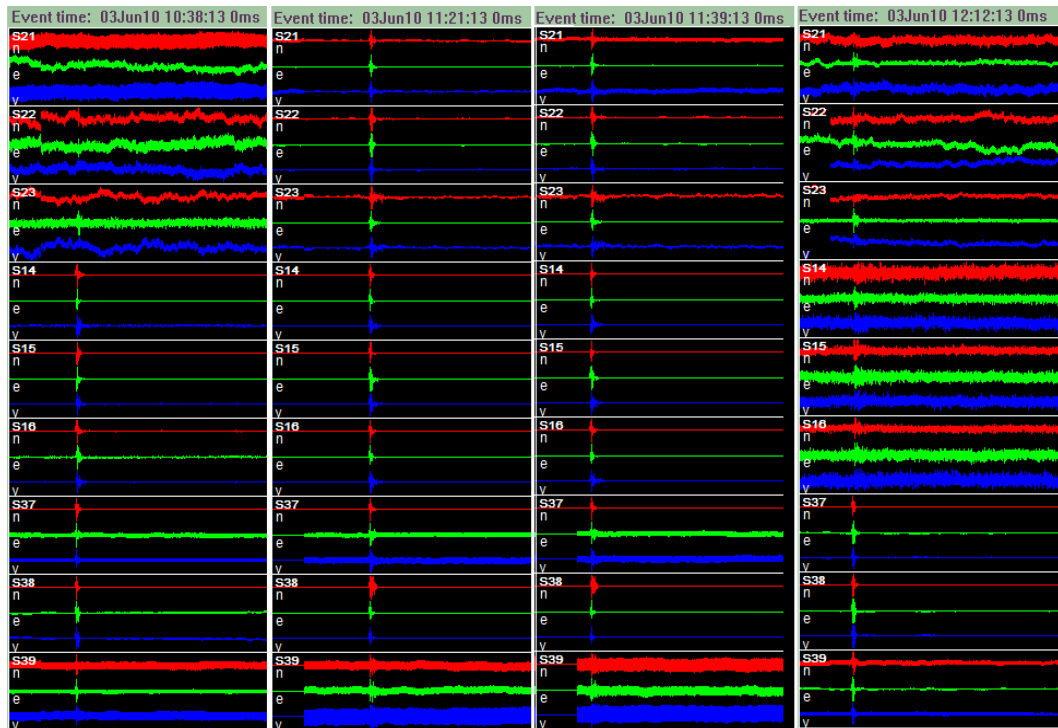


Figure 4-7. Seismic waveforms associated with the four calibration shots. Red, green and blue curves are waveforms on the north, east and vertical geophone components, respectively.

Table 4-3. The arrival times of the calibration shots and distances between each pair of the geophone station and shot.

Shot1			Shot2			Shot3			Shot4		
Geophn	Dist	Time	Geophn	Dist	Time	Geophn	Dist	Time	Geophn	Dist	Tim
s11	263.99	40915	s11	223.05	55242	s11	224.1	59108	s11	541	38470
s12	257.34	40913	s12	216.94	55238	s12	217.75	59105	s12	538.44	38475
s13	252.1	40914	s13	212.55	55236	s13	213.09	59103	s13	536.61	38481
s21	471.2		s21	337.64	55266	s21	338.33	59103	s21	536.61	38430
s22	466.72		s22	332.82	55266	s22	333.31	59134	s22	344.62	38430
s23	463.55		s23	329.84	55267	s23	330.1	59135	s23	341.6	38433
s31	207.48	40897	s31	255.33	55246	s31	256.38	59113	s31	191.22	38385
s32	197.85	40893	s32	249.13	55244	s32	249.97	59111	s32	182.65	38382
s33	189.83	40892	s33	244.42	55243	s33	245.03	59110	s33	175.95	38379

Dist: the distance (in m) from a shot to a geophone site;  
 Time: arrival time (in ms) of a shot signal at a geophone site.

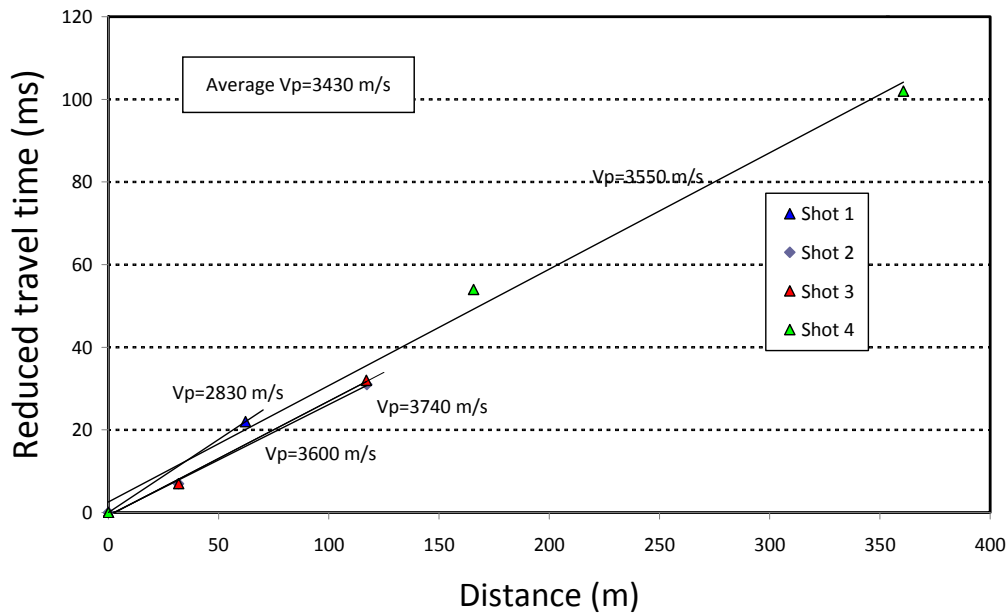


Figure 4-8. The average seismic velocity model determined for Collingwood Park, using seismic arrival times associated with the four calibration shots.

## 4.4 Data processing and interpretation

The microseismic monitoring system was in full operation on 4 May 2010, after an instrument tuning period. Up to 5 September 2010, about 50 events associated with ground movements were recorded. However, none of the events were recorded by more than one station. Most of the events are recorded by geophones in borehole S1. Records of geophones in boreholes S2 and S3 are heavily contaminated by electrical noise most probably induced by nearby electrical power lines.

### 4.4.1 Discrimination between traffic and seismic events

Discrimination between trigger associated with traffic noise and ground movement is done using two approaches: waveform attenuation and a delay of seismic arrival times. If a trigger is induced by a moving vehicle, the seismic amplitude for geophones in a drill hole should show a decay function from the shallowest to the deepest geophones. If the trigger is associated ground movement below the drill holes, the bottom geophone should have the maximum amplitude.

In order to discriminate a seismic event from traffic noise, we installed an extra triaxial geophone, S14, on the ground surface at the top of S1 borehole on 5 July 2010. We use the following formula for the waveform amplitude calculation

$$A = \sqrt{A_{e,\max}^2 + A_{n,\max}^2 + A_{v,\max}^2}$$

where  $A_{e,max}$ ,  $A_{n,max}$ ,  $A_{v,max}$  are maximum waveform amplitudes on the east, north and vertical components, respectively. Table 4-4 shows examples of event discrimination for several selected triggers.

Table 4-4. Examples of event discrimination for several selected triggers.

Geophone station		S14	S13	S12	S11	Source
Depth (m)		0	64	84	104	
Combined waveform amplitude A ( $\times 10^{-4}$ m/s) (arrival time)	5/08/2010 8:56	10.643	0.225	0.174	0.129	Trucks
	10/08/2010 14:55	-	0.279	0.316	0.381	Seismic event
	10/08/2010 17:00	69.956	0.308	0.252	0.175	Vehicle
	14/08/2010 19:41	44.703	0.508	0.616	0.667	Seismic event
	15/08/2010 0:16	-	0.252	0.427	0.62	Seismic event
	15/08/2010 12:33	22.183	0.513	0.689	0.943	Seismic event
	15/08/2010 1:05	22.324	0.454	0.65	0.889	Unknown

The blue column indicates the date and time when event was recorded.

#### 4.4.2 Seismic waveforms of traffic related events and seismic events

As well as event discrimination using the variation of waveforms and arrival times, the waveform characteristics were also used for event classification. Traffic related waveforms are always associated with successive seismic wave trains or harmonic vibrations (Figures 4-9 and 4-10). However, seismic events associated with ground movement show very different waveform characteristics compared to traffic events. Figures 4-11 to 4-14 show typical seismic events recorded at station S1.

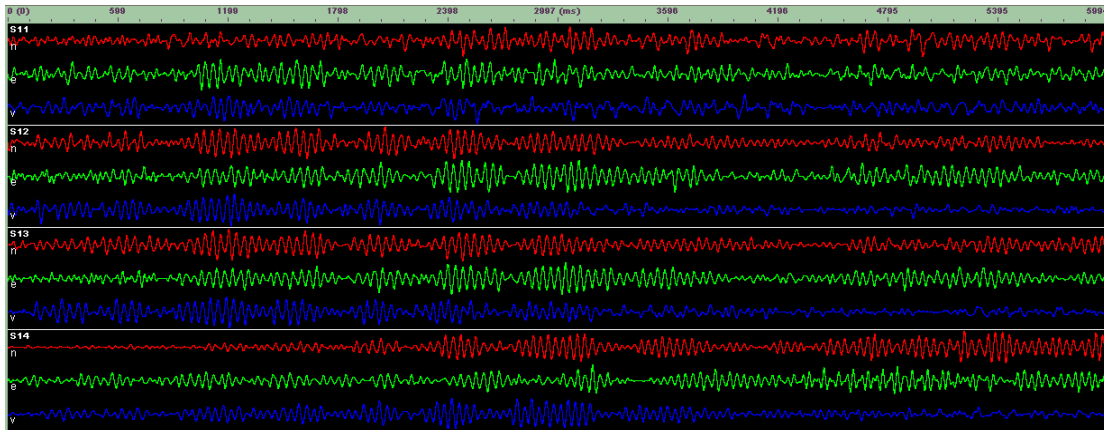


Figure 4-9. Seismograms associated with traffic on Collingwood Drive, recorded at geophones S11-S14 at 8:56:12 am on 5 August 2010. The dominant frequency is from 20-38Hz. The waveforms are band filtered using [5, 8 – 45, 48 Hz]. The waveforms are scaled in reference to their maximum amplitudes, hereafter.

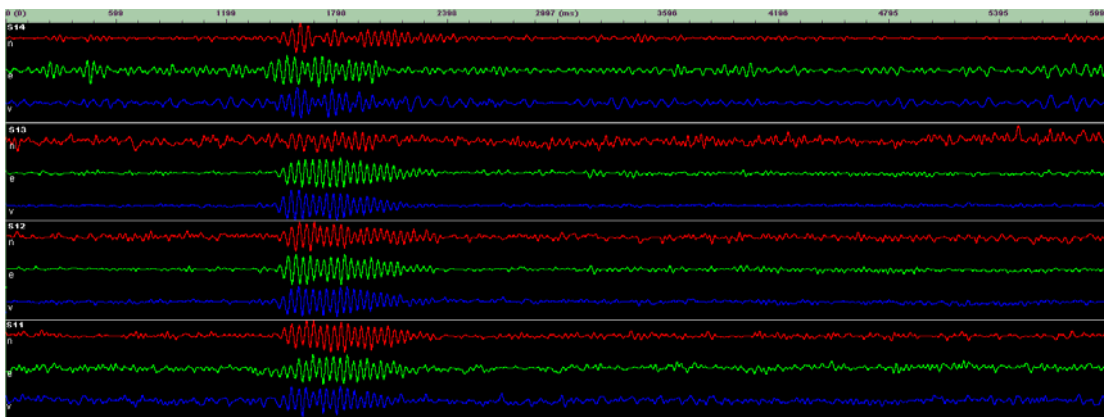


Figure 4-10. Seismograms possibly associated with traffic, recorded at geophones S11-S14 at 17:00:45 on 10 August 2010. The dominant frequency is about 28 Hz. The waveforms are low pass filtered using [45, 48 Hz].

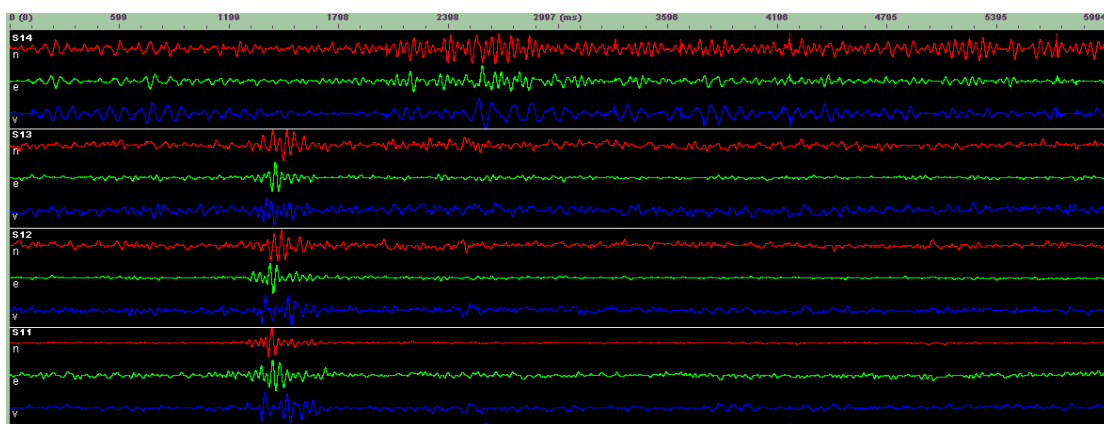


Figure 4-11. Seismograms possibly associated with ground movement, recorded at geophones S11-S14 at 14:44:06 on 10 August 2010. The dominant frequency is about 30 Hz. The waveforms are low pass filtered using [45, 48 Hz]. The seismic signal is not seen on the ground surface (S14).

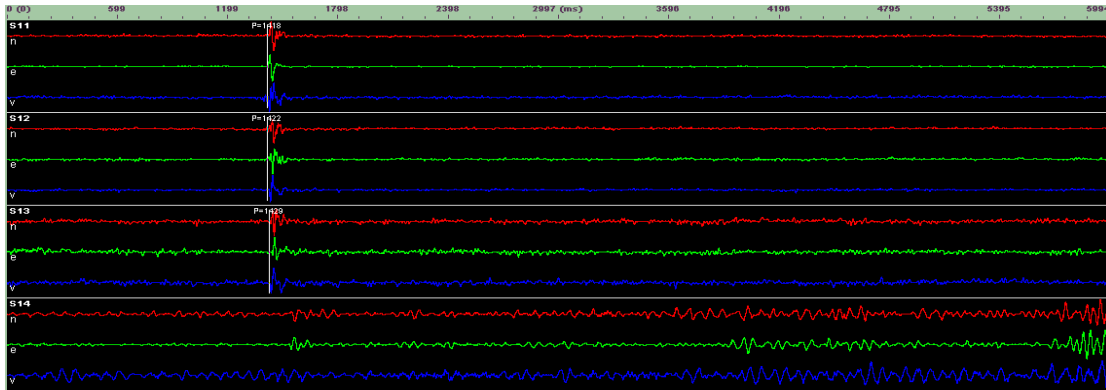


Figure 4-12. Seismograms possibly associated with a small seismic event, recorded at geophones S11-S14 at 00:16:28 on 15 August 2010. The dominant frequency range is about 12-55 Hz. The waveforms are low pass filtered using [75, 78 Hz]. The seismic signal is not seen on the ground surface (S14).

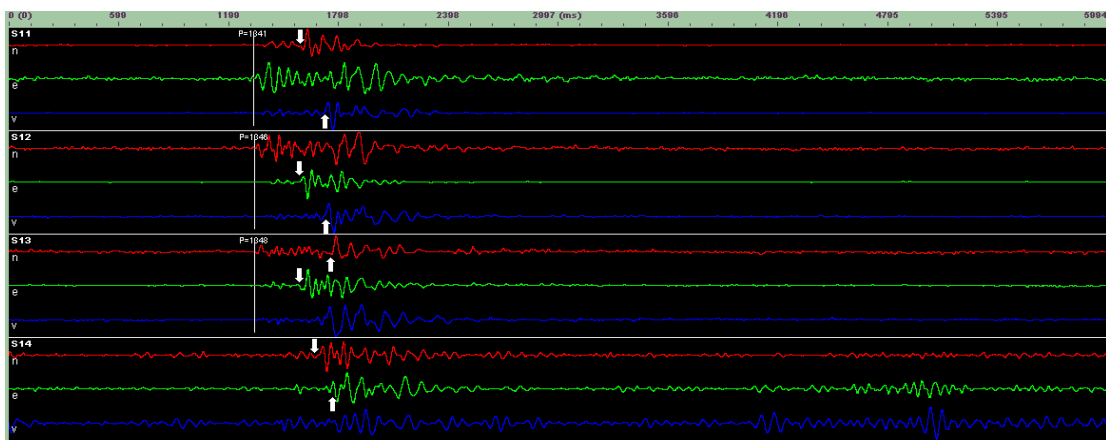


Figure 4-13. Seismograms possibly associated with a relatively strong seismic event, recorded at geophones S11-S14 at 19:41:35 on 14 August 2010. The seismograms recorded at borehole S1 at 19:41:35 on 14 August 2010 clearly show P- and S-waves. The dominant frequency range is about 12-25 Hz. The waveforms are low pass filtered using [45, 48 Hz].

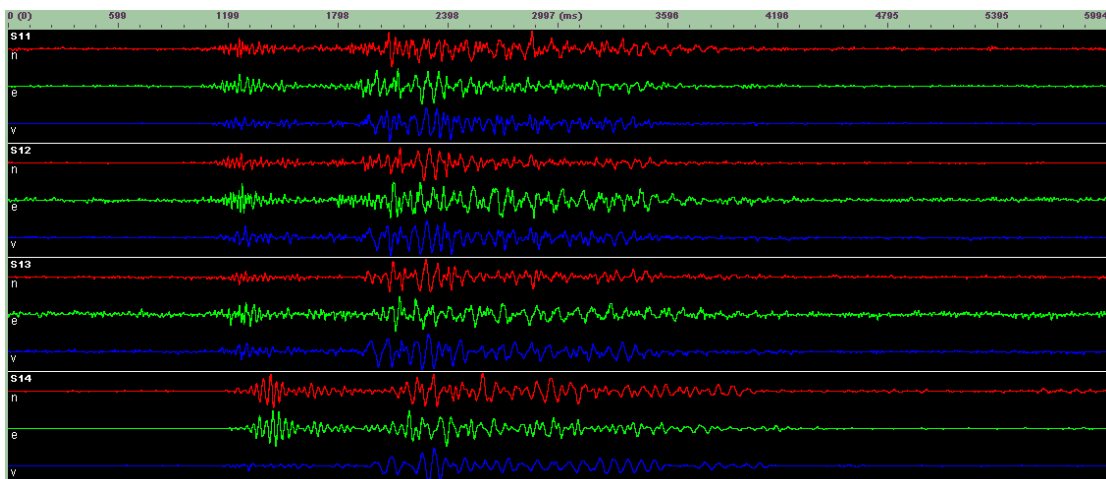


Figure 4-14. Seismograms possibly associated with a small seismic event, recorded at geophones S11-S14 at 01:05:55 on 15 August 2010. The dominant frequency range is about 12-55 Hz. The waveforms are low pass filtered using [75, 78 Hz].

### 4.4.3 Seismicity analysis

The discussion below refers to seismic events only. The traffic induced events have been excluded from this analysis.

Seismic events occurred through out the monitoring period. However, few events were recorded from May to June 2010. It appears that there is a tendency of increasing seismicity from July. Figure 4-15 shows the time of event occurrence from 1 July to 5 September, recorded at S1. Figure 4-16 shows the daily seismicity during this period.

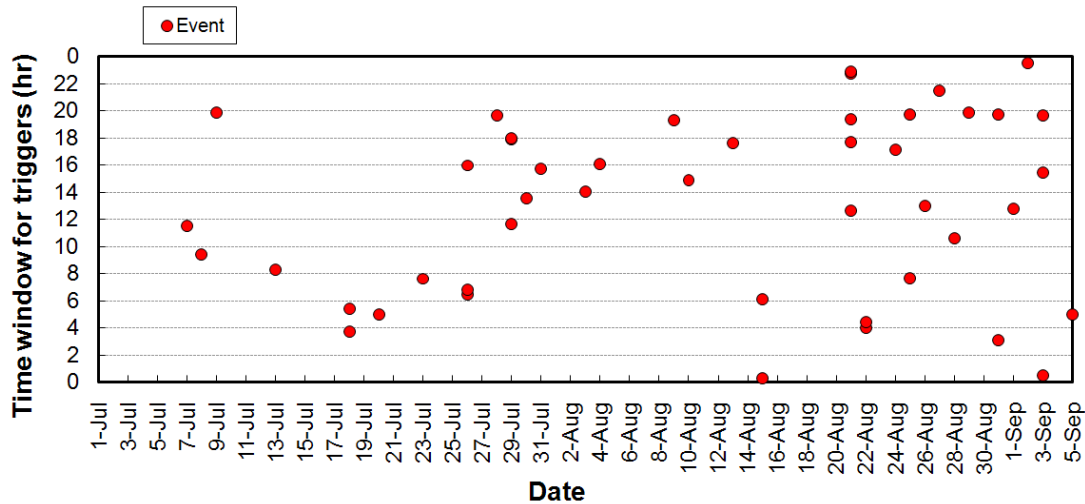


Figure 4-15. The occurrence time of seismic events from 1 July to 5 September, recorded at S1 (traffic induced events are excluded).

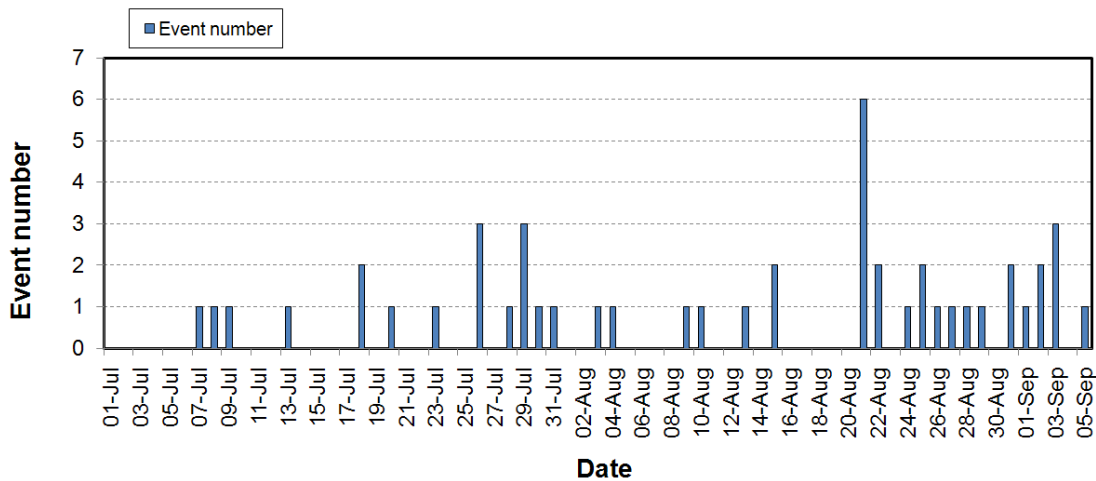


Figure 4-16. Daily seismicity from 1 July to 5 September, recorded at S1 (traffic induced events are excluded).

### 4.4.4 Event location estimation

As none of the seismic events have been recorded by geophones in more than one monitoring station, event location using the triangulation method cannot be applied. Accurate locations of these events cannot be obtained. However, using waveform

particle motion analysis, the azimuth of a source location can be estimated. We used the particle motion along the east and north axes of the P-wave to infer the source azimuth in reference to the S1 borehole. Figures 17 to 24 show particle motion diagrams (on the right) of P-waves recorded by S11, S12 and S13. The particle motions consistently indicate that these seismic events occurred either to the northeast or southwest of this drill hole.

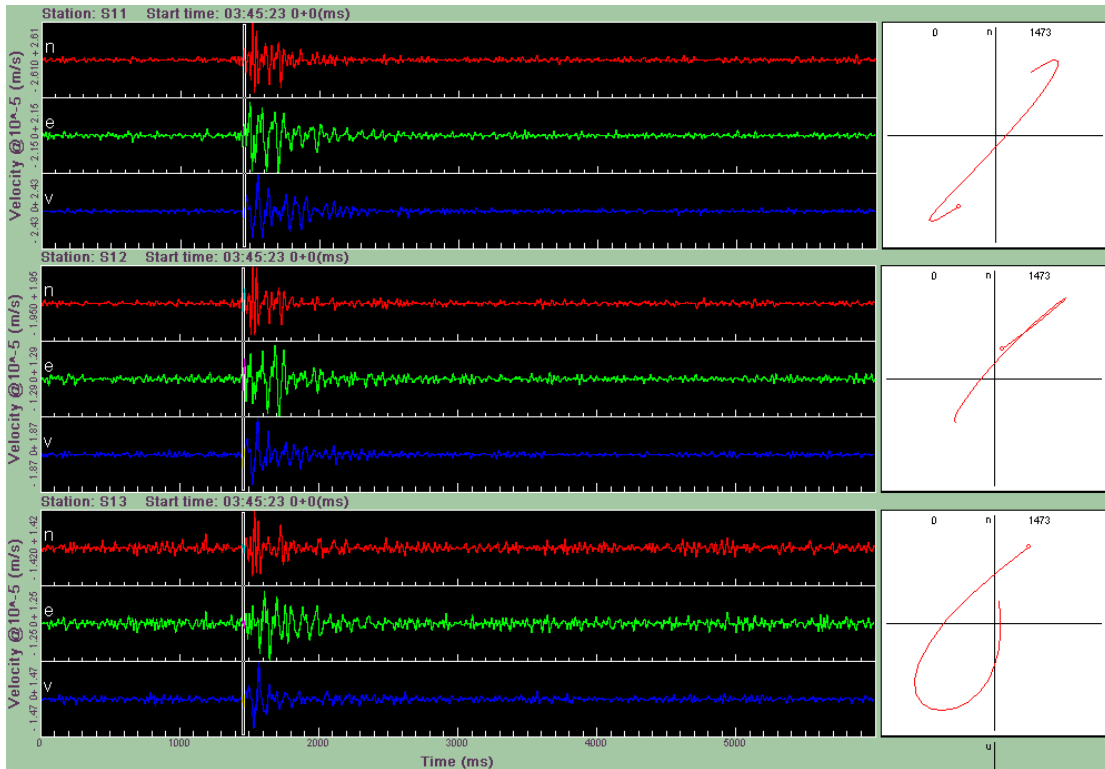


Figure 4-17. Particle motion diagrams of the P-wave recorded at S11, S12 and S13 at 03:45:23 on 18 July.

Figures 4-18 to 4-24 show particle motion diagrams for selected events recorded by S1. It is evident that most of the events are northeast or southwest of the seismic station.

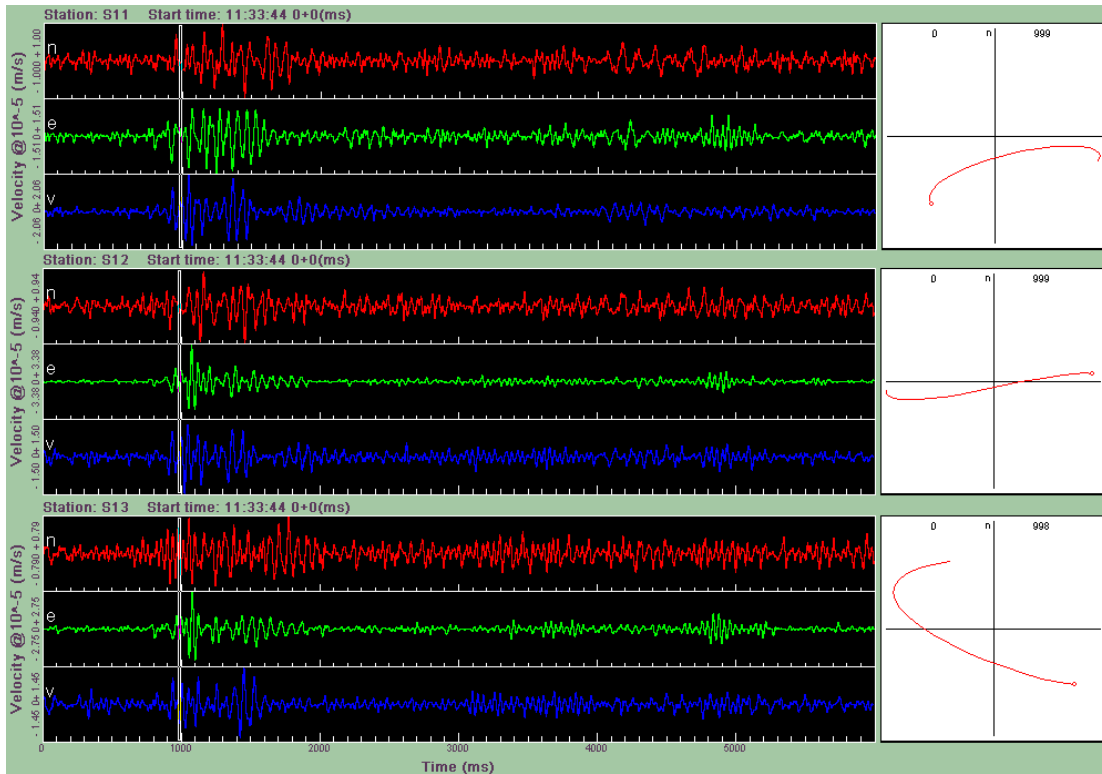


Figure 4-18. Particle motion of event recorded at 11:33:44 on 7 Jul.

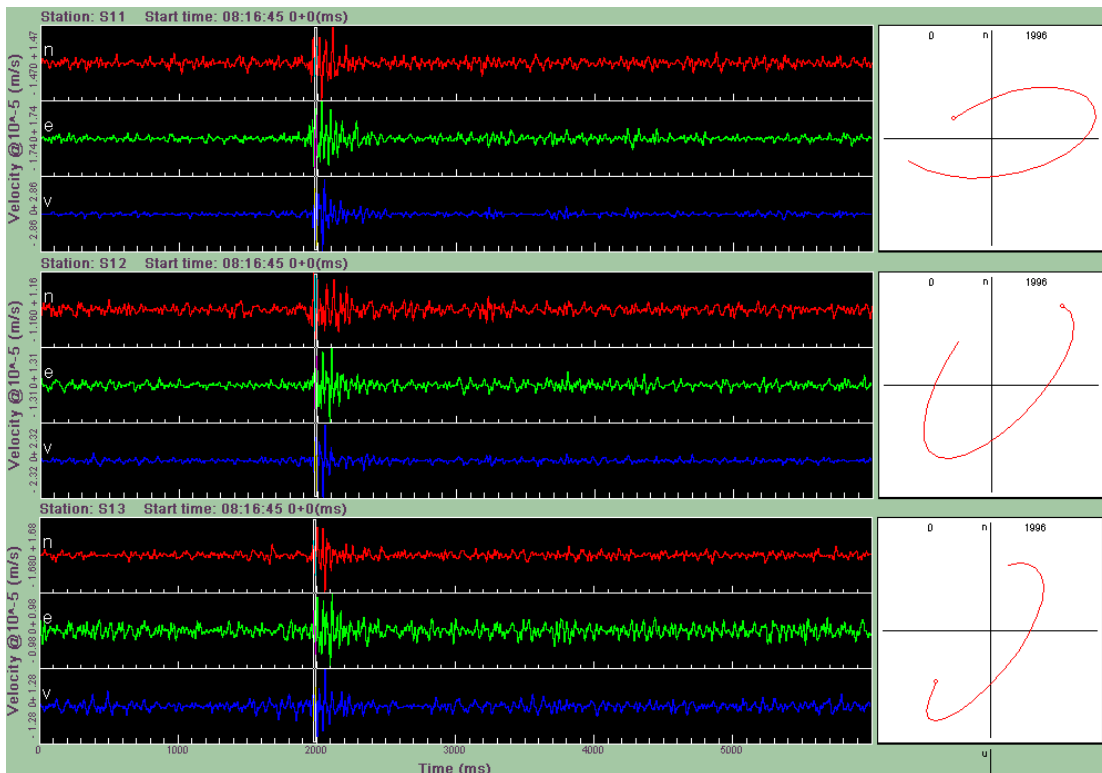


Figure 4-19. Particle motion of event recorded at 08:16:45 on 13 Jul.

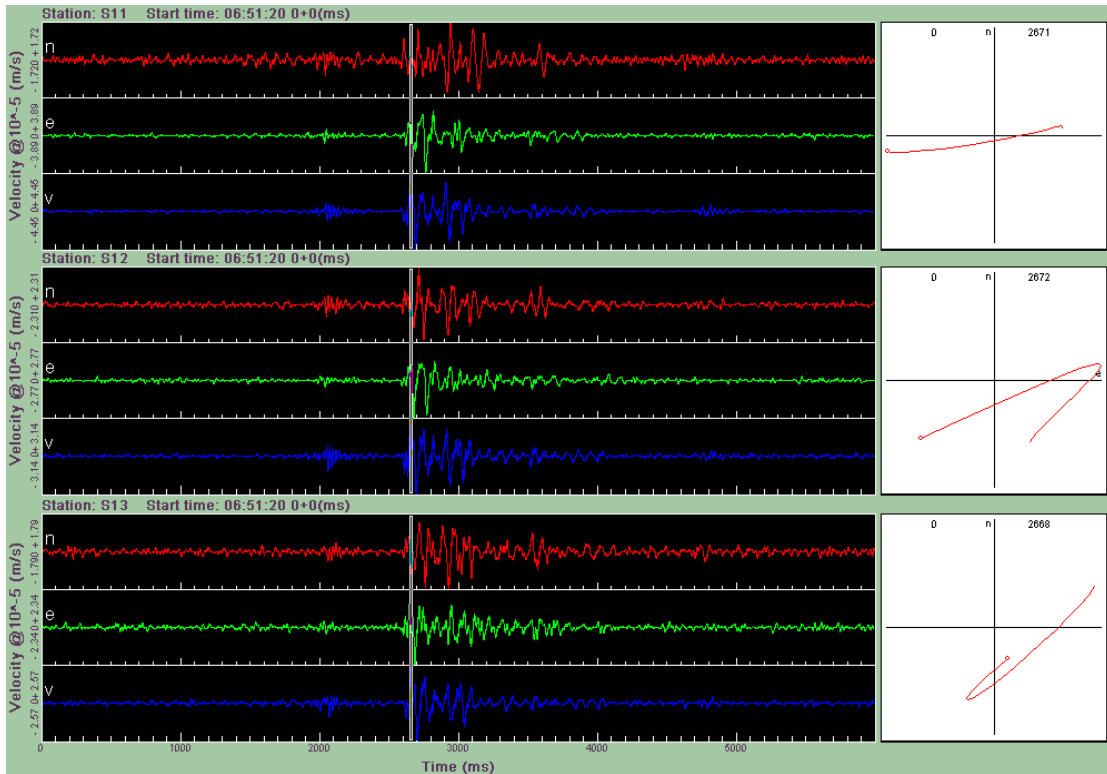


Figure 4-20. Particle motion of event recorded at 06:51:20 on 26 Jul.

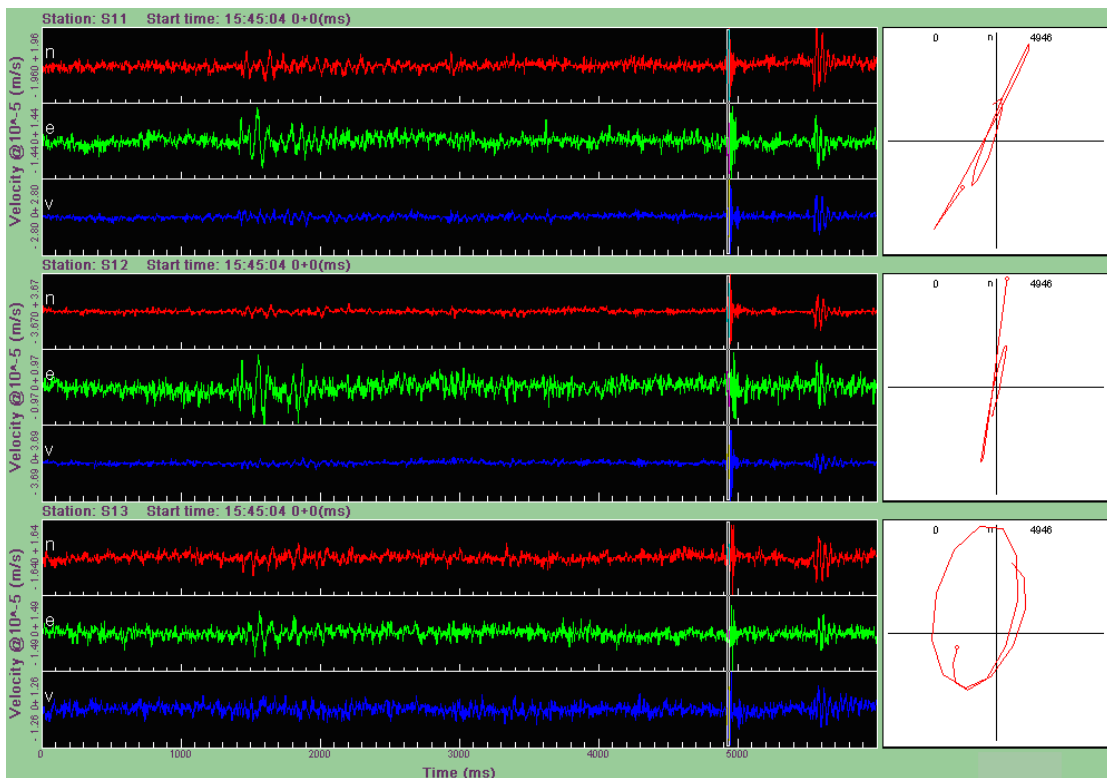


Figure 4-21. Particle motion of event recorded at 15:45:04 on 31 Jul.

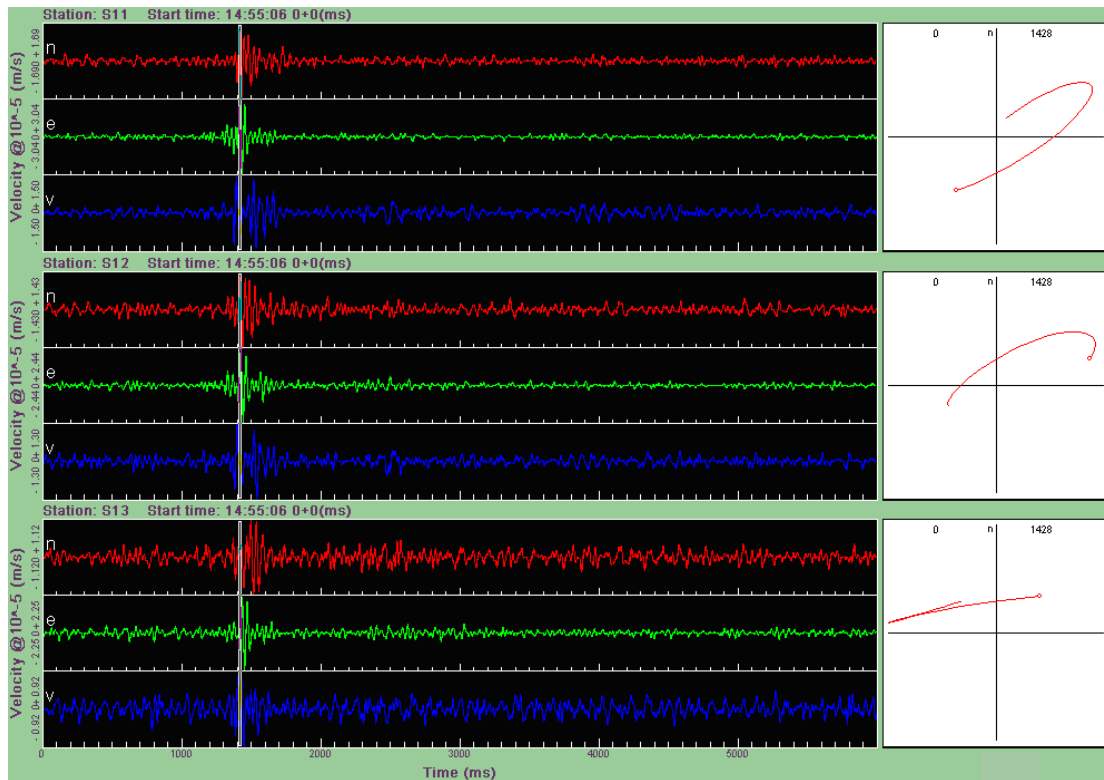


Figure 4-22. Particle motion of event recorded at 14:55:06 on 10 Aug.

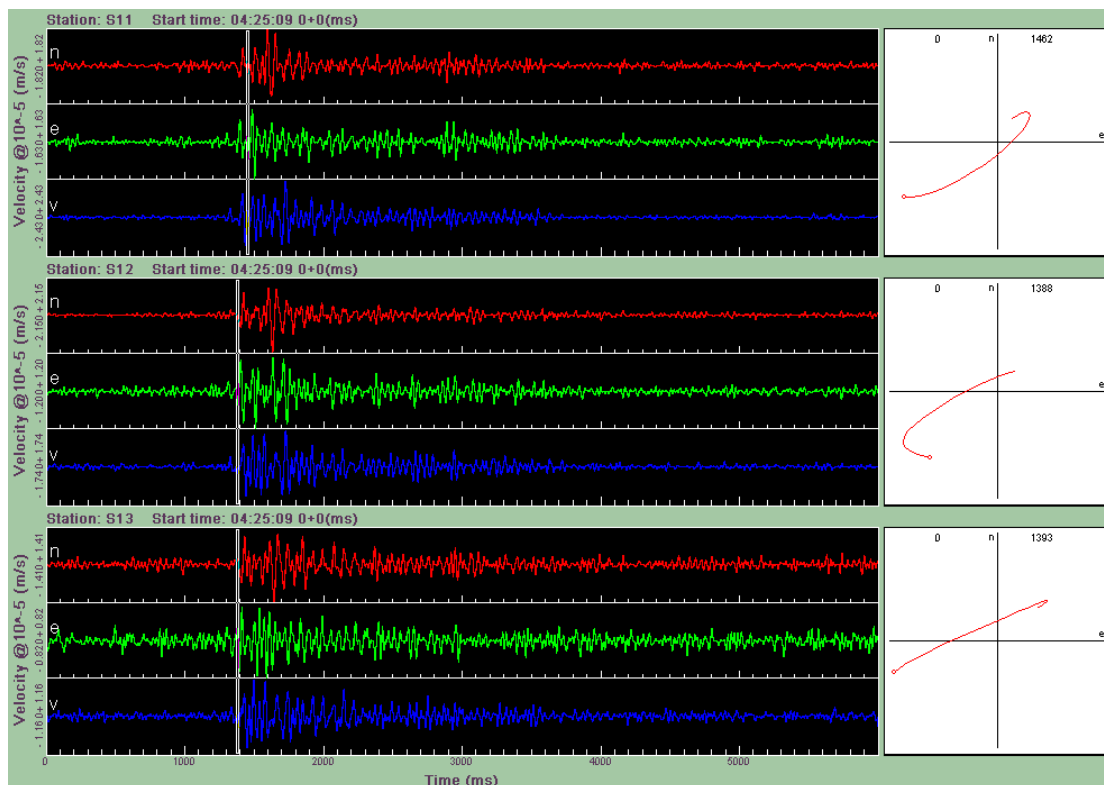


Figure 4-23. Particle motion of event recorded at 04:25:09 on 22 Aug.

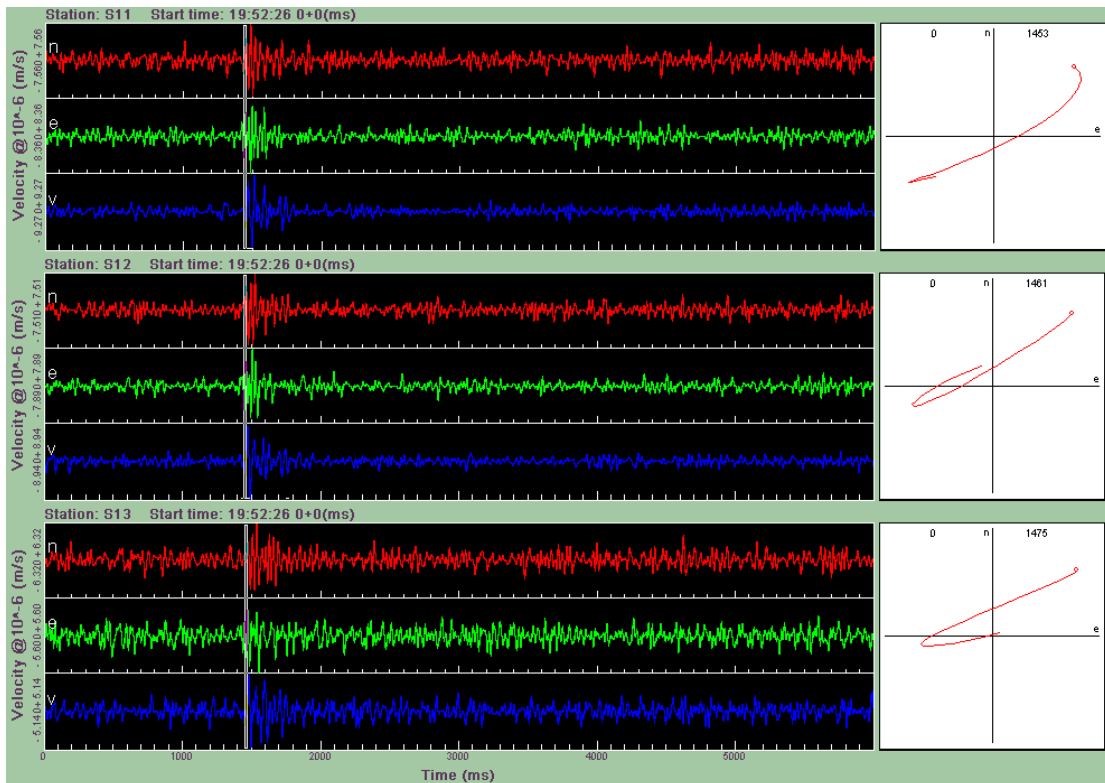


Figure 4-24. Particle motion of event recorded at 19:52:26 on 29 Aug.

## 4.5 Conclusions

- A three-station CSIRO microseismic monitoring network was installed at Collingwood Park and all seismic sensors and data recording instruments were in good working condition through out the monitoring period from 4 May to 5 September 2010.
- Data recorded from 1 July to 5 September were manually processed. During this period, the three stations recorded more than 2,000 trigger events. Most of the triggers are associated with moving vehicles. Only 50 events were recognised to be induced by ground movement.
- The 50 seismic events were all observed by station S1 (near Collingwood Drive). No seismic event has been identified at stations S2 (near the church) and S3 (at Cnr Duncan St. and Herman Av.). None of the events triggered S1 were recorded by S2 and S3.
- Few events were recorded from May to June 2010. It appears that there is a tendency of increasing seismicity from July. Most of the seismic events are weak.
- Seismic particle motion analysis indicated that ground instability may exist either northeast or southwest to borehole S1, at a distance less than 200m. The locations of these events cannot be determined as they were only detected by one monitoring station.

- The microseismic monitoring network is an effective tool for detecting rock fractures associated with ground instability at Collingwood Park. We recommend one more seismic station to be installed approximately 200m east of S1, in order to accurately locate these seismic events. It will help determine which part of the Central Panel may have ongoing ground movement and seismic activities.

## 5. NUMERICAL MODELLING AND PILLAR/PANEL STABILITY ASSESSMENT

### 5.1 Summary

A systematic numerical study was done to investigate the strength of pillars with common shapes and dimensions at Westfalen No. 3 Colliery. The effect of backfill on pillar strength using both cohesive fill material (fly ash and cement) and non-cohesive material (fly ash) was also investigated. Following these fundamental studies, large scale 3D numerical models were built to simulate the 2008 subsidence event and investigate the panel stability in a high risk area at Westfalen No. 3 Colliery.

The key findings from the pillar stability investigation are:

- Coal pillar stability depends mainly on the height, cross sectional dimensions, shape (square, rectangle, diamond, triangle, etc.), and modulus of the pillar and its interaction with roof strata. Presence of mine water may have adverse effects on pillar stability but is not considered in this study. Both analytical and numerical methods have been used to estimate pillar strength.
- A numerical model of a coal pillar was created and calibrated against the analytical strength formula developed by Salamon and Munro (1967) and modified by the University of New South Wales (Galvin, 1999).
- Coal pillar peak strength and post-peak residual strength were estimated for pillar shapes common to the Westfalen No. 3 Colliery. Of specific interest were diamond shaped pillars. It was found that the effective width of diamond shaped pillars can be estimated by hydraulic radius analogy (i.e. effective width = minimum width).
- The strength of pillars with irregular shapes has been analysed. It was aimed to simulate cases where the surrounding roadways have different cut heights and widths created by the multi-pass cutting mining method. Pillar strengths obtained using numerical methods agreed well with those obtained using analytical formula with average pillar height and minimum pillar width.
- It is predicted that pillars exhibit strain-softening behaviour at width-to-height ratio below approximately 5 and strain-hardening above this value. This is in agreement with field observations by Das (1986) in Indian mines. The residual strength of a pillar has been estimated from these models and the results have been used in estimating panel stability where stress transfer from yielded pillars to their neighbours is critical.
- Backfill is predicted to increase pillar strength and the percentage of strength increase is found to depend on the roadway fill percentage. For example, as displayed in the following table, the percentage of strength increase from 0.5MPa cohesive fill for a 20m x 20m square pillar with a height of 7m is 39% at a 60% backfill, and 57% at 90% backfill.

---

% roadwayfill	Non-cohesive backfill	0.5 MPa cohesive backfill
---------------	-----------------------	---------------------------

---

	% strength increase	% strength increase
60	13.5	38.8
70	18.3	43.2
80	20.8	47.4
90	29.1	57.2

- Backfill is predicted to reduce the critical width-to-height ratio at which pillar's post-peak behaviour transforms from strain-softening to strain-hardening.
- When backfill is placed after a pillar has yielded, the pillar is predicted to be able to carry additional load and stop softening.

The key observations from the 3D numerical models of mining panels include:

- The mine panel in the 2008 event model is predicted to fail when the pillar height is 9m.
- The panel in the central region adjacent to the 2008 event is predicted to be 20% stronger than the panel that failed in the 2008 event.
- Empirical, or semi-analytical estimates of pillar Factors of Safety (FoS) are in acceptable agreement with those from numerical models.
- Effect of backfill on panel strength is predicted to be similar to that on a single pillar. A panel strength increase of 60%-70% is predicted with 83% roadway backfill using 1.0MPa cohesive fill material.
- With a 83% backfill in the 2008 event model, the predicted maximum surface subsidence from a forced failure, is approximately 220mm.
- Stresses in the pillars surrounding the 2008 subsidence area are predicted to be elevated above the *in situ* level. The zone of influence is predicted to extend a horizontal distance of approximately 80m from the edge of the failed panel. This is in general agreement with the load transfer distance as described by Abel (1988) and used in pressure arch theory of 74m for a 20m pillar at this depth (Poulsen, 2010). The results suggest that the 2008 event was not initiated by the 1988 event that is located approximately 270m distant. However the central panel (identified as the high risk panel located adjacent to the 2008 event to the northeast) is likely to be affected by the 2008 subsidence due to elevated stresses from the failed panel.

## 5.2 Introduction

A series of numerical modelling studies were undertaken to assist in the evaluation of backfilling strategies to prevent future pillar/panel instability in Collingwood Park. It is expected that backfilling roadways surrounding pillars will have the following benefits:

- increase both immediate pillar strength and reduce the rate of pillar strength degradation from pillar spalling due to exposure to the environment, and roof instability that may increase the pillar working height
- change the post-peak pillar behaviour from rapid strength reduction to hardening so that pillars can continue to carry significant load even after yielding
- reduce roadway void space and hence significantly reduce the magnitude of surface subsidence from the unlikely event of panel failure.

This study started with numerical modelling of single pillars and was later extended to systems of pillars (or panels). The objectives of the study are:

- Determine strength of pillars with the dimensions and shapes observed at Westfalen No. 3 Colliery and determine the strength improvement from backfilling surrounding roadways.
- Investigate the pillar post-peak behaviour due to backfill.
- Estimate the response of the 2008 subsidence region to various backfilling strategies including estimating the pre-failure panel strength, strength improvement from backfill, surface subsidence, and reduction in subsidence from backfill.
- Compare the panel strength of the 2008 event region and the central region immediately to the northeast of the Waterline Fault, due to the different pillar configurations.
- Estimate the extent of stress influence zone around the 2008 subsidence.

Analytical and empirical formulas for estimating coal pillar strength and stress are well established for pillar design purposes and can be found in the literature. However there are issues in applying design approaches to the back-analysis of pillar failure because a conservative estimate of pillar stress is appropriate in design but this may give little, or misleading, information in a back-analysis. This is particularly true when the conditions for empirical formula are not satisfied as will be further discussed when estimating safety factors of Westfalen No. 3 pillars.

### 5.2.1 Pillar strength formula

The empirical equation developed by Salamon & Munro [Salamon 1967, Salamon 1998] (in SI units) from a South African pillar database has been widely used in South Africa and Australia since its development in 1967. This equation has been successfully used in the design of approximately one million pillars in South Africa alone [Mark, 1999]:

The Salamon & Munro pillar strength formula is expressed by:

$$\text{Pillar strength} = 7.2 w^{0.46} / h^{0.66} \text{ [MPa]} \quad (5-1)$$

where

$w$  = pillar width;

$h$  = mining height.

In Australia, coal pillar strength has been estimated by UNSW using a database for Australian coal pillars in 1996 [Galvin, 1999], and it is given as:

$$\text{Pillar strength} = 8.60 w^{0.51} / h^{0.84} \text{ [MPa]} \quad (5-2)$$

Pillar strength estimated from the combined coal pillar databases of South African and Australian was also given by [Galvin, 1999] and is expressed by:

$$\text{Pillar strength} = 6.88 w^{0.50} / h^{0.70} \text{ [MPa]} \quad (5-3)$$

In the above equations, the pillar width ( $w$ ) is for square pillars. When applied to pillars of different cross sectional geometry, the constants of the equations need further adjustments and modifications as will be discussed.

Interestingly, Equations (5-1), (5-2) and (5-3) derived from field observations of pillar performance give very similar results even though they were derived from pillars on two different continents and in different geological settings [Mark, 1999, Galvin, 1999].

## 5.2.2 Pillar effective width

Wagner [Wagner 1974] developed the concept of hydraulic radius to define the effective width  $w_e$ , which becomes identical to  $w$  for square pillars, as [Wagner 1980]:

$$w_e = 4 A_p / C_p \quad (5-4)$$

where

$A_p$  = cross sectional area of the pillar ( $w^2$  for a square pillar)

$C_p$  = cross sectional circumference of the pillar ( $4w$  for a square pillar)

## 5.2.3 Pillar load formula

Pillar axial stress has been estimated by tributary area theory [Salamon 1967, Salamon 1974] as:

$$\text{Pillar stress} = \rho g H / (1 - e) \quad \text{[MPa]} \quad (5-5)$$

where  $H$  is depth-of-cover,  $e$  is the area extraction ratio, which is theoretically between zero (no extraction) and one (100% extraction). To keep consistency with the original parameters of equation (5-1), gravity and average overburden density in this study are assumed to be:

$$g = 10 \text{ m / sec}^2$$

$$\rho = 2488 \text{ kg / m}^3$$

Using tributary area theory, the original work of Salamon and Munro [Salamon 1967] calculates the load of a square pillars width  $w$ , bord width  $B$  and depth of mining  $H$  as:

$$\text{Pillar stress} = \rho g H [(w + B)/w]^2 \quad [\text{MPa}] \quad (5-6)$$

In equation (5-6) it is assumed that the stress is fully contained on the pillars that are uniform in size with constant bord width [Salamon 1974, Zipf 2001], which is a conservative assumption [Wagner 1980] and is acceptable if the panel width to depth ratio exceeds unity [Roberts 2002].

One of the outcomes of the present Collingwood Park investigation is the development of a method of estimating pillar loads, where the conditions for tributary area theory are not satisfied as is the case at Westfalen No. 3 Colliery in the western branch. This method is termed “pressure arch theory” and described in greater detail in [Poulsen 2010]. Based on the pressure arch theory, coal pillar stress is estimated as:

$$\text{Pillar stress} = \rho g H_c / (1 - e_i) \quad [\text{MPa}] \quad (5-7)$$

where the depth-of-cover  $H_c$  is estimated at the pillar centroid and the extraction ratio  $e_i$  is calculated within a zone-of-influence (ZI) defined by the depth and it is dependent on the Load Transfer Distance (LTD) defined as [Abel 1988, Poulsen 2010]:

$$\text{LTD} = -1 \times 10^{-4} H_c^2 + 0.2701 H_c \quad [\text{m}] \quad (5-8)$$

$$\text{ZI} = 2 \text{ LTD} + w_e / 2 \quad [\text{m}] \quad (5-9)$$

## 5.2.4 Numerical model calibration

The numerical code FLAC3D (F3D) developed by Itasca Consulting Group has been used for all numerical studies of single pillars and Westfalen No. 3 mining panels. F3D is a three dimensional continuum code with yield criteria suitably flexible for modelling the full stress/strain response of coal. Interfaces with Coulomb sliding can be defined in the model and it was needed to achieve a close match to analytical formula over a wide range of width-to-height ratios.

A strain softening yield criterion has been used for modelling coal. The Mohr-Coulomb material model with non-associated shear and associated tension flow rules [Fama, 1995; Itasca Consulting Group Inc., 2006; Pietruszczak, 1980; Hoek, 1990] was used. In this model the parameters representing material cohesion, friction, dilation and tensile strength may reduce or soften after the onset of plastic yield by a user defined piecewise linear function [Jiang, 2009; Zhou, 2009]. Softening curves after model calibration are displayed in Figure 5-1.

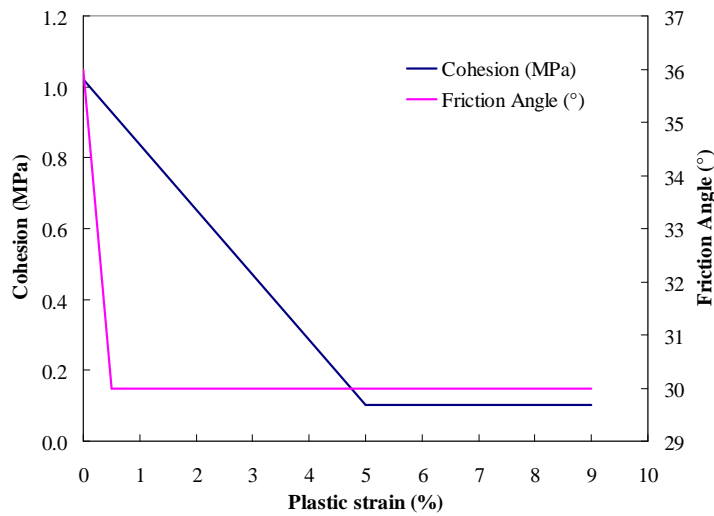


Figure 5-1. Variation of cohesion and friction angle with plastic strain.

Coal model properties are estimated from the reported values in literature and from calibration analyses matching Eq.(5-3) for a range of width-to-height ratios from 2 to 4. To estimate pillar strength the model as displayed in Figure 5-2 is compressed at a fixed vertical velocity while the average pillar stress is monitored.

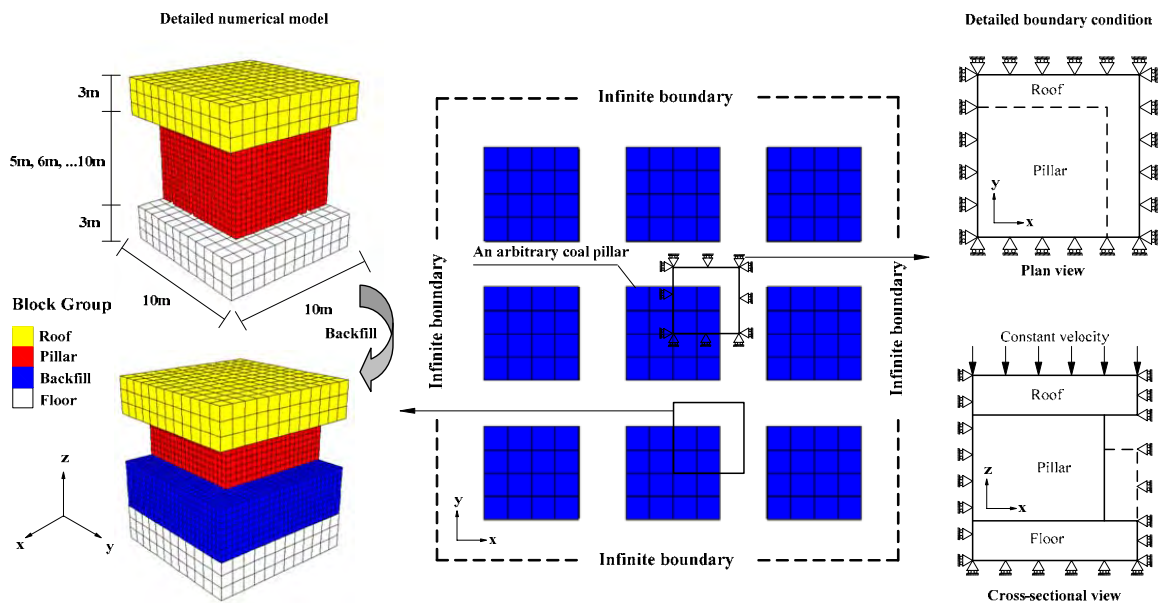


Figure 5-2. Example of single pillar model for examining pillar strength improvement from roadway fill.

The resultant material properties are presented in Table 5-1 and Table 5-2. Recognising that the response of softening models are sensitive to numerical element size, the calibrated element size of 0.5m x 0.5m x 0.5m is kept constant where possible.

Studies of the 2008 failure region are somewhat constrained by computer resources and numerical elements are unavoidably larger than the single pillar calibrated size and of variable size reflecting the irregular pillar shapes. Average dimensions in these models are 2m by 2m in plan and 1.5m in the vertical direction. Material properties at this calibration element size are presented in Table 5-3.

Table 5-1. Mechanical parameters for calibrated 0.5m element used for single pillar numerical model.

Property	Young's Modulus			Poisson's Ratio	UCS (MPa)	Tensile Strength (MPa)
	(GPa)					
Coal	1.10*			0.30	4.0**	0.04***
Roof	5.70			0.19	N/A	N/A
Floor	7.97			0.24	N/A	N/A

Property	Cohesion			Friction Angle			Dilation Angle (°)
	Original value (MPa)	Softening rate (%)	Residual value (MPa)	Original value (°)	Softening rate (%)	Residual value (°)	
Coal	1.02	5	0.102	36.0*	0.5	30.0	6.0

* from CSIRO report #42 [ref Schlanger HP, Enever JR, & Tsaganas S, 1983]

** from initial values of cohesion and friction angle

*** fixed at 1% UCS

As discussed in [Galvin 1981] with reference to physical models, there is a subtle difference in model response at specific width to height ratios, depending on whether the width or height of the model is fixed. This variation is attributed by Galvin to volume, stiffness and pillar end effect variation between width and height changes. In the Collingwood Park single pillar studies, generally the width is fixed at 20m and width-to-height changes are achieved with height variations and material properties are calibrated to this. In studies of diamond and other shaped pillars where the width or effective width varies a unique set of material properties calibrated over width-to-height 2 to 4 at fixed height is developed. In the full three dimensional 2008 event region models, the material properties are calibrated at fixed width but due to the irregular pillar arrangement there will be some unknown error due to effective width variations.

Table 5-2. Mechanical parameters of interface used in numerical model.

Interface property	Normal stiffness (GPa)	Shear stiffness (GPa)	Cohesion (MPa)	Friction Angle (°)
	2.0	2.0	0.5	20.0

Table 5-3. Mechanical parameters for calibrated 2m element used for studies of 2008 event region and adjacent region.

Property	UCS (MPa)	Tensile strength (MPa)	Cohesion (MPa)	Friction angle (degrees)
Coal (2m by 2m by 1.5m element)	2.79	0.0279	0.71 100% loss over 2.4% plastic strain	36 6 deg loss over 2% plastic strain

## 5.3 Summary of results on coal pillar strength

This section summarises the key findings from the numerical study on coal pillar strength. The detailed results are given in Appendix A.

### 5.3.1 Post peak strength

Das (1986) presented work on the post peak strength for Indian coals at various width-to height ratios. His results show some variability but have a general correlation between post peak strength and increasing w/h ratio. Beyond a w/h ratio of approximately 5 to 8 samples start to harden with increasing strain. This observation was confirmed in studies for Collingwood Park, Figure 5-3.

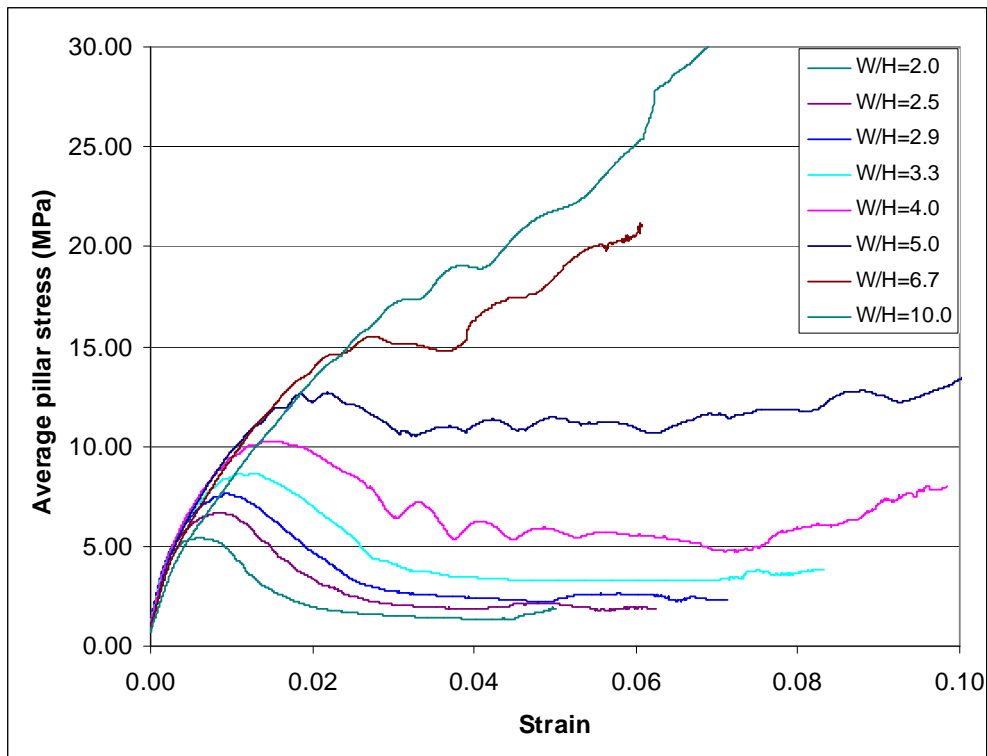


Figure 5-3. Post peak failure behaviour of numerical pillars of constant width,  $w = 20\text{m}$ , but variable height ( $h$ ).

### 5.3.2 Pillar shape influence on strength

Collingwood Park has many pillars of regular and irregular shapes, including diamond, triangular and other regular and irregular polygon shapes.

Diamond shaped pillars are common at the Duncan St failure panel and adjacent areas with side length 20-30m and acute internal angle of 50 degrees, Figure 5-4.

For a diamond shape defined by:

$$\text{Circumference} = C = 4 w$$

where  $w$  is the pillar side length. When the acute internal angle is  $\theta$  the area is:

$$\text{Area} = A = w^2 \sin \theta$$

The minimum width is:

$$\text{Minimum width} = w \sin \theta$$

Effective width by hydraulic radius analogy (e.g. 5-4) is:

$$w_{\text{eff}} = 4A/C = w \sin \theta = \text{minimum width}$$

Material properties used friction for calibrated model at  $w/h$  2 to 4 with fixed 6m pillar height are given in Table 5-4.

Table 5-4. Cohesion and friction for calibrated model at w/h 2 to 4 with fixed 6m pillar height.

Property	Cohesion			Friction Angle			Dilation Angle (°)
	Original value (MPa)	Softening rate (%)	Residual value (MPa)	Original value (°)	Softening rate (%)	Residual value (°)	
Coal	1.23	3.5	0.23	36.0	0.5	30.0	6.0

Results from the study of a number of pillar shapes found at Westfalen No. 3 are presented in Figure 5-4. In general it is found that the hydraulic radius analogy gives a good estimate of the effective width with errors under 5% for the range of shapes analysed.

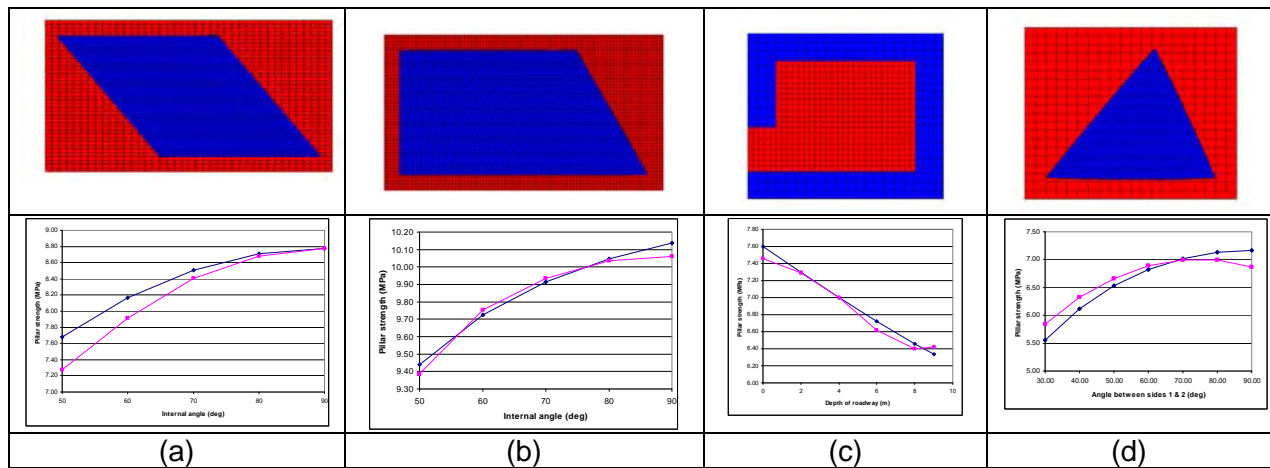


Figure 5-4. Pillar shapes from Westfalen No. 3 Colliery. (a) diamond, (b) quadrilateral with one acute internal angle < 90°, (c) rectangular pillar being split by roadway (note symmetry is applied to LH boundary, (d) triangular pillar. Magenta curve is the result with shape factor =  $4A^{0.5}/C$ .

### 5.3.3 Additional findings

Several numerical models were designed to study a realistic roof geometry, pillars surrounded by roadways of variable height and pillars cut narrower at the top than the base. The results are reported in detail in the Appendix A. Findings from these studies are summarised below.

- The idealised single pillar model with elastic roof gives good agreement with the detailed roof geology model. The differences in peak strength are less than 1% at 9m mining height and less than 4.5% at 5m mining height. This implies that the simplified model, which runs significantly faster, gives satisfactory results and makes it possible for more than 180 individual model runs.
- It was observed in the 1983 pillar site investigation [ref Hollingworth, Dames & Moore, 1990] that mining heights at Westfalen No. 3 are extremely variable with roadways surrounding individual pillars varying by up to 2m. It was found from the numerical modelling study that a pillar with 8m roadway on one side and 6m on the

other has a pillar strength equivalent to a 7m pillar. This leads to an assumption that the average pillar height can satisfactorily be used in calculating pillar strength.

- It was suggested by mine managers at the time that roadways at Westfalen No. 3 were cut in three passes with the upper cut wider than the lower. This is studied in a numerical model with pillar width 23m in lower two thirds and 20m in upper third. Modelling predicts the strength of this variable width pillar to be equal to the minimum pillar width, i.e. 20m in this case.

## 5.4 Roadway backfill and pillar strength improvement

Three backfill “types” were modelled referred to as non-cohesive (fly ash and water), 0.5MPa and 1.0MPa cohesive backfills (fly ash, cement, water etc with a unconfined uniaxial strength of 0.5MPa and 1.0MPa respectively (after settling). The percentage of pillar strength increase due to filling surrounding roadways was investigated using numerical models.

Backfill with a conservative estimated strength of 1.0MPa has been utilized in the nearby Ipswich Motorways Upgrade (IMU) for filling mine voids. A backfill of this strength was analysed together with the 0.5MPa backfill. Given the large volume required to fill the Westfalen #3 mine, it is more likely that the lower cost 0.5MPa fill be preferred should a cohesive mix be selected as the final remediation option.

Backfill properties used in this study are listed in Table 5-5.

Table 5-5. Backfill properties, data from various sources.

Backfill	Young's Modulus (GPa)	Poisson's Ratio	UCS (MPa)	Tensile Strength (MPa)	Cohesion (MPa)	Friction Angle (°)	Dilation Angle (°)
Cohesive	0.565	0.40	1.0	0.1	0.117000	40.0	10.0
0.5MPa-cohesive	0.565	0.40	0.5	0.05	0.060842	40.0	10.0
Non-cohesive	0.020	0.15	0.0	0.0	0.000000	42.0	7.5

### 5.4.1 Numerical results and analysis

In order to quantify the influence of backfill on pillar strength, 180 models (60 models each for non-cohesive, 0.5MPa and 1MPa cohesive backfills) were analysed for square coal pillars with a pillar width of 20m, mining heights of 5m to 10m (equivalent to w/h ratio of 2 to 4), and percentage of backfill from 0 to 90%. Predicted strength increases are presented in Table 5-6, Table 5-8 and Figure 5-5.

### 5.4.2 Post peak pillar strength increase

Post peak strength increase is presented to approximately 4% strain in Figure 5-7 and the approximate amount of backfill required to change from softening to hardening response is given in Table 5-7.

Table 5-6. Predicted strength increase of 7m high square pillar of 20m width from backfill types at 60 to 90% roadway fill.

% roadway fill	Non-cohesive backfill % strength increase	0.5 MPa cohesive backfill % strength increase	1.0 MPa cohesive backfill % strength increase
60	13.5	38.8	43.7
70	18.3	43.2	59.7
80	20.8	47.4	69.8
90	29.1	57.2	95.7

Table 5-7. Predicted amount of roadway backfill that leads to a change from strain softening to hardening.

Pillar height	Non-cohesive backfill	0.5MPa Cohesive backfill	1.0MPa Cohesive backfill
5m	30.0%	20.0%	20.0%
6m	50.0%	41.7%	33.3%
7m	57.1%	50.0%	42.9%
8m	62.5%	62.5%	50.0%
9m	72.2%	72.2%	61.1%
10m	80.0%	80.0%	70.0%

### 5.4.3 Backfill for diamond shaped pillars

A 7m high diamond shaped pillar with 50 degree skew angle was analysed with increasing level of backfill. Modelling results suggest a 66 percentage strength increase from 90% roadway fill using 0.5MPa cohesive backfill.

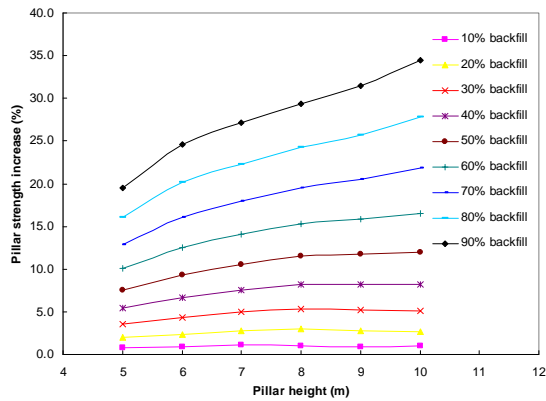
### 5.4.4 Backfill placed after significant pillar yield

A pillar model with 90% non-cohesive backfill placed after yielding of a 7m high pillar is presented in Figure 5-8. The percentage of strength increase is given in Table 5-9. It is found that the pillar strength increase is less significant if the pillar has undergone significant deformation before the placement of backfill. A 90% backfill is predicted to result in a strain-hardening pillar behaviour even if the pillar has previously yielded significantly.

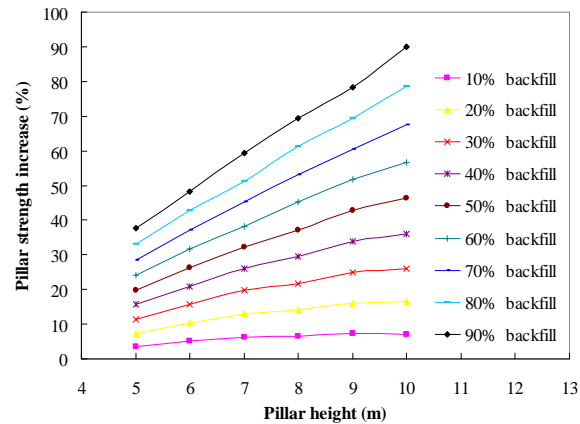
Table 5-8. Pillar strength with increasing cohesive backfill and non-cohesive backfill

Pillar strength	Backfill	Approximate percentage of backfill (%)	Pillar height (m)						
			5	6	7	8	9	10	
Pillar strength (MPa) for different percentage of backfill	Without backfill	0	10.07(0.0%)	8.94(0.0%)	7.95(0.0%)	7.14(0.0%)	6.47(0.0%)	5.96(0.0%)	
		10	10.49(10.0%)	9.40(8.3%)	8.33(7.1%)	7.85(12.5%)	7.20(11.1%)	6.50(10.0%)	
		20	11.04(20.0%)	9.83(16.7%)	9.09(21.4%)	8.20(18.8%)	7.71(22.2%)	7.10(20.0%)	
		30	11.40(30.0%)	10.69(33.3%)	9.47(28.6%)	8.89(31.3%)	8.03(27.8%)	7.58(30.0%)	
		1MPa Cohesive backfill	40	12.05(40.0%)	11.30(41.7%)	10.46(42.9%)	9.29(37.5%)	8.69(38.9%)	8.24(40.0%)
			50	12.34(50.0%)	11.78(50.0%)	10.95(50.0%)	10.16(50.0%)	9.43(50.0%)	8.94(50.0%)
			60	12.92(60.0%)	12.08(58.3%)	11.43(57.1%)	10.98(62.5%)	10.09(61.1%)	9.56(60.0%)
			70	13.42(70.0%)	12.71(66.7%)	12.70(71.4%)	11.58(68.8%)	11.20(72.2%)	10.35(70.0%)
			80	14.66(80.0%)	14.42(83.3%)	13.50(78.6%)	13.45(81.3%)	13.09(83.3%)	11.80(80.0%)
	90		15.93(90.0%)	15.80(91.7%)	15.56(92.9%)	14.70(87.5%)	14.40(88.9%)	14.00(90.0%)	
	0.5MPa Cohesive backfill		10	10.26(10.0%)	9.30(8.3%)	8.30(7.1%)	7.73(12.5%)	6.97(11.1%)	6.36(10.0%)
			20	10.81(20.0%)	9.68(16.7%)	8.96(21.4%)	8.03(18.8%)	7.54(22.2%)	6.87(20.0%)
			30	11.32(30.0%)	10.53(33.3%)	9.39(28.6%)	8.71(31.3%)	7.86(27.8%)	7.41(30.0%)
		40	11.84(40.0%)	10.98(41.7%)	10.18(42.9%)	9.01(37.5%)	8.53(38.9%)	7.99(40.0%)	
		50	12.17(50.0%)	11.41(50.0%)	10.65(50.0%)	10.00(50.0%)	9.36(50.0%)	8.73(50.0%)	
		60	12.40(60.0%)	11.67(58.3%)	11.02(57.1%)	10.54(62.5%)	10.09(61.1%)	9.54(60.0%)	
		70	12.69(70.0%)	11.89(66.7%)	12.37(71.4%)	10.93(68.8%)	10.44(72.2%)	10.14(70.0%)	
		80	13.22(80.0%)	12.80(83.3%)	11.67(78.6%)	11.43(81.3%)	11.05(83.3%)	10.61(80.0%)	
		90	14.10(90.0%)	13.50(91.7%)	12.50(92.9%)	12.02(87.5%)	11.50(88.9%)	11.20(90.0%)	
	Non-cohesive backfill	10	10.16(10.0%)	9.02(8.3%)	8.01(7.1%)	7.24(12.5%)	6.57(11.1%)	6.04(10.0%)	
		20	10.28(20.0%)	9.12(16.7%)	8.19(21.4%)	7.32(18.8%)	6.70(22.2%)	6.15(20.0%)	
		30	10.44(30.0%)	9.41(33.3%)	8.32(28.6%)	7.53(31.3%)	6.78(27.8%)	6.29(30.0%)	

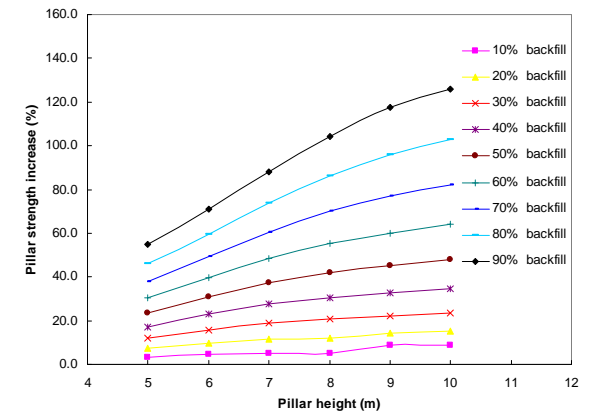
Pillar strength	Backfill	Approximate percentage of backfill (%)	Pillar height (m)					
			5	6	7	8	9	10
		40	10.63(40.0%)	9.61(41.7%)	8.65(42.9%)	7.67(37.5%)	7.02(38.9%)	6.49(40.0%)
		50	10.86(50.0%)	9.84(50.0%)	8.85(50.0%)	8.00(50.0%)	7.29(50.0%)	6.70(50.0%)
		60	11.13(60.0%)	10.06(58.3%)	9.04(57.1%)	8.35(62.5%)	7.60(61.1%)	6.96(60.0%)
		70	11.38(70.0%)	10.30(66.7%)	9.43(71.4%)	8.52(68.8%)	7.92(72.2%)	7.25(70.0%)
		80	11.68(80.0%)	10.83(83.3%)	9.63(78.6%)	8.89(81.3%)	8.29(83.3%)	7.65(80.0%)
		90	12.06(90.0%)	11.30(91.7%)	10.29(92.9%)	9.13(87.5%)	8.52(88.9%)	8.04(90.0%)



Non-cohesive backfill

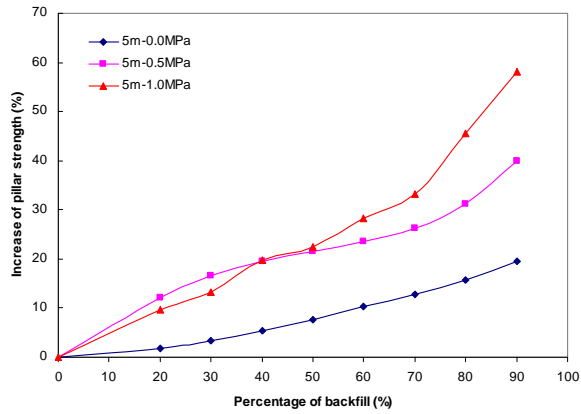


0.5MPa backfill

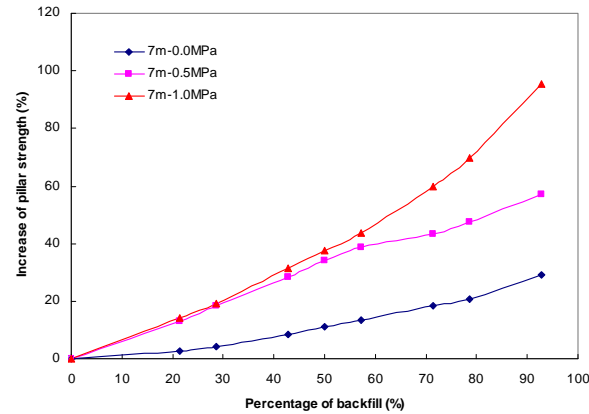


1.0MPa backfill

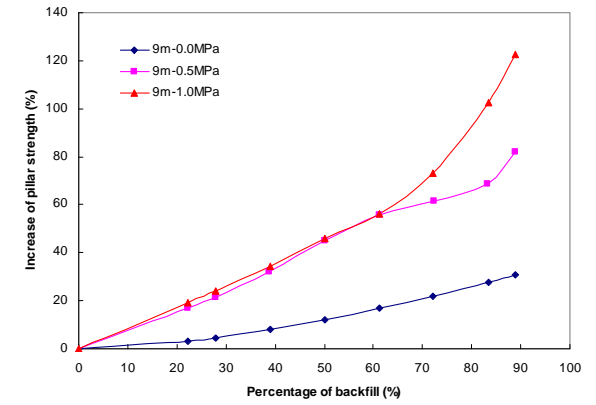
Figure 5-5. Percentage strength increase from roadway backfill.



5m high backfill

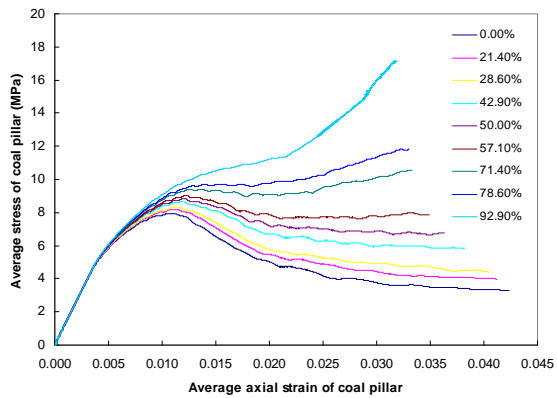


7m high backfill

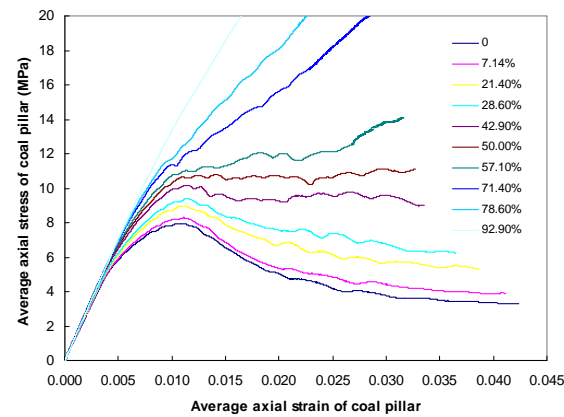


9m high backfill

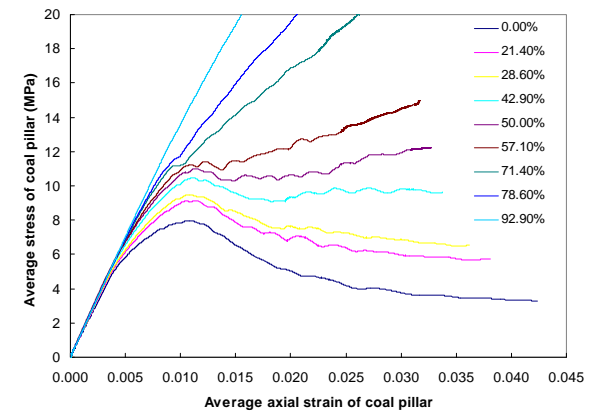
Figure 5-6. Comparison of strength increase from the different types of roadway backfill.



Non-cohesive backfill



0.5MPa backfill



1.0MPa backfill

Figure 5-7. Comparison of strength increase from the different types of backfill at 7m mining height.

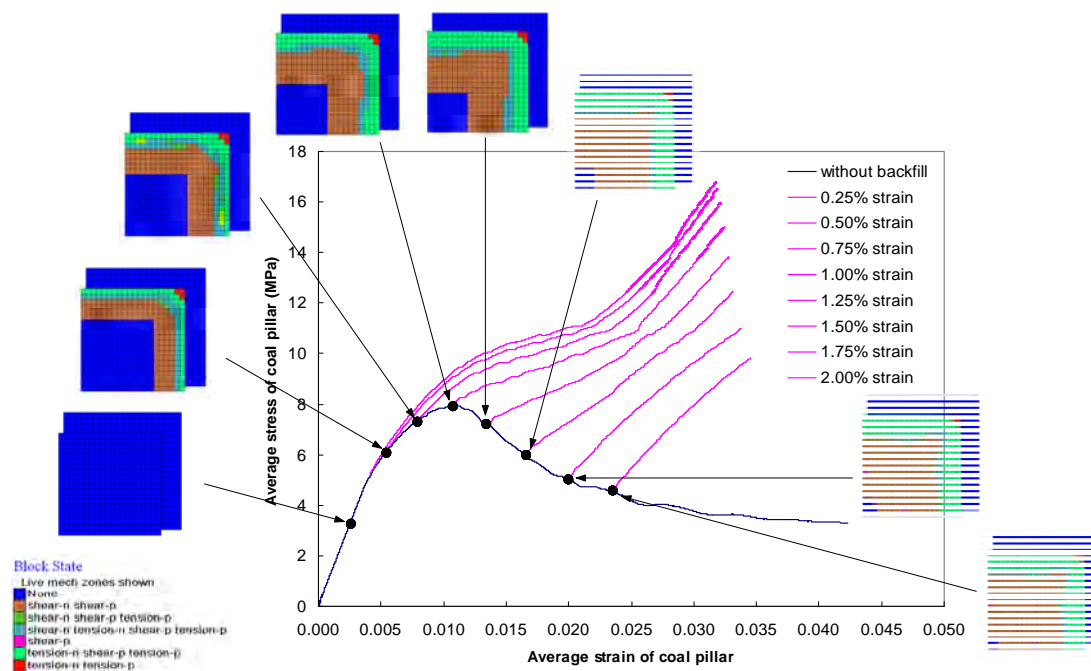


Figure 5-8. Stress strain curves for non-cohesive backfill placed around the pre-strained pillar displaying state of pillar core upon placement of backfill.

Table 5-9. Pillar strength with 90% non-cohesive backfill placed around a pre-strained 7m high square pillar of 20m width.

Percentage backfill (%)	Strain at placement of non-cohesive backfill (%)	Pillar strength (MPa)	Percentage increase in peak strength (%)	Percentage increase in post-peak strength at 3% strain (%)
0	0.00	7.953	0.00	/
90	0.00	10.290	29.39	/
90	0.25	9.156	15.13	/
90	0.50	8.965	12.72	/
90	0.75	8.526	7.20	/
90	1.00	7.945	/	260.06
90	1.25	7.951	/	226.08
90	1.50	7.951	/	189.17
90	1.75	7.951	/	156.29
90	2.00	7.951	/	111.34

## 5.5 3D models of 2008 failure panel and adjacent regions.

Two three dimensional models of panels in the 2008 failure region and adjacent central panel immediately to the northeast of the Waterline fault have been analysed in Flac3D, Figure 5-9.

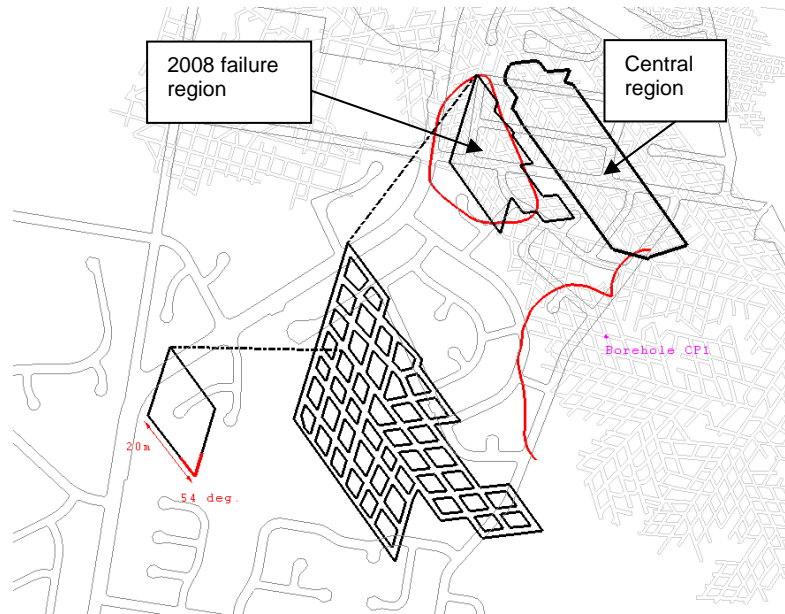


Figure 5-9. Location of two models of multiple pillars with expanded view of 2008 failure region panel. Note the location of representative open hole CP1. Westfalen No. 3 pillar layout, road network and subsidence contours are displayed.

The following observations are made from these models.

- In the 2008 subsidence region approximately 46 pillars are surrounded by unmined coal to the northwest, a large barrier pillar in the vicinity of the Waterline fault to the northeast and larger pillars to the southeast and north.
- In the central panel 76 pillars are bounded by the Waterline fault barrier pillar to the southwest, barrier pillars to the ventilation and conveyer roadways to the northeast and pillars of similar size north and southeast.
- 6m and 9m mining heights are studied in the 2008 event region model and 9m in the central panel.
- Depth of cover is 124m in both models, and the seam and all lithological units are the same to allow comparison of the relative strength of the two regions due to the pillar geometry.
- Representative hole CP1 is used to identify overburden rock units.

### 5.5.1 Results from 2008 event region model

- At 6m mining height, the minimum pillar FoS for these 46 pillars is calculated to be 1.31 using the Pressure Arch theory and UNSW strength formula. At 9m mining height the minimum FoS is calculated as 0.99.
- The probability of pillar failure for associated FoS calculated by the UNSW pillar strength formula, Eq.(5-2) is given in Galvin 2006 below. Caution is required when using this relationship because it was developed for square pillars using the Australian pillar database and tributary area theory:

Table 5-10. Factor of Safety (FoS) failure probabilities for UNSW pillar strength formula. (after Galvin 2006)

Safety Factor	Probability of pillar failure
0.87	8 / 10
1.00	5 / 10
1.22	1 / 10
1.3	5 / 100
1.38	2 / 100
1.44	1 / 100
1.63	1 / 1000
1.79	1 / 10000
1.95	1 / 100000
2.11	1 / 1000000

- From Table 5-10 there is a 1 in 20 probability of instability at 6m mining height, and a 1 in 2 probability at 9m mining height. Numerical modelling is however a deterministic approach, and it always predicts failure if the FoS is less than 1.0 and stability if  $FoS > 1.0$  since no variation in geotechnical properties or conditions is used.
- Although our numerical models predict no pillar failure at 6m and panel failure at 9m, in reality there remains approximately a 1 in 20 chance of failure at 6m mining height. If one pillar was to fail, load transferred to adjacent pillars would reduce the FoS of these adjacent pillars and could lead to the pillar failure and subsidence as observed at 2008 event region.
- Based on the numerical results obtained using two mining heights, the pillar and overburden failure is consistent with analytical predictions from Pressure Arch theory and UNSW pillar strength calculation.
- Surface subsidence predicted from the numerical model with a mining height of 9m is 1.96m. While this value is in general agreement with monitoring data, the model

was not sufficiently calibrated, since the real mining height in the region is uncertain, to be able to confidently predict final subsidence, strains and tilts at the site.

- With 1MPa cohesive backfill at a roadway fill ratio of 83%, the predicted strength increase is 70%. With non-cohesive backfill at the same fill ratio, the strength increase is 20%. These values are in agreement with the results for single pillars.
- The numerically predicted surface subsidence with 83% roadway fill is 0.22m. Maximum predicted tilt in east-west direction is 7mm/m and in north-south direction is 5mm/m. Analytical formula (ref Holla & Barclay) predict maximum tilt of 5.3mm/m for this amount of subsidence. Overall tilts in buildings less than 5 mm/m would generally have negligible impact on building structures (Mine Subsidence Engineering Consultants, 1997).
- Isolated cohesive backfill surrounding pillars of low w/h ratio is predicted to be effective in confining the pillar and increasing peak pillar strength and panel stability. Isolated non-cohesive backfill without barriers could not be analysed in this numerical model as backfill ‘flows’ and numerical stability could not be achieved.
- Stress transfer in the immediate roof sandstone unit (above the coal roof) are predicted to extend approximately 80m beyond the limits of collapsed panel. This is in reasonable agreement with theoretical studies.

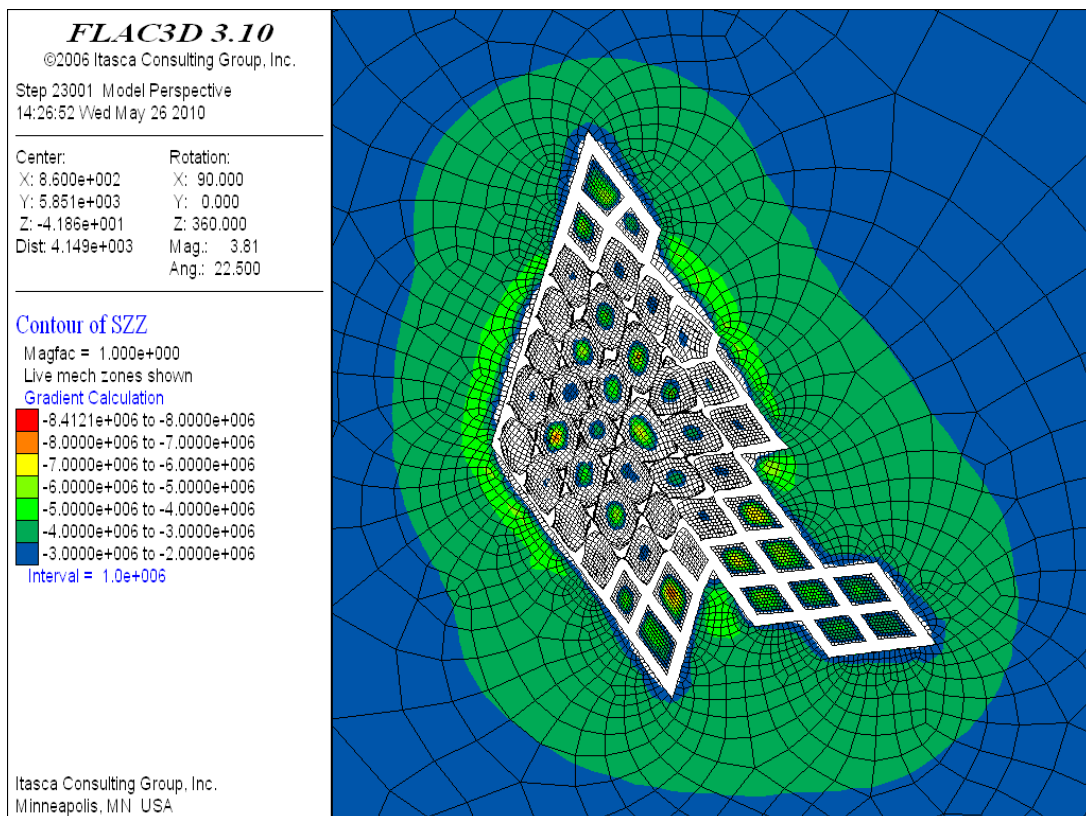


Figure 5-10. Predicted vertical stress at mid pillar height after the failure of 9m high pillars. In situ stress is 3.0MPa. Unyielded pillars and pillars hardening after yield are transferring vertical load while yielded pillars carry little load. Extent of abutment stress increase is approximately 80m.

## 5.5.2 Results from numerical model of the central panel

- At 9m mining height the model predicts a failure of 9 individual pillars but no significant overburden failure and the panel as an entity remains stable.
- With a 20% increase in vertical stress (achieved by increasing gravity) the panel is predicted to fail.

The result suggests that the central panel to the northeast of the Waterline fault is stronger by approximately 20% than the 2008 subsided region. This strength difference is due to pillar dimensions, layout and boundary conditions as it is assumed in the model the seam is horizontal and the depth-of-cover and overburden strata are identical to the 2008 event region model.

- Predicted surface subsidence (including compressive effects from gravity increase) is 1.65m. Note that numerical instability stopped the modelling and hence the ultimate subsidence may not have been achieved.
- Inspection of yield at mid-pillar height of the model after failure suggests the south western pillars in the model have intact core whereas pillars in the middle of the region failed entirely. Seam dips to the south-east and pillar stresses from the overburden will be higher in the southern pillars than that represented in the model.

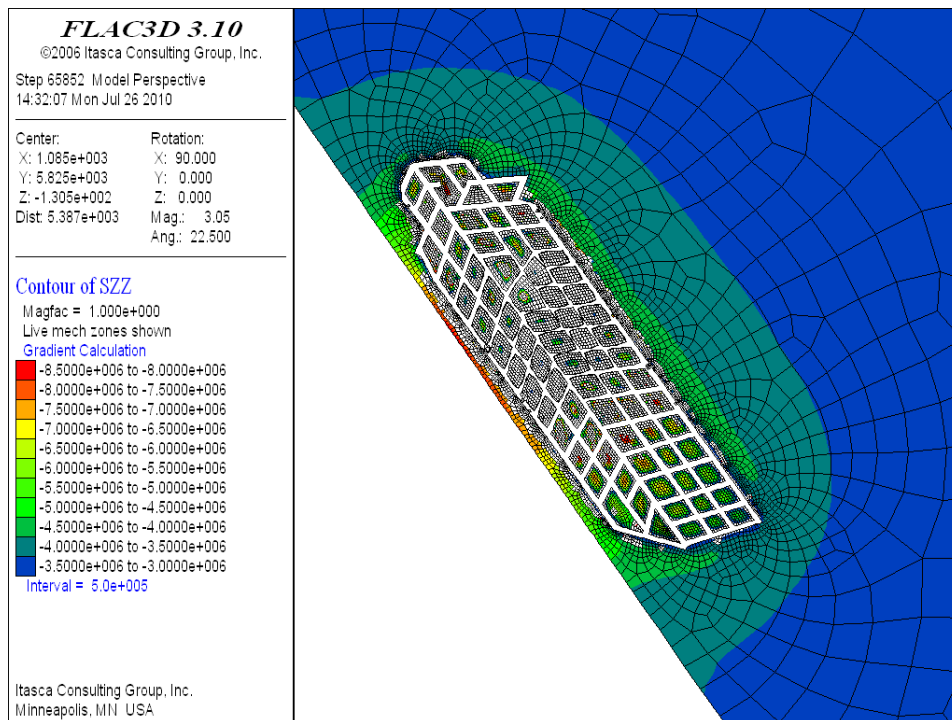


Figure 5-11. Vertical stress at mid-pillar height in the central panel. Insitu stress is approximately 3MPa. Displacements are restrained normal to the southwestern plane that is designed to represent the reduced stiffness of the Waterline fault.

## 6. HAZARD MAPPING AND RISK ASSESSMENT

### 6.1 Summary

Some of the undermined residential areas at Collingwood Park may have a high risk of future subsidence, particularly considering that two subsidence events have already occurred. To assist in the risk management process, an attempt was made to map and identify areas with a high likelihood of future subsidence. This exercise was limited to the Westfalen No. 3 Colliery within the given study area in Collingwood Park, where detailed information about the mining geometry and conditions is available. No such attempt has been made for the New Redbank Colliery due to the limitations of the information available for this mine.

The key results from this investigation are listed below.

- Hazard maps were created by estimating Factors of Safety (FoS) for every pillar based on the pillar's depth-of-cover, mining height and unique size attributes. Pillars interact with each other by shedding load if one fails, reducing the FoS of the adjacent pillars. The amount of load shed by a 'failed' pillar is dependent on its width-to-height ratio.
- Hazard maps produced in this study predict a pillar FoS of less than 1.0 in the two regions that subsided in 1988 and 2008 for an "after-mining" case. This agrees with the actual observation.
- Three remediation strategies were analysed; the first is a "Status Quo" approach with no backfill, the second involves targeted cohesive backfill of 0.5MPa strength in the central panel, the third approach involves total backfilling (with non-cohesive or cohesive fill).
- The central panel region from between Strachan Ct and Heysen Ct in the north extending southeast to Duncan St and beyond is predicted to have a FoS mostly < 1.4, which is considered to be too low to be stable in the long-term.
- Non-cohesive backfill to 90% roadway height is predicted to raise the FoS in the central region to above 1.6, which is the number often used in rock engineering design for long-term stability. A cohesive backfill with uniaxial compressive strength of 0.5MPa is predicted to raise the FoS to greater than 2.0 in the central region.
- Consequence maps have been created to estimate the amount of surface subsidence and surface tilt based on an empirical formula modified by observations from the site and numerical models.
- It is predicted that if pillars were to fail after backfilling roadways to 90% the surface subsidence would be less than 200mm and the surface tilt less than 5 mm/m. Overall tilts in buildings less than 5 mm/m would generally have negligible impact on building structures (Mine Subsidence Engineering Consultants, 1997).

## 6.2 Introduction

Some of the undermined residential areas at Collingwood Park may have a high risk of future subsidence, particularly considering that two subsidence events have already occurred. To assist in the risk management process, an attempt was made to map and identify areas with a high likelihood of future subsidence. This exercise was limited to the Westfalen No. 3 Colliery within the given study area in Collingwood Park, where detailed information about the mining geometry and conditions is available. No such attempt has been made for the New Redbank Colliery due to the limited information available for this mine.

The analyses were based on the best knowledge available about the mining geometries, mining heights, mining conditions. Various sources of information have been used to provide data for this study, including:

- Reports from previous studies in the area.
- Site investigation conducted as part of this study (SMEC, 2010).
- Interviews with previous mine managers of Westfalen No. 3.
- Information and comments from the Expert Panel employed by DIP.

Because it has been more than 20 years since mine closure and the 1974 flooding of the mine, significant uncertainties exist, particularly in estimating the pillar size and effective roadway heights. These uncertainties will inevitably affect the accuracy of this analysis, although measures have been taken (such as using probability approach) to minimise their effect. It is recommended that caution should be taken when using the results of this study.

### 6.2.1 Hazard maps

Hazard Maps of the study region are produced by colour filled contours of Factor of Safety (FoS) calculated for every pillar in Westfalen No. 3 Colliery.

For each pillar, the pillar strength is estimated using the strength formula developed at the UNSW [Gavin et al, 1999], namely:

$$\text{pillar strength} = 8.60 w_e^{0.51} / h^{0.84} \quad [\text{MPa}] \quad (6-1)$$

where  $h$  is the mining height and

$$w_e = 4 A / C \quad [\text{m}] \quad (6-2)$$

where

$A$  = area of pillar cross section

$C$  = pillar circumference

The mining height  $h$  in Westfalen No. 3 Colliery varies in the different mining zones. A range of mining heights has been ascribed to each mining zone by various sources including the site investigation, report data and correspondence with mine personnel. To take in to account this variation in possible mining heights in each zone, a Monte Carlo type simulation was used where the mining height was assumed to follow a normal distribution within the range of heights for each mining zone. A total of 10000 randomly generated combinations of the pillar heights in the study area were used to investigate the pillar/panel FoS and their confidence levels .

Pillar stress was estimated from Pressure Arch Theory (PAT) as discussed in [Poulsen 2010].

During the simulation to estimate FoS, it was assumed that a pillar “sheds” load to its neighbours within a zone-of-influence (ZI) if it is predicted to fail. The extent of the ZI is determined by the load transfer distance (LTD) that is dependent on the overburden depth [Abel, 1988, Poulsen,2010]. At a depth-of-cover of 120m the radius of the ZI is approximately 74m for a 20m square pillar.

The total vertical stress shed by failed pillars is a function of the width-to-height ratio. The quantity of shed stress is based on observations by Das (1986) in Indian mines and numerical modelling results with a square pillar of 20m width, see Table 6-1 and Figure 6-1 and Figure 6-2. Full details are presented in the Appendix I.

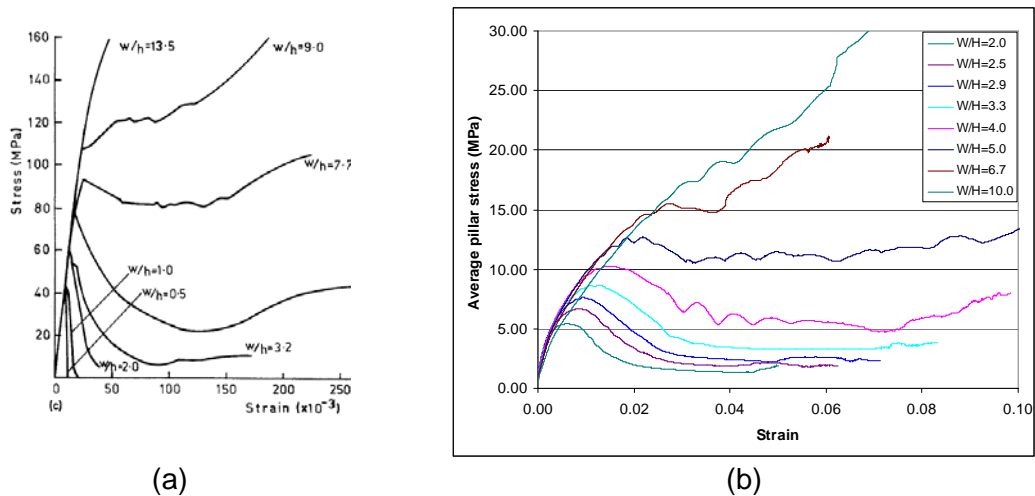
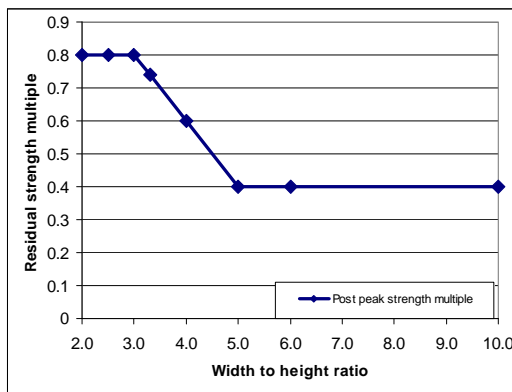


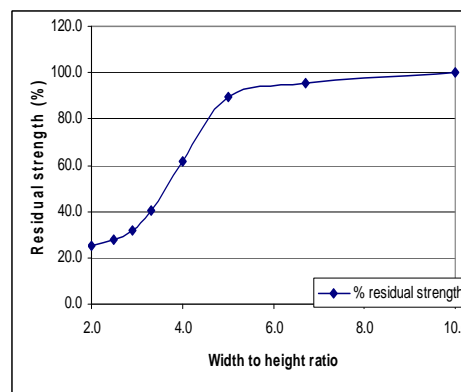
Figure 6-1. Stress-strain curves for pillars at various width-to-height ratios. (a) curves reported in [Das 1986]. The unmarked curve in the middle is  $w/h=4.5$  (b) numerical model for square pillar of width 20m, this study.

Table 6-1. Ratio of pillar residual strength to peak strength for the determination of the quantity of pillar stress shedding.

W/H ratio	Ratio of residual strength /peak strength
< 3.0	0.80
3.3	0.74
4.0	0.60
>= 5.0	0.40



(a)



(b)

Figure 6-2. Stress multiple as function of w/h ratio(a). Value of 1 means all pillar stress is shed to pillars within influence region. Values approximate (b) which in tern is derived from Fig 1-1(b) at 4% strain.

After the calculation of 10000 cases with random pillar heights, the FoS was obtained at the tenth, twenty fifth and fiftieth percentiles, which gives a level of confidence of 90%, 75% or 50% respectively that the “real” FoS is not BELOW the estimated value.

## 6.2.2 Mining zones

Mining heights are variable over Westfalen No. 3 Colliery, and no single source has been able to reliably estimate all heights. Based on a CSIRO site investigation in 1983, drilling by Morton Geotech Services in 1994, drilling within the current DIP/CSIRO project in 2010, interviews with site staff Mr J Edgar, Mr B Evans and Mr B Martin and various reports, a compilation of mining heights in 12 mining zones is presented in Figure 6-3. The resultant ranges of mining heights in each mining zone is given in the 2nd column from left, and they are used in this study.

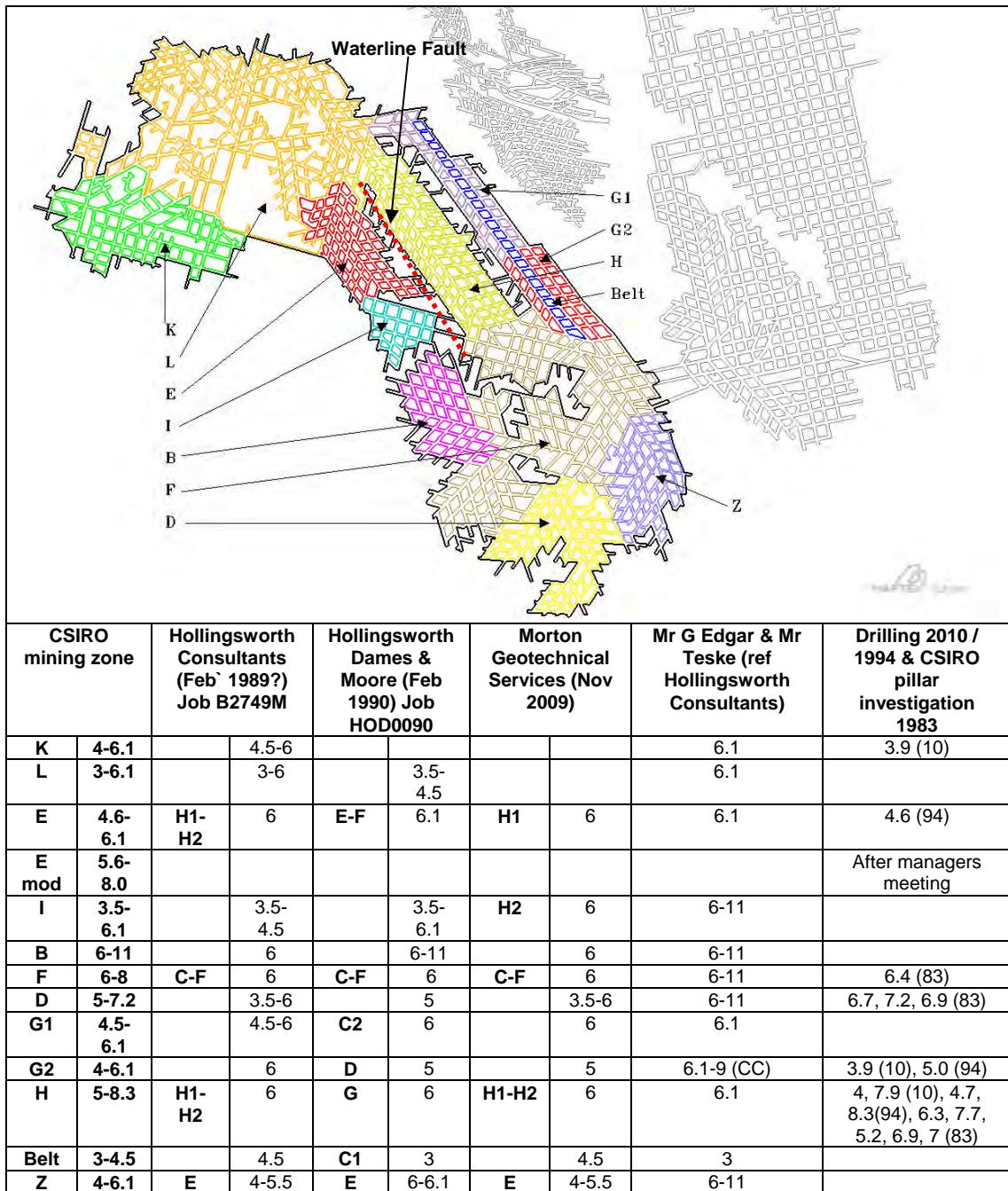


Figure 6-3. Mining zones with mining heights for Westfalen No. 3 Colliery. Note modified mining heights for Duncan St region after interviews with Mr Evans and Mr Martin who state there was no systematic variation in heights west and east of the Waterline Fault.

### 6.3 Hazard maps with and without backfill

A linear relationship between width to height ratio (w/h) and pillar strength increase from backfilling has been assumed based on the numerical studies. For a 90% roadway backfill, the following linear relationships describe the increase in pillar

strength with width to height ratio between 2 and 4. Below 2 and above 4 a constant strength increase is modelled equivalent to  $w/h=2$  or  $w/h=4$  respectively.

0.5 MPa cohesive backfill:

$$[\sigma_{c(\text{fill})} - \sigma_c] / \sigma_c = -0.23 (W/H) + 1.29 \quad (6-11)$$

Non-cohesive backfill:

$$[\sigma_{c(\text{fill})} - \sigma_c] / \sigma_c = -0.06 (W/H) + 0.46 \quad (6-13)$$

Separate hazard maps have been produced for the cases below:

- “No backfill” case (Figure 6-4 - Figure 6-6): This is an “after mining” case and the existing subsidence events are not considered; Three confidence levels are used, 90%, 75% and 50%
- “Targeted backfill” case (Figure 6-7). Mine roadways only in the central region are backfilled to 90% the original heights using 0.5MPa cohesive backfill.
- “Total non-cohesive backfill” case (Figure 6-8). All mine roadways (except those on the western side of Collingwood Drive) are backfilled to 90% the original heights using non-cohesive backfill.
- “Total cohesive backfill” case (Figure 6-9). All mine roadways (except those on the western side of Collingwood Drive) are backfilled to 90% the original heights using cohesive backfill with 0.5MPa strength.

### 6.3.1 Hazard map of Westfalen No. 3 Colliery without backfill

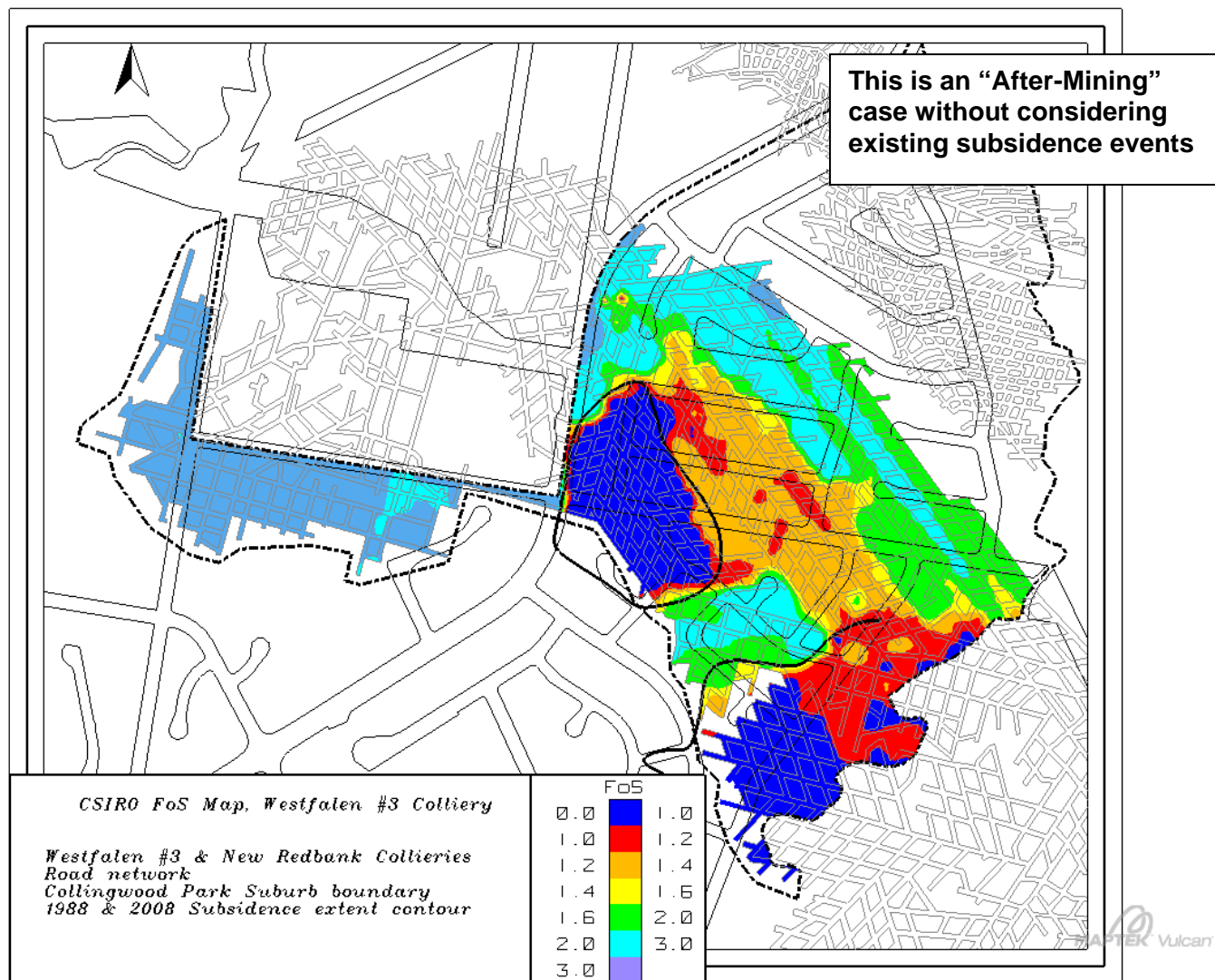


Figure 6-4. Factors of Safety (FoS) calculated without backfill. Minimum 10% FoS values (i.e 90% confidence level).

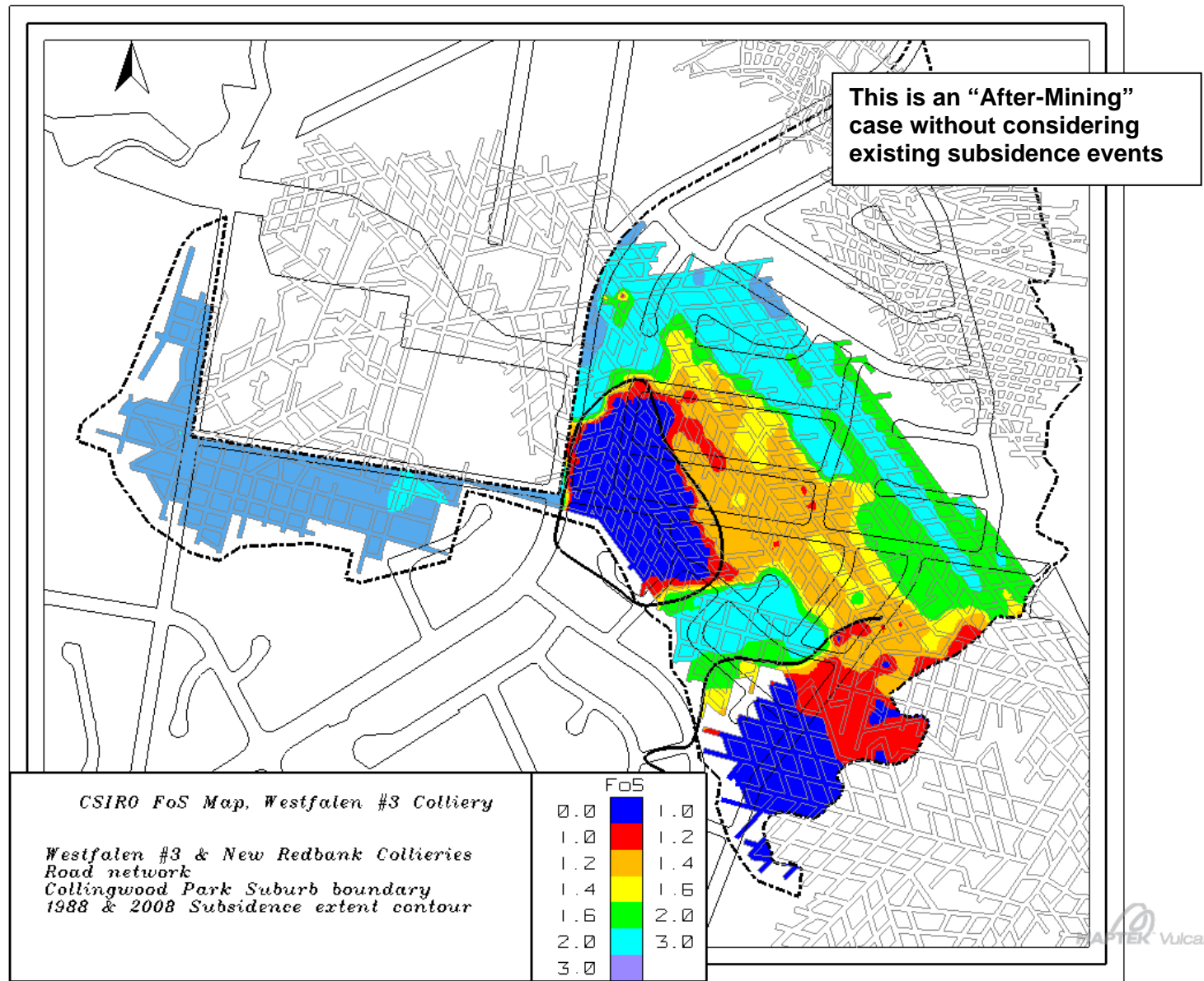


Figure 6-5. Factors of Safety (FoS) calculated without backfill. Minimum 25% FoS values (i.e 75% confidence level).

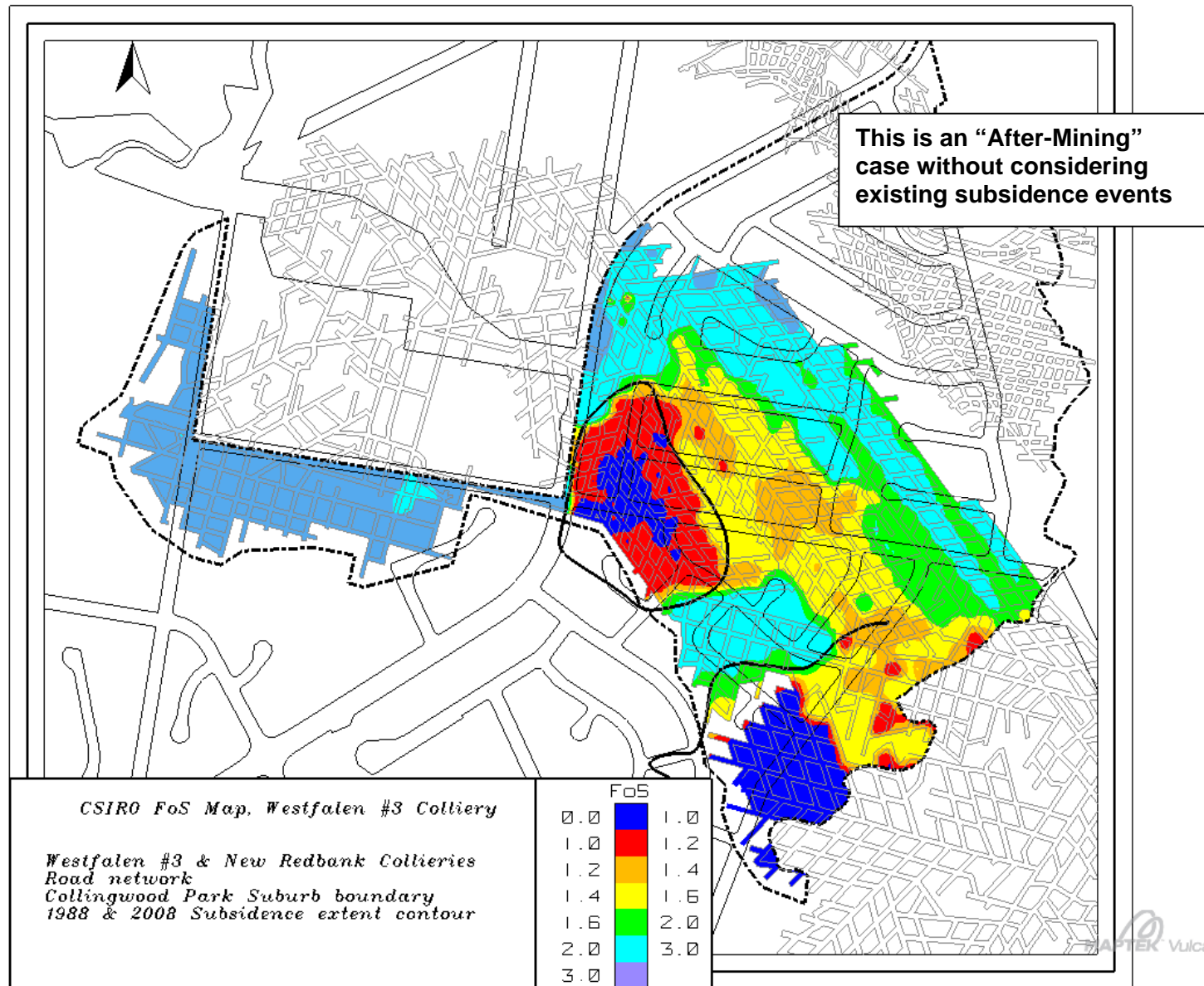


Figure 6-6. Factors of Safety (FoS) calculated without backfill. Mean FoS values (i.e 50% confidence level).

### 6.3.2 Hazard map with targeted 0.5MPa cohesive backfill

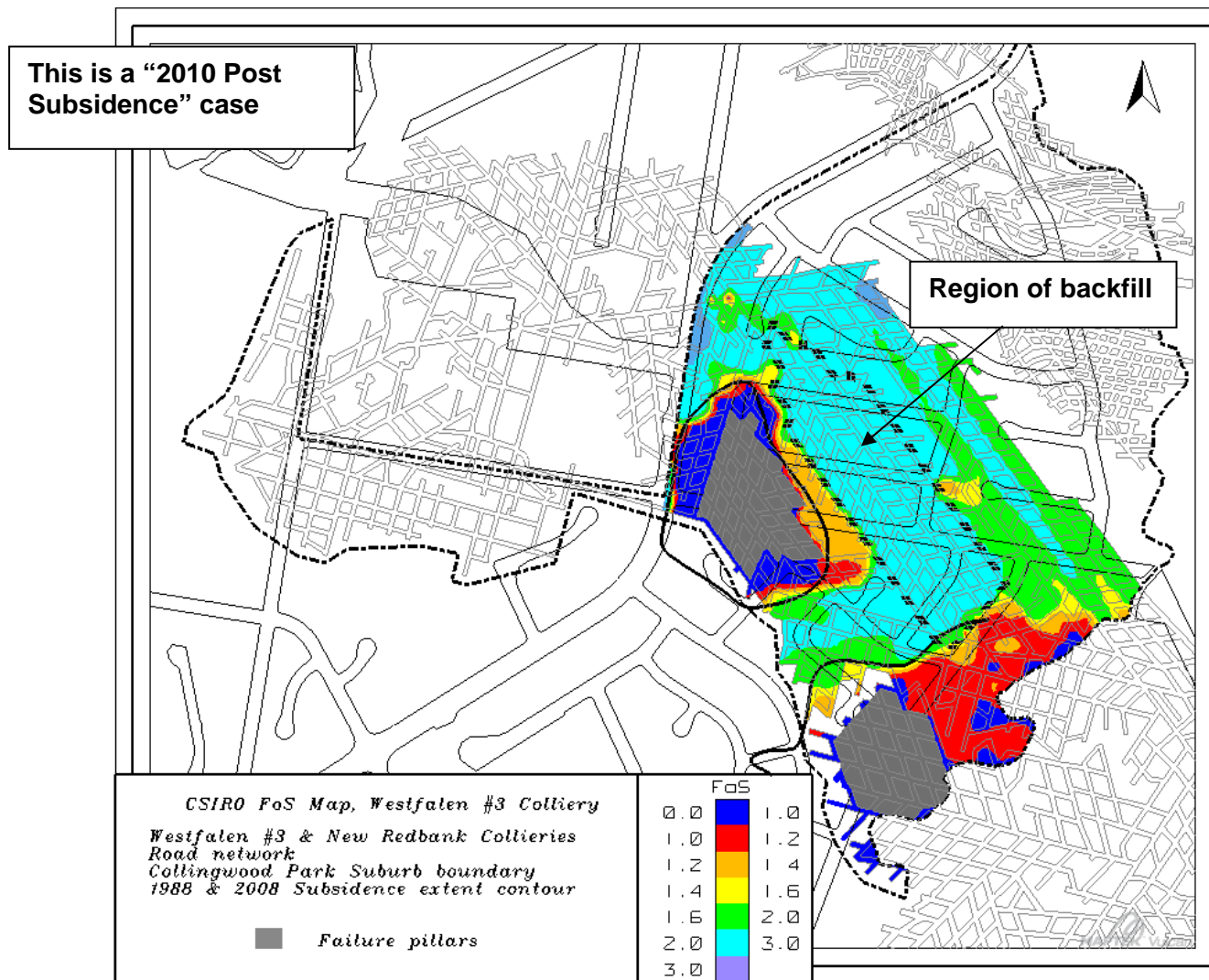


Figure 6-7. FoS Hazard Map with targeted 90% roadway fill using 0.5MPa cohesive backfill, minimum 10% FoS (i.e 90% confidence level). Backfill only in central region.

### 6.3.3 Hazard map with total non-cohesive backfill

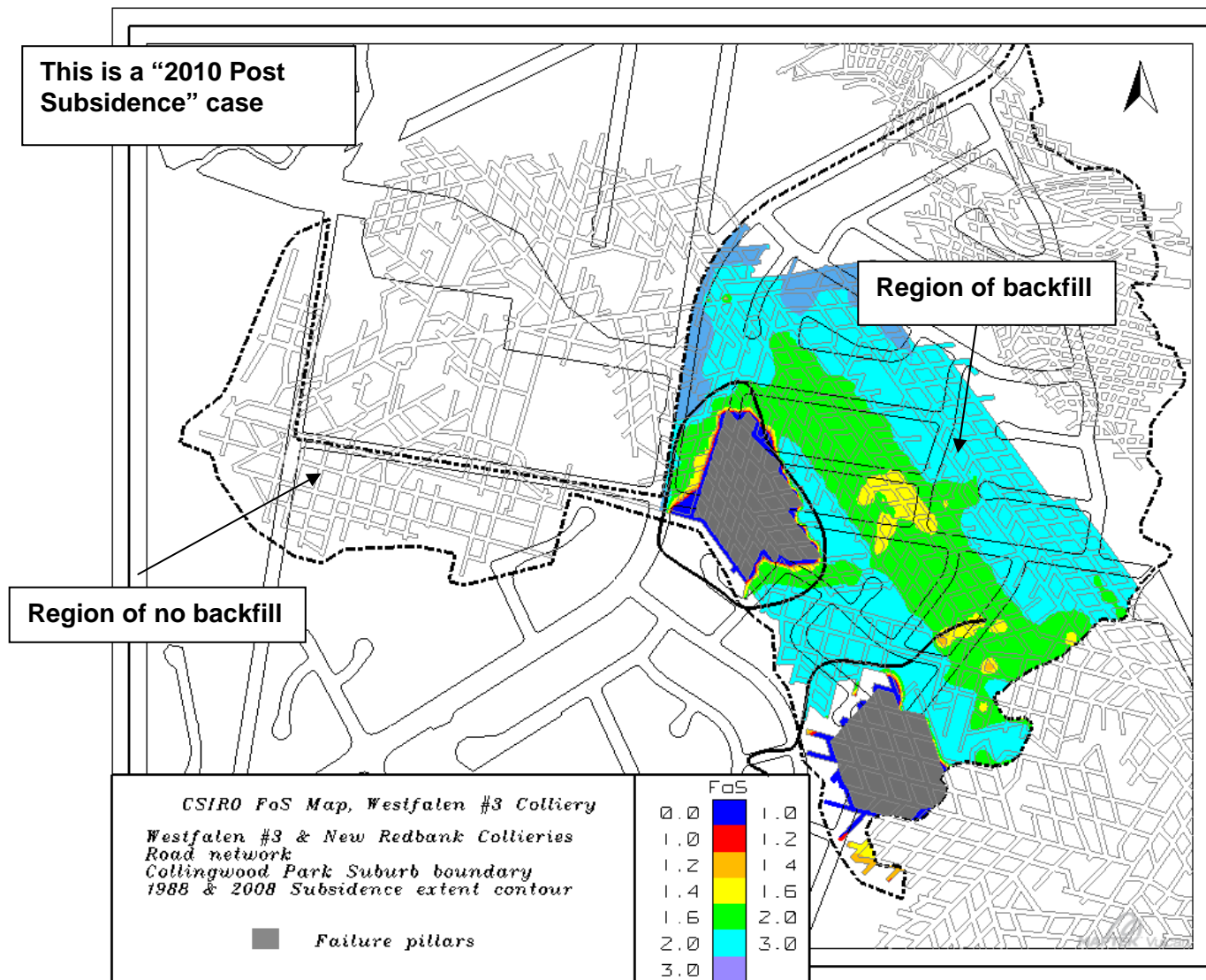


Figure 6-8. FoS Hazard Map with 90% roadway fill using non-cohesive backfill, minimum 10% FoS (i.e 90% confidence level). All roadways except those on the western side of Collingwood Drive are backfilled.

### 6.3.4 Hazard map with total cohesive backfill

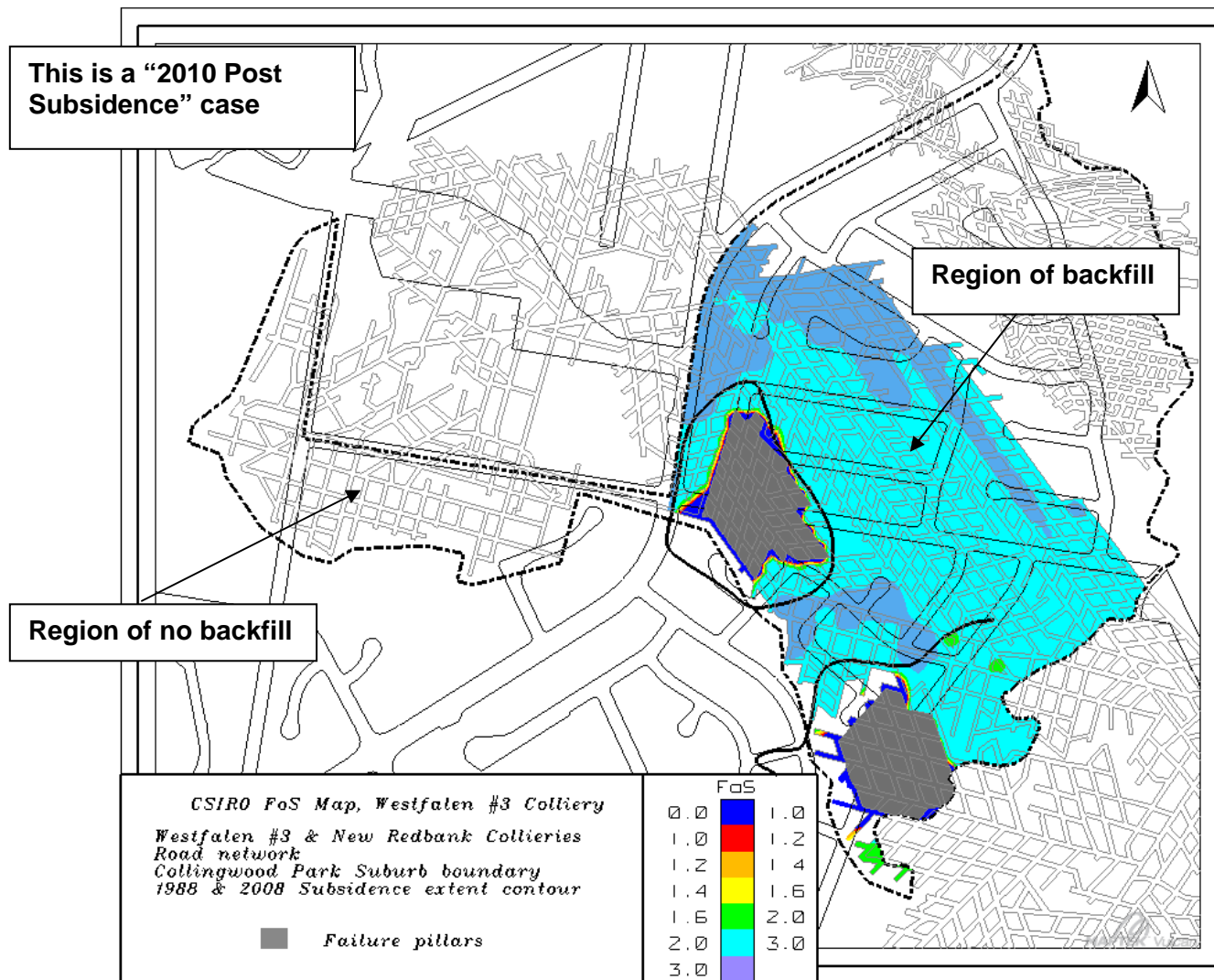


Figure 6-9. FoS Hazard Map with 90% roadway fill using 0.5MPa cohesive backfill, minimum 10% FoS (i.e 90% confidence level). All roadways except those on the western side of Collingwood Drive are backfilled.

## 6.4 Consequence maps – Surface subsidence

Theoretically subsidence,  $S$ , is a non-linear function of location  $(x,y)$ , time  $(t)$ , coal seam pillar height,  $h$ , coal seam area and/or volume extraction ratio,  $e$ , and overburden rock thickness or depth  $(z)$  and properties  $(r)$ , i.e.  $S = S(x, y, t, h, e, z, r)$ .

For practical purposes, surface subsidence has been calculated by a simple linear empirical formula using the Holla approach [Holla & Barclay, 2000], in which subsidence after ground stabilisation is directly proportional to extraction thickness,  $T$ , where  $T$  itself is the product of area extraction ratio,  $e$ , and the coal seam height,  $h$ . The maximum subsidence,  $S_{\max}$ , is estimated by using the Holla formula:

$$S_{\max} = K_1 * T \quad (6-3)$$

Where  $K_1$  is a constant mainly depending on time, and  $T$  is extraction thickness (m).

Holla estimates the multiplier  $K_1$  as 0.65 for longwall mining situation. However  $K_1 = 0.55$  has been found to be a better fit to the observed subsidence and the corresponding numerical results at Collingwood Park.

Holla reported that the influence of remnant pillars can be accounted for by modifying the mining height using the extraction ratio  $e$ , ie

$$T = h * e$$

where  $h$  is the average mining height, which is approximately equal to the average pillar height.

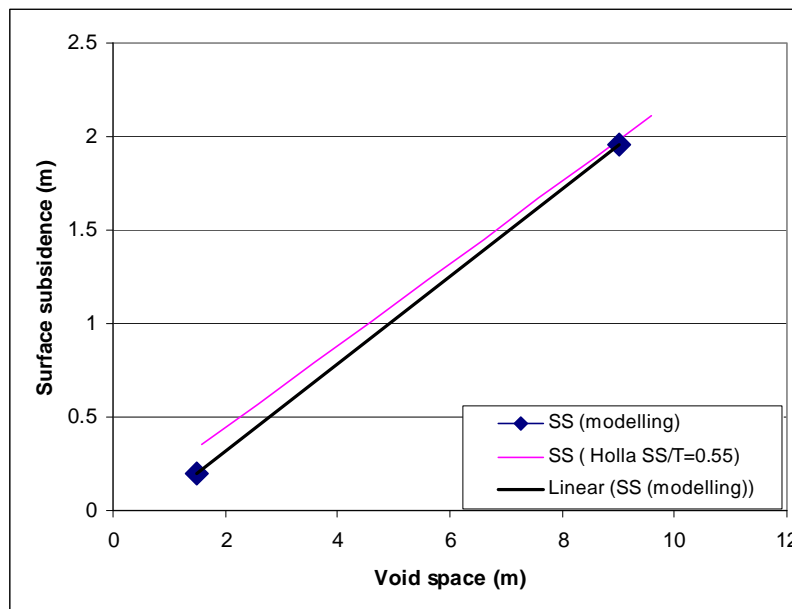


Figure 6-10. Comparison between surface subsidence predicted by two numerical models of Westfalen No. 3 and that predicted by Holla with  $S_{\max}/T=0.55$  and extraction ratio=40%.

By observation of the surface trough from the two existing subsidence events from failure of pillars with approximately 120-130m depth-of-cover it appears that the subsidence is extending a lateral distance of approximately 80m from the centre of the pillar. Therefore the predicted subsidence

from the failure of a pillar is distributed a radial distance of 80m with the maximum subsidence directly above the failed pillar and a cosine function describing the distribution of subsidence to the trough boundary.

Consequence maps (subsidence and tilt) are based on colour filled contouring of the predicted values when we assume that pillars in the region of interests were failed regardless the value of FoS.

The potential subsidence maps with backfill are designed to estimate the maximum surface subsidence **IF** pillars fail with 90% roadway backfill. The potential subsidence map is the same for both cohesive and non-cohesive backfill as it only depends upon the void space remaining in the mine. All maps are for “2010 post-subsidence” case and the subsided areas during the 2008 and 1988 events are assumed to have no further movement. Failure of pillars adjacent to those that failed in 1988 and 2008 will extend subsidence into previously subsided areas.

Potential subsidence maps have been produced for the four cases listed below:

- “No backfill” case (Figure 6-12).
- Failure of central region only. This central failure region includes pillars of similar size and extends further south than the “targeted backfill” region that has been clipped at a surface road centreline.
- “Targeted backfill” case (Figure 6-14). Mine roadways only in the central region of high risk are backfilled to 90% the original heights using cohesive or non-cohesive backfill.
- “Total non-cohesive/cohesive backfill” case (Figure 6-15). All mine roadways (except those on the western side of Collingwood Drive) are backfilled to 90% the original heights using non-cohesive or cohesive backfill.

The prediction of surface subsidence due to failure of irregular pillar layouts inherently has a high degree of uncertainty. The Holla approach with an extraction ratio calculated within a zone-of-influence is found to give a reasonable approximation to measured subsidence at Collingwood Park, Figure 6-11.

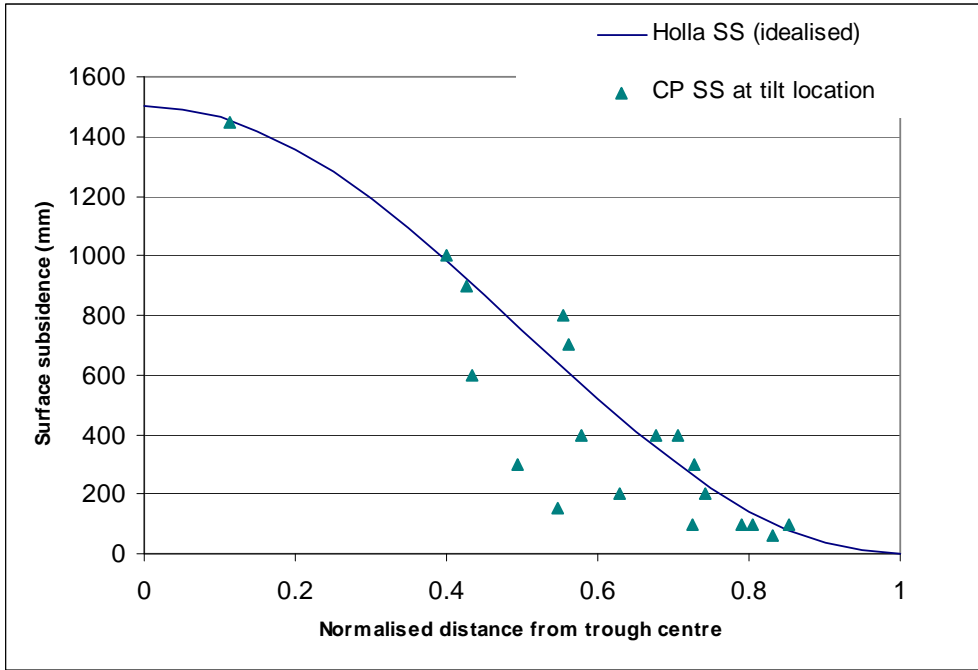


Figure 6-11. Collingwood Park measured subsidence with Holla ground subsidence formula.

### 6.4.1 Potential subsidence map assuming total failure without backfill

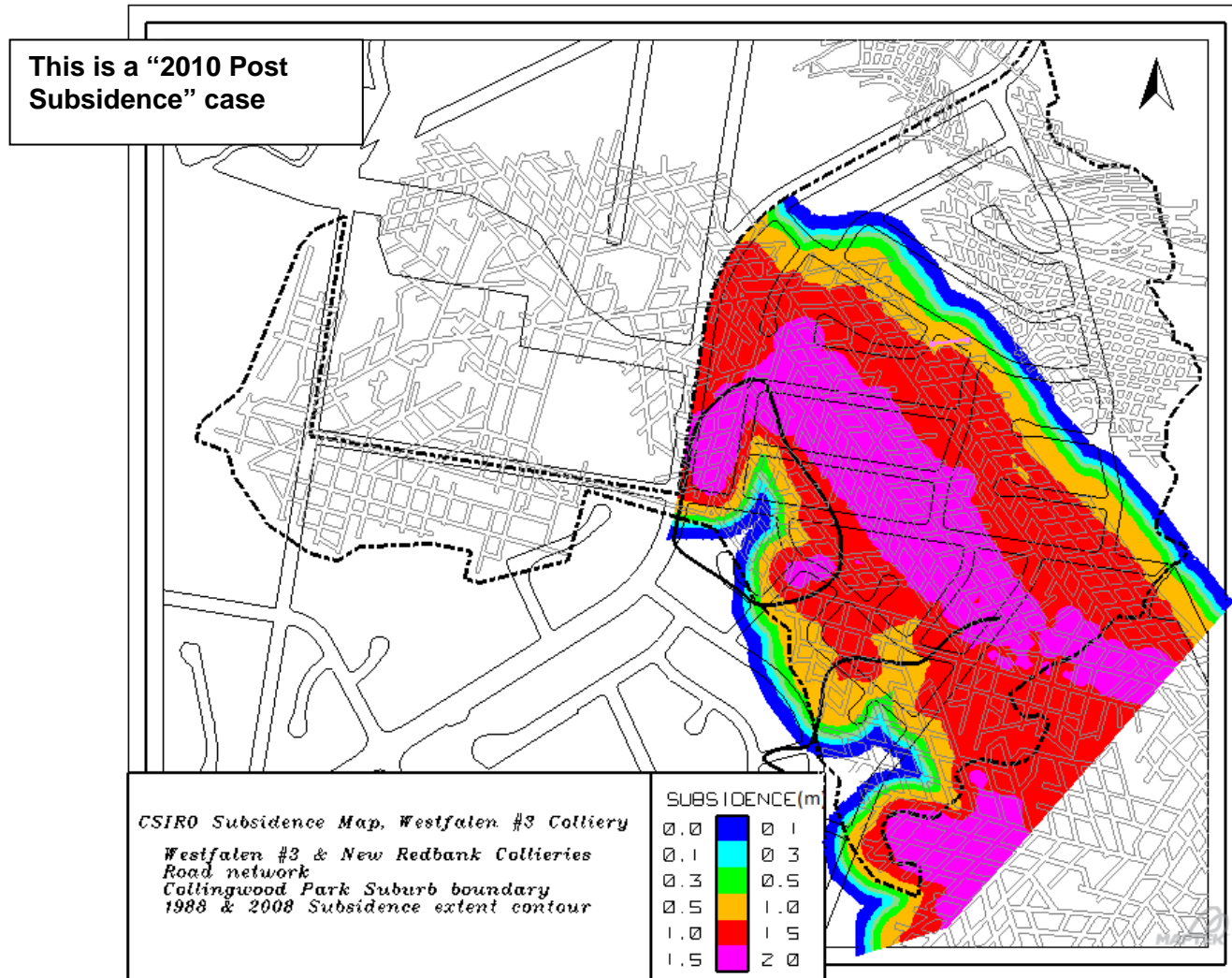


Figure 6-12. Estimated surface subsidence assuming ALL pillars fail with NO backfilling. Assumes height equal to 90% of the maximum reported height for each mining zone.

### 6.4.2 Potential subsidence map assuming failure of central region only without backfill

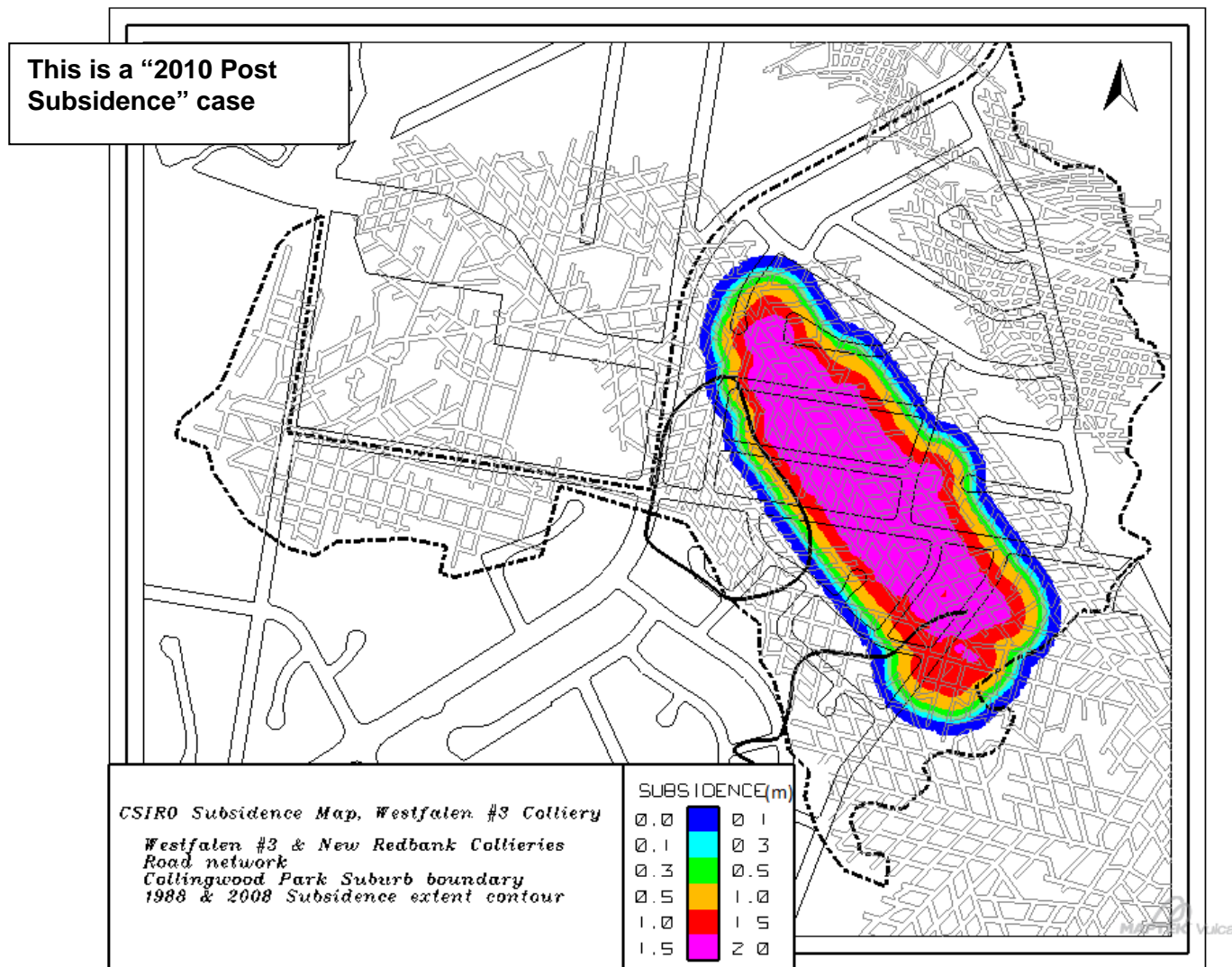


Figure 6-13. Estimated surface subsidence assuming central pillars fail with NO backfilling. Assumes height equal to 90% of the maximum reported height for each mining zone.

### 6.4.3 Potential subsidence map assuming total failure after targeted backfilling

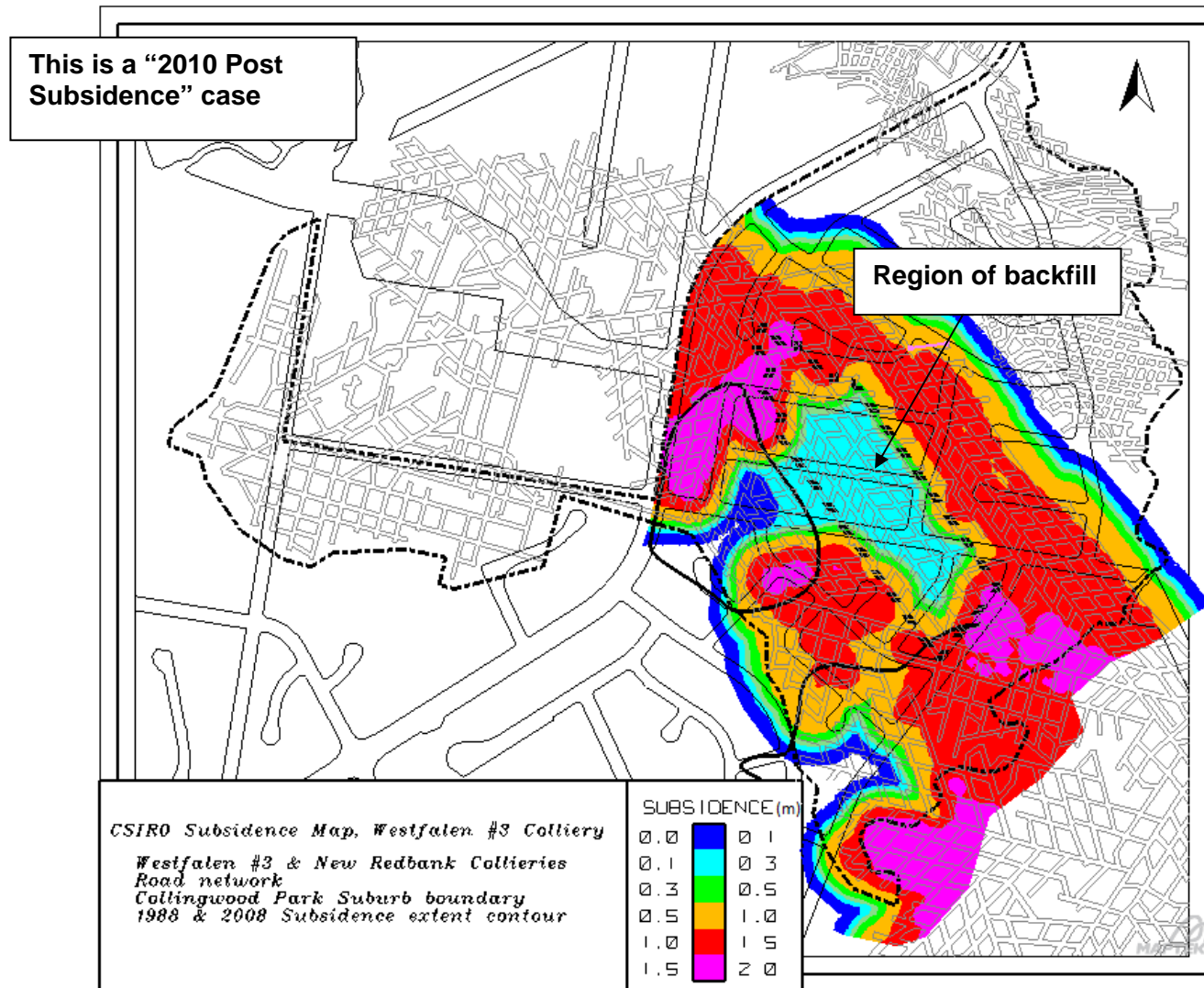


Figure 6-14. Estimated surface subsidence assuming ALL pillars fail after backfilling with 90% roadway fill. Assumes height equal to 90% of the maximum reported height for each mining zone. Backfill only in the central region.

#### 6.4.4 Potential subsidence map assuming total failure after total backfilling

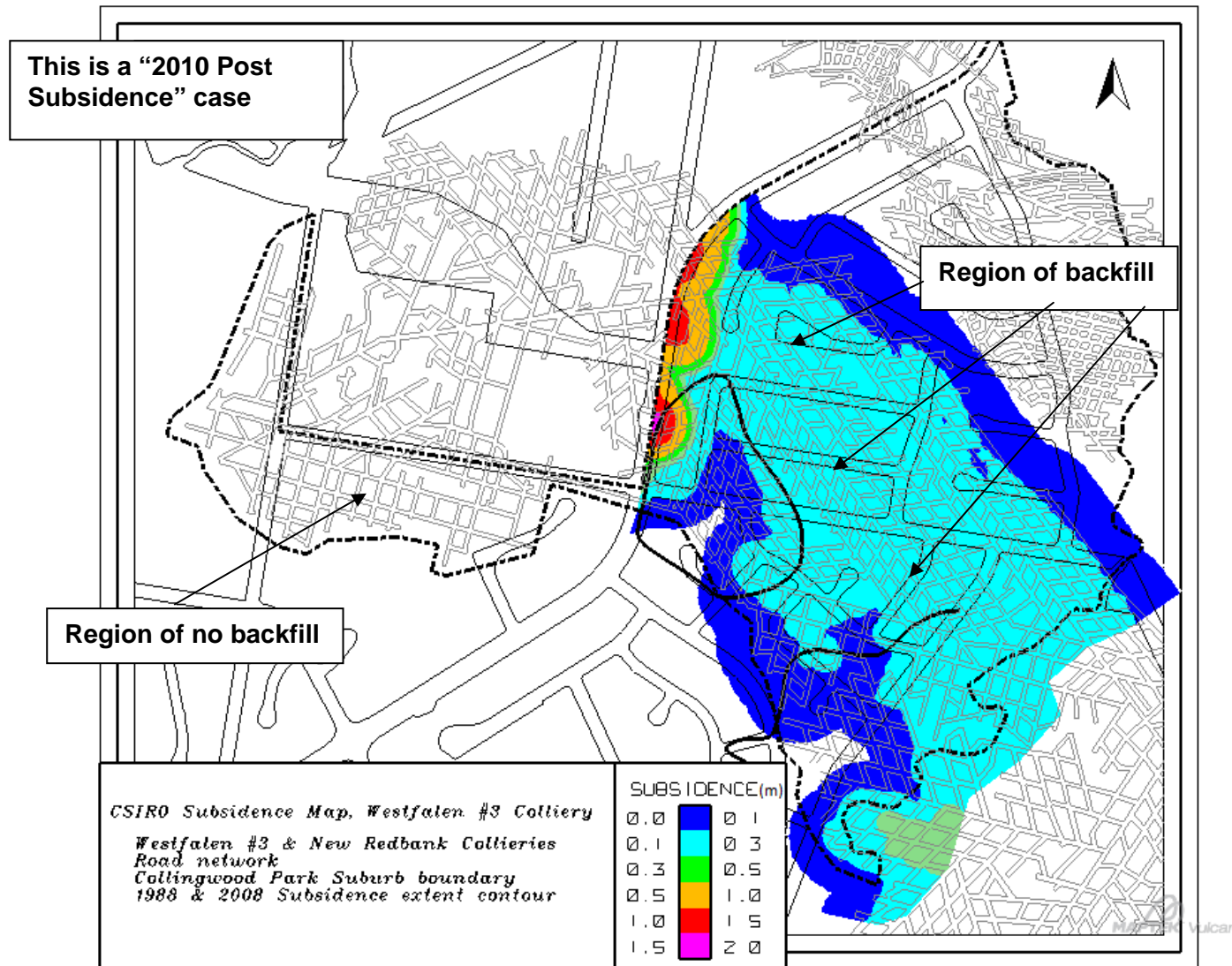


Figure 6-15. Estimated surface subsidence assuming ALL pillars fail after backfilling with 90% roadway fill (including cohesive or non-cohesive backfill). Assumes height equal to 90% of the maximum reported height for each mining zone. All roadways except those on the western side of Collingwood Drive are backfilled.

## 6.5 Consequence maps – Surface tilt

In the following study surface (ground) tilt is related to surface subsidence using Holla's formula:

$$G_{\max} = 1000 K_3 S_{\max} / H \quad (6-4)$$

where  $G_{\max}$  is maximum surface tilt in mm/m,  $S_{\max}$  is maximum surface subsidence in metres,  $H$  is depth-of-cover and  $K_3$  is a constant (= 3 for  $W/H > 1.0$ ).

The location of maximum tilt is approximately mid-way between the base of the subsidence trough and the limit of the trough at the surface. At Collingwood Park this is a distance of approximately 40-50m from the edge of the surface trough.

DEEDI officers have measured foundation tilts and subsidence at different locations in the 2008 subsidence area. For the same subsidence event with a maximum subsidence of 1.5m, we can obtain a predicted tilt distribution using Holla's empirical approach.

Figure 6-16 plots a comparison between the measured tilt and predicted tilt using Holla's approach. Note that the measurements were conducted on house foundations, rather than on the ground surface. It is expected that the measured foundation tilts tend to be less than the actual ground tilt.

The results in Figure 6-16 suggest that the predicted tilts using Holla's approach is generally consistent with the measured data, with the predicted results being slightly more conservative.

The above comparison provides us sufficient confidence that Holla's approach is applicable for the purpose of estimating the tilts at Collingwood Park.

By observation of the surface trough from the two existing subsidence events from failure of pillars with approximately 120-130m depth-of-cover it appear the subsidence is extending a lateral distance on the surface of approximately 80m from the pillar centre. Maximum tilt is assumed to be located mid-distance to the trough boundary and therefore predicted tilt from failure of a pillar is distributed a radial distance of 80m with the maximum tilt at 40m from the failure pillar and a sine function distributing tilt to the trough boundary.

At a given location, only the maximum possible tilt has been considered. Hence it may represent a value due to partial failure of a mine panel. It does not necessarily represent the case that mine panels fail together.

Four potential tilt maps have been produced. These are all for a "2010 post-subsidence" case and the subsided areas during the 2008 and 1988 events are considered to have no further movement.

- "No backfill" case (Figure 6-17).

- “No backfill” case with central region collapse only (Figure 6-18). This central failure region includes pillars of similar size and extends further south than the “targeted backfill” region that has been clipped at a surface road centreline.
- “Targeted backfill” case (Figure 6-19). Mine roadways only in the central region are backfilled to 90% the original heights using cohesive or non-cohesive backfill.
- “Total non-cohesive/cohesive backfill” case (Figure 6-20). All mine roadways (except those on the western side of Collingwood Drive) are backfilled to 90% the original heights using non-cohesive or cohesive backfill.

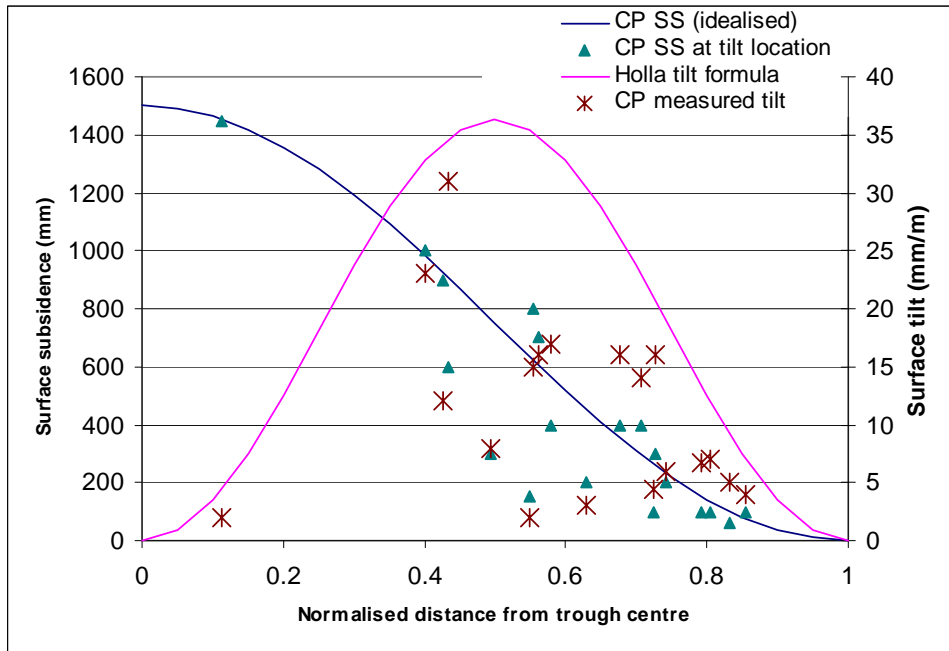


Figure 6-16. Measured tilts and subsidence at Collingwood Park are compared with Holla ground tilt formula. Note measured tilts are on foundations and will generally underestimated ground tilts.

### 6.5.1 Potential tilt map assuming total failure without backfill

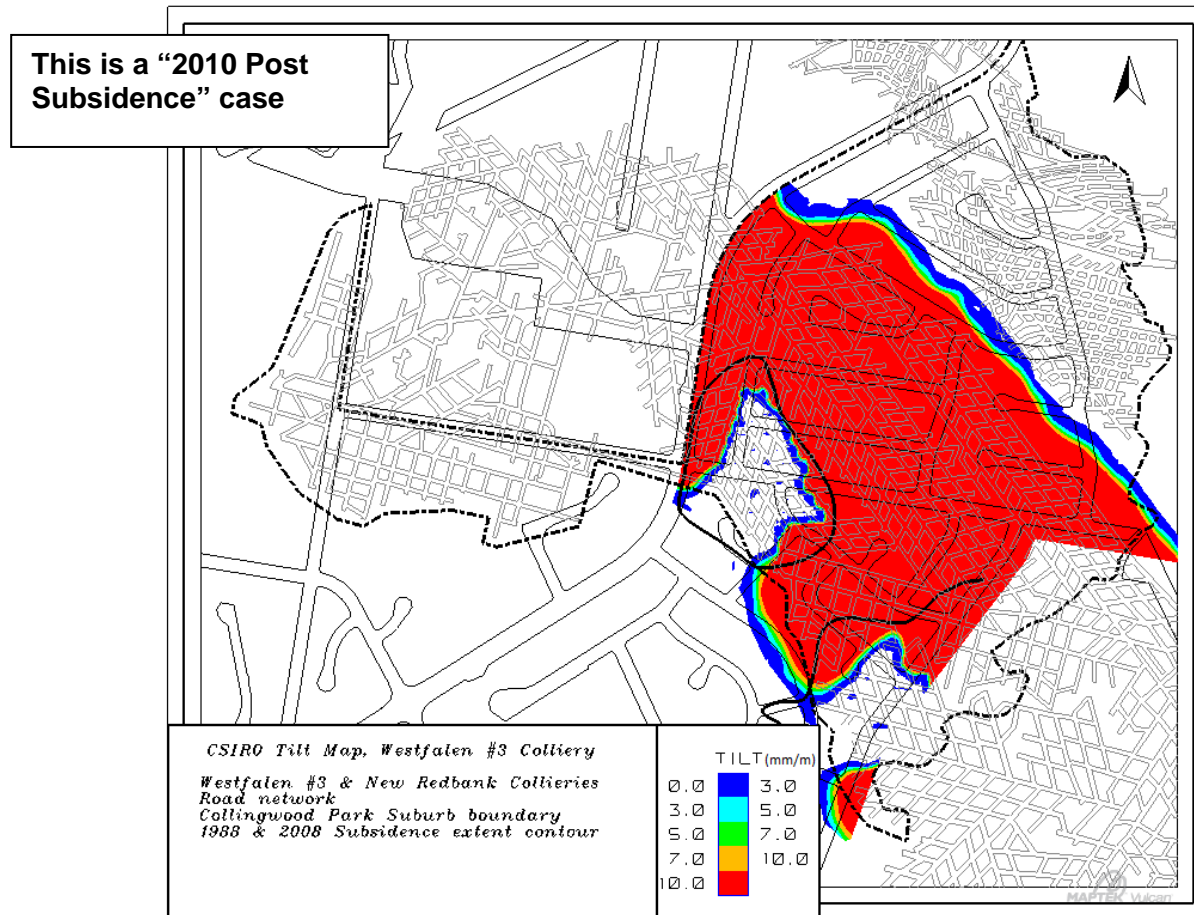


Figure 6-17. Estimated surface tilt assuming ALL pillars fail with NO backfilling. Assumes height equal to 90% of the maximum reported height for each mining zone.

### 6.5.2 Potential tilt map assuming failure of central region without backfill

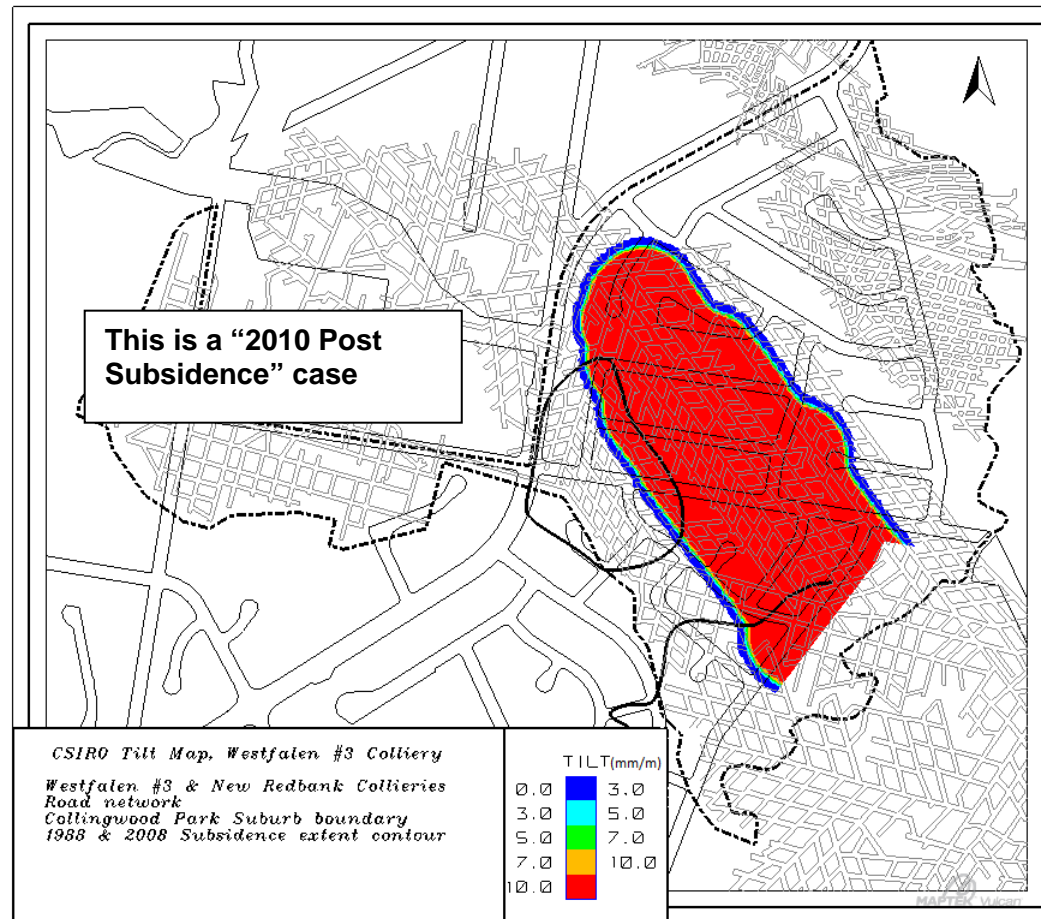


Figure 6-18. Estimated surface tilt assuming central pillars fail with NO backfilling. This central region includes pillars of similar size and extends further south than the proposed targeted backfilled region. Assumes height equal to 90% of the maximum reported height for each mining zone.

### 6.5.3 Potential tilt map assuming total failure after targeted backfilling

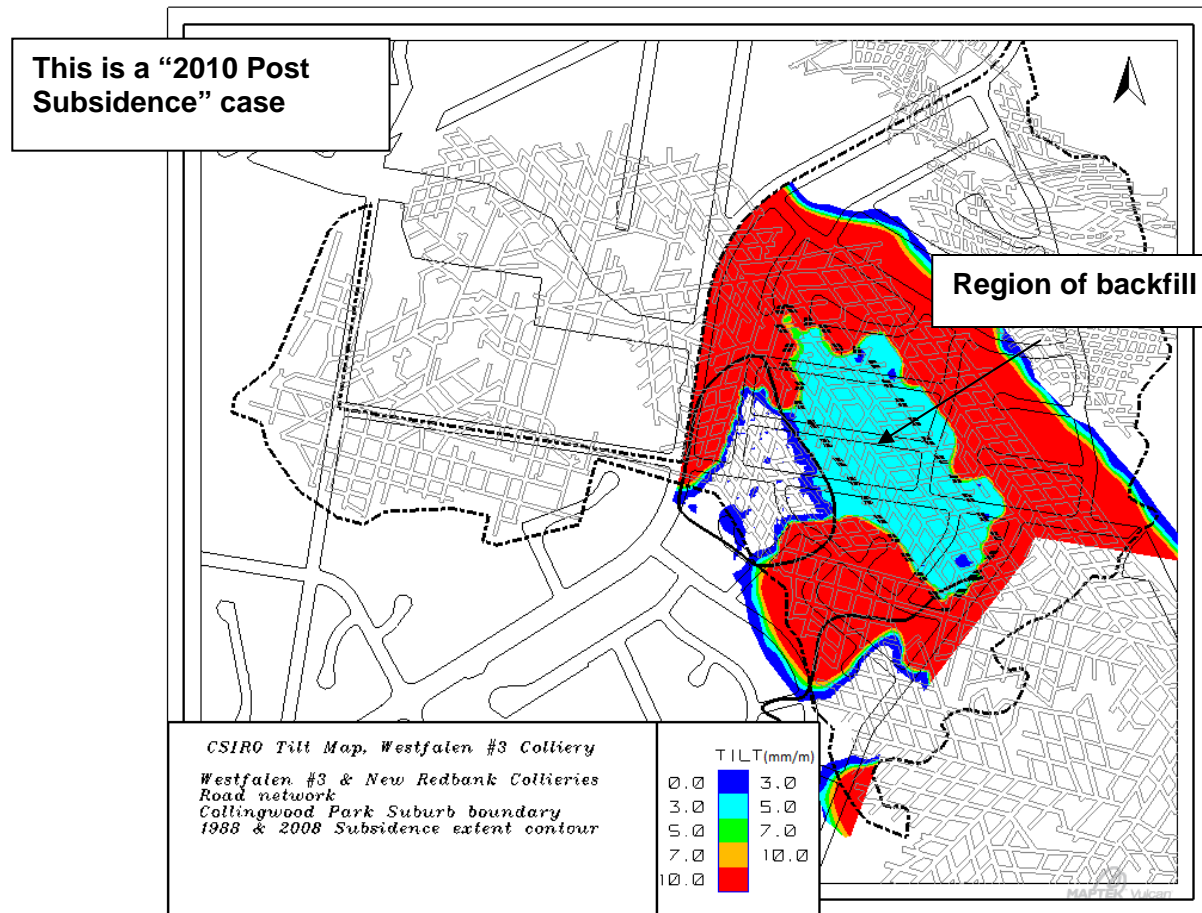


Figure 6-19. Estimated surface tilt assuming ALL pillars fail after backfilling with 90% roadway fill. Assumes height equal to 90% of the maximum reported height for each mining zone.

### 6.5.4 Potential tilt map assuming total failure after total backfilling

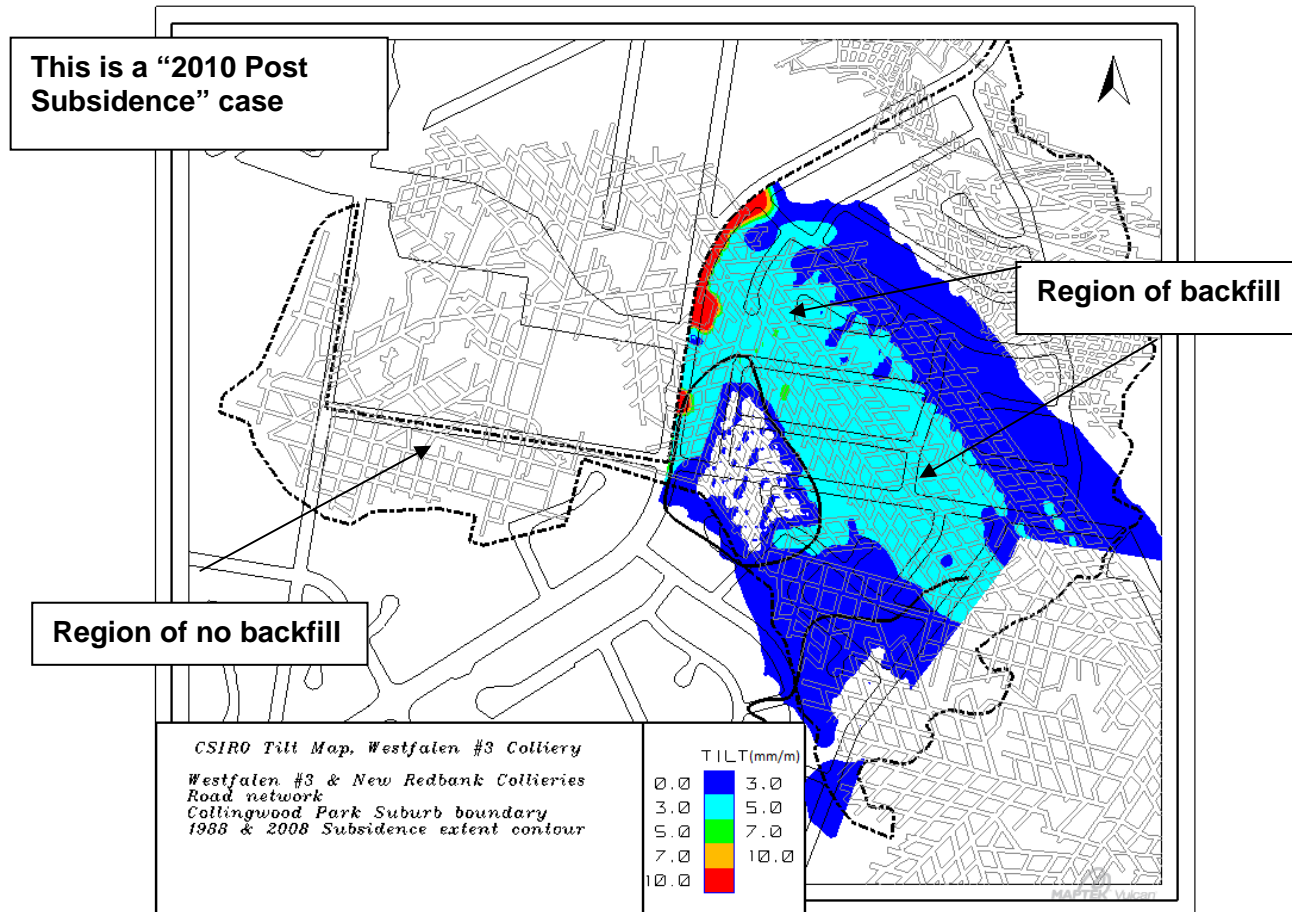


Figure 6-20. Estimated surface tilt assuming ALL pillars fail after backfilling with 90% roadway fill (including cohesive or non-cohesive backfill). Assumes height equal to 90% of the maximum reported height for each mining zone. All roadways except those on the western side of Collingwood Drive are backfilled.

## **7. LABORATORY TESTS AND INJECTION MATERIAL RECOMMENDATION**

### **7.1 Scope**

A set of laboratory experiments were conducted using fly ash and crusher dust supplied by Swanbank Power Station and Keller's batching plant at the Ipswich Motorway Upgrade construction site respectively. These experiments were conducted to establish the properties of potential slurry fill materials. The properties examined included: viscosity and consistency (flow-ability, inject-ability which determine the required pumping power); stiffness and strength (both under undrained and drained and consolidated conditions, which determining material deformation over time and under different loading conditions); long term stability of deposited material; cohesive and non-cohesive behaviour when used with or without cement, liquefaction, cementation, sedimentation, settlement and deposition rate, erosion, bleeding, segregation and dispersion due to water and dynamic loads. In addition to these test of material properties, extensive flume tests were conducted by the University of Queensland (UQ) to investigate the fly ash slurry flow, deposition and beach profile behaviour. Strength tests have also been conducted on hardened, dried, cohesive mixes as well as standard soil mechanics tests. An extracted summary of the results is presented here. More data and results are discussed in the **Appendix B**.

### **7.2 Recommendation**

From these laboratory studies, CSIRO's recommendation for backfilling a confined mine void structure (with no hazards from flooding and water or high seepage flow, which can cause liquefaction of fly ash particles) is a two phase non-cohesive slurry mixture of fly ash and water mix using 50 to 60 % solids by weight concentration. The injected non-cohesive fly ash will consolidate with time and becomes stiffer, harder and denser by the gradual drainage and dissipation of excess water accumulated in its pores. During the consolidation process, the friction angle of the confined consolidated fly ash can increase to close to 40 degrees and its hydraulic conductivity can reduce to less than one micrometre per second. Under high loads fly ash can be compacted and consolidated so that it only has 10% maximum moisture content.

A closed, confined, consolidated fly ash would not only provide sufficient confinement to the previously failed pillars and prevent them from further failure and collapse, but also would minimise any further ground subsidence by filling more than 90% of the voids left in the underground workings of the Westfalen No. 3 Colliery. However, in the lack of a closed or confined void structure, sealed barrier walls would need to be built using cohesive slurry, in which cement and crusher dust has to be added to the mix as well. These are similar to the T14 and T15 cohesive mixes, also considered in this study, which were used in the Ipswich Motorway Upgrade underground backfilling

project. In this chapter, the tests and studies considered are explained very briefly. More details are provided in **Appendix B**.

Although application of cohesive backfills of cement and fly ash are popular and their mechanical properties together with unit cost are discussed in Keller's report to DIP/DEEDI (Keller, 2010), very little comparisons can be found in the literature of their behaviour with the non-cohesive backfill, which is recommended in this study. The list below highlights the reasons why the non-cohesive (NC) mix was preferred to cohesive (C) mix for backfilling the Collingwood Park voids.

- NC mix doesn't set and harden with time due to lack of cement, hence it is much more flexible and desirable in terms of such potential operational problems as: flow interruptions, flow discontinuity, technical and operational pump and pipeline defects and blockages, and consequences associated with borehole loss.
- Both viscosity and yield values of C mix are higher than similar NC mix. They also increase rapidly and exponentially, causing pump power demand variations together with potential hardening and blocking problems in the entire pipeline-borehole system.
- NC mix normally has a beach angle (i.e. slope angle) of much lower than C mix, hence providing better penetration and backfilling result into tight and complicated void structures.
- Since NC friction and beach angles develop from zero to desirable large values with time (after removal of the excess pore pressure by natural consolidation and compaction), it provides a gradual smooth and almost flat layers of slurry deposition, ready for next layer deposition at any time, which is in total contrast to the irregular high slope deposits observed in the C mix slurry depositions.
- Because of the low beach angles and flat layering behaviour associated with the NC slurry depositions, better penetrations into the voids can be accomplished. In addition, injection boreholes can be spaced at a much larger distance. Initial estimates show that the borehole spacing is in the range of 100-200m in the case of NC, compared to the range of 50m required in the case of C mix (Keller, 2010).
- While porosity and density of C mixes remains fixed under closed and confined conditions, density of NC deposits can surpass the C mix density by up to 25%. NC mix deposits are much more flexible in reaching a maximum density, whereas the cement bond in the hardened C mix deposits had to be broken before they could allow any further densification.
- At 5% cement, Keller (Keller, 2010) estimated that the unit cost of a C mix is about 23% more than that of NC mix. The difference between the total cost estimates of backfill remediation of the key Collingwood undermined area above Westfalen No. 3 Colliery is about \$17M.
- NC mix is much more flexible than C mix in both transportation and deposition, e.g. even a 50% variation in its solid concentration (or water content) doesn't change the ultimate load bearing capacity of deposited, consolidated NC slurry, in contrast to the high sensitivity of C mix to variations in component proportions.

### 7.3 Result summary

To characterise and assess suitability of fly ash together with other mix materials for grout injection and backfilling design, the following laboratory tests were conducted at CSIRO laboratories on selected samples taken from the Swanbank Power Station and Ipswich Motorway Upgrade construction site (or D2G Project).

**Size distribution** tests were conducted both at CSIRO and UQ to determine the maximum, average and minimum sizes of solid particles of fly ash, crusher dust, cement and cohesive mixtures (Figure 7-1) for design of appropriate injection system.

From laser grain size analysis, the median size ( $d_{50}$ ) of fly ash particles was measured to be about 30-40  $\mu\text{m}$ . Hydrometer analysis of grain size for the same sample conducted by UQ showed a  $d_{50} = 15 \mu\text{m}$ . The difference in the two measurement techniques suggests a multi-modal size distribution, rather than a single S curve size distribution. The finer the slurry particles are, the less effort is normally required to pump such slurries through the pipeline and/or small holes and voids and gaps of the rock mass. See **Appendix B** for more details.

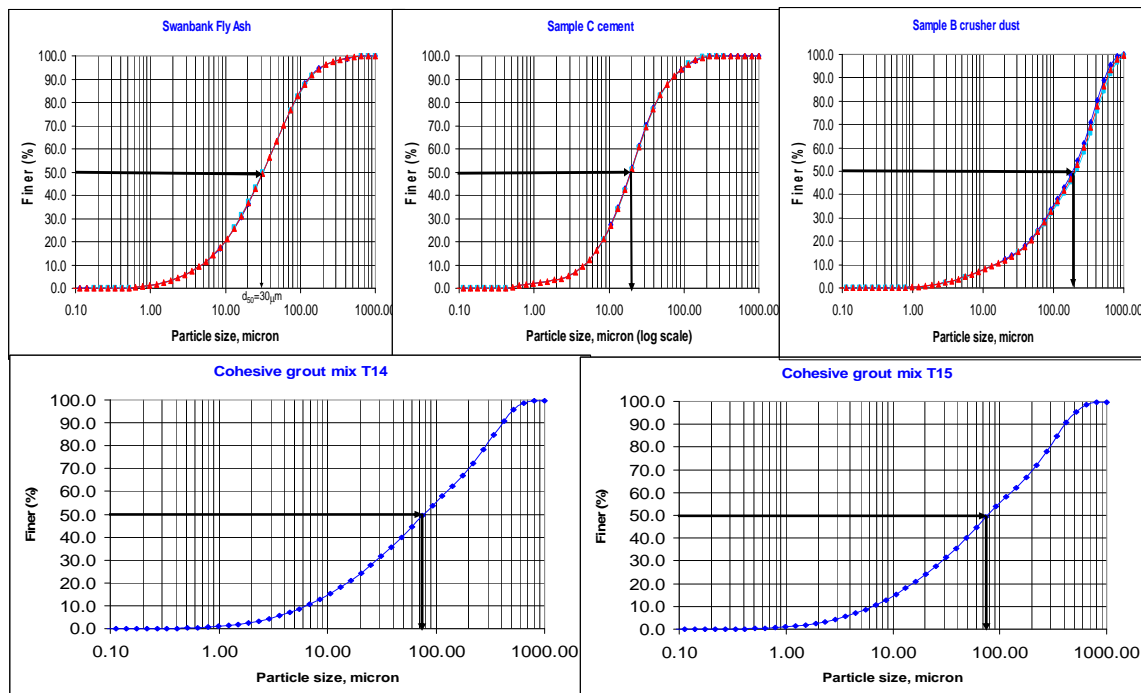


Figure 7-1. Size distribution of solid particles of fly ash, crush dust, cement and cohesive mixtures

**Sedimentation** tests were conducted in both to determine deposition time and velocity of floating particles. (Figure 7-2) to measure how quickly the submerged particles settle down.

Because the quicker the particles segregate and settle and the longer they remain stationary, the harder would be to pump them through the pipeline and borehole system, sedimentation or particle settlement tests versus time were carried out both in

glass beakers and graded buret (UQ) to measure the rate of sedimentation or settlement of separately moving submerged solid particles in slurry at low or zero flow velocities, or whenever separation and deposition of fly ash solid particles is possible. As shown in the figure the maximum rate of settlement occurs during the initial 20 minutes. More results are discussed in **Appendix B**.

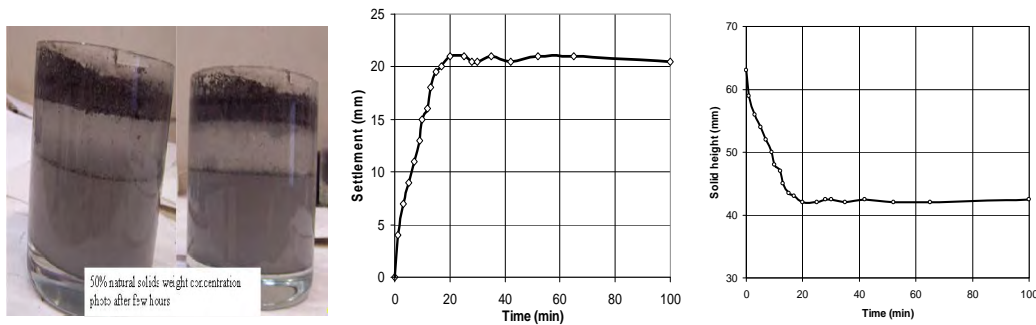


Figure 7-2. Deposition time and velocity of floating particles

**Viscosity** for grout flow-ability and pump pressure determination (Figure 7-3).

Pump power and energy efforts required for transportation of slurries depend primarily on their viscosity and initial plastic yield. A slurry's resistance to flow and shearing, and therefore the power required to pump it, is measured by a viscosity test. This test measures the shear stress resistance versus shear strain rate in terms of viscosity (slope of the curve) and plastic yield (vertical stress axis intercept). It is essential to determine the slurry viscosity and yield before any field trial operations for any slurry design.

Using CSIRO's viscometer, the viscosity and shear resistance of all possible fly ash slurries have been measured. The more fly ash particles in a slurry mix the more viscous, and hence more difficult to flow, that slurry will be, requiring more pumping power to make it flow.

There are correlations between material cohesion, friction and viscosity. As the viscous mixture becomes harder due to cement hardening effects, both its viscosity and cohesion will increase. The viscosity of fly ash is close to water, particularly at very low solid concentrations, however, it increases in orders of magnitude at high concentrations. When compared to all other coal washery mixed slurries, fly ash has proved to have the minimum shear resistance to flow and pump pressure both at low and high flow velocities.

The viscosity increases dramatically at concentrations > 75%, where the mix becomes more like a paste than a slurry. A practical range of solid concentration for all grout handling, transporting and backfill operations is in the range of 50% to 60%. Therefore, the selection of a pump meeting all the pump pressure and power requirements should

be straightforward and will not present a significant technical problem. See **Appendix B** for more details.

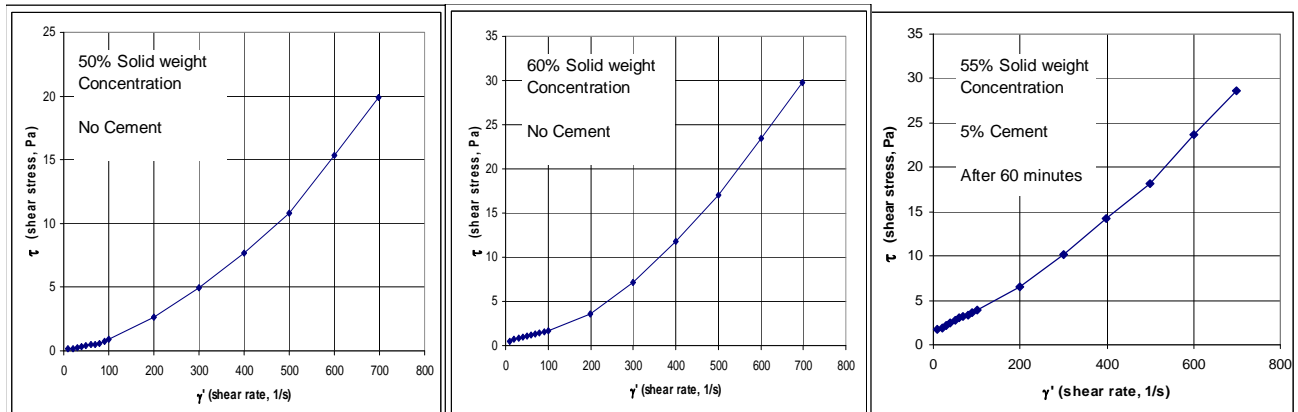


Figure 7-3. Viscosity measurements of non-cohesive slurry at solid by weight concentrations of 50% and 60% and cohesive slurry at solid concentration of 55% and 5% cement after one hour.

**Permeability/Hydraulic Conductivity** for seepage water flow analysis.

Like silt, the piping or liquefaction capacity of fly ash is very high and hence can be triggered very easily by shaking or any dynamic loading. On the contrary, once consolidated, it becomes dense and much less permeable. Permeability tests were carried out on consolidated samples of fly ash and its conductivity was found to be in the same range of silty soils, which can be less than a micron per second (**Appendix B**).

**Density** for measuring volumes and weights of fly ash slurry. It is one of the most important parameters for studying deformation and loading behaviour of backfilled fly ash.

Like soils, the density of fly ash is a function of its moisture content, void ratio, preloading and compaction and consolidation conditions. Unconsolidated fly ash solid particles sampled from the Swanbank Power Station, under an inherent moisture content of around 11% and loose contact conditions, exhibit a light density of around 0.81 g/ml, which can reach above unity by either dry compaction or submerged consolidation - See **Appendix B** for more results.

**Consolidation** for grout compressibility and deformation measurements. This test determines how the fly ash deposit deforms with its self weight and strata loading.

Backfill material needs not only to remain stable, but also needs to have the required stiffness and strength to carry potential overburden loads, which can change with time, with minimal compressive deformation. Under a total vertical load of 2 MPa, a saturated sample with an initial height of 17.9mm deformed to a final height of 15.8mm, i.e. approximately 12% compressive deformation took place. See **Appendix B** for more results and discussions.

**Friction angle** for stability analysis under different moisture contents and densities.

Friction coefficient between fly ash solid particles is not a fixed number. It varies with drained, undrained, consolidated and unconsolidated conditions of the fly ash samples. Therefore, the friction angle associated to the friction coefficient of fly ash is a function of density, void ratio (porosity), moisture content, degree of saturation, submergence and/or pore water pressure. It is expected that density, and hence the friction angle, in a deposited layer of fly ash increases with depth. It was also evident from direct shear tests conducted by UQ that fly ash dilates during plastic shearing tests. The fly ash internal friction angle can also be correlated to its beach profile angle. At the inherent moisture content of around 11% in fly ash samples from Swanbank Power Station, the small height restricted angle of repose was found to be as high as 40 to 45 degrees when measured from a pile of fly ash poured in air on to a dry surface at a relatively restricted small piling height of around 10-20 cm. However, when poured under submerged condition, this angle reduced to 1.5 to 2.2 degrees. Once the pore water is drained either by consolidation or by drying, at the same time the internal friction angle of fly ash increases, so that the denser the deposit, the higher is the friction angle. Fly ash slurries with 50% to 60% solids weight concentrations usually maintain a beach profile angle in the range of 2-10 degrees depending on the solids weight concentration. This implies that the higher the solids weight concentration of the slurry, the closer the injection boreholes would need to be drilled to guarantee a perfect backfilling operation. It also becomes harder to fill behind constrictions and obstacles at higher solids weight concentrations.

Strength of non-cohesive, non-pozzolanic fly ash deposits depends on internal friction angle, as non-cohesive slurries have no cohesion. However, strength of hardened cohesive deposits depends on both cohesion and friction angle. See **Appendix B** for more results.

Fly ash can stick to other materials with remarkably high **adhesion** at a critical moisture content and density. However, it can easily be liquefied and washed away by water flow.

**Strength** for measuring its ultimate tensile and compressive strength.

Unconfined, non-cohesive, non-pozzolanic fly ash has zero cohesion, zero tensile and zero unconfined compressive strength. However, when confined, it gains its confined compressive strength through its internal frictional contact resistance, which is a direct increasing function of its friction angle and confining stresses. Under fully confined conditions, a sample of consolidated fly ash having a friction angle of 40 degrees can take a shear load up to 83% of its applied axial compressive load, or an axial stress 3.3 times the confining pressure.

Unconfined, hardened, cohesive fly ash mix has 0.1-0.3 MPa cohesion, 0.1 - 0.2 Brazilian tensile strength, and 1 – 1.5 MPa unconfined compressive strength (UCS). However, when confined, its compressive strength increases through its internal frictional contact resistance, which is a direct increasing function of its friction angle and confining stresses. Under fully confined conditions, a solid sample of cohesive mix

can take shear loads up to 83% of the applied axial compressive load plus the original 0.1 to 0.3 MPa cohesion, or an axial stress 3.3 times the confining pressure plus the 1 – 1.5 MPa unconfined compressive strength (UCS). See **Appendix B** for more details.

**Disc grout flow** for measuring grout backfilling behaviour (Figure 7-4).

A series of disc grout tests were conducted on Swanbank Power Station fly ash both with and without cement at different solid weight concentrations. The testing gear consists of a disc of 1m diameter with an adjustable gap thickness, simulating a rock fracture opening, and a vertical pipe line at its centre, simulating an injection borehole. Left Figure 7-4 shows how a 60% solid weight concentration flows or disperses from the narrow central tube into a 4mm disc gap, while the right figure shows preparation of a curly narrow path, in which the same slurry flew successfully. See **Appendix B** for more details.



Figure 7-4. Disc grout flow experiments for measuring grout backfilling behaviour. Left: a 60% solid weight fly ash slurry flowing and dispersing through the 4mm gap of the disc. Right: a curly narrow path on a cemented deposit in the same disc installed to test if fly ash slurries can flow through the path.

**Fly Ash flow and deposition in tank** to determine profile beach angles, grout backfilling slopes, penetration distance and backfilling behaviour of roof voids.

A series of slurry flow tests for both cohesive (5% cement + 55% solids weight concentration) and non-cohesive (solid weight concentrations 50-60%) were conducted in a rectangular glass tank of 1.2m length, 400mm width and 600mm height. The tanks long axis could also be placed on a 5 degree slope to simulate the dip of the workings in the mine. The roof of the workings was replicated with a piece of corrugated plastic to simulate undulations in the roof. The grout flow rate was in the range of 10-30 litres per hour from a 12mm hose placed at the up-dip end of the tank under simple gravity. These tests showed that backfilling with non-cohesive slurry from boreholes spaced at large distances (100 m or so) is not a problem and is practically achievable. These tests also showed that more than 90% of the void space was filled. See **Appendix B** for more results.

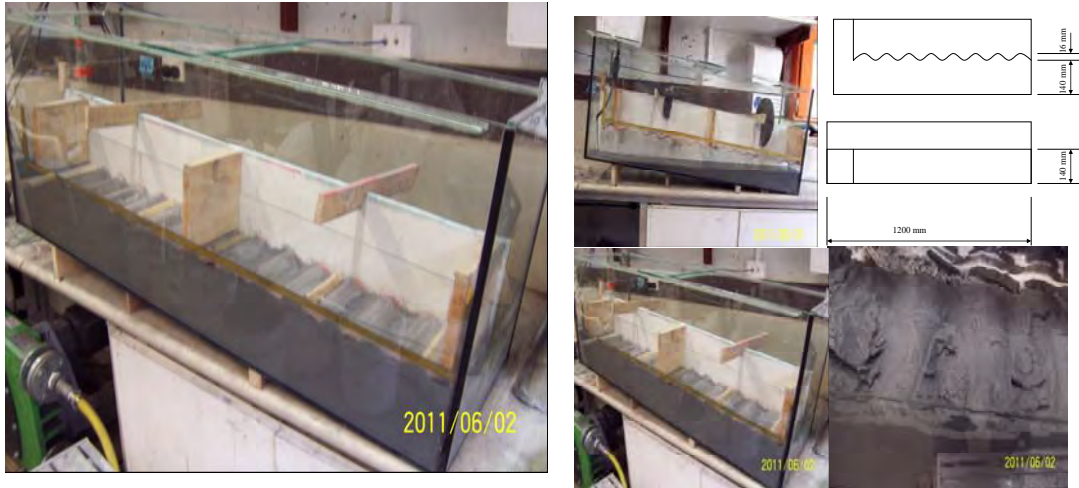
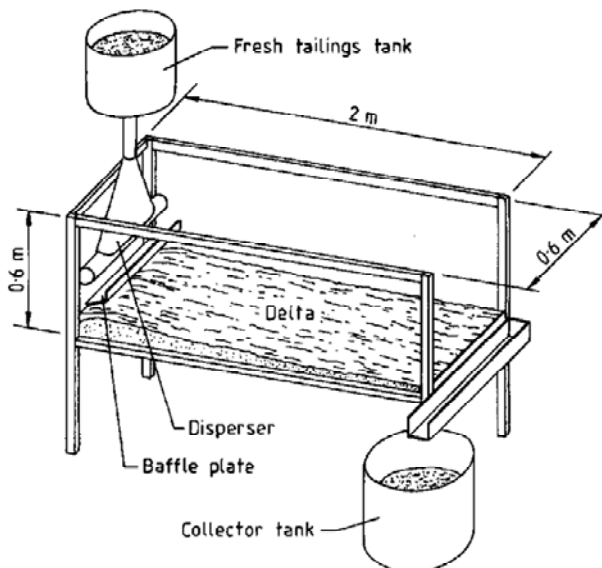


Figure 7-5. Experiment of fly ash flow and deposition in a confined roadway

### *UQ Fly ash slurry flume tests*

To simulate flooding effects on consolidated deposited fly ash, slurry flume tests were conducted at the Civil Engineering laboratory at the University of Queensland (UQ). The arrangement is shown in the figure below and some results are shown in the following figures. The complete UQ report on these tests is included in **Appendix B**.



(a) Schematic



(b) Constricted, under water set-up

Figure 7-6. UQ laboratory beaching flume for simulation of fly ash slurry flow, deposition and erosion

Figure 7-7 summarises all of the open-ended beach profiles obtained for Swanbank fly ash tested at different % solids in the laboratory flume. Clearly, the higher the initial %

solids, the steeper the beach profile, with  $\leq 35\%$  solids producing an almost flat beach. Notice the maximum measured beach angle is about 1%. Figure 7-8 shows the settled slurry profile resulting from flooded deposition of Swanbank slurry initially at 60% solids, under a high slurry head into a closed-ended constriction. Figure 7-9 compares the average laboratory and field beach slopes obtained for Swanbank fly ash at different initial % solids, which highlights that for unflooded, unconstricted beaching the average beach slope is highest (at about 1%) for an initial % solids of 55%, lower but insensitive over the intermediate range of initial % solids, and flat for an initial % solids of 15%. The average field beach slope of 0.014% is similar to that obtained in the laboratory for an initial % solids of 15% (similar to the field initial % solids), and the non-dimensional beach profile is similar to that for the field profile.

For unflooded, constricted beaching the average beach slope is significantly greater at high initial % solids, and only slightly greater at intermediate initial % solids. Flooding generally has little effect on the average beach slope for unconstricted beaching.

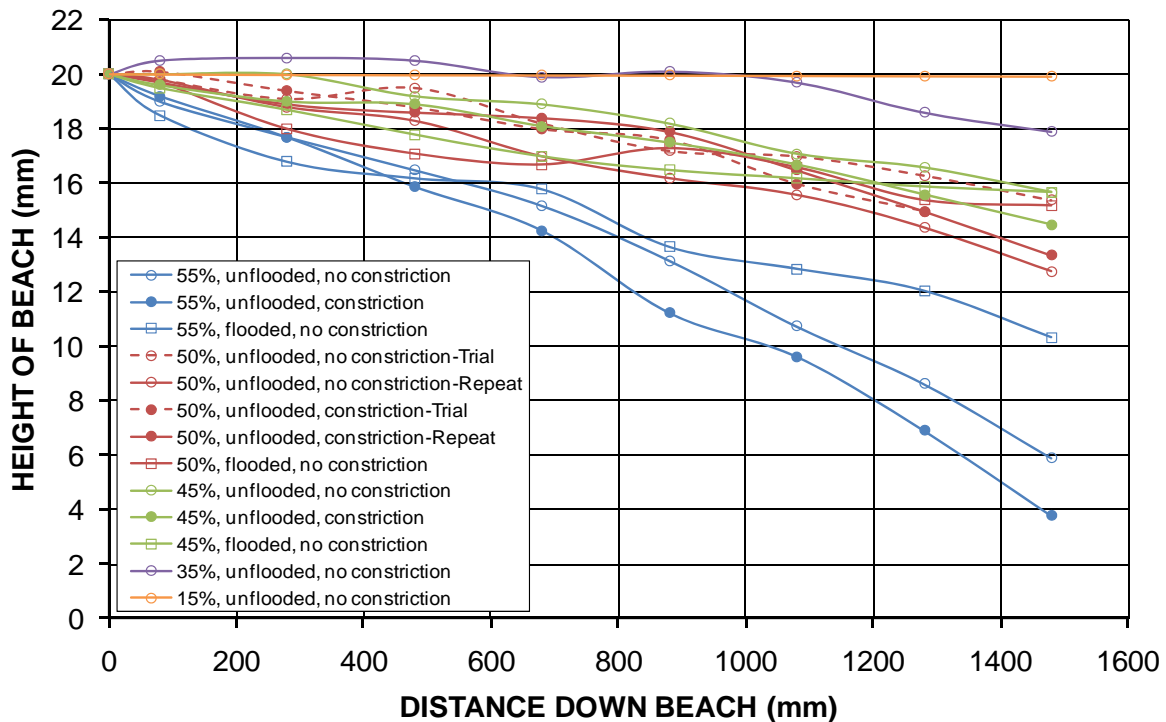


Figure 7-7. Summary of open-ended laboratory flume beach profiles for Swanbank fly ash

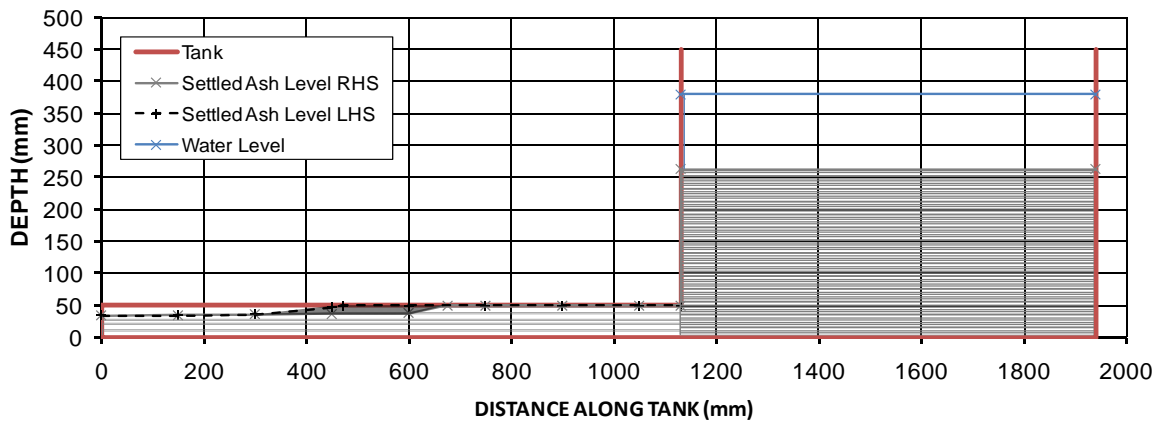


Figure 7-8. Constricted backfilling, under water and a high head of Swanbank fly ash slurry, initially at 60% solids

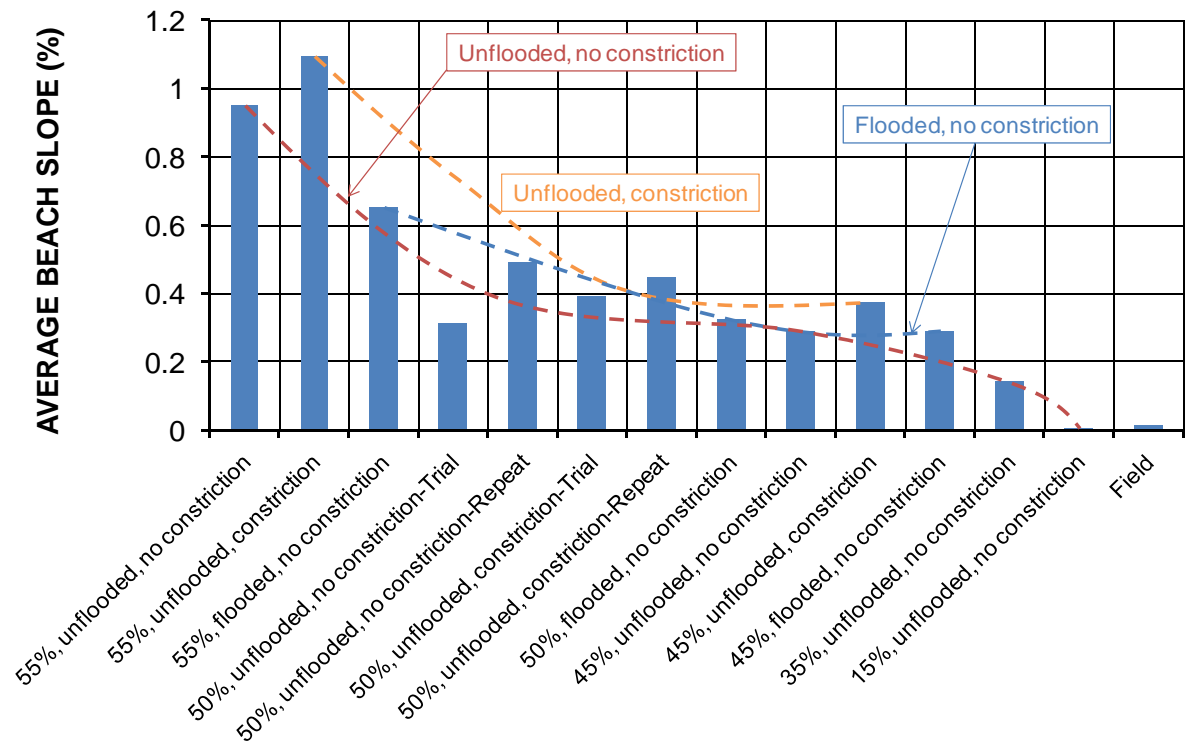


Figure 7-9. Comparison of average beach slopes of laboratory and field beach profiles for Swanbank fly ash.

**Pipeline transport** for grout transportation power and pump-ability requirements

Fly ash slurries would need to be pumped through pipes of varying lengths most likely with bends to reach boreholes for delivery in to the mine workings. Transportation of two phase slurries, in which solid particles are easily separated and deposited as sediments, is a challenging task because blockage of the flowing slurry can occur

whenever the speed of suspended particles drops below a critical threshold velocity. In this case, even injection of pure water, boosted by high pump pressures, may still be inadequate to remove blockages and to reactivate the flow in a long pipe or at a sharp bend. Therefore, the transportation characteristics of a slurry need to be determined before any field injection trials. We used flexible rubber pipes of 20mm diameter for experiments on Swanbank fly ash, as shown in Figure 7-10. The loop test results revealed the fact that fly ash slurry could successfully be pumped at all solids weight concentrations up to 75% without problems.



Figure 7-10. Pipeline transport tests on a range of fly ash slurries and paste from 50-70% solids weight concentration

## 7.4 Conclusions on laboratory tests

A number of basic tests at CSIRO and UQ laboratories were conducted on both cohesive and non-cohesive slurries and pastes of fly ash. Based on the test results, the following guidelines are suggested:

- Non-cohesive grout mixes are preferred to cohesive grout mixes. The major advantage of the non-cohesive mix over the cohesive mix is that its properties do not change rapidly with time and can penetrate more reliably into smaller voids.
- Smaller scale field testing trials should be tried with different fly ash concentrations and compositions before any full scale field operation.
- Voids should first be blocked off down slope of the delivery point for the fly ash slurry to contain the slurry.
- The optimum initial solid content for the fly ash slurry is about 50%. This solid content will be able to limit the average beach slope and hence maximise initial filling, capable of fluidising the slurry for better void filling following settling, and can increase the final dry density, strength and stiffness achieved.
- A head of slurry should be applied in the borehole used to deliver the fly ash slurry, which will enhance void filling and gain in dry density, strength and stiffness.

## 8. REMEDIATION SCENARIOS AND FURTHER INVESTIGATIONS

### 8.1 Summary

Based on the investigation results, CSIRO recommends the **Non-cohesive total backfill** approach as the most technically feasible option for Collingwood Park mine remediation.

Using the non-cohesive total backfill approach, all the mined areas between Collingwood Drive and Lawrie Drive/Namatjira Drive should be backfilled using the non-cohesive fill material (pond ash from Swanbank Power Station and water). Barrier walls would need to be built along Lawrie Drive/Namatjira Drive using cohesive grout with the same specifications as that used for the Ipswich Motorway Upgrade Project to stop grout escape to other regions of the mine. The workings would not need to be dewatered for backfilling purposes before the non-cohesive slurry was injected. However, it is considered to be the most economic and environmental friendly option that the existing mine water would be extracted and reused for grout mixing during the backfill operation. The void filling ratio is expected to be greater than 90%. With this backfill, the mine panels are estimated to remain stable in the longterm. Should panel instability occur the amount of subsidence at the surface is expected to be reduced to less than 0.2m.

For New Redbank Colliery where some 80 houses are located, however, the information available to date does provide us sufficient confidence to develop a feasible remediation scenario.

It is recommended that further work be conducted, as listed below:

#### *For remediation of Westfalen No. 3 Colliery*

Six key tasks are identified and should be carried out to ensure a successful remediation operation using the non-cohesive backfill:

- Expand the existing monitoring network in Collingwood Park by installing two additional extensometers and one micro-seismic station above the Central Panel of the former Westfalen Number 3 Colliery.
- Conduct a large-scale laboratory modelling of backfill.
- Conduct a full-scale field test of roadway backfill.
- Conduct a focused study to quantify the effect of rising water in Westfalen No.3 on the ground stability.
- Investigate and monitor groundwater flow and chemical transport during and after fly ash backfilling
- Continue ground monitoring and data analysis, including gas, in Collingwood Park.

## *For remediation of New Redbank Colliery*

- 3D seismic survey.

## **8.2 Introduction**

As part of current study for the DIP/CSIRO mine remediation project, extensive investigations have been carried out in the area undermined by Westfalen No. 3 Colliery, which included:

- 13 drill holes covering most of the undermined area in Collingwood Park.
- Geotechnical monitoring including piezometers and an extensometer.
- 3D seismic survey in an area of 390m×210m between Duncan Street, Herman Avenue and Collingwood Drive.
- Microseismic monitoring.
- Geotechnical numerical modelling and stability assessment.

Together with the existing data from various previous investigations and the mine plan, there is reasonably accurate knowledge about the mine layout, mining geometry and mining height etc in this part of the mine.

For New Redbank Colliery, where some 80 houses are located, the data available are limited. Two boreholes were drilled as part of this project in a public park to the east of the residential area. Both drill holes encountered voids at or above the estimated mining horizon, and showed signs that the mine may have collapsed. This is in contrast with the drilling results obtained by the D2G project in the western part of the mine near the Ipswich Motorway, where the mine was observed to be stable. Adding to the complexity and uncertainty is that different seams (Top, Middle and Bottom Seams) were reported to have been mined at different parts of the mine. But the details are yet to be verified. There is a mine plan in DEEDI's database. The accuracy of this plan however is largely unknown.

Based on the detail and confidence level of the information from the two mines at present, it is only possible to develop a remediation strategy for the Westfalen No. 3 Colliery. For New Redbank Colliery, however, the information available to date does provide us with sufficient confidence to develop a feasible remediation scenario.

This chapter presents the remediation options for Westfalen No. 3 Colliery, and the work that should be taken in the next step towards choosing and implementing the preferred scenario. A programme is also recommended to acquire the necessary data and knowledge for developing remediation options for the New Redbank Colliery.

## **8.3 Remediation scenarios at Westfalen No. 3 Colliery**

Based on the investigation results from this project, three most likely remediation scenarios have been identified: For completeness, two non-remediation options identified by DEEDI – Business as Usual (administering the Collingwood Park State

Government Guarantee) and Selective Property Purchase, have also been included in the discussion for Westfalen No. 3 Colliery. The five possible scenarios are:

#### *Scenario 1 – No remediation*

This scenario is also called "Business as usual", administering the Collingwood Park State Guarantee (S381 Mineral Resources Act 1989) for future mine subsidence events.

#### *Scenario 2 – No remediation*

This scenario is also called "Selective property purchasing" within areas identified as having a high risk of failure based on the latest mine subsidence risk assessment.

#### *Scenario 3 – Targeted remediation*

This scenario is also called "Selective mine panel filling" based on a review of mine subsidence risks using a cohesive grout to stabilise pillars in areas identified as having a high risk of subsidence in the future.

#### *Scenario 4 – Non-cohesive total backfill*

This scenario is also called "Complete non-cohesive backfill". All the mined areas between Collingwood Drive and Lawrie Drive/Namatjira Drive will be backfilled using non-cohesive fill material (pond ash from Swanbank Power Station and water). The void filling ratio is expected to be better than 90%. With this backfill, the mine panels are estimated to remain stable in the long term.

#### *Scenario 5 – Cohesive total backfill*

This scenario is also called "Complete cohesive backfill". The same area described in Scenario 4 will be backfilled using cohesive fill material (fly ash + cement + crusher dust + water). With this backfill, the Factor of Safety (FoS) for all the mined areas will be higher than 2.0, implying that long-term stability will be achieved.

In all the Scenarios 3, 4 and 5, barrier walls need to be built using cohesive paste to contain the grout mix in the regions of interest.

Among the five possible scenarios, CSIRO recommends Scenario 4 – Non-cohesive total backfill. The reasons are given below:

- Scenarios 1 and 2 have too high a risk for future subsidence. Large areas overlying Westfalen No. 3 Colliery in Collingwood Park have a pillar FoS less than 1.4, implying that they are potentially unstable over the long term. Recent extensometer and microseismic monitoring results suggest that the Central Panel is potentially unstable, and pose a high risk of future subsidence. It is our view that these areas should not be left untreated particularly considering the fact that two subsidence events have already occurred.

- Scenario 3 is insufficient to eliminate risk for the whole Collingwood Park area. Scenario 3 only backfills the central region where the risk of subsidence has been identified to be high. It may improve the pillar FoS in this region, but will not prevent pillar failures outside this region. If pillars outside this region collapse, the surface subsidence could extend into the central region and cause damage to properties in this area. In addition, this scenario requires barrier walls around the region which would make it less cost effective compared with other scenarios.
- Scenario 4 is considered to be the most cost effective. It uses only fly ash and water, and no cement. It requires fewer injection holes than the cohesive backfill because the non-cohesive slurry can flow much further than cohesive pastes. Non-cohesive backfill will provide sufficient reinforcement so that most of the pillars will have a FoS close to or greater than 1.6. More importantly, the scenario will lead to a maximum solid backfill of the mine voids and hence reduce or eliminate any surface subsidence, should some of the pillars fail.
- Scenario 5 is considered to be the safest but not most cost effective option. This scenario will result in a high pillar FoS (>2.0) in Collingwood Park. However, it uses a significant amount of cement which increases the cost of material. Because of the limit in flow distance of the cohesive paste, significantly more injection holes than the non-cohesive backfill have to be drilled, which not only increases the drilling costs but also the operational difficulties in the densely populated residential area. Based on the estimate by Keller (2010), this scenario will cost \$17M (or >20%) more than Scenario 4.

## **8.4 Recommended further studies for remediation scenarios at Westfalen No. 3 Colliery**

Each of the remediation scenarios outlined above for Westfalen No. 3 Colliery will require further studies to ensure that the risks at Collingwood Park are properly managed.

### **8.4.1 Scenarios 1 and 2 – No remediation**

The risk of future subsidence in this scenario is high based on the risk assessment and recent extensometer and microseismic monitoring results. The subsidence damage to existing properties could be severe. There is also a relatively low risk of mine gas explosion because the methane content in the mine gas is close to the explosive range and the oxygen content is increasing. In case of a large scale subsidence event, there will be a risk of mine gas escape to atmosphere, which could be a hazard to local residents.

In these scenarios, it is essential that the risk of future subsidence is accurately quantified, monitored and managed. The following tasks are suggested:

### *Understanding the effect of water and time on future subsidence*

It is known from the piezometer monitoring results that the water level in Westfalen No. 3 Colliery is increasing. The effect of water on pillar/panel stability is largely unknown. New theoretical, laboratory and field investigations are required to understand and quantify the effect of water on subsidence at Collingwood Park.

The effects of time on pillar/panel stability is also critical, considering that the 1988 and 2008 events both occurred many years after mining. The time effect includes the effect of water (which is time-dependent), and other time-dependent events such as gradual deterioration of the pillars and creep. The time effect will need to be studied more systematically to develop a better understanding and management strategy than the simple Factor of Safety (FoS) approach is required.

The effects of time and water are challenging topics in geomechanics, and the existing knowledge base is not sufficient to answer these questions. A future study will need to involve theoretical, laboratory and field investigations. Although such a study may not guarantee an answer to this question, it will significantly help to quantify the likelihood for future subsidence events in a given time frame.

It is expected that a focused preliminary study on the time effects on stability at Collingwood Park will require approximately 10 months at a cost of approximately \$200,000.

### *Monitoring of ground movement, mine gas, and water level.*

A microseismic monitoring system has been installed and is now fully operational. The microseismic system covers the main part of Westfalen No. 3 Colliery in Collingwood Park area. A 20-anchor extensometer was installed in the high risk area of Collingwood Park.

Judging from the extensometer and microseismic data up to early September 2010, we believe that the Central Panel is moving and is potentially unstable. We recommend the following actions be taken: 1) Install two additional extensometers close to either ends of the Central Panel to determine the size of the area with movement; 2) Install one additional geophone station close to CP_O07 to help detect and locate small seismic events in the Central Panel; 3) Continue the weekly data analysis, and if significant increase in the rate of displacement and seismicity is observed, increase the data analysis frequency (both extensometer and microseismic data) to minimum twice a week; and 4) DEEDI considers developing a response plan for any potential subsidence events.

The estimated costs for two additional extensometers and one microseismic station will be about \$140,000.

The estimated costs for weekly analysis of the microseismic data and extensometer and piezometer data will be \$2,000/week, or approximately \$8,700/month.

In order to minimise the potential risk imposed by underground methane, it is recommended that the current frequency of gas sampling and analysis should be increased to every three months for at least 2 years to confirm any long term trends. In the event of any major ground movement in the future (e.g. subsidence), the gas

sampling frequency should be increased to weekly. If the oxygen content is greater than 5% and the trend is continuing, remediation measures (such as injection of nitrogen) should be considered.

#### **8.4.2 Scenario 3 – Targeted remediation**

Although the identified high risk area will be backfilled with cohesive backfill material according to this scenario, there is a residual risk in other areas that are not remediated. In addition, there is a significant current risk before the backfill can be applied which will take at least 1 year from today. To manage this risk, the same studies of the effects of water and time on pillar stability and the expanded monitoring program suggested for Scenarios 1 and 2 should be put in place.

Before and during the backfill operation, the frequency of data processing and analysis should be maintained at once a week if the current movement trend continues. The frequency can be increased or decreased if the movement is slowed or accelerated.

After backfill, however, the frequency may be reduced from weekly to fortnightly. The estimated costs for a fortnightly analysis of the microseismic data and extensometer and piezometer data will be \$3,000/fortnight, or approximately \$6,500/month.

#### **8.4.3 Scenario 4 – Non-cohesive total backfill**

Further work needed for this scenario include:

##### *Large scale model tests*

Non-cohesive backfill is a new technology for bord-pillar mine remediation, although it has been used successfully before for longwall mine backfill. There is limited experience about grout flow and settlement in the actual roadways.

Large-scale model tests of the backfill operations will be extremely helpful not only for backfill design but also for demonstration and visualisation purposes. These tests will also be able to provide decision makers with good knowledge on how the backfilling operations can be done and how effective the backfill will be. This information will also be useful for communication with all stakeholder, including local residents.

The large-scale model tests should be conducted in a laboratory with appropriate facilities for a 1:20 model with maximum dimensions about 4-5m. It should include the detailed roadway/pillar geometries.

The large-scale model tests are expected to cost \$100,000 - \$150,000, depending on the number of tests required.

##### *Full scale field test*

A field-scale backfill test using the non-cohesive backfill is necessary before the actual backfill operation starts. It can be conducted at surface by digging a roadway-sized

trench and backfilling it with fly ash slurry. An underground trial at a shallow and isolated roadway is also possible if such a site can be located.

### *Monitoring of ground movement, mine gas, and water level.*

The expanded microseismic and extensometer monitoring program suggested for Scenarios 1 and 2 should be put in place. Before and during the backfill operation, the frequency of data processing and analysis should be maintained at once a week if the current movement trend continues. The frequency may be increased or decreased as movement is slowed or accelerated.

After the backfill, however, the frequency may be prolonged to once a month at an estimated cost of \$4,000/month until the ground is fully stabilised.

Piezometer monitoring should be continued well after the backfill. Data analysis should be conducted monthly.

Gas sampling and analysis should be conducted on a quarterly basis until the backfill operation is completed. Decision should then be made whether to continue the gas sampling in the untreated part of the mine to the west of Collingwood Drive.

### *Water effect assessment*

Non-cohesive backfill will displace the mine water in Westfalen No. 3 Colliery from the backfilled region to non-backfilled regions. The water level in the mine is likely to rise at a much faster rate than it is currently. Pillars in the currently dry areas will be submerged in water. Because the backfill operation may take more than one year to complete, many pillars that are currently dry in Westfalen No. 3 Colliery will become "wet" during the backfill operations before they are completely backfilled. In a worst-case scenario, some pillars could fail as a result of water level rise during backfill operations.

A study is recommended to investigate the effect of water on pillar stability. This study will use theoretical, numerical and experimental means to quantify the possible pillar strength reduction due to water saturation. Knowledge from soil mechanics and rock slope stability will be used in the study. A set of laboratory experiments on pillar strength under dry and wet conditions will be conducted in a rock mechanics laboratory. This will be combined with a set of numerical models using the mechanical properties for dry and wet coal.

As a result of this study, the effect of the water on pillar stability will be presented by a reduction factor to the dry Factor of Safety (FoS). For instance, if a pillar has a FoS = 1.2 in a dry condition, and the water reduction factor is 30%, this pillar will have a FoS = 0.84 when it is submerged in water. This means that the currently stable pillar could become unstable when submerged in water.

It is expected that a systematic study on water effect will require about ten months at a cost of approximately \$150,000 - \$200,000.

### *Modelling and monitoring of groundwater flow and chemical transportation*

Fly ash contains elements that may leach out and potentially pollute the ground water system in the residential area. Previous studies (e.g. Guo et al, 2006) suggest that fly ash from Australian power stations is normally considered to be environmentally safe compared with some overseas fly ash because of the less pozzolanic nature of the ash and different combustion processes in the power stations. Nevertheless, the environmental risk of fly ash backfill should be investigated before backfill operations proceed.

The recommended study includes laboratory tests of Swanbank fly ash, numerical modelling of the groundwater system in the Westfalen No. 3 Colliery and New Redbank Colliery areas and any changes in this system as a result of backfill operations. The study would also include chemical transportation modelling aimed at quantifying the concentration of heavy metal elements that may be transferred into the regional ground water system.

Long term monitoring of ground water quality should be put in place after the backfill.

It is estimated that this study will take about eight months at a cost of about \$150,000 excluding costs of long term ground water quality monitoring.

#### **8.4.4 Scenario 5 – Cohesive total backfill**

Cohesive backfill has been successfully used in the Ipswich Motorway Upgrade/D2G project near Collingwood Park, and a high level of confidence exists on this backfill method. If the backfill is done properly, there will be no need to continue geotechnical monitoring in the backfilled area after the remediation.

However, the expanded microseismic and extensometer monitoring program should still be put in place to manage the present risk that will last until the mine is totally backfilled.

It is also recommended that the water effect assessment and modelling of groundwater flow and chemical transportation recommended for scenario 4 should be carried out because both cohesive and non-cohesive backfills will use fly ash and will change the mine water level.

### **8.5 Recommended further work for developing remediation scenarios for New Redbank Colliery**

The New Redbank Colliery mined coal during the 1920s in an area that now underlies the north-east corner of Collingwood Park. Stability assessment of New Redbank Colliery is difficult due to the sparsity of data describing the mining operations. A mine plan exists but its accuracy is yet to be confirmed and little additional information is available on mining heights and working conditions.

If the mine plan is taken as accurate then a preliminary CSIRO investigation suggests majority of the workings, assuming 3m mining height, should have collapsed and additional mine related surface subsidence will be unlikely. Two boreholes drilled into

the New Redbank Colliery in 2010 determined that workings at those locations had indeed collapsed.

Even though considerable time has passed since mining operations ceased and given the lack of documented mine related surface subsidence events that give some reassurance new failures will not occur, CSIRO believes that further investigation of New Redbank Colliery is needed, particularly regarding the extent of the past mine collapse in this colliery.

Depending on the findings from this investigation at New Redbank, further site investigation and remediation recommendation may or may not be required. It is conceivable that all the old underground workings under residential housing at Collingwood Park had already collapsed and the risk of future ground subsidence is minimum.

It is recommended that a 3D seismic survey be conducted at New Redbank Colliery.

The 3D seismic survey is designed to map the locations of stable and collapsed mine sections. A 3D seismic survey conducted in the current DIP/CSIRO project near Duncan Street has successfully mapped the area of pillar collapse. It is highly likely that similar survey would be able to provide this critical information and clarify which parts of New Redbank Colliery have already collapsed.

The suggested area of the 3D seismic survey is shown in Figure 8-1. This area is about twice the area of the survey at Duncan Street. Because a large portion of the survey would be in an area with a higher density of residential properties, the difficulties for the 3D seismic survey will also increase.

It is expected the cost for this study will be in the range of \$150K-\$200K.



Figure 8-1. Recommended area of 3D seismic survey at New Redbank Colliery.

## 9. CONCLUSIONS

This study has been largely focused on the Westfalen No. 3 Colliery in the defined study region in Collingwood Park. Limited investigations have been done for the New Redbank Colliery. The following findings can be drawn from this study:

### *2008 subsidence event*

- The mine panel in the 2008 subsidence region is predicted to have a FoS close to 1.0. It is believed that the 2008 subsidence event was a result of pillar failure involving at least 38 pillars below Duncan Street.
- Based on the seismic interpretation, it is likely that the zone of pillar failure at seam level has extended across the Waterline fault to the north-east. Boreholes drilled after the 3D seismic survey also support the suggestion that pillar failure may have extended to the eastern side of the Waterline fault.
- An analysis was carried out to determine whether mine water may have had an influence on the 2008 subsidence. It was found that, based on the drill hole data, the mine water level in Westfalen No. 3 Colliery was unlikely to have reached the key area of subsidence at the time of the event. However, the effects of water on pillar strength and panel stability should not be discounted as past experience in geotechnical engineering showed that ground water can play a key role in rock mass instability.

### *Current condition in Westfalen No. 3 Colliery*

- Most of the holes drilled in Westfalen No. 3 Colliery successfully hit their intended targets (roadways or pillars). This indicates that the available mine plan is reasonably accurate. The mining heights obtained from this drilling programme are generally consistent with those previously reported in various sources.
- The water level in Westfalen No. 3 Colliery is at 108m below sea level in September 2010 and is increasing at a rate of about 11m/year, although the rate appears to be slowing. The water inflow is believed to come mainly from the overburden aquifers through drill holes and fractures.
- The FoS of the pillars in the central panel region from Strachan Ct and Heysen Ct in the north extending southeast to Duncan St and beyond are calculated by CSIRO to be mostly lower than 1.4, which is considered to be too low to warrant long term stability of this region.
- There was a small amount (8mm) of movement recorded in the overburden strata at Hole CP_O07 during a period of 47 days (up to the September 24, 2010). It may indicate that the ground in the vicinity of this borehole may be slowly moving or “creeping”, which could be a precursor of a future subsidence event. In this case we recommend the following actions be taken: 1) Install two additional extensometers close to either ends of the Central Panel to determine the size of the area with movement; 2) Install one additional geophone station close to CP_O07 to

help detect and locate small seismic events in the Central Panel; 3) Continue the weekly data analysis, and if significant increase in the rate of displacement and seismicity is observed, increase the data analysis frequency (both extensometer and microseismic data) to a minimum of twice a week; 4) Consider developing a response plan for any potential subsidence event;

### *Remediation method for Westfalen No. 3 Colliery*

- Based on the results of these investigations, CSIRO's recommendation is to backfill all open mine voids of the Westfalen No. 3 Colliery north of Lawrie Drive and east of Collingwood Drive using a backfill grout consisting of fly ash and water with 50-60% solid-to-water concentration to a minimum of 90% void volume.
- Non-cohesive backfill to 90% roadway height is predicted to raise FoS in the central region to above 1.6, which is the number often used in rock engineering design for long-term stability. A cohesive backfill with uniaxial compressive strength of 0.5MPa is predicted to raise FoS to greater than 2.0 in the same region.
- Consequence maps have been created to estimate the amount of surface subsidence and surface tilt based on empirical formula modified by observations from the site and numerical models. It is predicted that if pillars were to fail after backfilling roadways to 90% the surface subsidence would be less than 200mm and the surface tilt less than 5 mm/m. Overall tilts in buildings less than 5 mm/m would generally have negligible impact on building structures (Mine Subsidence Engineering Consultants, 1997).

### *Recommended further studies for remediation of Westfalen No. 3 Colliery*

Six key tasks are identified and should be carried out to ensure a successful remediation operation using the non-cohesive backfill:

- Expand the existing monitoring network in Collingwood Park by installing two additional extensometers and one micro-seismic station above the Central Panel of the former Westfalen Number 3 Colliery.
- Conduct a large-scale laboratory modelling of backfill.
- Conduct a full-scale field test of roadway backfill.
- Conduct a focused study to quantify the effect of rising water in Westfalen No.3 on the ground stability.
- Investigate and monitor groundwater flow and chemical transport during and after fly ash backfilling
- Continue ground monitoring and data analysis, including gas, in Collingwood Park.

### *Current conditions in New Redbank Colliery*

- Two boreholes were drilled into the New Redbank Colliery and they encountered large irregular voids. It is likely that the investigated section of the mine has collapsed.
- The water level in New Redbank Colliery is stable at 83m below sea level, which is about 26m higher than that at Westfalen No. 3 Colliery.
- The mine geometry is unverified and current mine conditions throughout the New Redbank Colliery are unknown.

### *Recommended further investigation for New Redbank Colliery*

The information available to date at New Redbank Colliery does not provide CSIRO with sufficient confidence to develop a feasible remediation solution.

It is recommended that a three dimensional seismic survey be carried out to determine the extend of the mine collapse. Depending on the findings from the seismic survey at New Redbank, further site investigation and/or remediation studies may or may not be required.

## 10. ACKNOWLEDGEMENTS

This study is financially supported by the Department of Employment, Economic Development and Innovation (DEEDI) and the Department of Infrastructure and Planning (DIP) of Queensland State Government and CSIRO.

We would like to thank our client representatives, Kate Browning, Grahame Wise, Stewart Bell, Andrew McNamara, Luke Whistler, David Foster, Damian Lewis, Ian Gould, Sonya Booth, Andrew Fynn for their excellent support and technical input to the project.

The project could not be made possible without the support and supervision from our division chief Dr Mike McWilliams who has provided enormous technical and management contributions during the project setup and execution. We would also like to acknowledge our colleague Dr Anthony van Herwaarden for his excellent work in helping to establish the collaboration for this project between CSIRO and DEEDI.

We would also like to thank the following individuals for their contributions to this study in various forms:

Mark Ballard (SMEC)

Dr Rao Balusu (CSIRO)

Dr John Carras (CSIRO)

Bob Chamberlain (CSIRO)

Dr Christian Dupuis (Curtin University)

Professor Jim Gavin (Gavin and Associates Pty Ltd)

Dr Ken Grubb (Moreton Geotechnical Services Pty Ltd)

Dr Hua Guo (CSIRO)

Dr Peter Heeley (Swanbank Power Station)

Bill Holz (Keller)

Chris Melville (SMEC)

Dr Ken Mills (Strata Control Technology)

Grace Penon (CSIRO)

Dr Ramesh Thiruvengkatachari (CSIRO)

Meg Rive (CSIRO)

Professor Milovan Urosevic (Curtin University)

Uros Urosevic (Curtin University)

Dr Andy Wilkins (CSIRO)

## 11. REFERENCES

- Abel J.F. Jr 1988 Soft rock pillars *Int. J. Min. & Geol. Eng.* 6, 215-248.
- Adhikary, D.P, Guo. H. 2002. An orthotropic Cosserat elasto-plastic model for layered rocks. *Rock Mech Rock Engng* 35(3): 161–170
- Alehossein, H, A triangular caving subsidence model. *Applied Earth Science: IMM Transactions Section B.* 118 (1), pp. 1-4. 590, 2009
- Alehossein, H., 2009. Viscous, cohesive, non-Newtonian, depositing, radial slurry flow. *Int. J. Miner. Process.* 93, 11–19.
- Alehossein, H., Shen, B., Qin, Z. 2010. Viscous, cohesive, non-Newtonian, depositing, pipe slurry flow. *Journal of Fluid Mechanics* (under review).
- Bell F.G. Bruyn I. A. 1999 Subsidence problems due to abandoned pillar workings in coal seams *Bull Eng Geol Env* (1999)
- Bocking K 2008 Use of fly ash as fill material Golders Assoc Pty Ltd Tech Memo
- Brady, B.H.G. and Brown, E.T. 1985 *Rock Mechanics for Underground Mining* George Allen & Urwin
- Carr, A.F., 1977. Coal Resources, West Moreton (Ipswich) Coalfield, Redbank – Goodna Area. *GSQ Record* 1977/14.
- Chopra, S., Negut, D., and Cilensek, S., 2009, Azimuth moveout transformation – some promising applications: *The Leading Edge*, 28, 510-521.
- Cosserat, E., Cosserat, F., 1909. *Theorie des corps deformables*. Hermann, Paris.
- Cranfield, L.C., Schwarzbock, H. and Day, R.W. 1976. Geology of the Ipswich and Brisbane 1:250 000 sheet areas. *Geological Survey of Queensland, Report* 95.
- Das 1986 Influence of width/height ratio on post-failure behaviour of coal *Int. J. Min. & Geol. Eng.* 4, 79-87
- Department of Mines and Energy, 2008. Scoping study for Collingwood Park subsidence 2008. Report prepared by Parsons Brinckerhoff Australia Pty Limited.
- Dixson, O., 1989, Collingwood Park seismic reflection investigation: Velseis report.
- Edgar J, 1976 Thick seam mining as practised at Westfalen Colliery, Qld Aust. *I.M.M.*
- Falkner, A.J., Fielding, C.R. and Saunders, B.J. 1988. The Ipswich and Walloon Coal Measures. In *Field Excursions Handbook for the Ninth Australian Geological Convention*, edited by Hamilton, L.H. 81 – 93.
- Fama M.E. et al 1995 Two and three dimensional elasto-plastic analysis for coal pillar design and its application to highwall mining. *Int. J. Mech. Min. Sci. & Geomech. Abstr.* Vol. 32, pp. 215-225.

Galvin JM 1981 The mining of South African thick coal seams – rock mechanics and mining considerations. Chapter 8 PhD Thesis.

Galvin, J.M. 2006 Considerations associated with the application of UNSW and other pillar design formulae. 41st U.S. Symposium on Rock Mechanics.

Galvin, J.M., Hebblewhite, B.K. and Salamon, M.D.G., 1999 UNSW Pillar strength determinations for Australian and South African Conditions. 37th US Rock Mechanics Symposium pp63-71

Grubb, K 1994, Mining Subsidence Assessment Report at Collingwood Park, Moreton Geotechnical Services Pty Ltd.

Guo Guang-li, et al Sept 2007 Study of “3-Step Mining” subsidence control in coal mining under buildings

Guo, H., Shen B. and Pala J. 2005. Overburden grout injection project for targeted subsidence reduction at BHP Billiton Illawarra Coal Operations – A desk top study. CSIRO Exploration and Mining Report P2005/334

Guo, H., Shen, B and Chen, S. 2007. Investigation of overburden movement and a grout injection trial for mine subsidence control. In Eberhardt, Stead & Morrison (eds): Rock Mechanics: Meeting Society’s Challenges and Demands. Proceedings of 1st Canada-U.S. Symposium, May 2007, Vancouver . Vol. 2, pp.1559-1566.

Guo, H., Shen, B., Chen, S. and Poole G. 2005. Feasibility study of subsidence control using overburden grout injection technology - ACARP Project C12019 Final Report; CSIRO Exploration and Mining Report P2005/335

Heasley, K.A., 2000 The forgotten denominator, pillar loading Pacific Rocks 2000 – Proc Fourth Nth American R. Mech. Symp.

Hoek E., 1990. Estimating mohr-coulomb friction and cohesion values from the Hoek-Brown failure criterion. Int J Rock Mech Min Sci & Geomech Abstr, 1990; 27: 227-229.

Hill, D. 2005 Coal pillar design criteria for surface protection. Coal2005 Conference, Brisbane Qld

Itasca Consulting Group Inc., 2006 FLAC3D (Fast Lagrangian Analysis of Continua in 3 Dimensions), version 3.1. Minneapolis, Minnesota, USA.

Jiang Y.D., Wang, H.W. and Zhao, Y.X., 2009. Study of complementary supporting technology of extremely soft rock mining roadway. Chinese Journal of Rock Mechanics and Engineering; 28: 2383-2390 (in Chinese)

Kathage WA, 1980 Roof control associated with a borer miner and multiple slicing in thick seams at Wesfalen No. 3 mine. Aist.I.M.M

Keller, 2010, Collingwood Park – Final Report on Mine Void Filling Logistics. Keller Document Reference No. K10066-03-BH PC 10339/00793.

Maconochie, D Forster, G 1982, Mining Subsidence Study, Collingwood Park Estate (plus Appendix), Peter Hollingsworth & Associated Consultants.

Mark, C. 1999 The state-of-the-art in coal pillar design Soc. For Mining, Metallurgy and Exploration Mar pp1-8

Mine Subsidence Engineering Consultants 1997. Mine Subsidence Damage to Building Structures. Mine Subsidence Engineering Consultants Report.

Mokgokong P.S. and Peng S.S. 1991 Investigation of pillar failure in the Emaswati Coal Mine, Swaziland Min. Sci. & Tech. 12 113-125

Pietruszczak S. and Mroz Z., 1980. Numerical analysis of elastic-plastic compression of pillars accounting for material hardening and softening. Int J Rock Mech Min Sci & Geomech Abstr, 17: 199-207.

Poulsen BA 2010 Coal pillar load calculation by pressure arch theory and near field extraction ratio Int.J.Rock.Mech.Min.Sci

Roberts D.P. et al, 2002 Development of a method to estimate coal pillar loading. Safety in Mines Research Advisory Committee Report 2001-0651

Salamon M.D.G., Ozbay M.U. and Madden B.J. 1998 Life and design of bord-and-pillar workings affected by pillar scaling J. Sth. Afr. Inst. Min. Metal. May/June 1998

Salamon MDG 1974. Rock mechanics of underground excavations Proc 3rd Cong. Int. Soc. Rock. Mech. Denver, CO, USA pp951-

Salamon, M.D.G. and Munro, A.H. 1967 A study of the strength of coal pillars. J. Sth. Afr. Inst. Min. Metal. Vol 68. 56-67.

Schlanger HP, Eniver JR, Tsaganas S & Kelly P., 1983 An hypothesis to predict the strength of banded coal pillars at Westfalen No. 3 Colliery, Ipswich Qld. CSIRO Division of Applied Geomechanics Report #42.

Shen B., Alehossein H., Pousen B. and Waddington A, 2010. ACARP Project C16023 Final Report – Subsidence control using coal washery waste. CSIRO Earth Science and Resource Engineering Report P2010/65.

Shen, B. and Guo, H. 2007. A laboratory study of grout flow and settlement in open fractures. In Eberhardt, Stead & Morrison (eds): Rock Mechanics: Meeting Society's Challenges and Demands. Proceedings of 1st Canada-U.S. Symposium, May 2007, Vancouver . Vol. 1, pp.747-754.

Shen, B., Alehossein, H., Guo, H., Pala J., Armstrong, M., Poole, G., and Riley P. 2006. Overburden Grout Injection Project for Targeted Subsidence Reduction at BHPBilliton Illawarra Coal Operations - Phase 2 Site Investigation and System Design CSIRO Exploration and Mining Report P2006/118

SMEC, 2010. Collingwood Park Mine Remediation - Geotechnical Field Investigation Factual Report, Reference Number 3003469.

Tesarik DR et al 2002 Post-failure behaviour of two mine pillars confined with backfill

Tesarik DR et al 2009 Long-term stability of a backfilled room-and-pillar test section at the Buick Mine, Missouri, USA

van der Merwe J.N. 2003 New pillar strength formula for South African coal. J. Sth. Afr. Inst. Min. Metal. June 2003

Waddington Kay & Associates, 2002. The Prediction of Subsidence Parameters and the Assessment of Subsidence Impacts on Natural Features and Surface Infrastructure. BHP Billion Endeavour Coal Pty Ltd, West Cliff Colliery Longwalls 5A5 to 5A8. Report Number WKA118.

Wagner, H. 1974. Determination of the complete load deformation characteristics of coal pillars. Proc 3rd Cong. Int. Soc. Rock. Mech. Denver, CO, USA pp 1076-81

Wagner, H. 1980 Pillar design in coal mines. J. Sth. Afr. Inst. Min. Metal. January 1980

Wang Xin-min et al 2009 Paste-like self-flowing transportation backfilling technology based on coal gangue.

Yilmaz, 2001, Seismic data Analysis - Processing, Inversion, and Interpretation of seismic data: Society of Exploration Geophysics.

Zhou, J.W., Xu, W.Y. and Li, M.W., 2009. Application of rock strain softening model to numerical analysis of deep tunnel. Chinese Journal of Rock Mechanics and Engineering; 28: 1116-1127 (in Chinese)

Zipf, K.R. 2001 Towards pillar design to prevent collapse of room-and-pillar mines. 108th Annual Exhibit and Meeting, Soc. For Mining, Metallurgy and Exploration

## **APPENDIX A**

### **Numerical modelling and pillar/panel stability assessment**

## **APPENDIX B**

### **Laboratory tests and injection material recommendation**

## **APPENDIX C**

**University of Queensland Report:**

**POTENTIAL FOR BACKFILLING BORD AND PILLAR VOIDS USING  
FLY ASH SLURRY**